STUDIES ON MIXED LAYER AND HEAT BUDGET OF THE NORTHERN INDIAN OCEAN

THESIS SUBMITTED TO

THE COCHIN UNIVERSITY OF SCIENCE AND TECHNOLOGY

FOR THE DEGREE OF

DOCTOR OF PHILOSOPHY

IN

PHYSICAL OCEANOGRAPHY

BY

DHOULATH K.A., M.Sc.

PHYSICAL OCEANOGRAPHY AND METEOROLOGY DIVISION

SCHOOL OF MARINE SCIENCES

COCHIN UNIVERSITY OF SCIENCE AND TECHNOLOGY

COCHIN - 682 016, INDIA

NOVEMBER - 1992

CERTIFICATE

This is to certify that this thesis is an authentic record of research work carried out by Smt. Dhoulath.K.A, under my supervision and guidance in the Physical Oceanography and Meteorology Division, School of Marine Sciences for the award of Ph.D degree of Cochin University of Science and Technology, and no part of this has been previously presented for the award of any degree in any University.

Cochin-682016,

November-1992.

(Prof.P.G.KURUP)

Head, Physical Oceanography and Meteorology Division,
School of Marine Sciences.
(Supervising guide)

CONTENTS

PREFACE

The marine boundary layer plays a vital role in the energy exchange processes between ocean and atmosphere. Due to their large thermal inertia, the oceans control the overall weather and climate. The energy exchange at the air-sea interface influences the oceanic and atmospheric circulations through wind and current regimes.

The reversing monsoonal winds in the Indian Ocean cause considerable changes in the circulation and thermal conditions of the ocean mixed layer. The thickness and heat content of this layer vary seasonally due to vertical mixing and surface heat exchanges, thus modifying the oceanic and atmospheric circulations. Heat budget parameters also exhibit seasonal variations in association with the reversing winds.

Recent studies have revealed that most areas of north Indian Ocean, especially western Indian Ocean are warm enough for the development of onset vortex. Considerable lowering of the surface temperature occurs as a consequence of surface heat loss during the monsoon season.

The present study is an attempt to understand the upper ocean conditions in the northern Indian Ocean in relation to India monsoon on a seasonal and daily basis. It is also aimed at examining the relative role of ocean heat potential on the development of cyclonic storms. Variations of different energy exchange components in the northern Indian Ocean are studied during pre-onset, onset and break periods of monsoon. Heat

storage and heat advection of the mixed layer and 0-200m layer are also analysed with an aim of quantifying the heat export or import during the monsoon season.

The thesis is divided into five chapters. The general introduction, literature review, scope, area of study and the data and methodology employed in the present study are included in the first chapter.

The second chapter deals with the estimation of mixed layer depth (MLD) and the spatial variations of Sea Surface Temperature (SST) and MLD in the northern Indian Ocean on a seasonal and daily basis using climatological data and data during 1977-1986. Mixed layer slope variations in the equatorial Indian Ocean have also been discussed in this chapter.

Seasonal and daily variations of heat content of each 50m layer upto 200m have been presented in the third chapter. The role of cyclone heat potential on atmospheric disturbances have also been discussed.

The fourth chapter deals with the variations of different heat budget parameters in the north Indian Ocean during pre-onset, onset and break-monsoon periods. Heat storage and heat advection have also been presented for different latitude belts.

At the end of chapters II, III and IV, the discussions of the result obtained are included.

Last chapter provides the overall summary and conclusion of the present study.

CHAPTER-I

INTRODUCTION

It is recognised that oceans exert a major role on weather and climate. They provide moisture for the hydrologic cycle and also influence the general circulation of the atmosphere. The oceans have larger thermal inertia which contributes to the spatial and temporal variations of climate. Oceans also transport heat horizontally and modify the climate and affect its variability. The poleward heat transport by the ocean currents implies that the ocean gains heat in the low latitudes and loses in high latitudes.

Oceans derive energy mainly from the sun in the form of solar radiation. Part of this is radiated as long-wave radiation and another part heats the atmosphere and the remainder returns to space. The loss of energy from the earth's surface must balance the incoming radiation for otherwise, the temperature of the earth would rise by an average of about 3^{o} F per day. But there is a net gain in the tropics and loss in the extra tropics maintaining a balance aruond 30^{o} N and 30^{o} S.

It is noted that the changes in the circulation of the global atmosphere have been found to be strongly correlated with the anomalies in the thermal and current structure of the upper layers of the tropical ocean. The ocean boundary layer is therefore important in the large scale climatology of the ocean. It also influences the changes in the temperature and density of water masses through air-sea interaction processes.

The net heat energy at the air-sea interface propagates into the sea with exponential decay and its absorption within the ocean layer creates negative temperature gradient with depth. Heat absorbed and the heat stored in the upper homogeneous layer (the mixed layer), affects the oceanic and atmospheric circulations. Over the central Arabian Sea, Rao and Rao (1986) observed dominance of surface wind speed in deciding the evaporative patterns during monsoon. Preliminary heat budget studies indicate that evaporative cooling and possibly the upward flux of cold water driven by wind mixing can have a major role in mixed layer tempareture and heat content (Rao,1987,a). The thickness and heat content of this layer varies seasonally depending upon the oceanic processes such as downward mixing of heat due to entrainment and surface energy exchanges. Most of these exchanges are mainly controlled by the wind stress acting over the ocean (Ali et al, 1987).

Due to the reversal of monsoonal winds in the Indian Ocean, there is a seasonal variation in the parameters controlling the heat budget components and oceanic heat content. During pre-monsoon season, the surplus energy at the sea surface warms the surface layer and reduces the mixed layer depth (MLD). Heat loss during winter decreases the surface layer temperature, which produces a deep mixed layer. This cooling and deepening of mixed layer reduces the heat content of surface layers. Hence it is very probable that the heat content of the Indian Ocean has great

impact on Indian monsoon, on which the economy of Indian sub-continent largely depends.

The net radiation increases from a minimum in winter to a maximum in April-May and thereafter decreases sharply with the onset of monsoon. The resulting net heat loss at the ocean surface during monsoon creates a prominent cooling in the surface layer. MLD deepens under the action of turbulent motion associated with the strong winds, swift currents, and heat losses at the ocean surface. Rao (1987,b) is of the opinion that local cooling process in the mixed layer caused by upwelling may be dominant over the eastern section. Evaporation at the sea surface plays a direct role in driving local boundary layer mixing, as well as providing latent energy for the development of cumulus convection.

The seasonal reversal of the monsoonal wind system produces unique responses in the equatorial Indian Ocean also. These responses are characterised by a rapid built up of the surface current jet, reversal of the mixed layer zonal slope and the under current (Ali et al,1987) and cooling of the sea surface (Rao et al,1983).

1.2 Scope of the study

It is clear that the atmosphere and the ocean form a coupled interacting system. The atmospheric circulation pattern determines the oceanic flow, which in turn influences where and how much energy is released to the atmosphere. Quantification of the energy budget over the Indian Ocean and identification of

principal spatial and temporal features of the budget components help in complete understanding of the air-sea interaction processes. A knowledge of the heat fluxes across the sea surface and the heat content in the ocean mixed layer would be helpful in improving monsoon and weather forecast. Mixed layer determines the characteristics of sound duct, a layer in which underwater objects can be detected from farther distances. The density anomaly and mixed layer depth also decide the propagation speed of the internal waves (Christenson and Macarenhas,1979). In order to understand the basic nature of air-sea coupling and behaviour of the Indian monsoon, a comprehensive study of the heat balance and the thermal condition of the upper layer is essential.

1.3 Review of literature

The rythmic reversing monsoons over the Indian Ocean and associated oceanic and atmospheric circulations have particularly attracted the attention of several workers. During the past, several investigations have been carried out on the interaction between Indian monsoon, surface energy exchanges and thermal structure of the Indian Ocean, using a variety of data sets. A brief review if the investigations related to the present study is presented here.

1.3.1 Heat budget components

Jeffry (1918) and Giblett (1921) were amoung the earliest workers to study the problem of evaporation in terms of atmospheric turbulence. Applying the heat budget equation and

using the available seasonal climatic data, Jacob (1951) computed the amonut of evaporation, sensible heat and total energy exchanged between sea and atmosphere within each 5^{o} square grids for the North Pacific and Atlantic Oceans. Differnt aspects of radiation were analysed by Anderson (1952), Black (1956) and Burdicky (1958). The atlas of heat balance by Budycko (1963), world maps of global solar radiation by Black (1956) and Ashbel (1961), the review of surface measurements of solar and terrestrial radiation by Robinson (1964) and oceanographic Atlas of Wyrtki (1971) are some of the important works in this aspect.

Determination of the different heat budget terms, in the Indian Ocean are carried out using ship observations. Computation of mean monthly sea surface temperature (SST) and air-sea exchange parameters were carried out by Miller et al,(1963) under the Meteorological programme of the International Indian Ocean Expedition (IIOE, 1963-64). Colon (1964) and Colborn (1975) discussed the southwest monsoon interaction over the Arabina Sea and Indian Ocean in relation to heat budget parameters. Computation of evaporation flux for the year 1963 has been presented by Suryanarayana and Sikka (1965). Pisharoty (1965) discussed the evaporation from the Arabian sea and its relation to the India southwest monsoon. Roll (1965) discussed the different aspects of air-sea interaction and the importance of drag coefficient in the exchange of heat and momentum.

Mani et al, (1967) studied the distribution of global solar and net terrestrial radiation over the Indian Ocean. They concluded that, the net radiation over the ocean is always

positive and greater than that over land and its distribution is zonal with maxima over ocean and minima over land. Subsequently, heat budget components for all the months of 1963-64 were copmuted from IIOE data and presented for the Indian Ocean north of 40^{o} S (Ramage et al,1972). The role of vertical motion in the heat budget of upper ocean is discussed by Kaiser (1976) who also computed the heat budget components of the upper 30m layer in the Bermuda area.

With the implementation of experiments like Indo-Soviet Monsoon Experiments (ISMEX) and MONSOON experiments (MONSOON-77 and MONEX-79), information regarding the monsoonal heat budget components were published by Pant (1977), Rao et al, (1978) and Rao (1987,a & b). Bunker (1978) estimated the monthly seasonal and annual means of energy fluxes over the Atlantic Ocean for the period 1948-1972. The heat budget of the ocean-atmosphere-land system in the Indian Ocean area (30^{o} N-30^{o} S, 30^{o} E-120^{o} E) was studied by Hatenrath and Lamb (1979,b) on the basis of ocean surface heat flux calculations from long-term ship observations and satellite derived estimates of net radiation at the top of the atmosphere. This study revealed that the oceanic heat import or export is small for the study area during Novomber-April and May-October and nearly zero for the whole year. They also concluded that during northern summer, the atmospheric energy export from the southern tropical Indian Ocean was largely in the form of latent heat and was directed northward across the equator. Later this work was extended to estimate the heat budget

of the tropical oceans by Hasterath (1980). Another study by Hastenrath and Lamb (1980) sugested that the energy had to be exported across the equatorial Indian Ocean at an annual average of $5*10^{14} W/M^2$. Duing and Leetma (1980) in a similar work, assessed the relative contribution of the different energy exchange processes involved in cooling the surface layers of the Arabian Sea in summer.

Mohanty et al,(1982) studied the effect of large scale heat budget during the onset and active phases of southwest Asian monsoon during May-July 1979. Rao et al, (1985) estimated the surface heat budget over the north Indian Ocean using MONSOON 77 USSR ship data, and concluded that energy input to the atmosphere from the ocean surface during disturbed weather condition was approximately double the corresponding value during fair weather period. Rao (1988) estimated the seasonal heat budget of the upper layers in central Arabian Sea using ship observations and observed a mixed layer cooling of about 2^{o} C during monsoon onset.

1.3.2 SST and monsoon

The large scale interaction between ocean and atmosphere has been examined by observational studies and by numerical simulations by several authors. From a series of quantitative anlyses of observation from the ocean and atmosphere, Bjerknes (1966) has shown that large and intense SST anomalies exist in the equatorial regions. Utilising the SST data collected during IIOE, Saha (1970) showed the existence of zonal anomalies of SST

in the Indian Ocean and its possible effect upon the monsoon circulations. Sastry and D' souza (1970) presented the thermal structure of the Arabian Sea between 5^{o} N-20^{o} N during the summer monsoon of 1963. This study revealed that large spatial variations in surface temperature were due to radiation imbalance and intense upwelling off Somali coast. Rao et al, (1978) studied the lowering of surface temperature in the Arabian Sea with the advance of southwest monsoon and found that the SST was high during May-June while a lowering (ranging from 1-4.5^{o}C) is observed in July. The surface layer was uniform in the region west of 60^{o} E and showed a phenominal increase in its thickness and heat content east of 60^{o} E. Raghavan et al,(1978) showed that during the weak monsoon over India, the SST drops significantly over a large area compared to strong monsoon. Ramesh Babu et al, (1978) attributed the drop of 1-2^{o} C in the SST to the strong winds off Sourashtra coast during southwest monsoon.

Upwelling appears to be the dominant factor in determining the heat balance of Arabian Sea. Anjaneyulu (1980) reported that the lowest SST during the southwest monsoon observed in Bay of Bengal and Arabian Sea was due to upwelling and the large amount of heat loss from the sea. Duing and Leetma (1980) examined this cooling in relation to heat fluxes, advection and upwelling over the Arabina Sea and concluded that it was mainly due to upwelling. Ramam et al, (1982) while analysing the hydrgraphic data collected in the central Arabian Sea during MONSOON 77, have found that the thermal structure of the surface layer upto 20m

depth was influenced by the transit of a severe cyclonic storm. Riverdine (1983) attributed the heat budget of the tropical Atlantic Ocean to seasonal upwelling, and concluded that the transient upwelling close to the equator was associated with the largest oceanic heat gains in the tropics.

Rao et al, (1981 & 1983) and Rao & Rao (1986) investigated the surface layer cooling in the seas around India from MONEX data sets and related it to the heat losses from the sea and upwelling, while Ramesh Babu and Sastry (1984) suggested that this cooling was due to entrainment. Murthy et al, (1983) studied the thermal conditions in the east central Arabian Sea associated with a cyclone. By examining the SST pattern in the Arabian Sea, Sastry and Ramesh Babu (1985) related the initial cooling of the sea surface to the heat loss and cooling due to entrinment during June. Joseph and Pillai (1986) observed surface cooling in the Arabian Sea and Bay of Bengal, and suggested that SST anomaly as an indicator of the strength of Indian monsoon.

1.3.3 Ocean mixed layer

Apart from the above studies, many workers investigated the variability of surface mixed layer in a quantitative manner. Patil and Ramamirtham (1962) observed a mixed layer depth of 65-80m during December around Laccadive Islands. Patil et al, (1964) noticed low MLD of 20-30m off Veravel during January-May. Sastry and D'souza (1970) related the spatial varaibility of mixed layer in the eastern and central Arabian Sea during southwest monsoon

to the oceanic circulation. David (1974) suggested the variations in MLD as due to synoptic meteorological disturbances, and reported that the change in heat content of the upper mixed layer was (less than + 5 %) as the mixed layer deepens. Creegan and Johnson (1978) developed an advective mixed layer model for the prediction of surface temperature, MLD and circulation from wind stress and surface heat flux distribution. Elsbery and Camp (1978) studied the oceanic thermal response during a strong atmospheric disturbance using bulk turbulent kinetic energy model.

According to Merle (1980), annual variations of heat content in the upper layer is mainly due to the vertical movement of thermocline associated with seasonal winds. Ramesh Babu et al. (1980) reported a progressive fall in the mixed layer thickness of the north eastern Arabian Sea during March. In the northern Arabian Sea, during January-May Varma et al, (1980) found winter cooling leading to the deepening of mixed layer, and eddy flow along 64^{o} E causing southward shoaling of mixed layer depth. Rao et al, (1981) examined the short term variations of MLD in relation to the surface energy exchanges over the northern Bay of Bengal during break monsoon of 1977. Basil Mathew (1982) attempted to explain the seasonal variability of the mixed layer along the west coast of India in relation to upwelling and sinking. Washburn and Gibson (1984) observed the temperature microstructure during Mixed Layer Experiment (MILE) and showed that the distribution of mixing activity in the seasonal

thermocline at the base of the surface mixed layer was highly intermittent in the horizontal plane.

Heat budget analysis of mixed layer by Rao et al, (1985) indicated that the surface cooling of 2-3^{o} C in the central Arabian Sea with the onset and sway of the MONSOON 77 was mostly due to net oceanic heat losses. Numerical model studies of the upper ocean thermal structure by Shetye (1986), indicated that the surface heat fluxes influence the mixed layer processes during all seasons except during southwest monsoon. Joseph (1987) studied the mixed layer characteristics in the Arabian Sea with special reference to energy transfer from eddies. Ali and Desai (1989) obseved a mixed layer deepening from east to west in the equatorial Indian Ocean after the onset of monsoon during 1979.

1.3.4. Studies using satellite data

Besides the studies mainly concerned with ship data, some attempts were made using satellite data also. Based on past satellite data, Yamamotto and Wark (1962) estimated infra-red flux and SST. Vonder Haar and Ellis (1974) and Oort and Vonder Haar (1977) observed in their anlysis of satellite radiation parameters during 1962-65 that more than 30% of solar energy was absorbed in the tropics. A numerical relation has been developed between hourly values of net radiation and global solar radiation by Kelkar and Pradhan (1977) who showned that for a given amount of solar radiation. the net radiation is greater in the afternoon than in the forenoon. Using a regression analysis, Tarpley (1979) determined the hourly insolation from satellite

derived daily insolation, and the accuracy being ± 10% when compared with pyranometer data. Hastenrath (1980) studied the inter annual variability of poleward transport and storage of heat in the ocean-atmosphere system using the satellite radiation measurements at the top of the atmosphere.

Gautier (1981) estimated the short-wave energy budget from geostationary satellite data over the Indian Ocean. Satellite derived SST distribution over the north Indian Ocean has been studied by Mishra (1981) using NOAA-5 and TIROS -N data and found that lowest SST of about 22^{o} C was noticed off Somali coast during July and August 1979. This delayed low SST over the region is associated with the delayed and weak monsoon onset. Zandlo et al, (1981) presented a method to depict quasi-continous surface temperature features using GOES and TIROS-N radiation measurements. While estimating surface insolation from geostationary satellite data, Gautier (1982) compared the insolation from satellite parameters with those from pyranometer measurements and obtained an r.m.s difference of ± 8% of the mean measurements.

Deshamps and Frouin (1983) studied the diurnal heating of the sea surface utilizing the data from HCMR satellite. In this study glitter reflectance was modeled to retrieve an equivalent wind speed. Timothy (1983) estimated the average wind speed from SEASAT scatterometer data and reported that, this wind speed was higher than that obtained from ship measurements. Ohring and Gruber (1984) developed a relation between long-wave radiation

flux and infra-red window radiance from regression analysis utilising the NIMBUS-7 radiation data. Their results indicate that there is a very high correlation between the flux equivalent brightness temperature and the window brightness temperature.

Simon and Desai (1986) estimated the evaporation over the equatorial Indian Ocean using TIROS-N moisture profile and GOES low level cloud motion vector winds extrapolated to the surface. Their results suggest that latent heat flux estimates are more satisfactory than the sensible heat flux. By monitoring the heat flux over the Indian Ocean, some inferences related to monsoon onset were also discussed. Joshi and Desai (1986) explained the thermal features of the monsoon circulation in the atmosphere with NOAA data during monsoon onset, active and break periods. Ali et al,(1987) attributed the surface wind stress change to the vertical processes in the equatorial Indian Ocean using GOES winds and TIROS-N SST data. Gautier and Frouin (1988) attempted to estimate the net surface heat flux over the Indian Ocean from satellite parameters and found that the variations in net heat flux are consistent with the monsoon activity.

Miller (1985) studied the heat storage change in the upper ocean on seasonal and annual time scales from SEASAT wind stress and SST data. Hsiung et al,(1989) presented the heat storage and heat transport for the Pacific, Atlantic and Indain Ocean on monthly basis, and observed largest annual amplitude in regions where western boundary currents are predominant. Ali and Desai (1989) studied the variations in the heat transport associated

with the mixed layer slope in the equatorial India Ocean, considering heat budget on weekly time scales. Their study showed that there is a net heat loss from the ocean during the onset of southwest monsoon due to the increased evaporation and reduced insolation.

1.4. Area of study

Indian Ocean occupies almost $28*10^6$ sq. miles ie about 14% of the total surface area of the earth. Indian Ocean is mostly an enclosed area with Africa on the west and Asia on the north. It is partially enclosed on the east by Australia and eastern Archipelago and is open towards the Antartica. In the present study, north Indian Ocean comprising three regions viz. Arabian Sea which lies north of 5^oN and west of Cylone (5^o-20^oN, 50^o-80^oE), Bay of Bengal which lies north of 5^oN and east of Cylone (5^o-20^oN, 80^o-100^oE), and north equatorial Indian Ocean that lies between 0^o-5^oN, 50^o-100^oE) is studied. Fig.1.1 shows the study area for which the horizontal distributions of different parameters were presented and the positions of different polygon areas for which daily variations were presented.

1.4.1. Climatic features of the study area

Indian Ocean is largely influenced by reversing monsoons. Monsoon is a planetary scale land-sea breeze circulation that arises because of heating contrast between the land masses of the Asian continent and water masses of the Indian Ocean. The Asiatic monsoon with its pattern of extensive seasonal precipitation and associated heating of the middle troposphere exercises a very

significant influence on the general circulation of the atmosphere, The Indian monsoon is a geographically bound cyclonic system less than 6 km in thickness embedded in the equatorial easterlies. The monsoon strengthens when there is fresh input of moist air and weaken owing to friction and dispersal of water vapour.

The low pressure developed over the Indian sub-continent causes intense southwesterly winds which flow for longer periods from May to September in the Arabian Sea. During winter, a high pressure system over the Tibetan region initiates the northeasterly winds which are weaker over the Arabian Sea lasting for a shorter duration from December to January. Precipitation is more during southwest monsoon than the northeast monsoon. When the monsoon trough over the north India shifts to the Himalayas, there is a general cessation or break in the monsoon rains over the plains of India although heavy rains continue over the foothills, flooding the Himalayan rivers. The major synoptic features identified in the break monsoon are the southward extension of a westerly trough in the extra- tropical westerlies over Pakistan (Ramaswamy, 1962) and westward moving lows or mid-troposphere cyclones over the southern Bay and south peninsula causing showers there (Koteswaram, 1958).

Cyclones over the Arabian Sea and Bay of Bengal are typical however they are most frequent in the weeks preceding the onset of monsoon rains in the western Indian Ocean and in the weeks following the retreat ie May, early June and in November. The

extensive areas of north Indian Ocean are warm enough for tropical cyclogenesis throughout the rainy period in western India. The reversal of monsoonal wind and current system also influences the surface heat transfer processes, thermal structure and MLD variation.

The major energy exchange components which exhibit large seasonal variation are net radiative flux and latent heat flux. The net radiation rises from a winter minimum to maximum during April-May and thereafter decreases sharply with the onset of monsoon. Rates of evaporation are larger in winter because of dry northeasterly trade winds over the Arabian Sea and maximum in summer on account of the strength of southwest monsoon winds. Heat fluxes in the ocean are directed upward during monsoon and winter seasons, but, during pre-monsoon and post-monsoon seasons, large quantities of heat are transmitted from the ocean surface to deeper layers (Pickard and Emery,1983).

The annual average of net short-wave radiation input to the ocean surface ranges from $90W/M^2$ at 80^oN to $229W/M^2$ between 20^o-25^oN. The back radiation term varies between $20-50W/M^2$ on annual scale (Pickard,1965). The value of sensible heat ranges from -10 to $-40W/M^2$ being smaller in most of the regions. Latent heat flux, on the otherhand, ranges from -25 to $-150W/M^2$. Negative sign shows heat loss term.

1.4.2. Circulation and thermal features

The circulation in the Indian Ocean is dominantly controlled by the monsoonal wind reversals. A major anticyclonic

system of current is present during summer and the system persists for a longer duration (March-september) intensifying during June-August. In winter, a weak cyclonic circulation system is present from November-January. Reversal of flow towards north takes place after October (Pickard,1965). Circulation in the north Indian Ocean as deduced from dynamic topography indicates the presence of several eddies (Duing, 1970). Sastry and D'souza (1970) observed cyclonic and anticyclonic eddies in the Arabian Sea during southwest monsoon and Das et al,(1980) reported eddies in the north Arabian Sea during Feb-April. Along the east coast of Africa, during southwest monsoon season, a swift northeasterly current known as Somali current develops.

In rhythm with the semiannual changes in winds and currents, Indian Ocean exhibits cyclic characteristics of upwelling during south west monsoon and sinking during northeast monsoon season along much of the coastal zones. Regions of extensive upwelling along the Somalia and Arabian coasts are caused by strong offshore wind stress components.

The thermal structure in the Indian Ocean shows typical deviations compared to tropical oceans. The ocean bounded by the Asian continent on the three sides reflect the effect of continentality on the thermal conditions in the upper layers. The annual cycle of SST in most parts of the ocean shows a strong bimodal signal. Large meridional and zonal temperature gradients exist at the surface and sub-surface levels. Summer cooling in the Arabian Sea is a combined effect of different factors like

reduced insolation, increased evaporation and turbulent mixing resulting in the deepening of mixed layer and the spreading of cold upwelled waters.

1.5. Data and Methodology

Ship observations and scientific expeditions have provided a sparse collection of data from which a general pattern of different processes can be inferred but, detailed studies over the whole ocean may not be possible. Satellite observations provide global real-time data needed for climatic studies. Hence in this study, data from two complimentary sources are utilized ie data from ship observations coupled with satellite observations. Satellite measurements provide good coverage over most of the Indian Ocean during the study period for radiation parameters,SST and air-temperature during monsoon 1979. For cloud motion vector winds over the north Arabian Sea and Bay of Bengal, there is less coverage for certain months eg ,May 1979. Ship observations are coupled with these observations in order to get a global coverage. The source of data used for the present study is shown in Table.1.1

Net short-wave radiation at the ocean surface is estimated from a regression analysis utilizing ship measured net radiation, satellite derived radiation at the top of the atmosphere, planetary absorbed radiation, cloud amount and total water vapour content of the atmosphere (which are available from NOAA satellite series). Sensible and latent heat fluxes are determined using bulk aerodynamic formula utilizing NOAA satellite derived

Table.1.1 Sources of data used in the present study

S. No	Type of data	period	Source
1.	MONEX-79 temperature profiles and NOAA/GOES satellite finished products	1979	Space Applications Centre, Ahmedabad.
2.	MONEX -79 and MONSOON-77 marine meteorological data	1977 and 1979	Indian Daily Weather Report and Naval Physical Oceanographic Laboratory, Cochin.
3.	MONSOON-77 temperature profiles	1977	Naval Physical Oceanographic Laboratory, Cochin.
4.	Temperature profiles	1977-1986	National Institute o Oceanography, Goa.
5.	Climatological temperature profiles	1885-1965	Levitus (1982)

SST and air temperature, cloud motion vector winds (obtained from GOES) and ship observed SST, air temperature, dew point temperature, sea surface pressure. As the satellite measured relative humidity is difficult to retrieve, dew point temperature is taken from ship observations to compute vapour pressure. For the computation of MLD, mixed layer heat content and heat content of different layers, the temperature profiles obtained from both indian ships including R.V. Sagarkanya and Gaveshini during 1977-1986, and USSR ships during 1977 and 1979 are utilised. Distribution of data points is presented in Table.1.2. The temperature data is selected for standard depths. In data sparse regions, data have been interpolated using linear interpolations. The data are checked and obvious errors have been removed manually. For the horizontal distribution of MLD, SST and heat content during 1977-1986, seasonal averages are determined for each of $2.5^{o} \times 2.5^{o}$ grid boxes. Six hourly temperature profiles are averaged on a daily basis in order to analyse the daily variations.

The various parameters used in the present study are computed as follows.

Estimation of Energy exchange components

The heat budget equation is given by

$$Q = Q_n - (Q_{lh} + Q_{sh}) \qquad (1.1)$$

where Q is the net heat gain or loss, Q_n is the net radiation term, Q_{lh} the latent heat flux and Qsh sensible heat flux.

Table.1.2 Monthly depth-wise distribution of data points during 1977-1986.

Depth (m)	Jan	Feb	Mar	Apr	May	June	July	Aug	Sep	Oct	Nov	Dec
0	29	66	48	110	128	1019	860	319	124	127	143	111
10	29	66	48	110	128	1019	860	319	124	127	143	111
20	29	66	48	110	128	1019	860	319	124	127	143	111
30	29	66	48	110	128	1019	860	319	124	127	143	111
50	29	66	48	110	128	1019	860	319	124	127	143	111
75	28	66	47	108	128	1019	860	311	120	123	141	106
100	28	64	47	108	122	1011	854	309	116	120	138	101
125	27	63	41	106	118	1006	851	306	113	120	137	101
150	27	61	40	102	116	1002	848	298	108	118	128	98
200	26	61	40	101	116	1002	848	296	104	118	128	98

Estimation of net radiation (Q_n)

In thi study, net radiation at the ocean surface has been estimated from the absorbed radiation of the ocean-atmosphere system (planetary values) as obtained from NOAA finished products. For this purpose, a regression equation has been fitted between the net radiation measured by the MONEX-79 ships, planetary value of the absorbed solar radiation at the top of the atmosphere, amount of water vapour and cloud amount. All the later four parameters are available from NOAA satellite. The regression is of the form

$$Q_n = Q_{pb} * 0.2- (Q_{av}* 0.6+ W*5.4 - cl*0.8)+112.5 \qquad (1.2)$$

where Q_{pb} is the planetary absorbed radiation, cl is the cloud amount in tens, W is the water vapour content of the atmosphere in millimeters of perceptible water vapour, Q_{av} is the available radiation at the top of the atmosphere. The number of data points are 30 (simultaneous ship observed net radiation) and the correlation coefficient is found to be equal to 0.86. The net radiation values obtained from the regression equation are compared with the actual ship measured values and the R.M.S error is found to be 20% for the measured net radiationin range of $108W/M^2$ to $210W/M^2$. The table of comparison is given in chapter-IV. Net radiation at more number of points could thus be estimated from satellite observations using this regression equation (Dhoulath et al,1992).

Estimation of latent and sensible heat

Latent heat flux (Q_{lh}) and sensible heat flux (Q_{sh}) have been computed using the bulk aerodynamic formula as·

$$Q_{lh} = \rho C_D L V (q_s - q_a) \quad (1.3)$$

$$Q_{sh} = \rho C_D C_p V (T_s - T_a) \quad (1.4)$$

where, ρ is the density of air, C_D is the drag coefficient, L is the latent heat of vaporization, V is the surface wind speed, q_s is the saturated specific humidity at the sea surface, q_a is the specific humidity of air near the seas surface, $C_p$is the specific heat at constant pressure, T_s is the SST and T_a is the air temperature, = 1.2 kg/m , L = 24.5*10 J/kg and C_p = 1005 J/kg/^{o}K and C_D = $1.3*10^{-3}$ following Camp and Elsberry (1978). q_s and q_a are estimated as

$$q_s = 5/8 (e_s/p) \quad (1.5)$$

$$q_a = 5/8 (e_a/p) \quad (1.6)$$

where, e_s and e_a are the vapour pressure of air and saturated vapour pressure at the sea surface.

e_s and e_a are computed following Simon and Desai (1986), which is given by

$$e_a = T_d + 10^{(b+c/T_d)} \quad (1.7)$$

$$e_s = T_s + 10^{(b+c/T_s)} \quad (1.8)$$

where, T_d is the dew point temperature, a = -4.928, b = 23.55 and c = -2937.

Estimation of MLD

Mixed layer depth is estimated using gradient method followed by Ali et al, (1987) details of which are given in chapter-II. Briefly, the depth at which temperature at 10m is $1^{o}C$ less than that is first determined. From this depth, the gradient is checked towards the surface untill the gradient is less than $0.08^{o}C/m$. Then the MLD is determined as the mean of this depth and the next lower level where the gradient is more than $0.08^{o}C/m$. If the gradient check is satisfied in the very first layer, then the average depth of this layer is considered as the MLD. Two conditions are satified by this criterian. One, mixed layer can not extend to a depth where temperature is one degree less than that at 10m and two, if a sharp temperature gradient exists within this layer, then that particular depth is considered as MLD. Here the depth of temperature at 10m minus $1^{o}C$ is determined as

$$D_{10}\text{-}1 = D_2 + [(T_2\text{-}(T_{10}\text{-}1))/(T_2\text{-}T_3) * (D_3\text{-} D_2)] \qquad (1.9)$$

where, D_2 and D_3 are the depth where the temperature is more and less than $T_{10}\text{-}1^{o}$ C , T_2 and T_3 are the temperature at depths D_2 and D_3 respectively. Then MLD is determined as

$$MLD = (D_m + D_m\text{-}1)/2 \qquad (1.10)$$

where, D_m is the depth at which the gradient is more than $0.08^{o}C/m$ and D_m-1 is the depth where the gradient is less than $0.08^{o}C/m$.

For the MONSOON-77 and MONEX-79 period, the temperature profiles have been plotted and the MLD obtained from the plots have been compared with other methods. Details described in chapter-II. The standard error of estimate (SEE) is computed as

$$SEE = \sqrt{\frac{\sum_{i=1}^{n}(x_i - \bar{x})^2}{n}} \qquad (1.11)$$

where, x_i is the difference between graph value and that obtained from each methods, $\bar{x}$ is the mean of this difference and n is the number of stations taken for each seasons.

Estimation of oceanic heat content

Heat content of the mixed layer and of the different layers of 50m thickness upto a depth of 200m have been estimated as

$$HC = \rho_w C_p \int_{D_1}^{D_2} T_z \, dz \qquad (1.12)$$

where, ρ_w is the water density, T_z average temperature of the two layers, dz the difference in depth, D_1 and D_2 are the upper and lower depth limit of each layers. The factor C_p is taken to be $0.977 cal/cm^2/^oK$ following Bathen (1971) which is equal to $4.1*10$ $J/M^2/^oK$.

Estimation of heat storage change

The average heat content of the mixed layer and the total heat content of the 0-200m layer are evaluated on a seasonal basis using equation (1.12). Then the seasonal heat storage change (Q_t) is given by

$$Q_t = [HC_{n+1} - HC_{n-1}] / dt \qquad (1.13)$$

where, H_{Cn+1} and HC_{n-1} are the heat stored in the succeeding and preceding seasons and dt is the time difference between preceding and succeeding months. Hastenrath and Merle (1986) and Levitus (1987) also adopted this method. The heat advection has been estimated as the heat storage change minus the surface heat gain/loss.

Estimation of Cyclone heat potential from ship data (CHP_{28})

The CHP_{28} is estimated as the heat content over 28°C isotherm from

$$CHP_{28} = \rho_w C_p \int_0^D T_z \, dz \qquad (1.14)$$

where D is the depth of 28°C isotherm and the other parameters are same as in eqn(1.12). The 28°C isotherm is chosen as most of the tropical cyclones are formed when SST > 26°C (Rao,1987,b).

Estimation of CHP_{28} from satellite data

In order to estimate CHP_{28} from satellite derived values of SST and wind speed, a regression analysis has been carried out between values of CHP_{28} estimated from eqn. (1.14), the NOAA satellite derived SST corrected for water vapour and the GOES satellite derived cloud motion vector winds extrapolated to the surface.

GOES satellite derived 900mb cloud motion vector winds were extrapolated to the surface using the relation adopted by Wylie and Hinton (1982) given by

$$V = 0.72\ Wc + 1.2 \qquad (1.15)$$

where, V is the surface wind speed and Wc is the wind speed derived from cloud motion at the 900m level in m/s. The accuracy of wind speed using this method is about 2.6m/s.

The SST values obtained as finished products from NOAA differ on an average, by 1.5°C from the in-situ bucket temperature (Pathak, 1982). The difference in SST and the total water vapour content are empirically related as

$$T_S = T_{sat} + 0.13 * W - 5.1 \qquad (1.16)$$

where, T_S is the corrected SST, T_{sat} is the SST derived from NOAA before applying this correction and W is the water vapour content of the atmosphere in millimeters of perceptible water (Pathak,1982).

Cyclone heat potential is estimated from the following regression equation (Dhoulath et al,1990) which is of the form

$$CHP_{28} = A + B*V + C*T_S \qquad (1.17)$$

where, A= -0.5030, B = 120.22, C = 6988.88, V is the wind speed extrapolated to the surface from cloud motion vector winds, T_S is the satellite derived SST corrected for water vapour.

The regression formula developed in the present study is based on 466 data points (using hydrographic data) with an R.M.S difference of ±8% for the range of 6.3 to $6.7*10^8 J/M^2$ and a correlation coefficient equal to 0.968. This regression equation has been used to compute CHP_{28} using satellite observations of

SST and wind speed over Bay of BengalOwing to the lack of simultaneous observations of satellite and ship, CHP_{28} obtained from satellite observations were compared at nine points only. The comparison table is presented in Chapter-III.

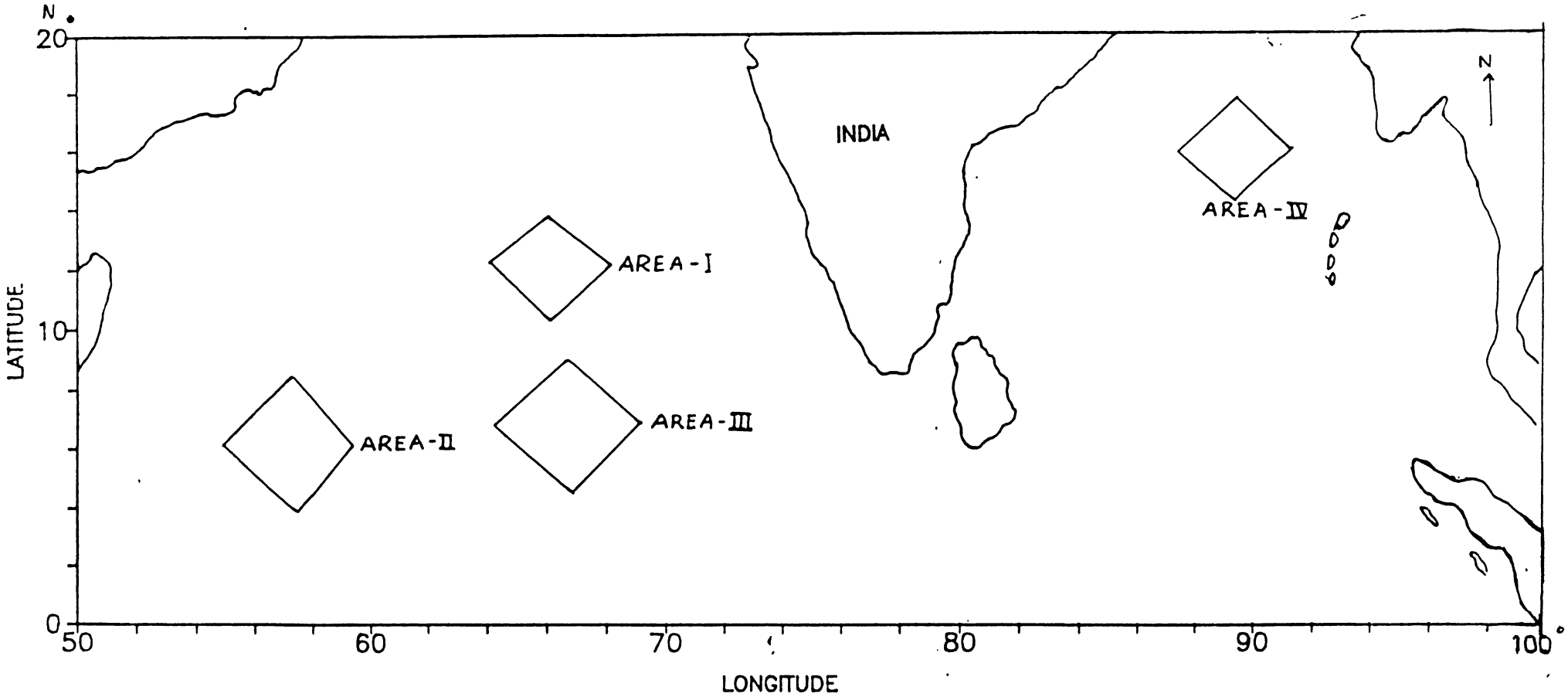

Fig.1.1 Area of study and the polygon positions

CHAPTER - II

MIXED LAYER DEPTH

2.1 Introduction

This chapter deals with the estimation and comparison of MLD by different methods and selecting an appropriate method needed for the present study. Variations of MLD during four seasons (Pre-monsoon, Monsoon, Post-monsoo and Winter season) are discussed in detail using the temperature climatology of Levitus (1982) and the seasonal averages during 1977-1986.

MLD is defined as the layer where temperature remains almost uniform. Below this layer a sharp negative temperature gradient exists which is called as thermocline. MLD extends approximately upto the upper 100-150m layer within which the interaction of the atmosphere with the ocean has been mainly confined. .Due to the effect of wind stress and heat exchange at the ocean surface, turbulent mixing takes place which results in an almost uniform temperature in surface layer. This surface layer absorbs most of the solar energy incident at the ocean surface and contains the momentum impatred by the wind stress and hence acting as a buffer modifying the energy exchanges between the atmosphere and the deeper layers. Most of the seasonal heat storage are confined to this layer and therefore many short-term and seasonal anomalies can be explained by the variations in the mixed layer depth. The atmosphere derives back an immense amount of energy from the mixed layer in the form of ocean heat

potential, thereby significantly influencing the weather and climate. Convergences and divergences associated with the mixed layer lead to modification of the circulation patterns in deeper layers (Pond and Pickard,1983). Over the Indian Ocean, where seasonal wind reversal occurs, MLD and its variations are important tool for the monsoon weather forecast. The surface mixed layer can be easily identified from the vertical temperature structure of the ocean, which will have an isothermal part in the top layers.

2.2.Factors influencing MLD

The factors controlling MLD are heat exchange at the surface, mixing by wind stress, convection, vertical and horizontal advection and internal oscillations.

For periods from few hrs to a month, the vertical one-dimensional processes of heat and momentum transfer at the ocean surface control the vertical structure of temperature and MLD (Niiler and Kraus,1977). Over longer periods, horizontal processes due to advection are equally important, as the poleward transport of heat by currents is to be taken in to account (Pond and Pickard,1983).

Increase in MLD and decrease in sea surface temperature (SST) are related to high wind speed and upward heat flux and, conversely, decrease in MLD is related to low wind speed and downward heat flux (Elsberry and Camp, 1978, Elsberry and Raney, 1978).

When there is heat input to the surface, an increasing stabilizing density gradient inhibits mixing. When there is net cooling at night in winter, convection extends to the mixed layer entraining cooler water from below (Mc Alister and Mc Leish).

2.3 Estimation of MLD

In view of the importance of MLD in the ocean atmosphere interaction, many investigators have developed different techniques to determine MLD. It is rather difficult to make a rational selection of the most appropriate one among these techniques. The available methods are reviewed below.

Method-1(a)

Rao and Rao (1986) defined MLD as the depth at which the sub-surface temperature is 0.2^{o} C colder than the surface temperature.

$$MLD = D_2 + ([T_2 - (T_s - 0.2)] / (T_2 - T_3)) * (D_3 - D_2) \qquad (2.1)$$

where T_s is the surface temperature D_2 and D_3 are the depths where the temperature is higher and lower than $T_s - 0.2^{o}C$, T_2 and T_3 are the temperatures at the respective depths D_2 and D_3. In case, if the temperature gradient falls on a particular measured depth, then that depth is considered as MLD. Since 0.2^{o} C is a small difference, this method may underestimate the MLD.

Method-1(b)

The above method is repeated for the gradient Ts-o.5^{o}C. Here the MLD is computed as

$$MLD = D_2 + ([T_2-(T_s -0.5)]/ (T_2-T_3)) * (D_3-D_2) \qquad (2.2)$$

where, T_s-0.5 is the temperature where it is less than 0.5^{o}C from the surface, D_2 and D_3 are the depths where the tempeartue is higher and lower than T_s-0.5, T_2 and T_3 are the temperatures at depths D_2 and D_3 respectively. Some times there may be error in the measurement of surface temperature. In such cases, the MLD obtained by this method will not be accurate.

Method-1(c)

MLD has also been defined as the depth at which the temperature is 1^{o} C lower than the surface temperature (Rao et al,1983). MLD is given by

$$MLD = D_2 + ([T_2-(T_s-1)]/ (T_2-T_3)) * (D_3 -D_2) \qquad (2.3)$$

where T_s-1 is the temperature which is less than at the surface, D_2 and D_3 are the depths where the temperature is higher and lower than T_s-1^{o} C. T_2 and T_3 are the temperatures at depths D_2 and D_3 respectively. This method also yields a wrong estimation of MLD when there may be some error in the measurement of SST.

Method-2

Ostapoff and Wortherm (1974) defined MLD as the depth at which the temperature is lower by 1^{o} C than the temperature at 10m depth and this method was followed by Rao et al,(1981). In this method MLD is estimated as

$$MLD = D_2 + ([T_2-(T_{10}-1)]/ (T_2-T_3)) * (D_3 -D_2) \qquad (2.4)$$

Where, T_{10}-1 is the Temperature a which is 1^{o} C less than at 10m depth . D_2 and D_3 are the depth where the temperature is higher and lower than T_{10}-1^{o}C, T_2 and T_3 are the temperatures at D_2 and D_3 respectively. Since by definition, a maximum variation of only 1^{o} C can be tolerated within the mixed layer, this method overestimates MLD.

Method-3 (Gradient method, Ali et al,1987)

MLD can also be determined using temperature gradient (Ali et al,1987). Some times the gradient check is satisfied very close to the surface, yielding unduly small MLD. Here the depth at which the temperature is lower by 1^{o} C less than at the 10m is first estimated. Then from this point the gradient is checked towards surface where the gradient is lower than 0.08^{o}C/m. Then MLD is determined as the mean depth of this layer and the last layer with temperature gradient greater than 0.08^{o}C /m. If the first layer fails the check, then the mean of first checked layer and the next deeper level is taken as the MLD. From method-2 the depth of T_{10}-1^{o}C is first determined. Then MLD is estimated as

$$MLD = (D_m + D_m - 1) / 2 \qquad (2.5)$$

where, D_m is the depth where the gradient is greater than $0.08^{o}C/m$ and D_m-1 is the depth where it is less than $0.08^{o}C/m$. The gradient is checked using a computer programme.

The accurate method of obtaining MLD is by plotting the depth-temperature profile graph and thereby determining the depth of isothermal layer (fig 2.1 to 2.4). Since this is a time consuming method to determine MLD of many profiles for a longer period, a comparison has been made between the MLD obtained by plotting the graph and the one obtained by all the above methods. Table (2.1 to 2.4) gives the comparison of MLD for different methods. In this section, MLD is estimated using all the above methods for different seasons and locations. The study has been carried out for pre-monsoon, monsoon, post-monsoon and winter seasons over the northern Indian Ocean. Considering the MLD values obtained from the graph as standard, the difference in MLD between the standard value and that obtained from the individual method is found out. The SEE is compared for each of this difference.

2.4. Comparison of MLD

Fig (2.1 to 2.4) shows the depth -temperature graph for the pre-monsoon, monsoon, post-monsoon and winter seasons in the Arabian Sea and Bay of Bengal. The numbers indicated in the graph represents the location, and MLD values using different methods are given in Table.2.1 to 2.4.

MLD values obtained using method 1(a) are found to be mostly less than the graph values. In the case of graphs 1,2 and 5 in fig (2.2), and graph 5 in fig (2.4), there have been much difference in MLD values because the temperature gradient is more in the top few meters followed by a homogeneous layer up to a depth of 50-100 m. Similar variations were observed during other seasons also, (graph 3 & 4, fig,2.3; graph 3 & 6, fig 2.1). The SEE obtained using this method gives a very high value between 10 to 35 compared to other methods.

Eventhough method 1(b) yields MLD values almost nearer to the graph values in some cases, it fails in majority of the cases. The SEE for this method does not give consistent values during most of the seasons. However, during monsoon season, MLD obtained using this method is comparable with graph values.

MLD obtained by method 1(c) gives higher values during most of the seasons. The SEE for this method is less than other methods and more or less nearer to that of method (3) during monsoon season.

Results of MLD obtained by method-2 gives much higher values than the earlier methods.

MLD values almost nearer to the graph values are provided by the gradient method (method 3). The SEE for all seasons are found to be the lowest compared to the earlier methods excepting during monsoon season (Table.2.2).

Table.2.1.(a) MLD values obtained using different methods in the Arabian Sea during pre-monsoon season.

S.No	Latitude ^{o} N	Longitude ^{o} E	Graph	MLD values in metres 1(a)	1(b)	1(c)	2	3
1	8	63	19	23.5	26	39	30	24.5
2	8	71	23	17	24.5	31.5	33	25.1
3	13	62	21	06	16.5	23	23.5	21.8
4	11	70	75	53	70	77	76	74
5	15	69	100	52	62	77	77	65
6	15	72	99	04	15	98	103.5	97.2

Table 2.1(b) Standard Error of Estimate for different methods

S.No	Difference from the graph 1(a)	1(b)	1(c)	2	3	$(x-x)^2$ 1(a)	1(b)	1(c)	2	3
1	+4.5	+7	+20	+11	+5.5	462.2	110.2	134.6	11.56	8.42
2	-6	+1.5	+8.5	+10	+2.1	361	256	0.01	5.76	0.25
3	-15	-5.5	+2	+2.5	+0.8	100	144	41	26	3.24
4	-22	-5	+2	+1	-1	9	156	41	43	2.5
5	-48	-2	+17	+17	+5	289	240	74	88.4	5.7
6	-95	-84	-1	+4.5	-1.8	4900	4422	55	9.6	.64
				SEE		31.9	23.7	7.58	5.5	1.9

Table 2.2.(a) MLD values obtained using different methods in Arabian Sea (monsoon season)

S.No	Latitude °N	Longitude °E	MLD Graph	values in metres 1(a)	1(b)	1(c)	2	3
1	12 20′	73 20′	24	7	28	34	42	31
2	12 16′	73 22′	32	6	33	38	43	34
3	2	77 52′	51	52	55	58	58	54
4	10 27′	66 13′	71	60	74	79	82	73.5
5	15	68	78	48	81	84	85	82.5
6	12 36′	64	76.5	78	84	90	90.5	86.5
7	10 24′	66	103	90	109	117.5	118	108.3
8	7 10′	77 25′	32	25	41	53	55	43.2

Table 2.2(b) Standard Error of Estimate for different methods

	Difference from the graph					$(x-x)^2$				
S.No	1(a)	1(b)	1(c)	2	3	1(a)	1(b)	1(c)	2	3
1	-14	+4	+10	+18	+7	1	0.5	0.5	23	0.5
2	-26	+1	+6	+11	+2	169	13.7	22	4.8	13.7
3	+1	+4	+7	+7	+3	144	0.5	13.7	38.4	0.5
4	-11	+3	+8	+11	+2.5	4	2.8	7.3	4.8	2.9
5	-30	+3	+6	+7	+4.5	289	2.9	22	38.4	2.89
6	+1.5	+7.5	+13.5	+14	+10	132	7.8	7.8	0.6	7.8
7	-13	+6	+14.5	+15	+5.3	0	1.69	14.4	3.24	1.69
8	-7	+9	+21	+23	+11.2	36	18.5	106	96	18.5
				SEE		9.8	2.5	4.9	5.1	3.3

Table.2.3. MLD values obtained using different methods in Bay of Bengal (post-monsoon season)

S.No	Latitude ^{o} N	Longitude ^{o} E	Graph	MLD values in metres 1 (a)	1 (b)	1 (c)	2	3
1	8 08'	93 1'	17.5	11.5	19.1	25	28.5	19.5
2	12	68	26.5	24	30	35.6	35.6	30.5
3	17 30'	89'	30	32	35.1	38.2	38	31.6
4	17 32'	89 35'	37.2	08	41	44	46.5	38.8
5	17 06'	88	39.5	42	49	51	52.6	43.8
6	19 07'	89	48.5	10.5	50	54	57	50.2
7	14 05'	88 02'	54.5	13.5	61.5	64	66.1	60.5

Table. 2.3.(b) Standard Error of Estimate for different methods

	Difference from the graph					$(x-x)^2$				
S.No	1(a)	1(b)	1(c)	2	3	1(a)	1(b)	1(c)	2	3
1	-6	+1.6	+7.5	+11	+2	123.2	9	0.01	1	1
2	-2.5	+3.5	+9.1	+9.1	+4	213.2	1.2	2.25	0.81	1
3	+2	+5	+8	+8	+1.6	228	0.16	0.16	4	1.96
4	-29	+4	+7	+9.5	+1.8	141.6	0.36	0.36	0.25	1.44
5	+2.5	+9.5	+10.5	+13.1	+4.3	213.2	24	8.41	9.61	1.69
6	-38	+1.5	+5.5	+8.5	+1.7	436.8	9.61	4.41	2.25	1.69
7	-41	+7.5	+9.5	+11.6	+6	517.2	8.4	3.6	2.56	9
				SEE		16.6	2.7	1.6	1.7	1.5

Table. 2.4.(a) MLD values obtained using different methods in Arabian Sea (winter season)

S.No	Latitude ^{o} N	Longitude ^{o} E	Graph	MLD values in metres 1(a)	1(b)	1(c)	2	3
1	15	73	19	16	19.5	21.5	21.5	20
2	15	72 30'	22	14	21.5	23	22.5	21.8
3	15	60 2'	56	38	57	61.5	62	58
4	15	60 12'	56	41	57	63	62.5	58.5
5	12	74	58	6	11	61	63	59

Table 2.4(b) Standard Error of Estimate for different methods

S.No	Difference from the graph 1(a)	1(b)	1(c)	2	3	$(x-x)^2$ 1(a)	1(b)	1(c)	2	3
1	-3	+0.5	+2.5	+2.5	+1	262	83	1.7	0.04	0.1
2	-8	-0.5	+1	+0.5	-2	125	83	7.84	3.2	1.2
3	-18	+1	+5.5	+6	+2	1.4	74	2.9	13.7	0.5
4	-15	+1	+7	+6.5	+2.5	17.6	74	10	17.6	1.4
5	-52	-47	+3	+5	+1	1076	1398	0.6	7.3	0.1
				SEE		17.2	18.5	1.8	2.8	0.9

After comparing the different methods to estimate MLD, it has been found the the gradient method gives MLD values comparable to the actual graph value. Hence in the present study, the gradient method is adopted for the estimation of MLD.

2.5 MLD Variations

The day time heating of the surface layers increases the negative temperature gradient in the upper layers and results in the decrease of MLD. In the night the surface layer gets cooled due to the reduction in solar radiation making the surface layer isothermal to a greater depth (La Fond,1966).

During winter MLD is deeper when the sea loses heat to the atmosphere except in areas near current boundaries. The net heat gain during summer causes shallow seasonal thermocline and low MLD. Over the Indian Ocean this pattern, is however, disturbed by the reversing monsoonal winds and currents modifying the divergence and convergence patterns.

In view of the importance of mixed layer depth on weather and climate related studies, the variations of MLD over the Indian Ocean during different seasons namely Pre-monsoon (Feb-April), Monsoon (May-July), Post-monsoon (Aug- Oct), Winter (Nov-Jan) seasons have been studied using the seasonal averages during 1977-1986. Though the monsoon season is from May-september, these months have been selected because of the limitations of Levitus (1982) data. The short-term variations of MLD over the four polygon areas (Ref. fig.1.1) during MONSOON-77

and MONEX-79 were also been analysed. Climatic data of temperature profile from Levitus (1982) were utilized in order to compare the variations in MLD obtained during 1977-1986 for different seasons. As the mixed layer heat budget governs the evolution of SST (Rao.1987,b), seasonal variations of SST are also taken in to account.

2.5.1 Climatic variation of MLD (from Levitus's temperature climatology,1982)

Fig (2.5) shows the distribution of MLD in the northern Indian Ocean during pre-monsoon season. Maximum MLD of 60m is noticed around 10^{o} N, 85^{o} E and low values of around 35m in the western Arabian Sea and in the south western Bay of Bengal. This is due to high SST observed in this region (fig.2.9). In the south western Arabian Sea, the contours are closely spaced. Less variations in MLD are observed in the northern Arabian Sea while Bay of Bengal shows large variations which shows that the zonal variations in MLD are very sharp in this region due to strong upwelling.

During the monsoon season (fig.2.6), MLD shows an increase from west to east very near to the equator. The maximum MLD observed over Bay of Bengal during the previous season is found to have shifted towards the equator with an increase of 15m. The area of maximum MLD during pre-monsoon season has been replaced by minimum MLD (25m) in this season probably due to vertical mixing caused by strong monsoon winds. Much variations in MLD are observed south of the Indian continent. Compared to the pre-

monsoon season, MLD shows a general decrease except around 10^{o} N, 90^{o} E where, it has increased by about 10m. An increase of 15m is also noticed at 0^{o}, 88^{o} E.

Fig (2.7) shows the distribution of MLD during the post-monsoon season. Maximum MLD of 75m is seen around 5^{o} N,60^{o} E. Generally MLD decreases towards north except near the central Arabian Sea where, a slight increase is found. Minimum MLD is observed around 20^{o} N,64^{o} E because of comparatively high SST. Higher MLD values have been noticed during this period than the monsoon period. In the Arabian Sea much variations in MLD are noticed compared to Bay of Bengal.

During the winter season, MLD is deep about 70m observed around 5^{o} N, 95^{o} E. MLD varies between 30- 50m in the Arabian Sea and between 30-70m in the Bay of Bengal (fig.2.8). In the western Indian Ocean MLD increases in all direction from 10^{o} N,60^{o} E. In the north equatorial Indian Ocean MLD increases from west to east which was in the reverse direction during post-monsoon period could be due to the reversal in northeast trade winds.

2.5.2 Climatic variations of SST (from Levitus's temperature climatology,1982)

Fig (2.9) shows the distribution of SST during pre-monsoon season. It is seen that in the northern Indian Ocean SST varies from a minimum of 30^{o}C at 15^{o} N, 81^{o} E to a maximum of 25^{o} C at 19^{o} N,71^{o} E. Maximum SST in the western Arabian Sea almost coincides with minimum MLD and vice-versa. SST variations during

the monsoon period show maximum value of 30^{o} C in the area of minimum MLD in the Arabian Sea (fig.2.10). However the minimum SST of 28^{o} C in Arabian Sea does not corresponds to maximum MLD. Variations in SST are more in the western and eastern parts with uniform SST values in the intermediate region. The minimum MLD observed around 0^{o} , 80^{o} E corresponds to a surface temperature of 28.5^{o} C. MLD values showed much variations in the souther Bay of Bengal without corresponding variations in SST.

During post-monsoon period, SST shows a regular increase towards east and north from 10^{o} N,54^{o} E (fig 2.11). The minimum MLD of 40m around 19^{o} N,60^{o} E coincides with an SST of 28^{o} C. The minimum SST of 24^{o} C at 10^{o} N, 54^{o} E corresponds to maximum MLD.

Distribution of SST in the winter season (fig 2.12) shows a minimum SST of 25^{o} C in northeastern Bay of Bengal, which corresponds to maximum MLD value. Minimum MLD of 30m at 10^{o} N,98^{o} E coincides with an SST of 28^{o} C . Another minimum SST 26.5^{o} C is observed around 10^{o} N, 90^{o} E which does not corresponds to maximum MLD. In the Arabian Sea SST shows an increasing trend towards east while in Bay of Bengal, it increased towards southwest. However MLD does not a regular pattern in Arabian Sea, though in Bay of Bengal it gradually decreased to east and increased to north and south from 10^{o} N,90^{o} E.

2.5.3. Variation of MLD during the period 1977-1986

Spatial distribution of seasonal averages of MLD for the pre-monsoon season is shown on Fig (2.13). During this season

sufficient data was not available over Bay of Bengal. So the study has been carried out for Arabian Sea only. Low MLD value of 25m is observed west of 60^{o} E. The variations in MLD show a regular increase towards northeast reaching a maximum of 65m around 16^{o} N,72^{o} E. Considerable variations are observed along 9-15^{o} N,67-72^{o} E where, the MLD increases rapidly towards north. During the monsoon period, minimum MLD observed in the previous season has been replaced by seasonal maximum of about 120m in the central part of the southern Arabian Sea (fig.2.14). Unlike the pre-monsoon season, MLD increases towards east up to 61^{o} E thereafter it shows a decrease. Maximum MLD of 130m is observed in south western Arabian Sea. Lowest MLD is seen in the western Arabian Sea. Comparatively shallow MLD is observed in Bay of Bengal than in the Arabian Sea. During post-monsoon season, mixed layer is deep in the western Arabian Sea with small pockets of alternate lower MLD (fig.2.15). Subsequently, MLD decreases both towards north and east reaching a minimum value of 30m near south west coast of India. In the eastern parts of Bay of Bengal, shallow MLD prevails. Large variations in MLD are observed in the western Arabian Sea. During winter season, the picture is drastically different in the western Arabian Sea (fig.2.16). The minimum value of 30m is seen just near the area where maximum MLD was reached for the previous season. During this season also higher MLD values are observed in the western Arabian Sea. The minimum MLD of 30 m is observed around 15^{o} N,71^{o} E. In the Bay of Bengal, maximum value of 70 m is seen near the central Bay from where, the MLD decreases in all directions.

2.5.4. Variation of SST during 1977-1986

The distribution of SST for the pre-monsoon season is depicted in fig (2.17). Maximum SST of 31^{o} C is seen near the southwest coast of India coinciding almost with minimum MLD of 30m. Maximum MLD almost coincides with area of minimum SST off the central west coast of India. Lowest MLD values in this season corresponds to an SST of 29.5^{o} C around 11^{o} N, 62^{o} E. In general, SST decreases towards north . In the north equatorial Indian Ocean, SST increases towards east. During the monsoon season, a cooling of 3.8^{o} C in SST is noticed compared to the previous period in the western Arabian Sea (fig.2.18). Maximum SST of 30^{o}C is seen near the western coast of India. Along the eastern boundary of Arabian Sea SST increases towards north and south from a minimum of 27^{o} C at 11^{o} N. In the Bay of Bengal, SST exhibits alternately warm and cold waters extending from the shore towards offshore coinciding with corresponding shallow and deep MLD.

The low SST during monsoon period continues in the post-monsoon period also with increased cooling of 0.7^{o} C in the western Arabian Sea (fig.2.19). From this region, SST increases towards east from a minimum of about 24^{o} C in the western Arabian Sea to a maximum of 29^{o} C in the coastal waters off the southwest coast of India. In the Bay of Bengal SST further decreases towards east reaching about 29^{o} C in the mid Bay. These SST variations are reflected in the corresponding variations in MLD.

Maximum SST of 31^{o} C is seen near the Madras coast and minimum of around 24^{o}C in the westerb Arabian Sea . Minimum MLD is seen around 8^{o} N, 71^{o} E for a comparatively higher SST of 30^{o} C . The general trend in SST is an increase towards east and north. Large variations are seen in the Arabian Sea compared to Bay of Bengal. During the winter season lowest SST of 26^{o} C is recorded near northern Arabian Sea which corresponds to maximum MLD area (fig.2.20). Variations in SST show an increase towards east in the Arabian Sea reaching a maximum of 29.5^{o} C around 12^{o} N,71^{o} E. The minimum SST in Bay of Bengal corresponds to a comparatively deeper MLD of 65m off the central east coast of India.

2.5.5. Daily variations of MLD and SST

During MONSOON 77 in area I the observations are taken for two phases ie, phase-I 6-20 June, phase-II 30 June- 15 July.

Daily average values of MLD for the polygon areas shown in fig (1.1) were analysed. Fig (2.21,a) shows the daily variations in MLD and SST in Area-I during 6-20 June 1977 (phase-I). SST shows a decrease of 0.7^{o} C from 6-11 June. It again decreases by 1.7^{o} C reaching 28.8^{o} C on 20 June. The corresponding MLD shows an Increasing trend throughout this period. Maximum MLD of 60 m is noticed on 11 June.

During 30 June to 6 July (phase-II), SST decreases from 27.9^{o} C to 27.5^{o} C and then increases to a maximum of 28.2^{o} C on 10 July (fig.2.21,b). After 10 July, it shows a gentle decrease to 27.8^{o}C on 15th July. During this period, MLD shows gradual

decrease of 12m from 30 June to 9 July. After this MLD decreases to a minimum value of 55m on 10 July and subsequently increased rapidly up to 15 july.

Fig (2.22) shows the daily variations of MLD and SST in the polygon area II,III and IV during May- July 1979. In area II, SST shows values over 30^{o}C during May (fig.2.22,a). An increase in SST of 0.3^{o}C is noticed from 17-22 May. MLD shows a slight decrease of about 6m during 16-22 May.

In area-III, maximum SST of 30^{o} C is seen during 4-5 June and then it decrease up to 10th June reaching a value of 29.8^{o}C (fig.2.22,b). During this period MLD decreases by about 4m from 2nd to 3rd and increases by 4m on the next day. Subsequently, MLD shows a decrease of 14m during 4-8 June followed by an increase of 16m up to 10 th June.

During July, SST varies between a minimum of 29.6^{o} C and a maximum of 30.5^{o} C in Bay of Bengal (fig.2.22,c). MLD shows much variations in Bay of Bengal during 10-22 July. MLD increases from 37m on 10th to 60m on 12th July. This is followed by a decrease of 32m and a sudden increase of 33m between 16th-18th July. Subsequently, MLD increases by 18m on 22nd July.

2.5.6. Equatorial MLD slope

The behavior of equatorial Indian Ocean during the monsoon period is mainly controlled by the wind stress distribution. Reversal of mixed layer slope after the onset of monsoon as one

aspect of this response. Observational evidences are available on this response with periods ranging from few days (Wunch and Gill,1976; Weisberg et al,1980), to several months (Wunch,1978). The seasonal variability in the east-west slope of the tropical thermocline appears to be in phase with changes in the zonal wind stress. When the trade winds are strongest, the tilt of thermocline is the maximum and vice versa. In the transition between the monsoons, westerly winds appear along the equator with associated eastward oceanic jet. This leads to rise in the sea level and a simultaneous depression in the thermocline off Sumatra (Wyrtki,1973).

Polousky and Shapiro (1983) observed eastward flow in the top 100m water column from 26th April to 19th May at 61^{O} E along the equator. Nearly after two months, the flow reversed towards west in the upper 55m during 13th July-2nd August 1980 at the same location. Ali et al,(1987) studied the vertical motion of the thermocline in the equatorial Indian Ocean using MONEX-79 data and concluded that the thermocline displacements are associated with jet like surface response of the equatorial Indian Ocean to the zonal wind stress during the onset of monsoon. Due to strong seasonal variability in the wind stress over the equatorial Indian Ocean, the corresponding oceanic responses are expected to differ in the east-west direction (Hastenrath and Lamb, 1979,a). During the summer monsoon, western equatorial Indian Ocean experiences stronger wind stress compared to central or eastern equatorial Indian Ocean. Accordingly, the

upper oceanic response is distinct in the western equatorial Indian Ocean.

In order to understand the zonal variations of MLD in the equatorial Indian Ocean, vertical temperature sections are drawn during different phases of summer monsoon using MONSOON-77 and MONEX-79 hydrocast data for the region between 5^{o} N-2^{o} S, 50-95^{o}E. Fig (2.23 to 2.24) shows the vertical section of temperature from May-July 1977. During May 26-31st, MLD varied between 40m at 90^{o} E to 65m at 86^{o} E. (fig.2.23). MLD shows a decreasing trend from west to east with almost steady value up to 8^{o}E. MLD shows a gentle increase between 82^{o} and 85^{o} E. The corresponding SST shows lower values ($<29^{o}$ C)in this region. Isotherms are closely spaced between 100-150m indicating thermocline of high temperature gradient. In this depth isotherms exhibit a wavy pattern.

During 1-4th June 1977, the MLD decreased sharply by about 10m from west to east and after that it becomes deeper with an increase of 26m towards east (fig.2.24). In general MLD is deepened by 18m over 8^{o} longitude from west to east during this period. The SST also shows an increase of 0.35^{o} C from west to east. The vertical oscillations of isotherms are not prominent in this period. Thermocline extends from about 60-150m. Beyond 72^{o}E, isotherms show a regular descending tendency throughout the 200m column may be because of descend of warm sueface water.

After the monsoon onset , during July 1977, MLD shows a rapid decrease from west to east which is opposite to what

occurred in May. MLD decreased from 72m at 73°E to 40m at 76°E and subsequently, shows a mild decrease of 6m at 77°E. During this period SST also decreased in the same direction. Throughout the 200m column, all the isotherms are sloping upward up to 76°E and descend slightly afterwards. Eventhough SST is low in the eastern side, shoaling of MLD is noticed in this region. Hence it is clear that the thermohaline processes in the equatorial Indian Ocean can not be explained on the basis of SST alone but, are controlled by surface wind stress also. Using ERS-1 wind stress data with simultaneous temperature profiles, this phenomena can be better studied.

Fig (2.25) shows the vertical thermal section during 25-31 May 15-23rd and 27-30th June 1979. It is seen that, in May, MLD becomes shallow by about 10m from 50-55°E. A sharp increase in MLD is noticed between 55-57°E and afterwards it decreases towards east to a minimum of 60m at 66°E. In general, MLD shows a decrease from west to east. During this period SST increases in the same direction with maximum at 67°E.

After a fifteen days period, the slope of MLD has been reversed. MLD increased by 12m in the west compared to May. Almost uniform MLD is observed till 71° E afterwards increases by 22m towards east. SST decreases by 0.25 c from 68° E and afterwards the cooling is more about 0.6° C . MLD shows a wavy pattern during 27-30 June 1979 (fig.2.25). By this time MLD decreases by 10m between 85° and 87° E and shows a sudden increase of 26m towards east. The overall increase in MLD is 14m

during this period. A cooling of 0.5^{o} C is also noticed during 27-30th June.

2.7. Discussion

In the foregoing sections a comparison of the estimation of MLD using different methods were presented. Variations of MLD and SST using the temperature climatology of Levitus (1982) and the seasonal averages during 1977-1986, the daily variations of MLD and SST and the reversal of equatorial mixed layer slope during 1977 and 1979 were also presented in the earlier sections. It was found that the MLD values provided by the gradient method gave sufficient accuracy.

During pre-monsoon season, the mixed layer is comparatively shallow on the western side while, it is deeper towards the central Arabian Sea. Similar variations have earlier been obtained using the temperature climatology of (Levitus,1982). The zonal gradient in MLD is more near the southwestern Arabian Sea. MLD shows a gradual decrease from west to east in the equatorial Indian Ocean up to 80^{o} E. Ali and Desai (1989) observed a decrease in MLD from west to east in the equatorial Indian Ocean during May 1979. During monsoon season, contrary to the climatological variations of MLD obtained from Levitus (1982), zonal distribution of MLD in the equatorial Indian Ocean shows a slight decrease from west to east upto 65^{o}E and an increase towards east beyond 65^{o}E. These variations in MLD are accompanied by more or less reverse variations in SST. Sastry and D'souza (1970) have studied the nature and variations of the

thickness of mixed layer during summer monsoon and concluded that it is related more closely to the surface circulation than the wind distribution. In a numerical simulation of mixed layer, Camp and Elsberry (1978) indicated that large changes in SST are normally accompanied by changes in MLD. Ali (1990,b) suggested that the eastward increase of MLD is due to the piling up of water at the eastern end of the basin by wind forcing.

During post-monsoon season, maximum MLD of 120m is recorded near the southwest Arabian Sea and minimum of 40m in the northern Arabian Sea. During this season, Bay of Bengal shows comparatively shallower MLD than Arabian Sea . Using Levitus (1982) temperature climatology, an MLD of 75m is recorded in the western Arabian Sea and a minimum of 25m near the northern Arabian Sea. Small pockets of deep MLD areas with alternate low MLD are due to low SST and less mixing . During winter season, the magnitude of maximum and minimum values observed in both Arabian Sea and Bay of Bengal coincide with the Levitus (1982)

The horizontal distribution of SST during all the seasons suggest that, in most of the cases deep MLD corresponds to low surface temperature and shallow MLD to high SST. SST varies from 29.5^{o} C to 31^{o} C during pre-monsoon and a cooling of about 3^{o} C is noticed during monsoon season. High SST observed during post-monsoon season is a result of maximum surface heat gain as can be seen from Hastenrath and Lamb (1979,a). Simpson and Paulson (1980) related the shallowness of MLD to warmer sea surface temperature during monsoon months. Ramesh Babu et al, (1991)

noticed an average temperature rise of 0.5^{o} C mainly due to surface exchange processes in the central Arabian Sea during pre-monsoon months.

During monsoon season, net heat loss and vertical mixing associated with monsoonal winds result in surface cooling. MLD variations in Bay of Bengal during this season do not show any correspondence with SST variations. A mixed layer cooling of 2^{o}C is reported in the Arabian Sea and Bay of Bengal during southwest monsoon which is related to the prevailing meteorological conditions (Ramam et al,1979; Anjaneyulu,1980; Rao et al,1984; Joseph and Pillai,1986), heat losses from the sea and current shear (Rao et al, 1981 & 1983; Ramesh Babu and Sastry, 1984) and entrainment (Sastry and Ramesh Babu, 1985).

A cooling of less than 1^{o} C is found during the post-monsoon season. Temperature climatology of Levitus (1982) does not provide such marked cooling in SST during monsoon season, though a cooling of 2-3^{o} C is noticed during post-monsoon season. During winter, lowest SST of 26^{o} C is noticed in the eastern Arabian Sea and southwestern Bay of Bengal. In the climatological SST distribution, the minimum SST is about 25^{o} C in the eastern Arabian Sea less rate of cooling during winter season. Daily variations of SST and MLD were analysed during June-July 1977 and May- July 1979. It can be seen that, in Area-I, the daily variation of SST decreases throughout the period and MLD gradually decreases during the first phase. In the second phase, SST shows an increasing trend and the MLD decreases correspondingly. However, a cooling of 1^{o} C and MLD deepening of

16m are evident compared to the first phase. This cooling and deepening of mixed layer is a result of wind mixing due to the passage of a cyclonic storm (discussed in the next chapter). Camp and Elsberry (1978) reported mixed layer cooling and deepening caused by vertical mixing during the passage of storm. Rao (1987,a) observed a cooling of 1.3^{o} C and MLD deepening of 30m during June 1977. The deepening of MLD is also related to surface heat loss and downwelling on account of negative curl of wind stress favoring convergence within the layer (Rao,1987,b).

During 16-22nd May 1979, in Area-II, MLD does not exhibit marked variations with changes in SST . This could be due to intense mixing below the surface throughout the period. In the central Arabian Sea (Area-III), a deepening of 14m is observed during 2-10th June 1979. Wavy patterns in the variations in MLD during 10-23rd July 1979 over Bay of Bengal are mostly governed by the respective SST variations (Area-IV). Similar variations in SST and MLD are encountered in Bay of Bengal by Ramesh Babu and Sastry (1984) and Rao (1987,a).

Reversal of MLD slope after the onset of monsoon in the equatorial Indian Ocean is very important in the case of ocean currents. The vertical temperature sections during 26-31st May 1977 show a decrease of 20m in MLD over 14^{o} longitude from west to east. MLD slope reversal is observed with a decrease of 18m over 8^{o} longitude from east to west during 1-4 June 1977 in association with the wind reversal at the equator. Prominent deepening of MLD is clearly seen (about 22m over a longitude of

5^{o}) from west to east after onset during 19-23rd July 1977.

MLD slope reversal is also obvious in May-June associated with strong winds of monsoon onset 1979. During pre-onset (May 25-31st), the decrease in MLD from west to east amounts to 15m over a longitude of 16^{o}, and the increase from west to east during onset is 22m over 17^{o} longitude which diminishes by 8m within a longitude of 7^{o} in the end of June 1979. In the equatorial Indian Ocean, low SST does not always leads to deep MLD and high SST to shallow MLD. Thus, MLD variations in this region are not primarily controlled by surface temperature alone. Ali et al, (1987) have earlier reported reversal of the equatorial mixed layer slope during monsoon onset, the depth being more at east than in the west. Rao (1987,a) noticed similar eastward deepening of MLD in the eastern side of the polygon area in the central Arabian Sea and ascribed it to the initiation of upwelling at the eastern side. Ali and Desai (1989) observed mixed layer deepening towards east after the onset of monsoon and a decrease in heat content in the same direction in association with heat transport by the under current from west to east.

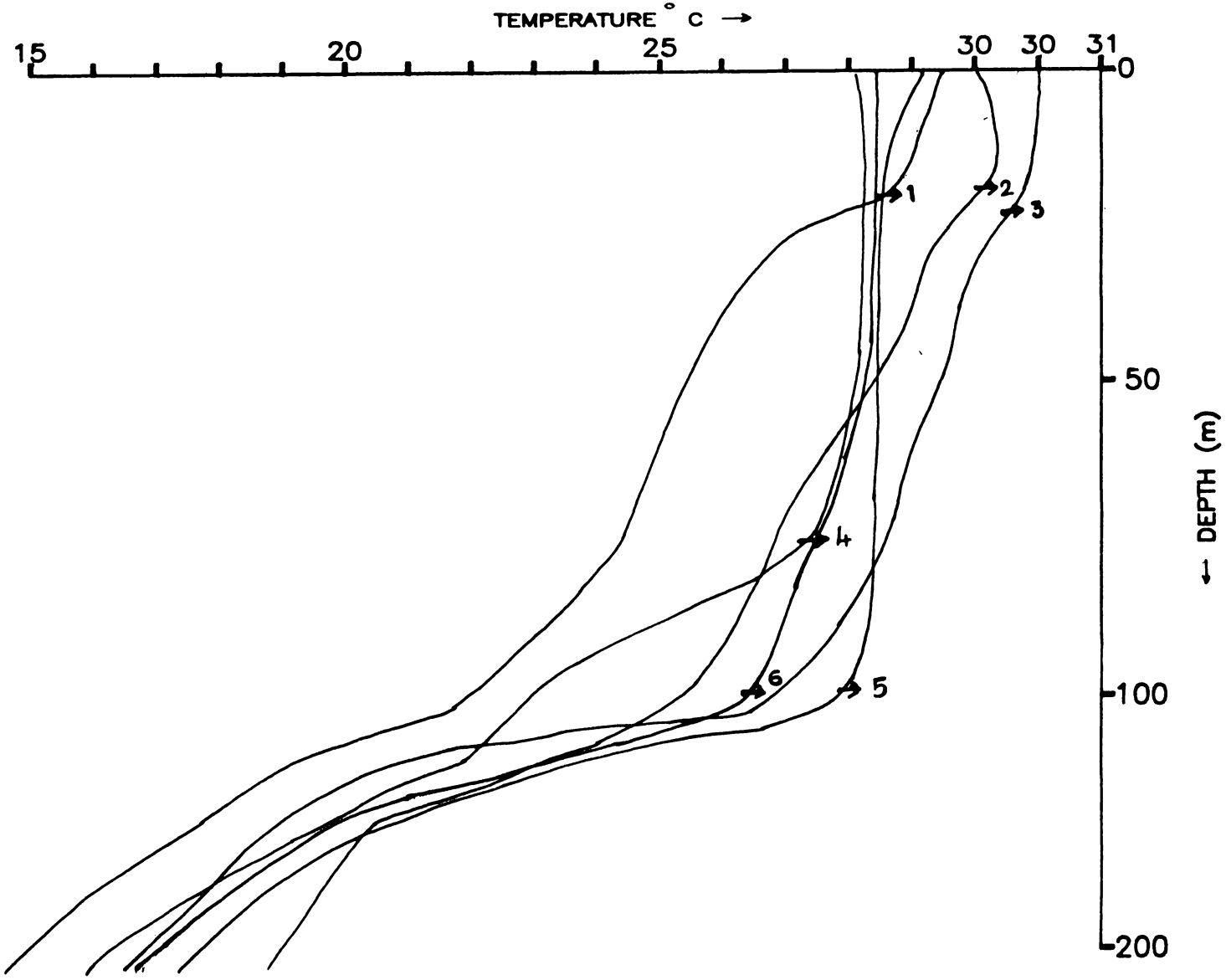

Fig.2.1 Temperature profiles during pre-monsoon season

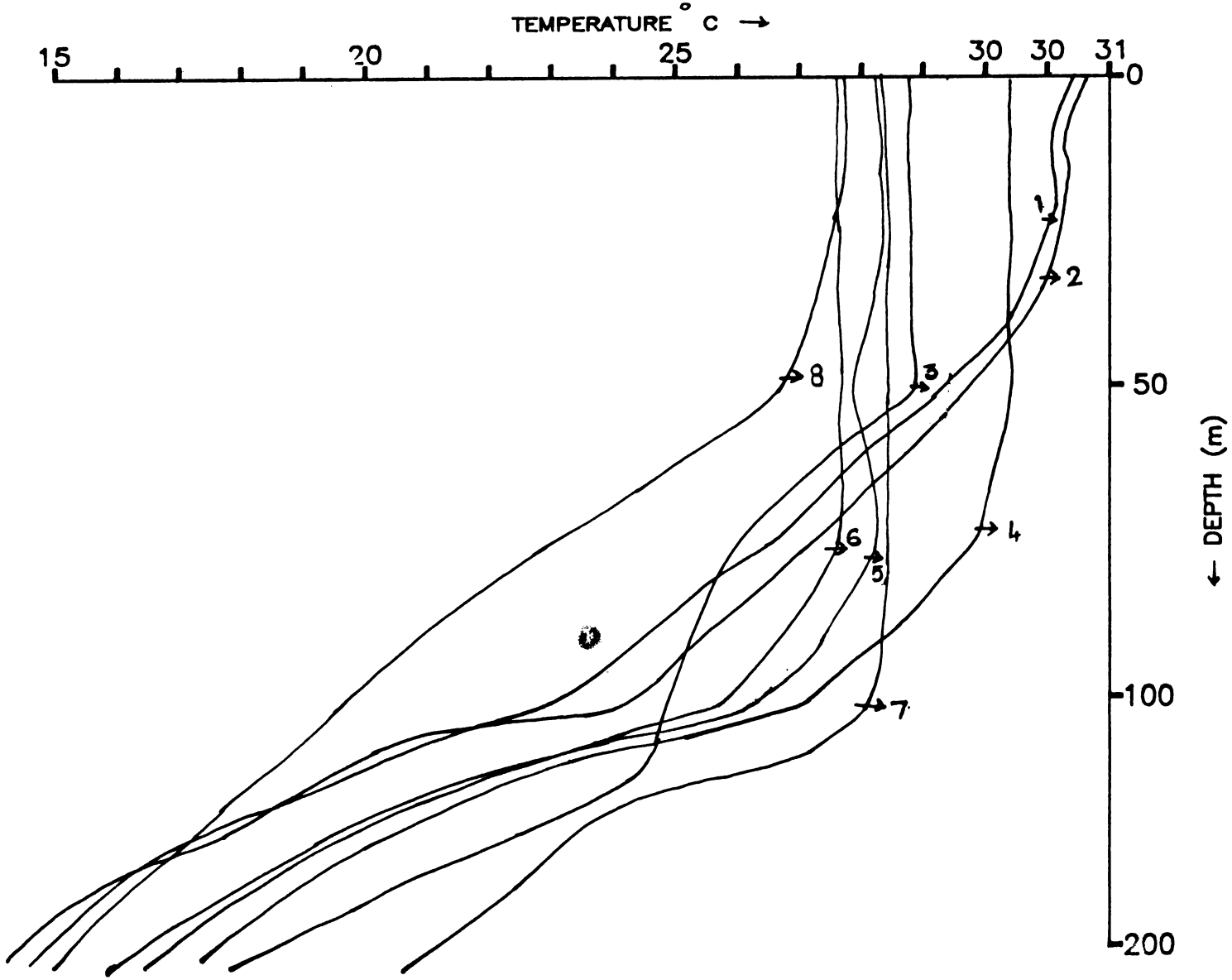

Fig.2.2 Temperature profiles during monsoon season

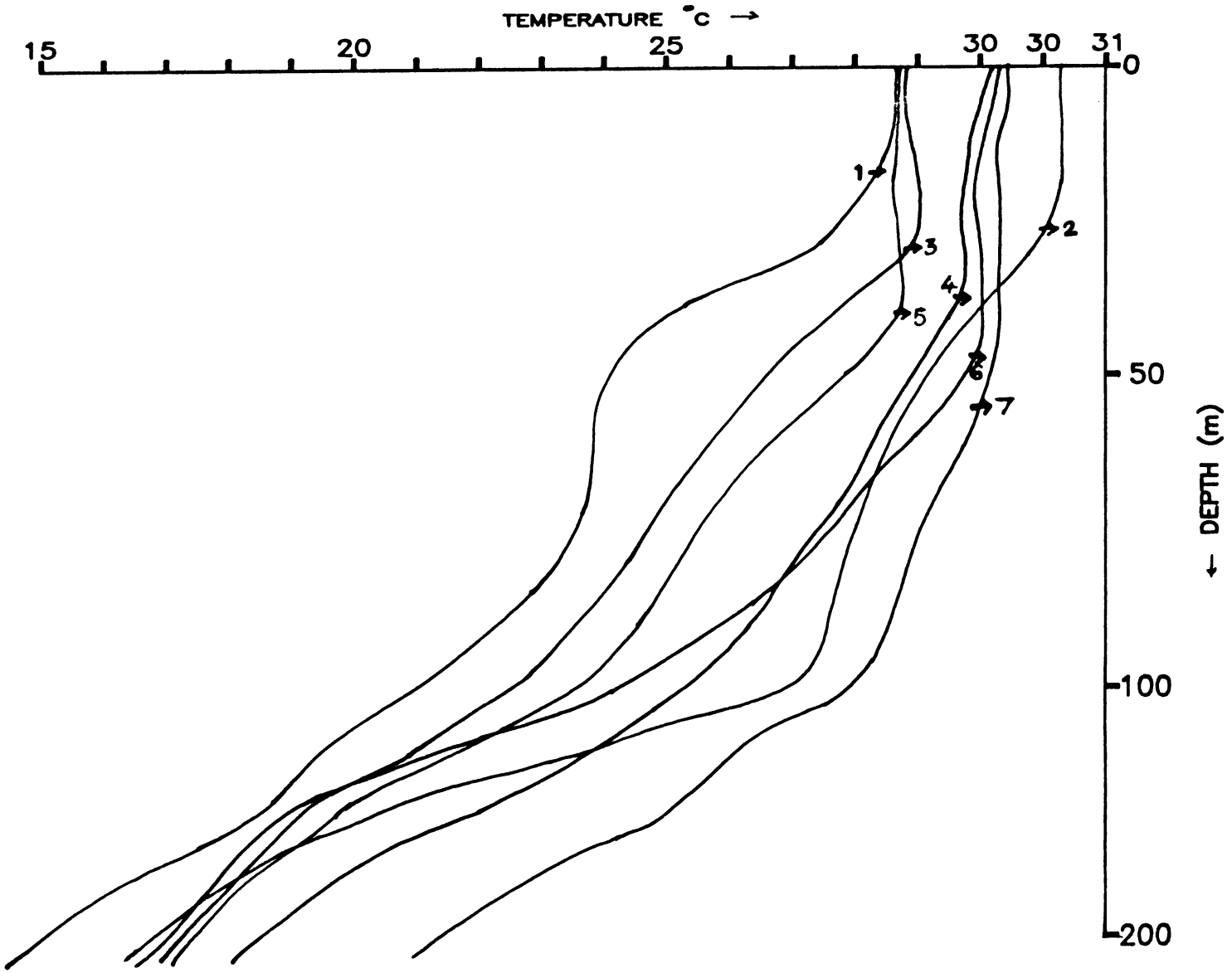

Fig.2.3 Temperature profiles during post-monsoon season

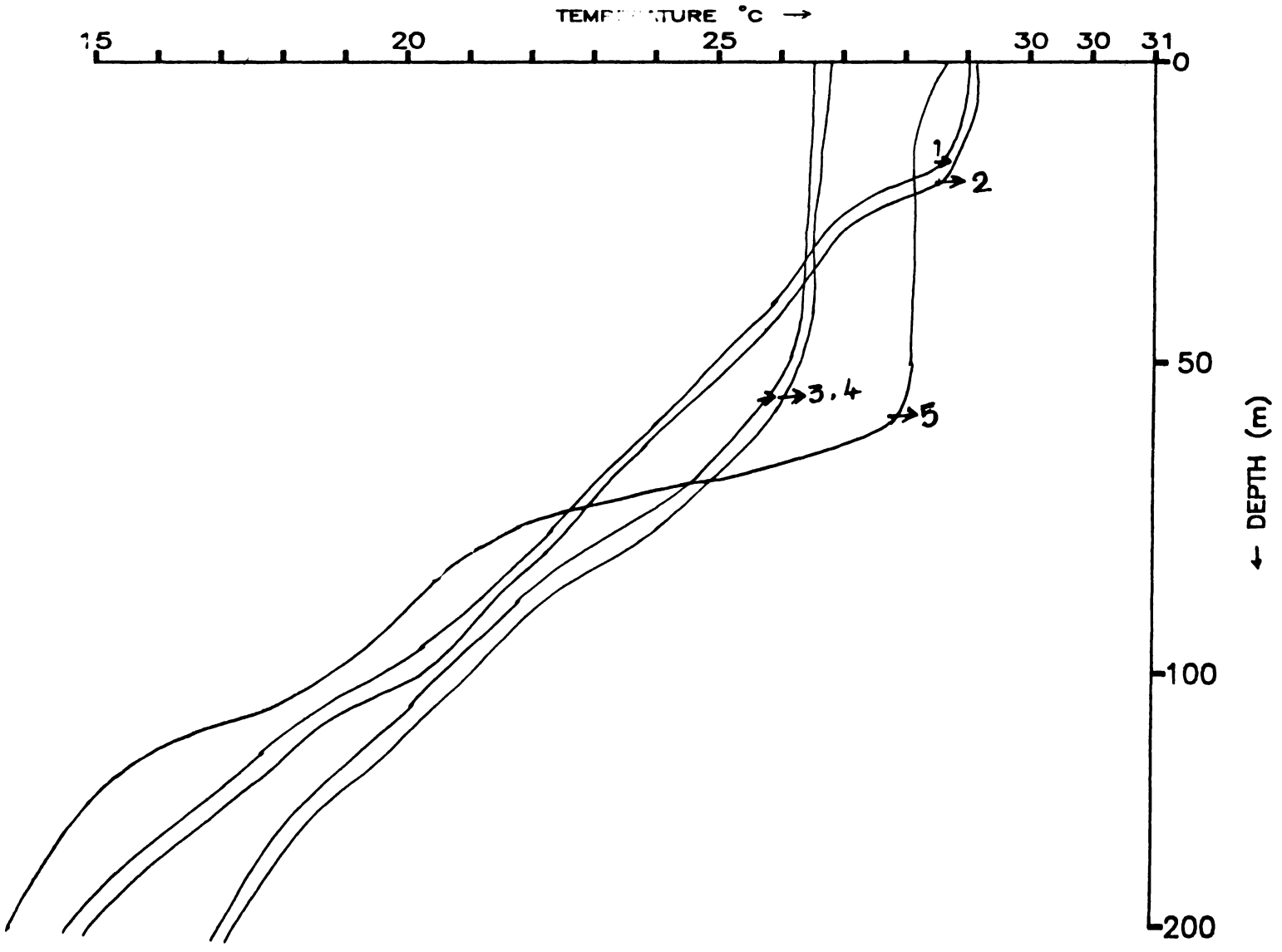

Fig.2.4 Temperature profiles during winter season

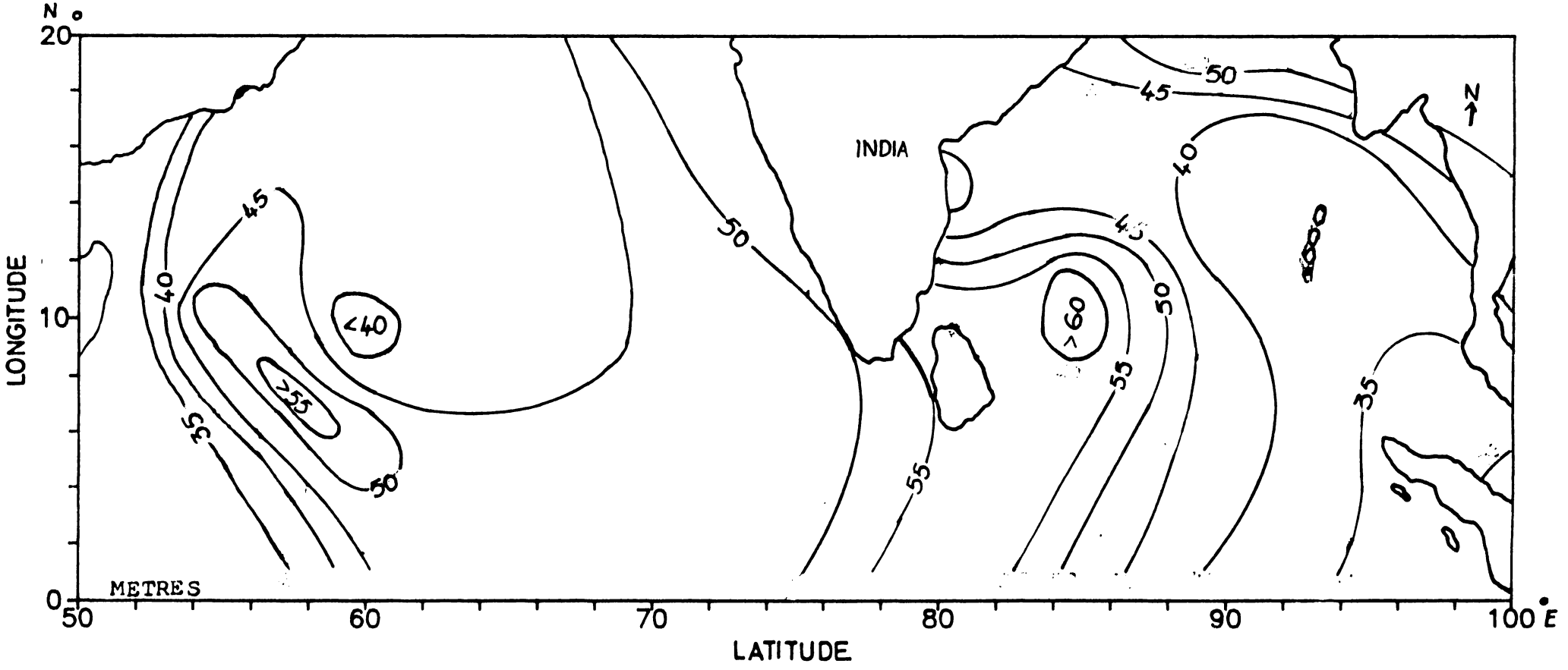

Fig.2.5 Pre-monsoonal distribution of MLD (Levitus, 1982)

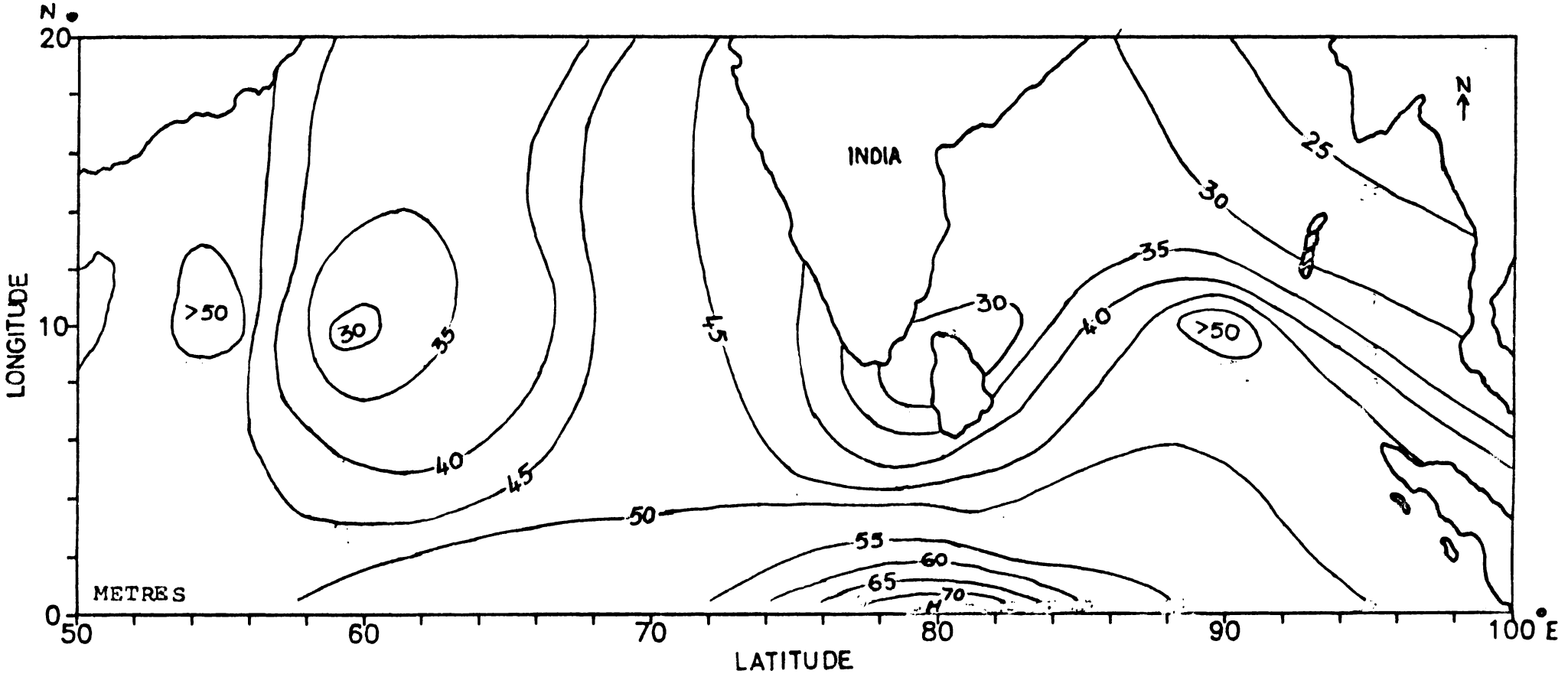

Fig.2.6 Monsoonal distribution of MLD (Levitus, 1982)

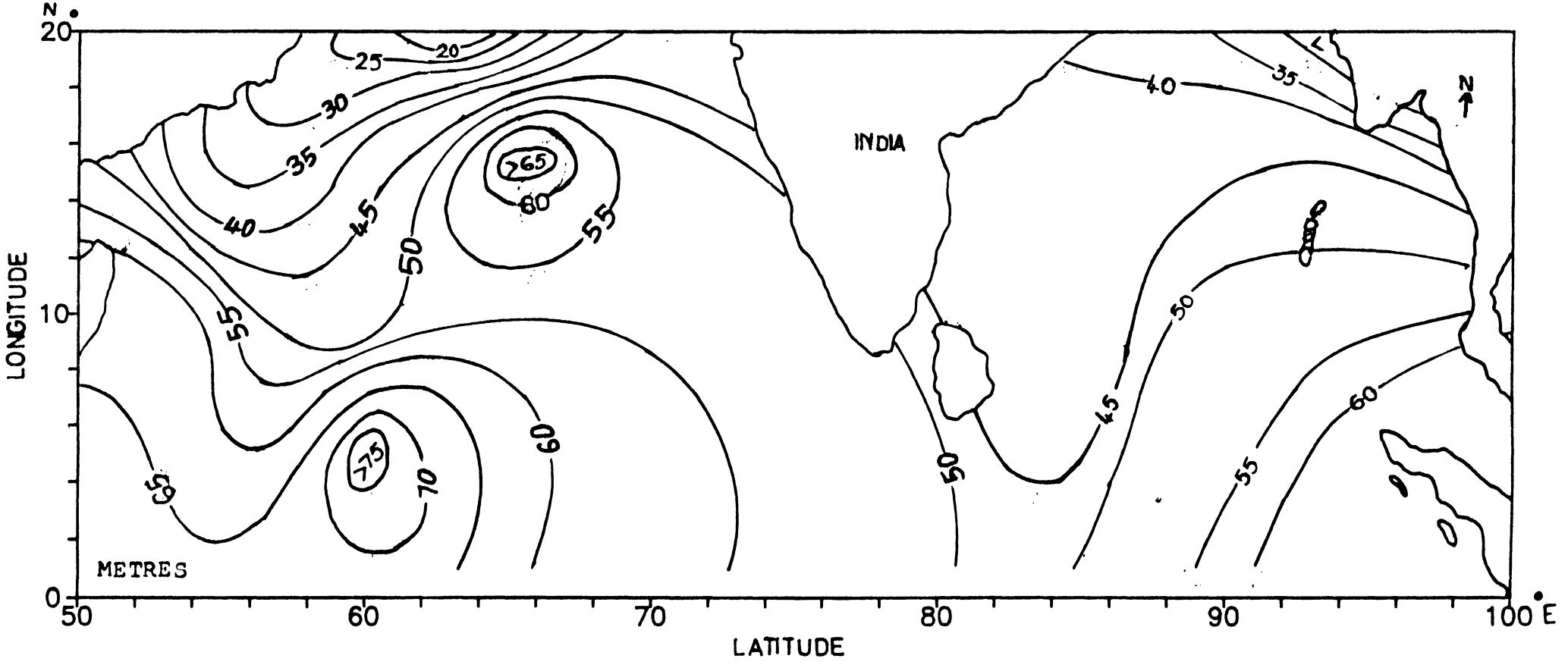

Fig.2.7 Post-monsoonal distribution of MLD (Levitus, 1982)

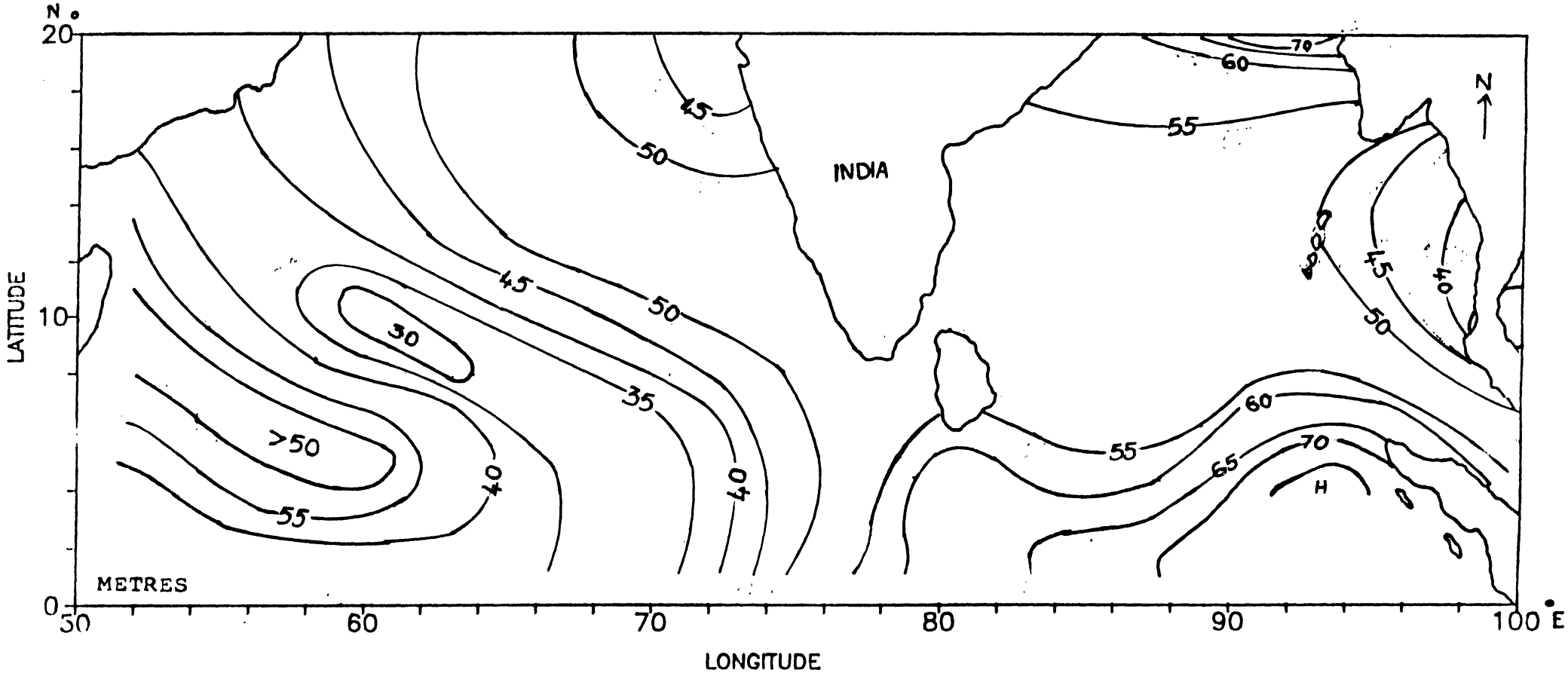

Fig.2.8 MLD distribution during winter (Levitus, 1982)

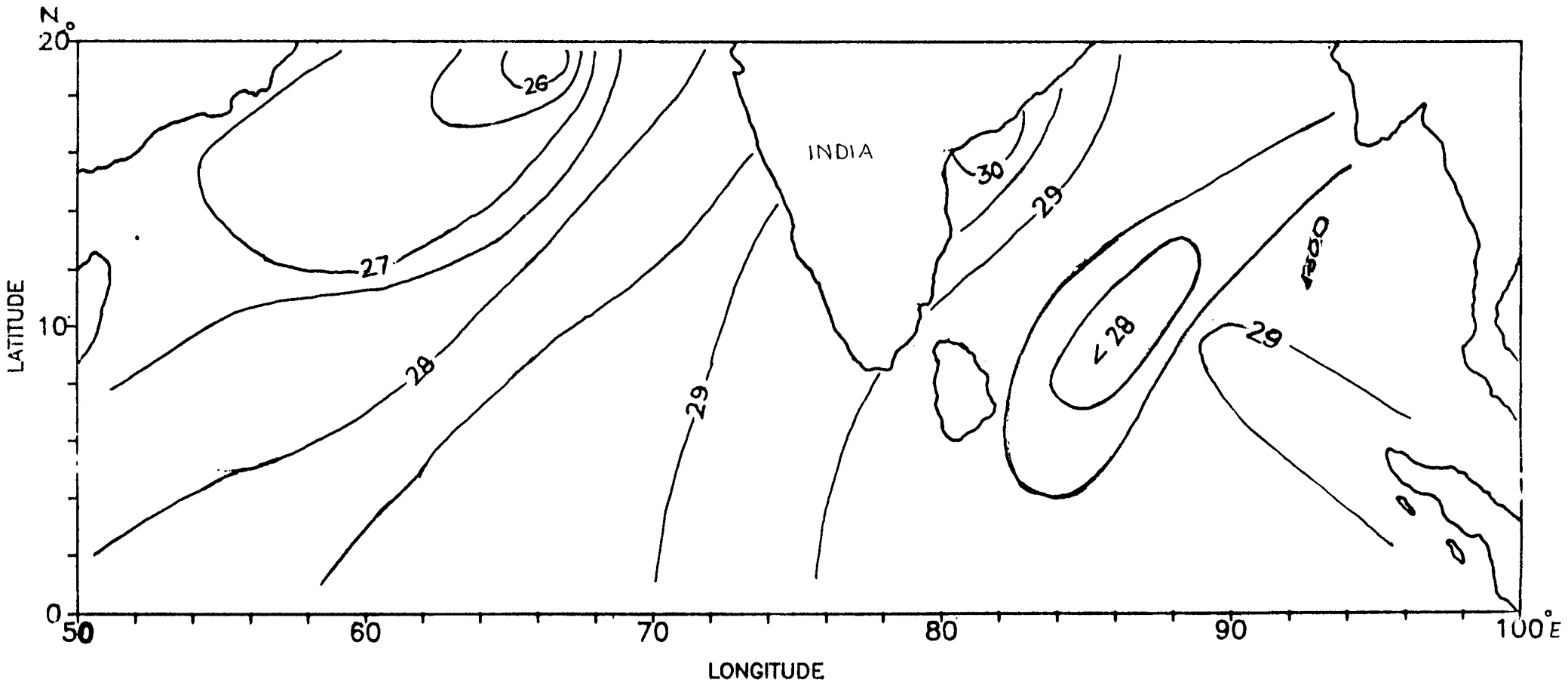

Fig.2.9 Pre-monsoonal distribution of SST (Levitus, 1982) °C

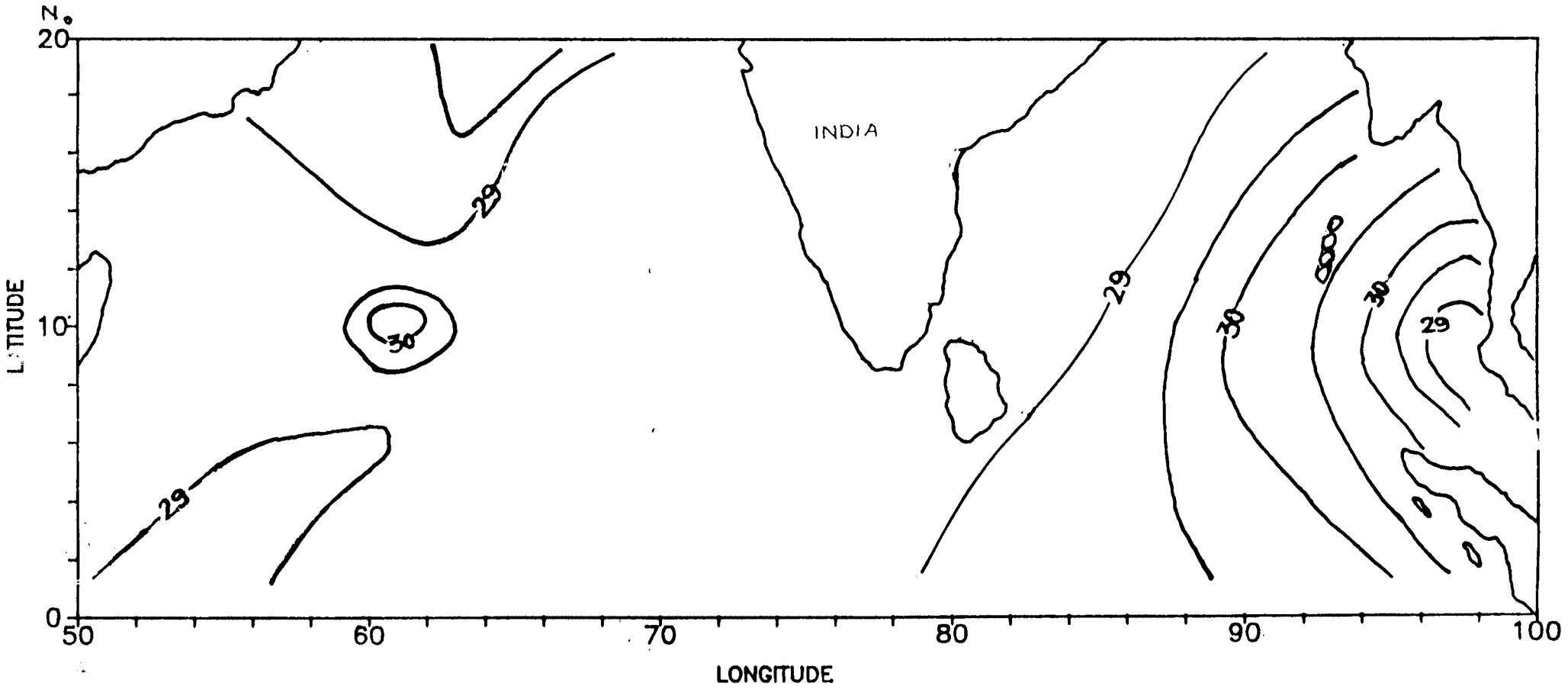

Fig.2.10 Monsoonal distribution of SST (Levitus, 1982) °C

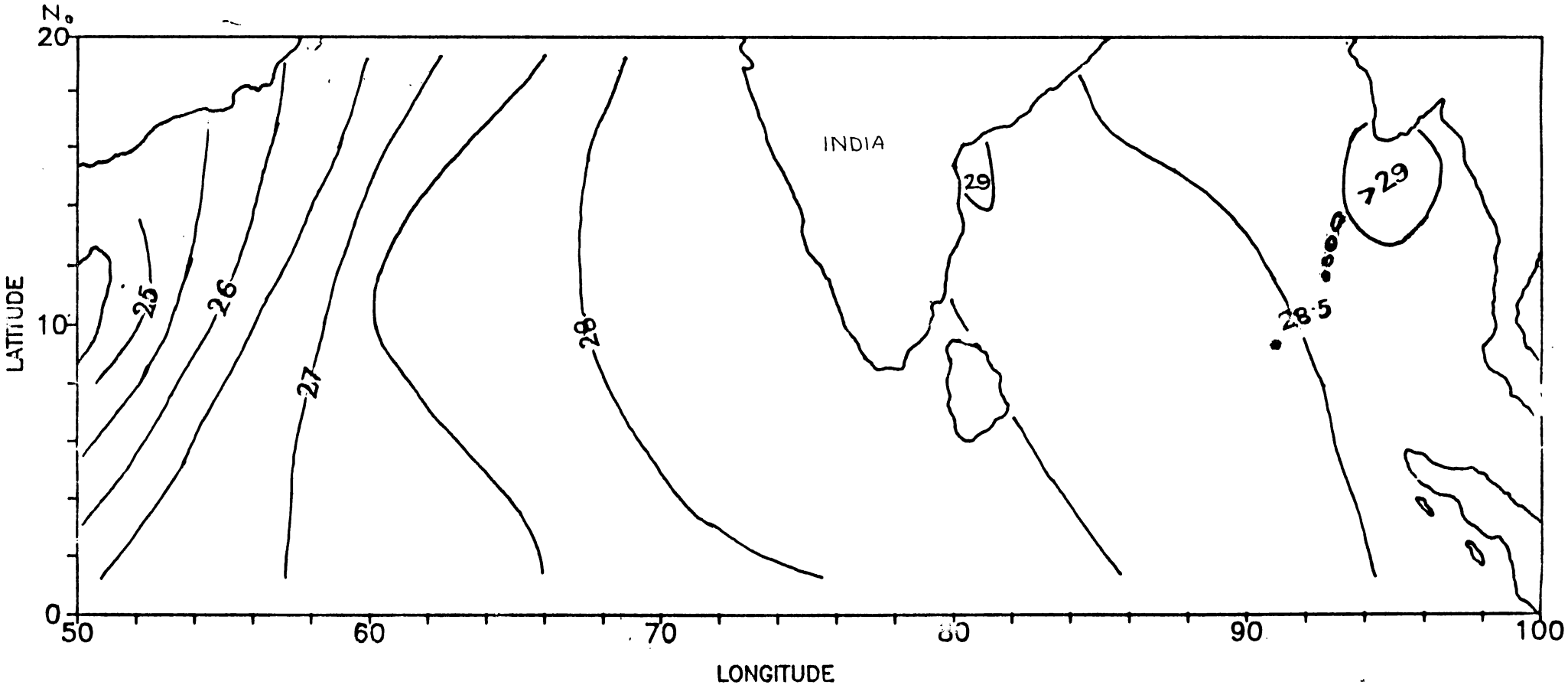

Fig.2.11 Post-monsoonal distribution of SST (Levitus, 1982) °C

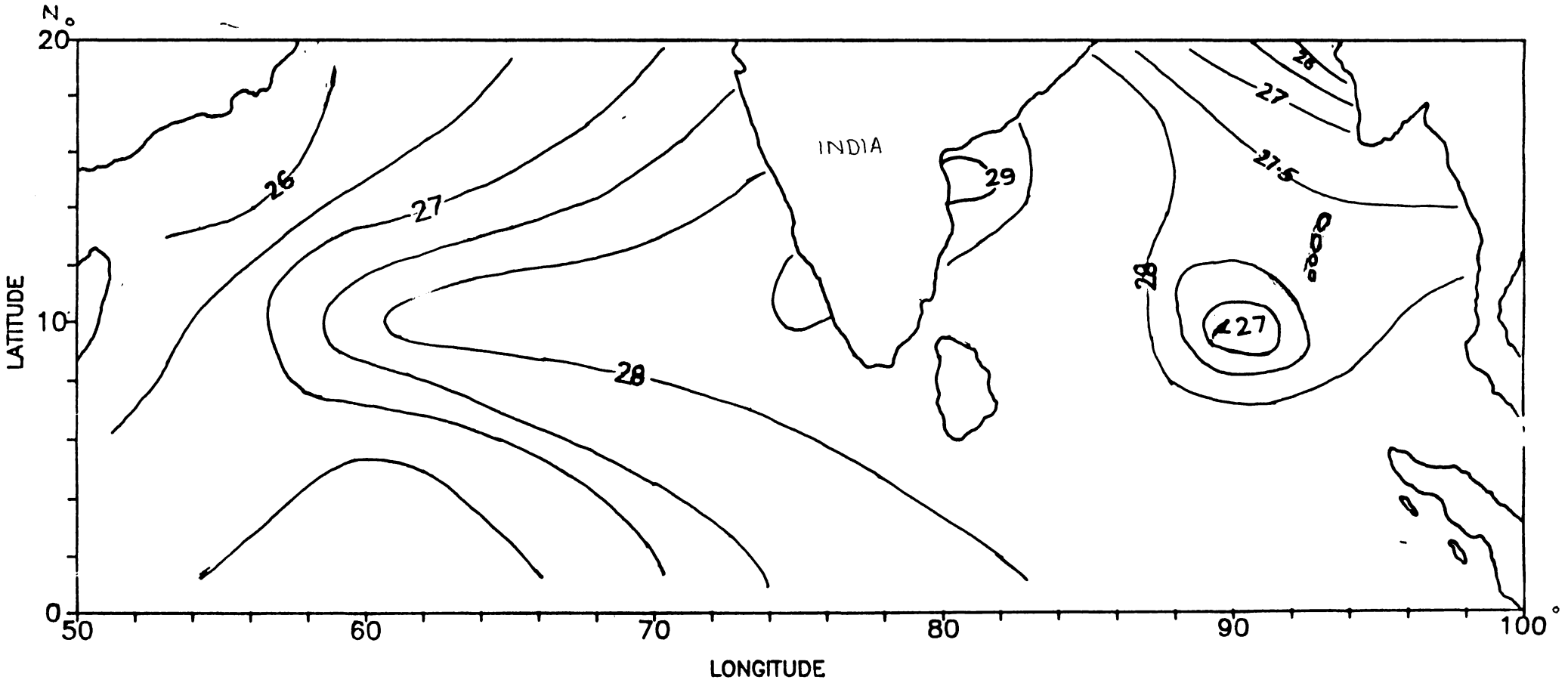

Fig.2.12 SST distribution during winter (Levitus, 1982) °C

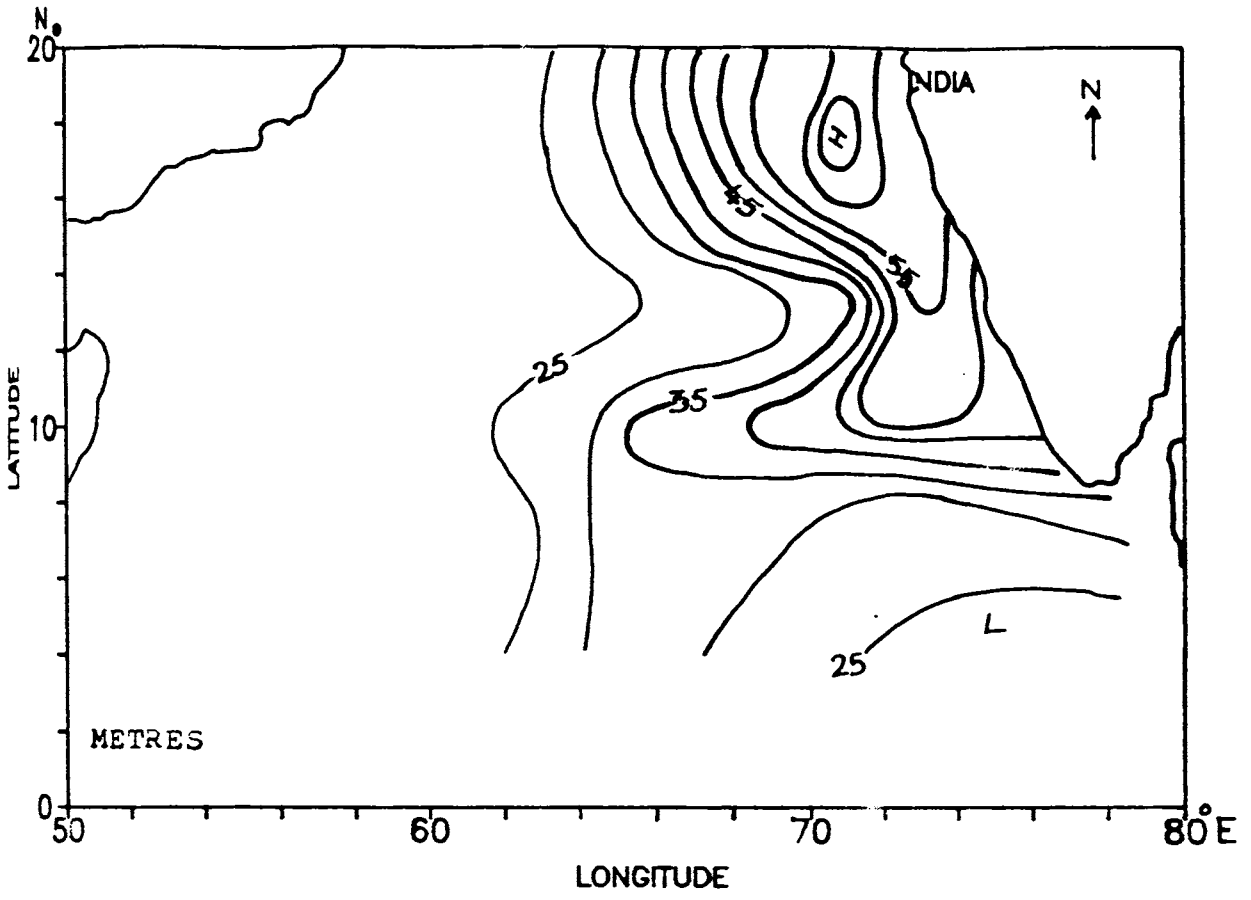

Fig.2.13 Distribution of MLD during pre-monsoon season (1977 - 1986)

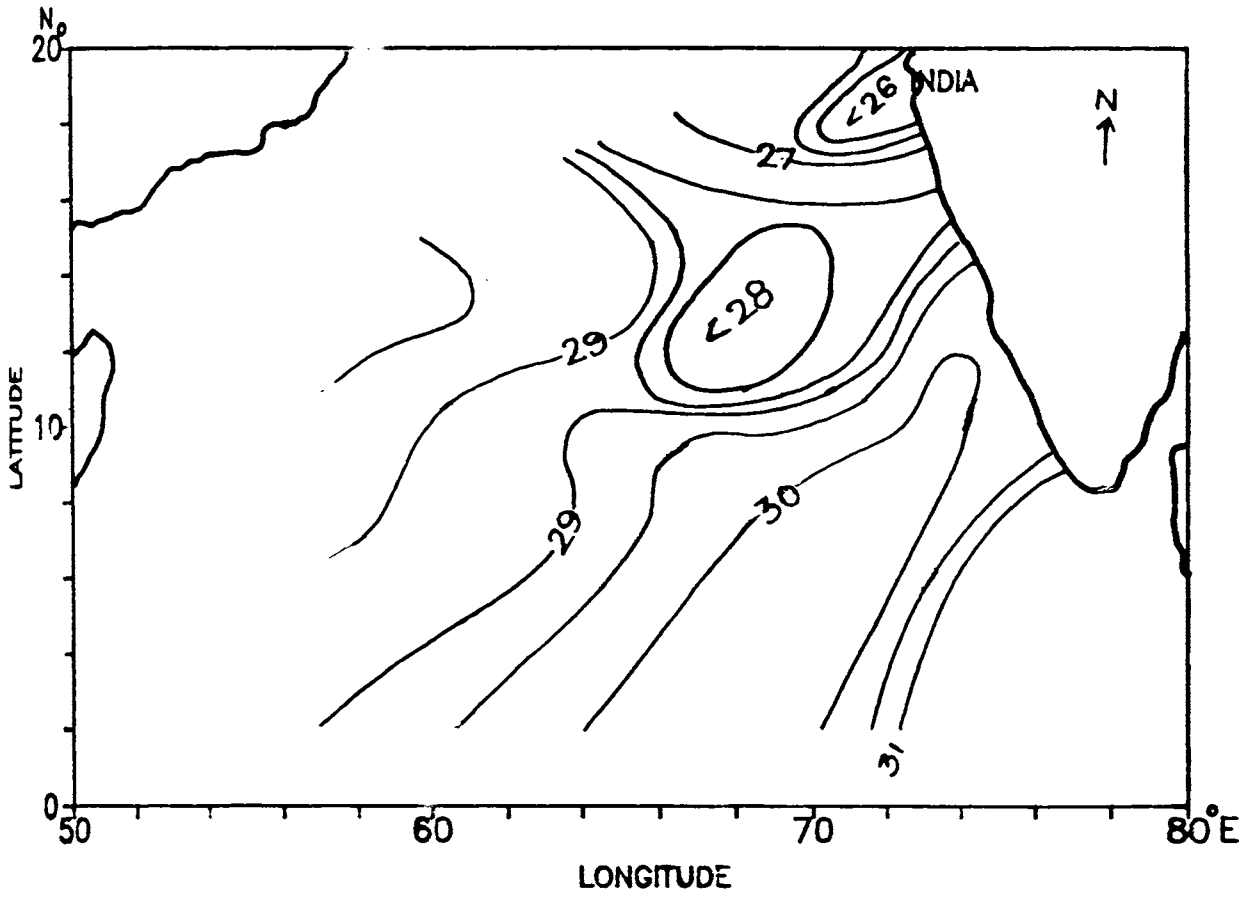

Fig.2.17 Distribution of SST during pre-monsoon seasor 1977 - 1986) °C

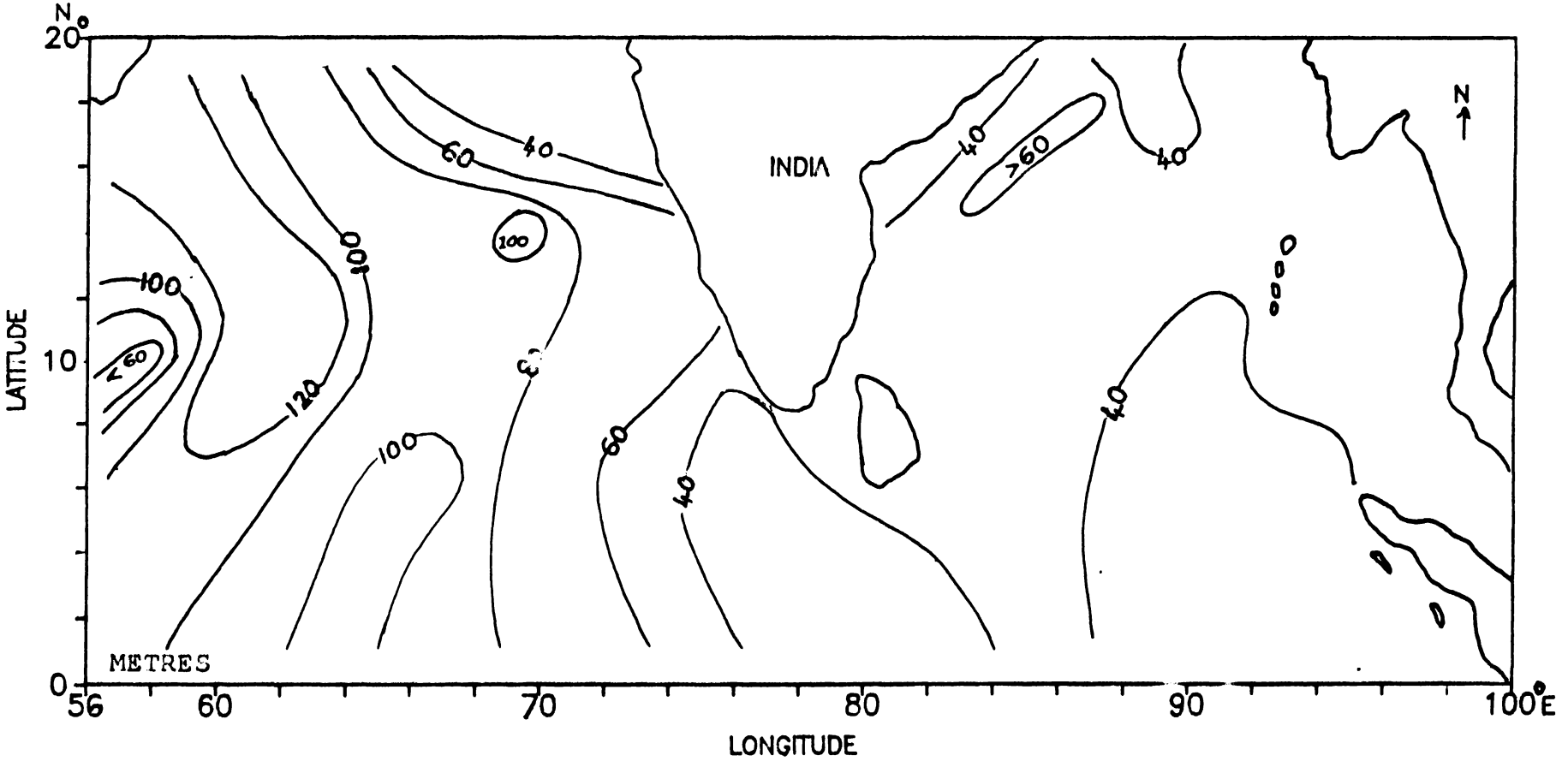

Fig.2.14 Distribution of MLD during monsoon season (1977 - 1986)

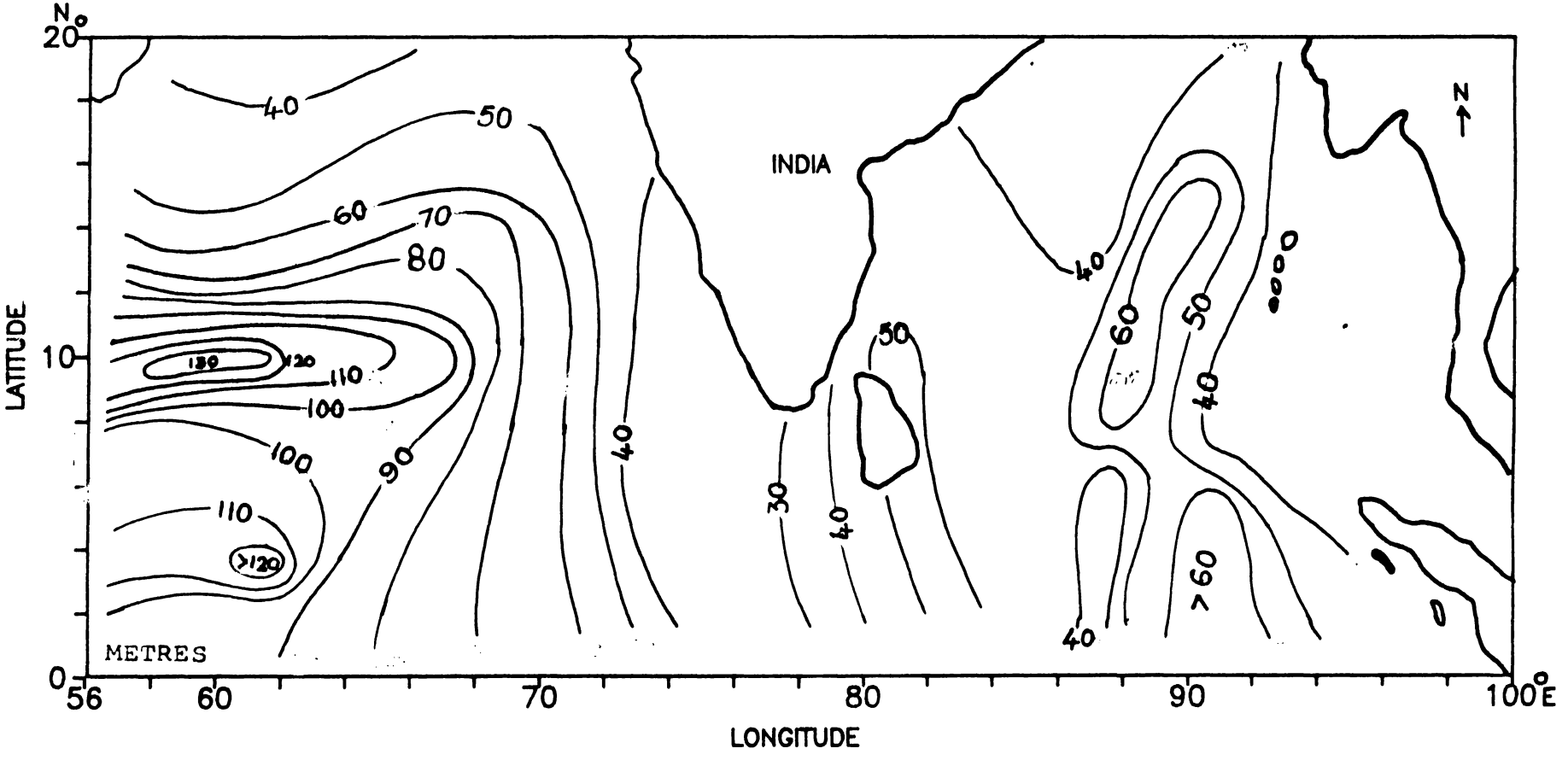

Fig.2.15 Distribution of MLD during Post-monsoon season (1977 - 1986)

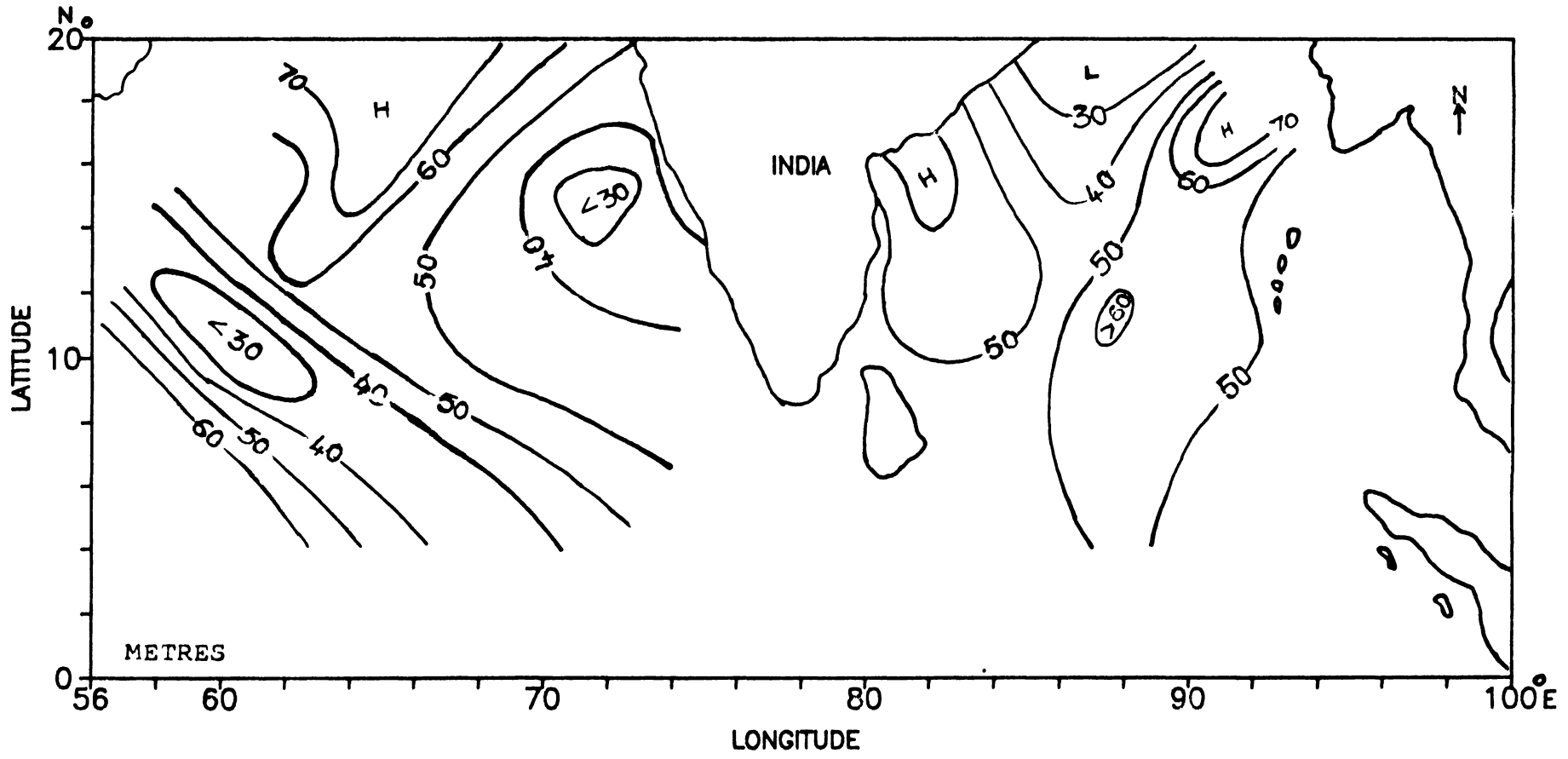

Fig.?.16 Distribution of MLD during winter season (1977 - 1986)

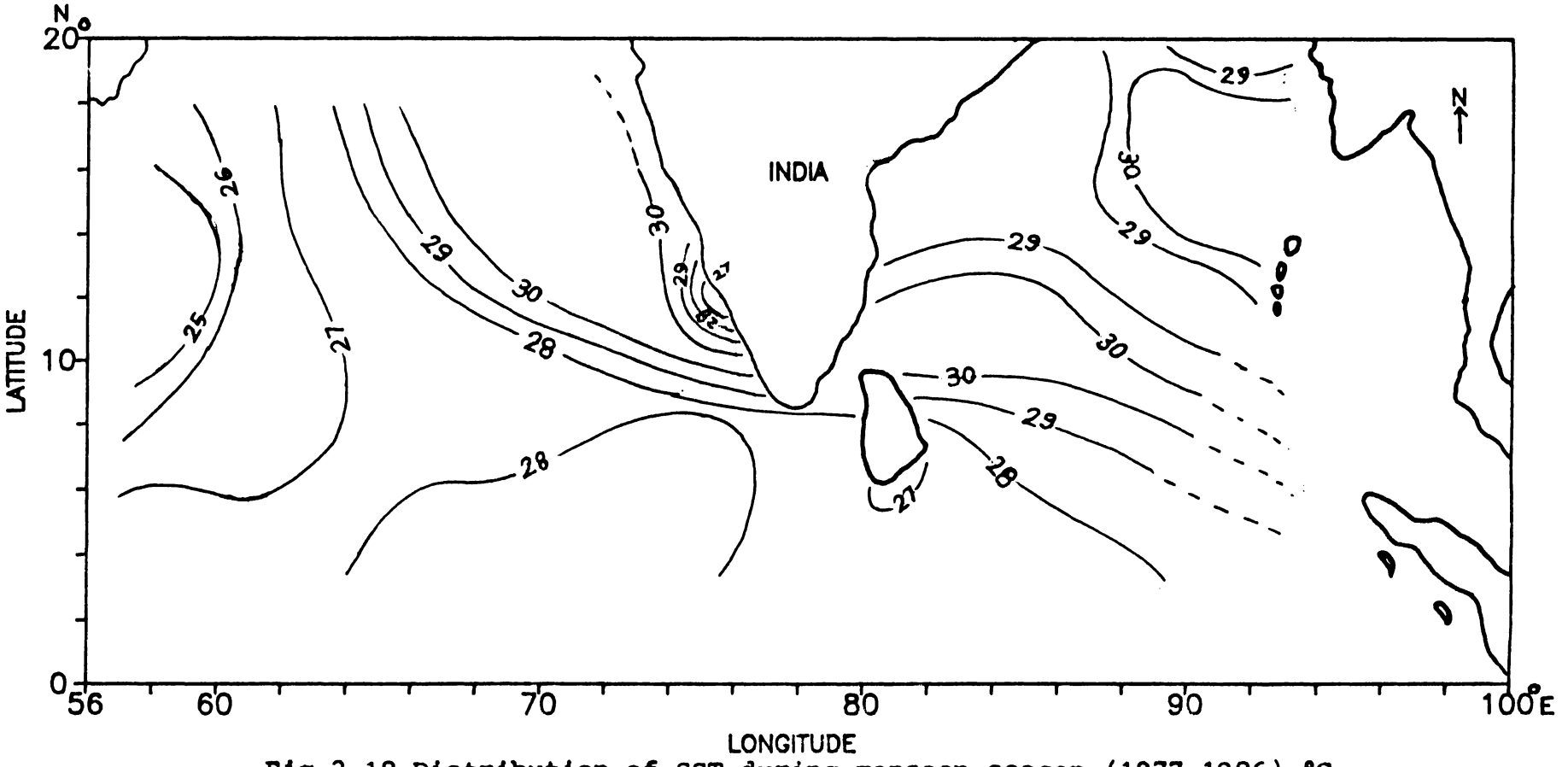

Fig.2.18 Distribution of SST during monsoon season (1977-1986) °C

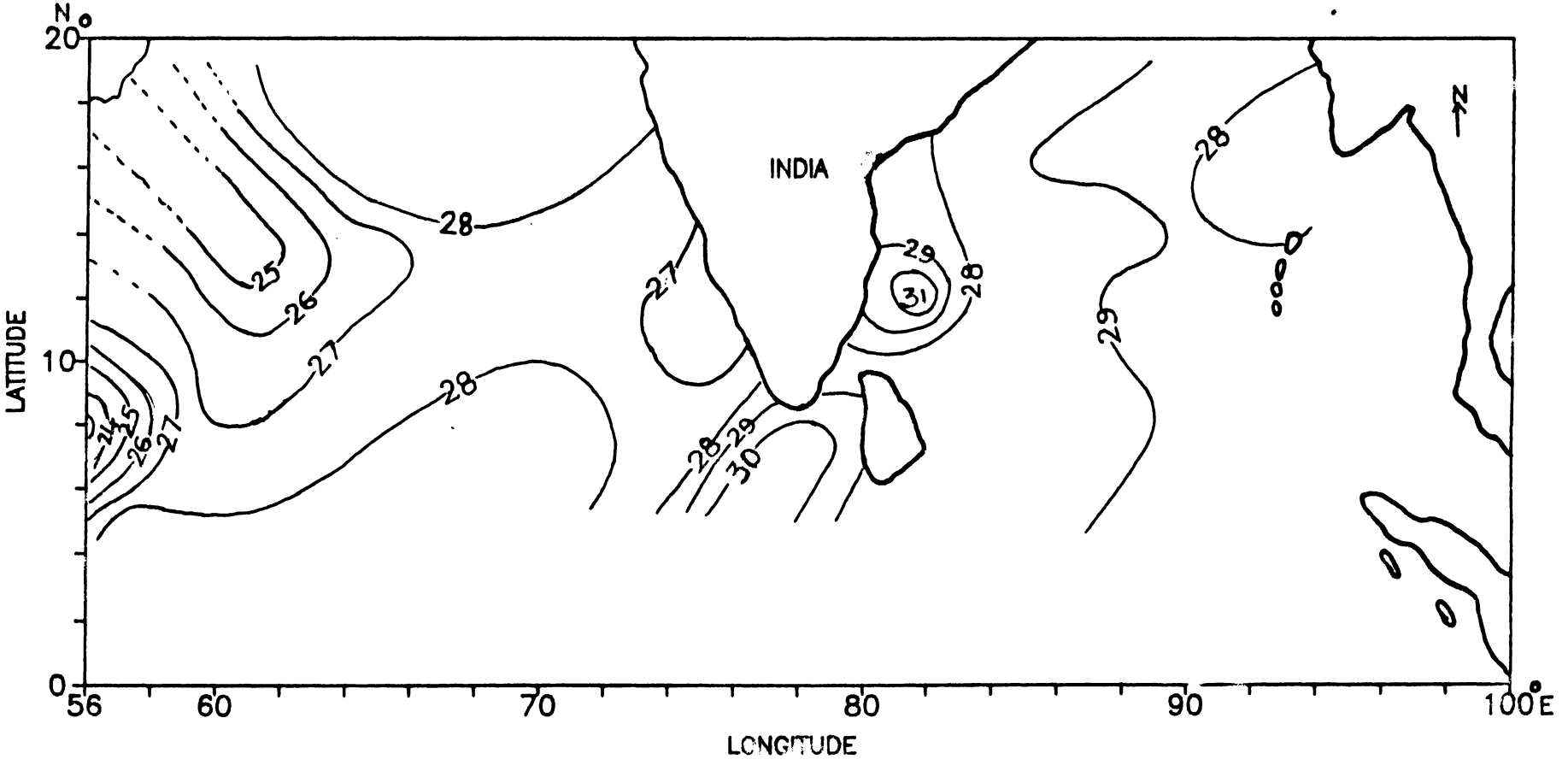

Fig.2.19 Distribution of SST during post-monsoon season (1977-1986) °C

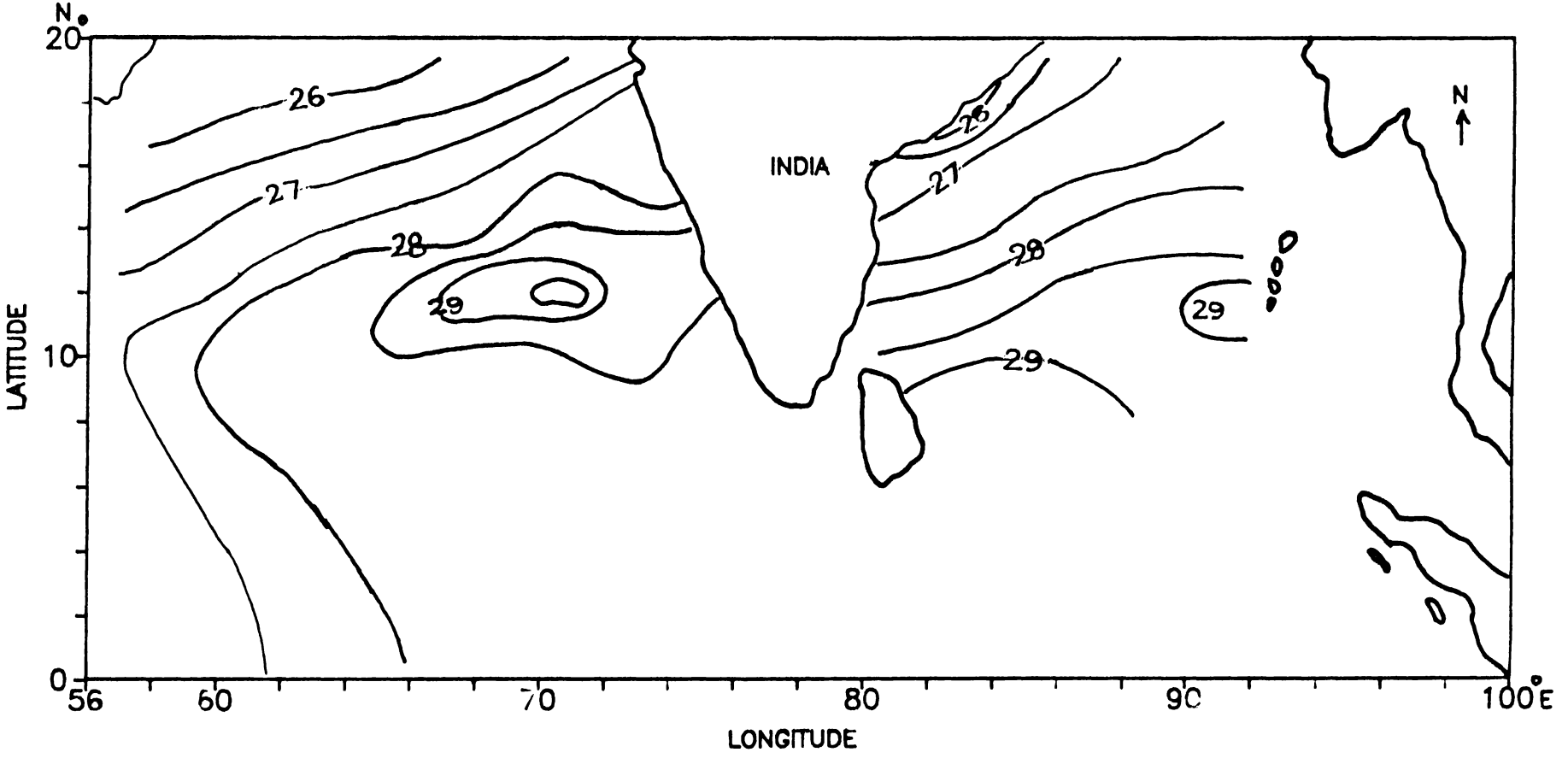

Fig.2.20 Distribution of SST during winter season (1977-1986) °C

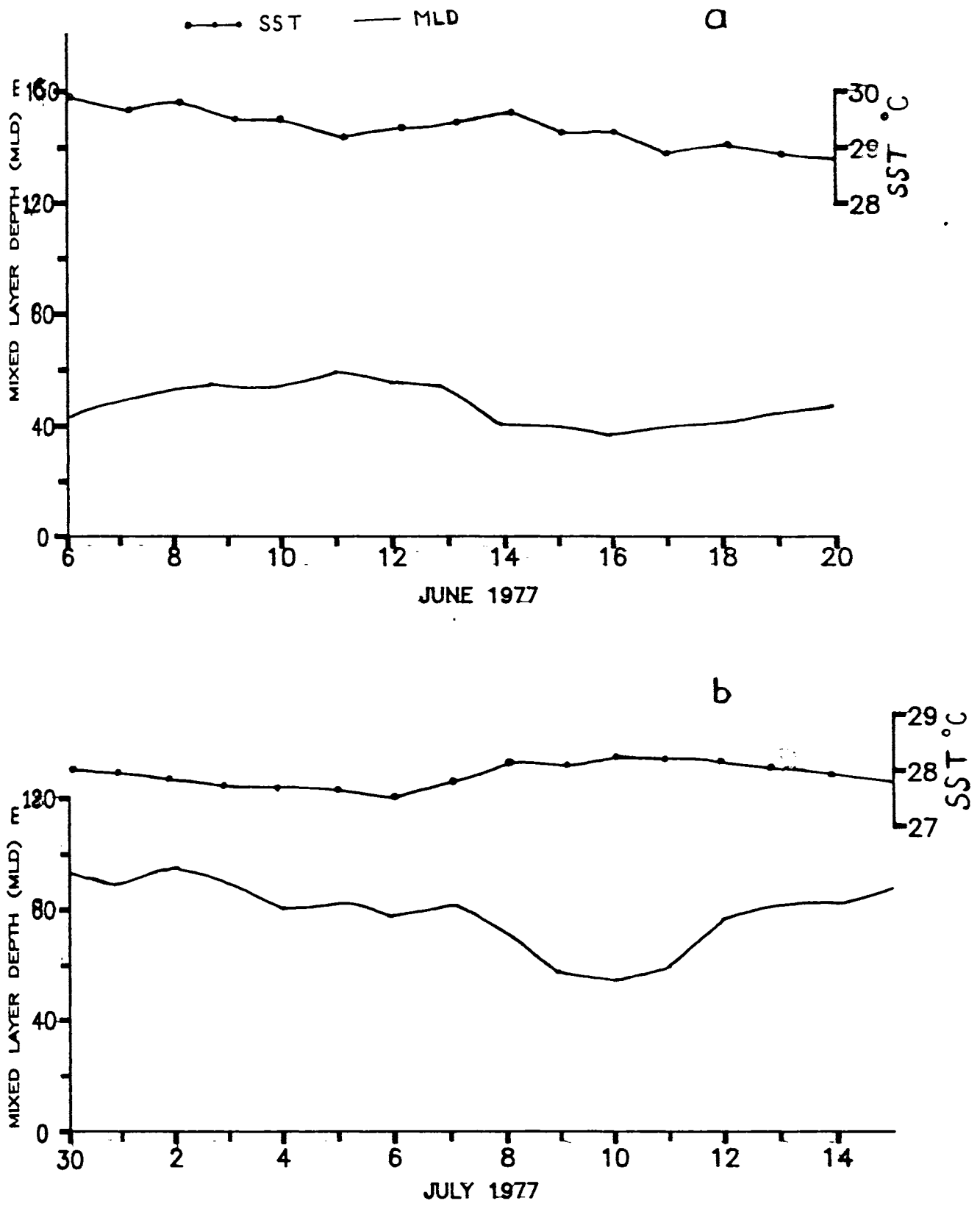

Fig.2.21 Daily variation of MLD & SST in Area - I (a) phase - I (b) Phase-II.

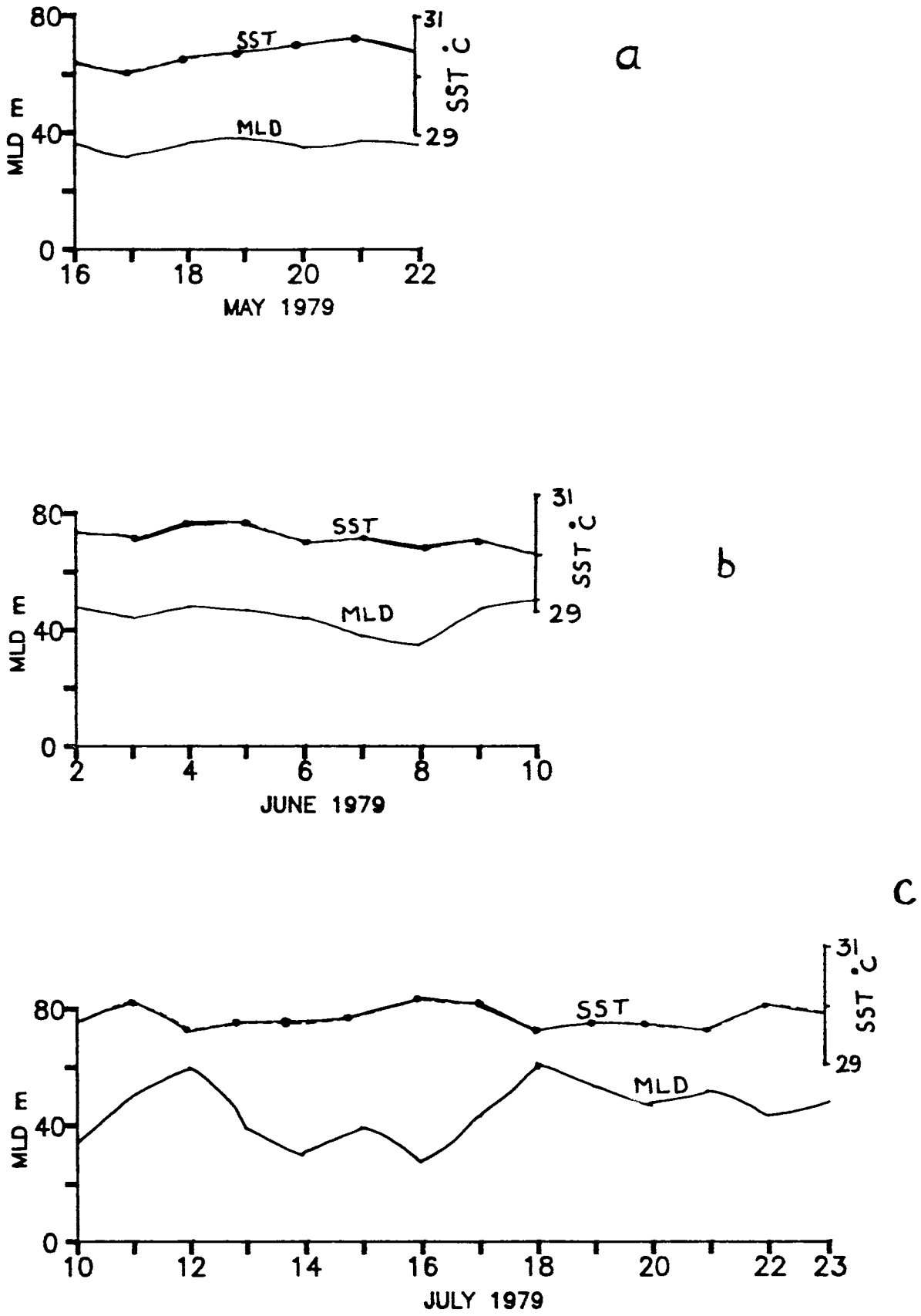

Fig.2.22 Daily variation of MLD & SST in (a) Area - II (b) Area-III (c) Area - IV

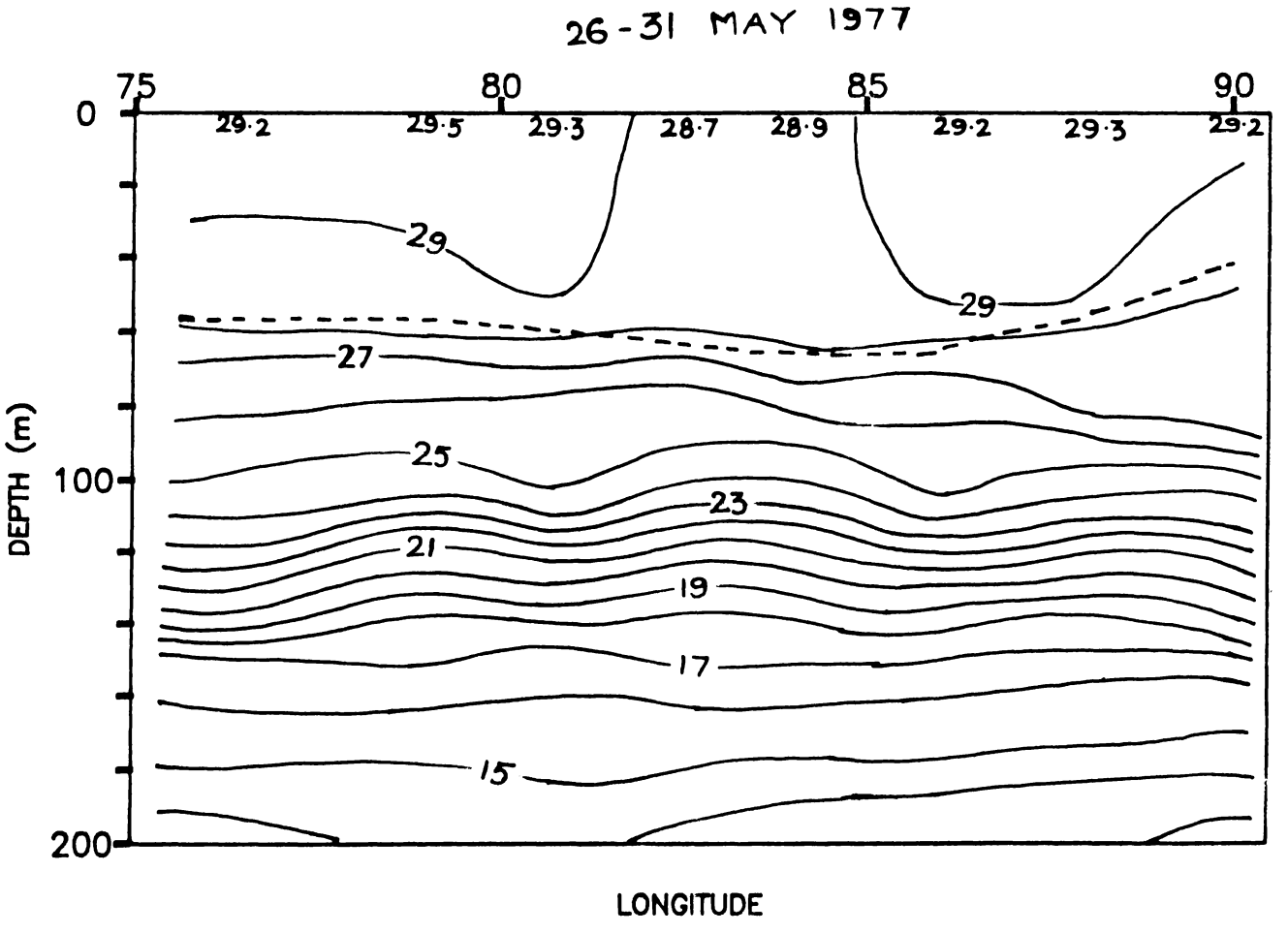

Fig.2.23 Zonal temperature sections in equatorial Indian Ocean, May 1977

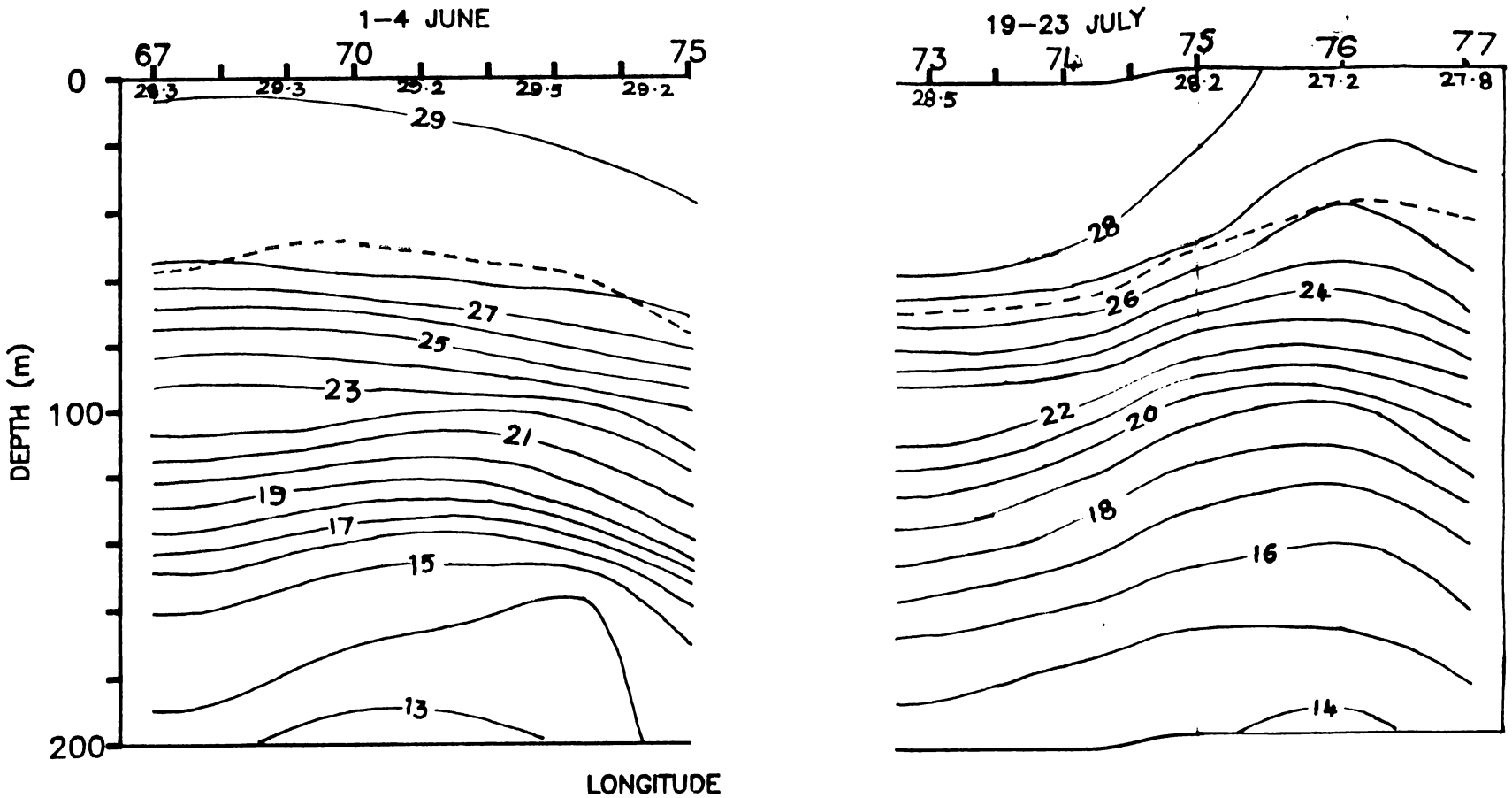

Fig.2.24 Zonal temperature sections in equatorial Indian Ocean, June-July 1977

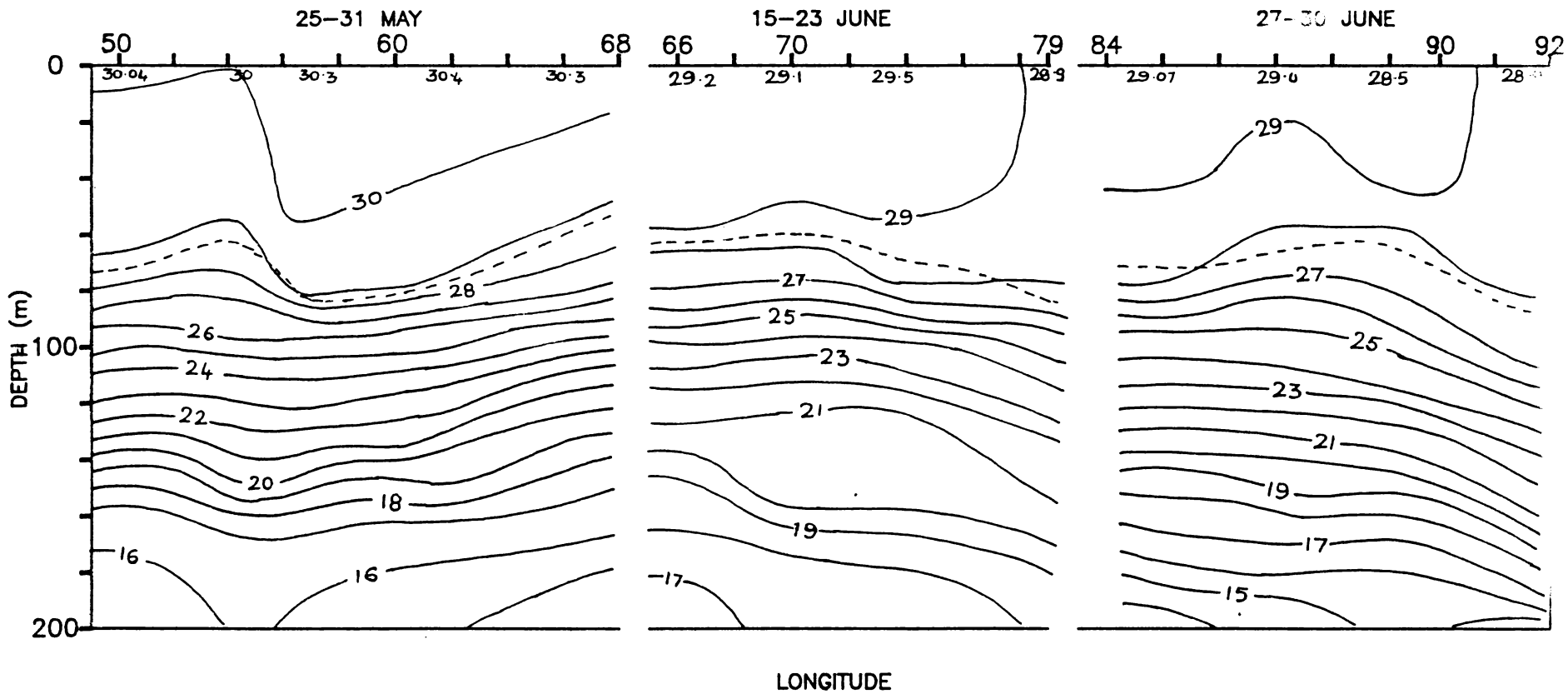

Fig.2.25 Zonal temperature sections in equatorial Indian Ocean, May-June 1979

CHAPTER - III

HEAT CONTENT VARIATIONS

3.1. Introduction

This chapter deals with the seasonal variations of heat content upto a depth of 200m in different layers of 50m thickness in the northern Indian Ocean during the period 1977-1986. Daily variations of heat content of different layers for different polygon areas (Ref. fig.1.1) and variations of cyclone heat potential (CHP_{28}) before and after three storm events were analysed over Arabian Sea and Bay of Bengal during June 1977 and May-June 1979.

Heat storage in the Indian Ocean is greatly influenced by the forcing signals of semi-annual monsoons. Various investigators have pointed out that the local heat exchange with the atmosphere can hardly account for the large amounts of heat stored seasonally in the upper ocean at low latitudes. Duing and Leetma (1980), suggested that the Arabian Sea coastal upwelling is a major cause of heat storage variability. In the western equatorial Atlantic, Merle (1980) observed that the annual cycle of heat content appeared to be the result of vertical movement of thermocline associated with the dynamic response of the ocean to the seasonally varying winds. In fact, he showed that the rate of heat storage could be up to ten times larger than the net input through the sea surface.

Vertical and horizontal advections are of significant importance over the Indian Ocean, because of the intensity of eddy circulation during the monsoon. Bruce and Beatty (1985) and Molinari et al, (1986) are of the opinion that SST and heat storage of the surface layer control the amplitude of air-sea interaction to a great extent. Heat received from the atmosphere by the ocean at low latitudes has to be exported meridionally to higher latitudes. In the case of Arabian Sea and Somali basin, most of this heat must leave southward across the equator (Bruce,1987). According to him, the energy of eddy field plays a significant role in the heat storage and vertical and horizontal transfer, in the western Indian Ocean during southwest monsoon.

Studies on the heat content of the upper ocean layer have received considerable attention in recent years because of its importance in Ocean- atmosphere energy exchanges. Long period weather fluctuations are related to the larger thermal memory of the ocean. According to Rao (1987,b), the heat content of top 100-200m layer is strongly influenced by the surface mixed layer cooling and the associated vertical advective processes in the upper thermocline.

The coventional method of monitoring heat content variations requires observations of vertical temperature profiles of the ocean either from ships or bouys. Attempts have also been made to estimate the heat content of the ocean form satellite data. Miller (1978) developed an algorithm to predict changes in the surface heat content using the satellite derived SST and

surface wind stress. Christenson and Mascarenhas (1979) computed heat storage of the ocean mixed layer by relating the density anomaly to temperature. Ali and Desai (1989) noticed a decrease in content of the upper 250m layer from west to east in the equatorial Indian Ocean during the onset of monsoon 1979. Dhoulath et al, (1990) estimated cyclone heat potential utilising the satellite derived SST and cloud motion vector winds extrapolated to the surface and examined the role of ocean heat potential on atmospheric disturbances.

3.2 Seasonal variations of heat content

The average heat content computed for the different seasons for different layer of 50m thickness over the northern indian Ocean during the period 1977-1986 are presented in the following sections. During pre-monsoon the study is limited for the Arabian Sea due to the paucity of data.

3.2.1 Pre-monsoon season

Distribution of average heat content in the 0-50m layer in the Arabian Sea is shown in fig (3.1). The heat content of this layer increases from west to east reaching a maximum of $62*10^8$ J/M^2 near the south west coast of India, where the mixed layer extends to about 50m. Similar increasing trend is also noticed for the MLD in this season (discussed in chapter-II). The maximum heat content area coincides with the area of warmer SST ($>31^{o}$ C) and the area of minimum heat content of $54*10^8 J/M^2$ coincides with cooler SST (26^{o} C) region. In the eastern Arabian Sea, heat

content decreases towards north along the west coast of India due to the increase in SST in the same direction. Maximum variations in heat content is observed around 12^{o} N, 62^{o} E. Heat content of 50-100m layer (fig.3.2) shows a decreasing trend from west to east south of 10^{o} N. In the central Arabian Sea, the heat content increases from west to east reaching a maximum of $56*10^{8}$ J/M^{2} around 10^{o} N, 59^{o} E . The minimum heat content is observed around 13^{o} N,63^{o} E. The decrease in heat content between this layer and the surface (0-50m) layer is minimum in the western Arabian Sea while, in the central Arabian Sea and near the Kerala coast, it is maximum. Maximum variations in heat content of this layer are found on the western side of the Arabian Sea.

Fig (3.3) shows the distribution of heat content for the 100-150m layer. It can be seen that, in this layer heat content varies between $42*10^{8}$ and $50*10^{8}$ J/M^{2} . The maximum heat content is observed around 8^{o} N,60^{o} E from where it decreases in a northeasterly direction and attains the minimum value in the central Arabian Sea. Low heat content of $44*10^{8}$ J/M^{2} is also observed near the Kerala coast. In the western region, a decrease of about $15*10^{8}$ J/M^{2} is seen between this layer and the 1st layer (0-50m) while, it is about $13*10^{8}$ J/M^{2} in the eastern region. In the northern Arabian Sea where the heat content is minimum for the 1st layer, a decrease in heat content of $17*10^{8}$ J/M^{2} is noticed between 100-150m and the next upper layer.

The 150-200m layer shows minimum heat content of $38*10^{8}$ J/M^{2} along 8-10^{o} N,66-69^{o} E (fig.3.4). The maximum is found in

the same region (around 13^{o} N,63^{o} E) as in the case of 100-150m layer with a decrease of $10*10^{8}$ J/M^{2} .The minimum heat content near the Kerala coast is seen shifted slightly towards west. Generally the heat content decreases in all direction from the south central Arabian Sea. The decrease in heat content is maximum between the upper 100m layer and the lower layers in the southeastern Arabian Sea. On the an average decrease of $20*10^{8}$ J/M^{2} in heat content is observed during this season between the 1st and last layer (150-200m).

3.2.2 Monsoon season

During this season, maximum heat content for the surface layer is observed in the western Equatorial region and in the central Bay of Bengal (fig.3.5). Heat content decreases towards east reaching a minimum of $50*10^{8}$ J/M^{2} near the Kerala coast. Maximum variations are observed in the Arabian Sea compared to Bay of Bengal where a comparatively high heat content values are seen. In this season MLD extends to 120m in the central Arabian Sea (fig.2.10) showing a similar decreasing trend towards east as that of heat content variations. The minimum heat content area coincides with almost cooler SST of 27^{o} C (Fig. 2.14). The low heat content near the southeastern Arabian Sea could be attributed to the upwelling phenomena prevailing during the monsoon period.

In the 50-100m layer, maximum heat content is found around 8^{o} N,59^{o} E and in the western parts of Bay of Bengal

(fig.3.6). The maximum heat content area observed for the surface (0-50m) layer in the western equatorial region has been changed to a low heat content area in the 2nd layer. In this region though the MLD extends to about 100m, considerable decrease of about 19*10 J/M in heat content is noticed between the upper two layers. In Bay of Bengal, the maximum heat content area corresponds to warmer SST and vice versa. The decrease in heat content between the upper two layers is more in the northern Bay while it is less in the southern parts.

Fig(3.7) shows the distribution of heat content in the third (100-150m) layer. Minimum heat content is encountered in the north equatorial region and near northern Bay of Bengal. The heat content increases towards northwest reaching a maximum of $50*10^8$ J/M^2 in the southwest Arabian Sea. In the Bay of Bengal, heat content increased towards the central Bay with maximum value of $52*10^8$ J/M^2 concentrated around 13^o N,86^o E. The decrease in heat content between 2nd and third layer is maximum in the northeastern Arabian Sea and northern Bay of Bengal while it is minimum in the central Bay of Bengal. Maximum variations are observed in the northern Bay and near the eastern parts of north equatorial region. The heat content of the 4th layer varies between $32*10^8$ and $42*10^8$ J/M^2 during this season (fig.3.8). This layer shows an increasing trend in heat content towards west in the central Arabian Sea with maximum around 13^o N, 59^o E. Almost uniform heat content of $36*10^8$ J/M^2 is noticed in the western parts of north equatorial Indian Ocean. Southern Bay Bengal

experiences minimum heat content for this layer where the heat loss between the 3rd and 4th layer is maximum about $18*10^8$ J/M^2. Along the western coats of India, the variations in heat content are more compared to other areas.

3.2.3 Post-monsoon Season

During this season, maximum heat content of $59*10^8$ J/M^2 is observed in the south central Arabian Sea and eastern coast of Bay of Bengal for the surface (0-50m) layer (fig.3.9). Heat content decreases in all directions in the Central Arabian Sea and towards west in the Bay of Bengal. Low heat content area observed in the previous season has now been changed into a high heat content area in the Arabian Sea. Along the western Bay of Bengal, variations in heat content are less while, it is more on the eastern side. Maximum heat content area corresponds to an SST of 28^{O} C and the MLD extends to about 70m. Minimum heat content is observed south of 10^{O} N which corresponds to moderately high SST and deep MLD. In the northwestern Arabian Sea, the maximum heat content corresponds to low MLD and almost high SST. The Maximum heat content in the central Bay coincides with high SST and low MLD.

Fig (3.10) illustrates the heat content distribution for the 50-100m layer in the northern Indian Ocean. In this layer, horizontal variations i heat content shows similar trend that of the 1st layer in the Arabian Sea. The maximum heat content area for the 1st layer observed in the central Arabian Sea remains at the same region with a slight decrease. Small pockets of

alternate high and low heat content are observed in the eastern Bay of Bengal. Maximum heat content variations in the eastern Bay of Bengal are found in the same region as in the surface layer.

The heat content distribution in the 3rd layer are more or less similar to that in the upper (50-100m) layer along most parts of the eastern Arabian Sea (fig.3.11). In the southwestern Arabian Sea, the decrease in heat content between this layer and 2nd layer is maximum about $12*10^8$ J/M^2 . Compared to Arabian Sea, Bay of Bengal shows in general,lower heat content values.

In the 4th layer, the maximum heat content area of the next upper layer has been disappeared and it is found near the southwestern Arabian Sea (fig.3.12). In Bay of Bengal, maximum heat content in this layer is of about $38*10^8$ J/M^2 recorded around 8^o N,93^o E. The difference in heat content between 3rd and 4th layer is maximum near north eastern Arabian Sea and minimum on the western Arabian Sea while, there is no such marked difference in Bay of Bengal.

3.2.4 Winter season

In this season, southcentral Arabian Sea registers maximum heat content of $59*10^8$ J/M^2 (fig.3.13). The area of maximum heat content remains in the same region as during the previous season. Lower heat content of $54*10^8$ J/M^2 is noticed in the central Bay of Bengal. The maximum heat content both in Arabian Sea and Bay of Bengal corresponds to warmer SST of 29^o C (Ref. fig.2.16). Compared to previous season, Bay of Bengal shows lower heat

content while Arabian Sea recorded higher heat content. The heat content variations in the 2nd layer shows an increasing trend from west to east in the Arabian Sea with maximum occurring around 10^{o} N,60-64^{o} E (fig.3.14). Rate of heat content variations is more near the southwest coast of India and in the western parts of Bay of Bengal. A decreasing trend is seen from west to east in the central Bay of Bengal while the trend is reversed in the northern Bay of Bengal.

In the Arabian Sea, variations in heat content in the 3rd layer are similar to to those in the next upper layer(fig3.15). Minimum heat content of $34*10^{8}$ J/M^{2} is noticed around 14^{o} N,85^{o} E, from where, it increases in all directions. The heat content of lower layer (4th) shows maximum of $39*10^{8}$ J/M^{2} in the same region as in the case of upper (100-150m) layer. In the central Arabian Sea heat content increases towards west while, it increases towards east in the southern Arabian Sea(fig.3.16).

The decrease in heat content between the surface (0-50m) layer and the next layer is minimum (about $2*10^{8}$ J/M^{2}) in the south western Arabian Sea and central Bay of Bengal but, it is maximum (about $8*10^{8}$ J/M^{2}) along the western coast of India and in the northeastern Bay. Almost similar decrease is seen in the layers between 2nd and 3rd. The reduction in heat content between the lower two layers is about $3*10^{8}$ J/M^{2} near the western coast of India and about $9*10^{8}$ J/M^{2} in the Central Arabian Sea. The heat loss between these two layers is almost uniform in most parts of Bay of Bengal.

3.3 Daily variations of heat content

In order to study the daily variations, average heat content of the polygon areas (Ref.fig.1.1) for different layers during 1977 and 1979 have been considered.

3.3.1 Area-I Phase I

During MONSOON-77, the first phase of observation was carried out during 6-20th June and the second phase during 30th June to 15th July. Fig(3.17,a) shows the daily variations in heat content of the different layers during the 1st phase. It is seen that, the heat content slightly decreases from 6th to 7th June in the surface layer (0-50m) and then decreases sharply to a maximum of $63*10^8$ J/M^2 on 9th. Subsequently, it decreases gradually reaching a minimum of $57*10^8$ J/M^2 on 18th June. The corresponding SST shows more or less a similar variation as that of the heat content of 0-50m layer. The 2nd layer shows more or less opposite variations compared to the above layer. From 6-13th June, heat content fluctuates by $3.5*10^8$ J/M^2 and afterwards remains steady up to 20th June. The lowering of heat content between the 1st and 2nd layers varies from $7.5*10^8$ J/M^2 to $13*10^8$ J/M^2. The corresponding values between 2nd and 3rd layers are $2*10^8$ J/M^2 and $8.5*10^8$ J/M^2 and those between the lower two layers are $8*10^8$ J/M^2 and $11.5*10^8$ J/M^2. The lower two layers show in general, an increasing trend contrast to the upper two layers. The daily fluctuations in heat content are not very prominent in this period probably because of the low variations in MLD.

3.3.2 Area-I Phase-II

The day to day variations of heat content during 30th June to 15th July are presented in fig(3.17,b). The heat content in all the four layers show gradual decrease up to 7th July thereafter it increases up to 13th July. Subsequently, the heat content decreases beyond 13th July,thus exhibiting a wavy pattern. The variations of heat content in the surface layer somewhat follows the daily variations of SST. The heat loss between successive 50m layers increases downwards. It varies between $4*10$ to $9*10^8$ J/M^2 between the 1st and 2nd layers. The corresponding values between the 2nd and 3rd layers are $5*10^8$ J/M^2 and $9*10^8$ J/M^2 and that between the next pair of layers are $5*10^8$ J/M^2 and $14.5*10^8$ J/M^2 .

During MONEX 79, heat content variations of different layers were analysed in three polygon areas viz. 1. Area-II (16-23 rd May) 2. Area-III (2-10th June) 3. Area-IV (10-23rd July).

3.3.3 Area-II (16-23rd May 1979)

Fig (3.18,a) shows the daily variations in heat content during May 1979. The heat content in the upper layer decreases from $60.5*10^8$ J/M^2 on 16th to $58*10^8$ J/M^2 on 19th May. Subsequently, the heat content shows an increase reaching $60.5*10^8$ J/M^2 on 21st, thereafter it shows slight decrease. The 2nd and 3rd layers however show more or less constant heat content. The variations of SST shows a trend similar to the variations in heat content of the top layer up to 18th May.

Subsequently, the SST gradually increases up to 21st May and decreases afterwards. The magnitude of heat loss between successive layers is more or less the same except during 16-18th May when the heat loss is slightly higher between the 3rd and 4th layers.

3.3.4 Area-III (2-10th June 1979)

In this area, the heat content in the upper two layers show more or less uniform value during the period of observations except for minor fluctuations amounting to $2*10^8$ J/M^2 (fig.3.18,b). The 3rd and 4th layers show an increasing trend with slight daily fluctuations not exceeding $3*10^8$ J/M^2 .Heat content in the upper layer and the SST show more or less similar variations during this period also. The lowering of heat content between 1st and 2nd layer and 3rd and4th layer exhibits equal magnitudes. However, the heat loss between the 2nd and 3rd layers seems to be slightly higher magnitude than the layers both above and below.

3.3.5 Area-IV (10-23rd July 1979)

In the Bay of Bengal polygon, the surface layer shows more or less constant heat content with minor fluctuations amounting to $3*10^8$ J/M^2 (fig.3.19). The fluctuations in SST are also small for this period. Thus the surface layer heat content is mainly controlled by the SST. All the layers show a minimum heat content on 12th July and maximum on 21 st July. ON 12th July, heat content of 50-100m layer in particular and all the other lower layers in general, is less while, the MLD of the same day is more

(fig.2.22,c). This could be possible if the heat from this region gets transported to the other region on this day. In contrast to the surface layer, the lower three layers exhibit much variations. The variations in MLD are also large in this period. In the 2nd layer heat content decreases sharply from a value of $51.5*10^8$ J/M^2 on 10th to $42*10^8$ J/M^2 on 12th July, afterwhich heat content increases upto 17th July, thereafter fluctuate considerably from day to day. The lower two layers also show similar trend in heat content variations as the 50-100m layer. The variations in SST also exhibit more or less similar trend as the heat content variations in the surface layer. The reduction in heat content between the first two layers varies between $7*10^8$ and $16*10^8$ J/M^2 . The corresponding values between the 2nd and 3rd layers are $8.5*10^8$ and $16*10^8$ J/M^2 and those between the lower two layers are $7.5*10^8$ and $12.5*10^8$ J/M^2.

3.4 Cyclone heat potential (CHP_{28})

The role of heat potential in atmospheric disturbances is examined using information from Indian Daily Weather Reports on the cyclonic storm formed in the eastern Arabian Sea and in south western Bay of Bengal. The track of three storms formed in the Arabian Sea and Bay of Bengal during June 1977, May and June 1979 are presented in fig (3.20). The variations of CHP_{28} has been studied in relation to surface wind speed.

Cyclone heat potential is estimated by two methods which were explained in chapter-I. Daily variations of CHP_{28} were analysed during June 6-20th 1977 and June 2-14th 1979 in the

Arabian Sea. For this, CHP_{28} has been estimated as the heat content over 28^{o} C isotherm.

Utilizing the satellite derived wind speed and SST, CHP_{28} has been estimated in the Bay of Bengal and Arabian Sea before and after two storms (fig.2.20 b & c) during both May and June 1979. The CHP_{28} estimated from satellite parameters were compared with the values estimated from temperature profiles. The correlation coefficient is equal to 0.968. Table 3.1 gives the comparison of CHP_{28} obtained from satellite and ship. The values obtained from ship and satellite parameters are comparable ($\pm$8% for a range of 5.8 to $6.7*10^{8}$ J/M^{2}). At three points the variations in CHP_{28} are wider, this can be expected considering that wind speed have been obtained by extrapolating cloud motion vector winds to the surface.

3.4.1. CHP_{28} during 8-12th June 1977

A low pressure area formed at 15^{o} N,70^{o} E on 8th June, deepened to depression in the next day and intensified in to a cyclonic storm and moved northwestward during 10-12th June (fig.3.20,a).

The temporal evolution of daily average temperature profile for the polygon area I before and after the above storm is shown in fig (3.21). It is clear that from 8-13th June, MLD deepened by 20m. Significant cooling up to 75m is noticed after the storm. This cooling and deepening of mixed layer is probably because of enhanced mixing caused by upwelling due to strong winds.

Table.3.1 Comparison of CHP_{28} estimated from satellite-derived parameters and ship measurements ($*10^8$ J/M^2)

Satellite derived	Ship derived	Difference
7.5	6.6	0.9
6.0	5.8	0.2
5.8	5.8	0.0
5.8	6.3	0.5
4.8	6.7	1.9
5.8	6.4	0.6
6.1	6.4	0.3
6.9	6.7	0.2
7.7	6.7	1

The daily variations of CHP_{28} and surface wind speed during 6-20th June 1977 are presented in fig (3.22,a). CHP28 increases from $5.8*10^8$ to $6.8*10^8$ J/M^2 during 6-9th June. A sharp decrease of about $1.4*10^8$ J/M^2 is noticed from 9-12th June afterwhich a gradual increase is seen on 13th June.

The surface wind speed shows a maximum on 10th June after which, it decreases sharply to a minimum on 14th June. The increase in CHP_{28} and wind speed during 6-9th June indicates a favorable condition for the formation of a depression. The sudden decrease in CHP_{28} from 9th to 12th June implies a net oceanic heat loss during the storm event. Similar fall in ocean heat potential has been observed during the onset of a cyclonic storm in the south western Bay of Bengal (Rao,1987,b). Low CHP_{28} observed during 12-15th June may be caused by mixing due to upwelling resulted by the passage of storm. The decrease in CHP_{28} due to upwelling at the center of the storm has been reported earlier in the Arabian Sea by Ramesh Babu and Sastry (1984) and Rao et al,(1983). Seetharamayya and Mullen (1987) found a fall of $3*10^8$ J/M^2 in cyclone heat potential during 9-18th June and the corresponding fall in SST is about 0.5^{o} C after the passage of onset vortex. This lowering of SST may be due to the entrainment of cold sub-surface water into the surface and the subsequent mixing between cold deep waters and warm waters results downward transfer of heat (Ramesh Babu and Sastry,1984).

3.4.2 CHP_{28} during 5-13th May 1979

The well marked low pressure, which intensified in to a depression on the evening of 5th May. lay around 7^{o} N,90^{o} E. Moving slowly westwards, the depression developed into storm by the morning of 7th May near 7^{o} N,88^{o} E (fig.3.20,b). The storm took a southwesterly track and developed into a cyclonic storm by the morning of 11th May and developed into a hurricane with maximum intensity on 11and 12th May. It crossed the Andhra coast between Nellore and Ongole by the evening of 12th May and gradually dissipated by the morning of 14th May.

The vertical temperature profile on 5th and 14th May at a fixed position around 7.5^{o} N,87^{o} E is presented in (fig. 3.21) shows a deepening of 25m in MLD after the storm.

Due to the scarcity of ship observations during this storm event in Bay of Bengal, CHP_{28} only from satellite parameters have been analysed. Fig (3.23) shows the distribution of CHP_{28} on 1st and 17th May 1979 (4 days before and 4 days after the storm). On 1st May, the heat potential increases in the southwesterly direction reaching a maximum of $6.6*10^{8}$ J/M^{2} around 13.5^{o} N.83^{o}E (fig.3.23,a). This increase in CHP_{28} also confirm the indication for the formation of depression as discussed in the earlier sections. Rao and Rao (1986) observed a gradual increase in heat potential before the formation of a depression in the northern Bay of Bengal. The low heat potential observed on 17th May, around 15^{o} N,81^{o} E could be because of heat taken away by

the storm in the form of latent heat as this area is along the track of cyclone (fig.3.23,b).

The distribution of surface wind speed on 1st and 17th May (fig.3.24) shows very low values near the central Bay on 1st May. Wind speed increases rapidly towards west, reaching a maximum of 7.5m/s at 14^{o} N 83^{o} E. Comparing this with fig (3.24,a) it is seen that for both wind speed and CHP_{28} the trends of gradient are same on 1st May. On 17th may wind speed increases in the direction of passage of the storm (fig.3.24,b).

3.4.3 CHP_{28} during 16-19th June 1979

A cyclonic cell, the monsoon onset vortex, which was noticed on 14th June intensified into a depression around 14^{o} N,70^{o} E (fig.3.20,c). Between 16-18th June, a core of strong winds of 60-70 knots was seen along 8-10^{o} N. On moving northwestwards, the depression intensified into a storm and crossed the Arabian coast by 20th June 1979.

From the temperature profile on 14th and 21st June 1979 (fig.3.21), mixed layer deepening of 18m is observed after the storm in the polygon area III.

Fig(3.22,b) shows the daily variations of CHP_{28} and wind speed during 2-14th June immediately before the commencement of a cyclonic storm. CHP28 shows a decrease of $2.1*10^{8}$ J/M^{2} from 2-4 June afterwards, it increases to a maximum heat potential on 14th June with small fluctuations in between. This increase in CHP_{28}

favours the intensification of low pressure which persisted near Lakshadweep during 8-13th June. The corresponding surface wind speed shows an increasing trend throughout the period.

The distribution of CHP_{28} and wind speed before and after this storm derived from satellite data can be seen in fig (3.25 and 3.26). Before the onset of storm,ie, on 10th June, maximum CHP_{28} is recorded near the southwest coast of India (fig.3.25,a). This also indicate a favorable response for the monsoon vortex, which deepened into a depression on 16th June around 13^{o} N,71^{o} E. The surface wind speed shows a maximum of 7m/s in the same area of maximum CHP_{28} (fig.3.26,a). After the monsoon vortex, CHP_{28} showed a fall of about 10^{8} J/M^{2} in the southeastern Arabian Sea (fig.2.25,b). On this day the CHP_{28} shows a decrease towards northwest. This may imply that heat has been taken away by the storm along its track. The corresponding wind speed shows an increasing trend towards northwest in the direction of passage of the storm (fig.3.26,b).

3.5 Discussion

In the preceding sections we have looked into the distribution of heat content in four different layers of 50m thickness analysed on a seasonal basis for the period 1977-1986 in the northern Indian Ocean. Daily variations in heat content of these layers in four different polygon areas and the variations in CHP_{28} during three storm events during MONSOON-77 and MONEX-79 were also studied. In the following section, the results obtained are discussed in detail in the light of earlier investigations.

The heat content of the surface layer (0-50m) shows maximum of $62*10^8$ J/M^2 during pre-monsoon season and a minimum of $50*10^8$ J/M^2 during monsoon season in the south centriole Arabian Sea. During the post-monsoon and winter seasons, the heat content values in this region are $58*10^8$ J/M^2 and $53*10^8$ J/M^2 respectively. Bruce (1987) reported a minimum heat content in the surface layer (0-100m) at the end of south west monsoon in the western Indian Ocean. He has noticed intense warming below 100m with the progress of southwest monsoon which was almost equal to the heat loss in the upper 100m layer. Varma (1989) observed a minimum heat content of about $52*10^8 J/M^2$ during July in the 0-50m layer both near the eastern central Arabian Sea and northern Somali coast. While analyzing the heat budget of the equatorial Atlantic, Merle (1980) also observed minimum heat content in the surface (0-50m) layer during monsoon season. The zonal variations of heat content in all the lower three layers more less follow the variations in the surface layer during monsoon. This could be because of vertical turbulent mixing caused by strong winds during monsoon season. During pre and post-monsoon seasons, the variations in heat content in the lower layers do not follow the variations in the surface layer may be due to relatively less mixing because of low surface winds.

Bay of Bengal exhibits higher heat content in the surface layer during monsoon compared to Arabian Sea. This could be due to comparatively high SST observed in this region during this season. But during the post-monsoon and winter seasons, when Bay

of Bengal and Arabian Sea shows similar magnitudes in SST lower heat content values are seen in the surface layer in Bay of Bengal. This low heat content is caused by mixing provided by upwelling above 100m. Rao (1987,b) noticed a gradual fall in heat content in the top 100m layer near southwestern Bay of Bengal which he attributed to vertical advective processes controlled by Ekman and probably geostrophic transports.

The decrease in heat content from west to east in the 1st layer in the north Equatorial region during monsoon season is mostly controlled by similar variations in the SST. Ali and Desai (1989) also observed similar variations in the equatorial Indian Ocean and suggested that the water below thermocline plays a greater role in determining the heat content variations. Rao (1987,a) reported a decrease in heat content from west to east in the central Arabian Sea during 7-13th June 1977. The decrease in heat content between the surface layer and the next layer (50-100m) is about $9*10^8$ J/M^2 in the eastern Arabian Sea which shows a continuous fall towards west. Varma (1989) observed a fall of $5*10^8$ J/M^2 in the eastern central Arabian Sea and near the Somali basin.

During monsoon, the reduction in heat content between the first and second layers is minimum in the eastern Arabian Sea (about $2*10^8$ J/M^2) and maximum (about $18*10^8$ J/M^2) in the western north equatorial Indian Ocean while the trend is different in Bay of Bengal. This maximum heat content variability in the western parts may be due to less mixing below 50m. A reduction of $8*10^8$ J/M^2 has been reported earlier (Varma,1989)

for the eastern central Arabian Sea and about $4*10^8$ J/M^2 for the northern part of Somali basin. Rao (1987,b) attempted to explain the heat content variations in the top 100m in terms of near surface mixed layer cooling and vertical advective processes in the upper thermocline.

During post-monsoon period, the lowering of heat content between the 1st and 2nd layers is comparatively less on the western side than the eastern region both in the Arabian Sea and Bay of Bengal. This is associated with the mixed layer cooling and deepening noticed on the western side and shallow MLD on the eastern side as discussed in the previous chapter.

In winter season, the decrease in heat content between the surface (0-50m) and the second layer is more in the southeastern Arabian Sea (about $10*10^8$ J/M^2) and less (about $2*10^8$ J/M^2) in its western side. Whereas in Bay of Bengal conspicuous variations are not present. This is probably due to a large temperature gradient associated with a shallow thermocline in the east and comparatively deep MLD in the west. Merle (1980) related the seasonal heat content variability to the shallowness of thermocline in the equatorial Atlantic region. Considerable reduction in heat content between the upper 100m and 100-200m layer has been noticed earlier along the Somali basin also (Bruce,1987).

The heat loss between successive layers beyond 100m exhibits higher values in the east and lower value in the west during both monsoon and winter seasons. During pre and post-

monsoon seasons, this trend ia more or less reversed in the Arabian Sea. Larger difference in heat content between successive layers encountered during the seasons when the temperature gradient is larger. Similar situation has been encountered while analyzing the heat content along the Somali region (Bruce,1987).

In Bay of Bengal, the lowering of heat content between successive layers beyond 100m shows higher values on the west and lower values on the east during pre and post-monsoon seasons. During monsoon season, larger heat loss between the 2nd and 3rd layers has been observed in the northwestern Bay of Bengal. This is because of shallow thermocline observed in this region. In winter season, the heat loss beyond 100m exhibits comparatively higher values on the west and lower values on the east.

Results of studies on daily variation of heat content during different periods have been presented in section 3.3. It is seen that in most of the cases, heat content variations in the surface layer coincides almost with SST variations. In Area- I, during 6-20th June 1977, the decrease in content between the upper and lower most layers is more compared to the middle layers (50-100m and 100-150m). This implies that downward advective transfer of heat decreases from the surface to deeper layers.

The variations in heat content during May 16-22nd and June 2-10th 1979 (Area II and III) are not significant compared to the variations during July 1979 in Bay of Bengal. The heat content in the surface layer is almost constant in the northern Bay of Bengal in July. The fluctuations of heat content observed

in the lower layers could be due to the vertical oscillations of thermocline.

Analyses of CHP_{28} during three storm events show in general, an increase in heat potential just before the storm and considerable decrease after the storm. Such lowering of heat potential due to passing storm has been observed earlier by few authors (Leipper,1967; Rao,et al,1983; Rao,1987(a); Ramesh Babu and Sastry,1984). Cooling and deepening of mixed layer is also noticed due to the passage of storms. Camp and Elsbery (1978) suggested that mixed layer cooling and deepening is mostly caused by vertical mixing during the passage of storm.

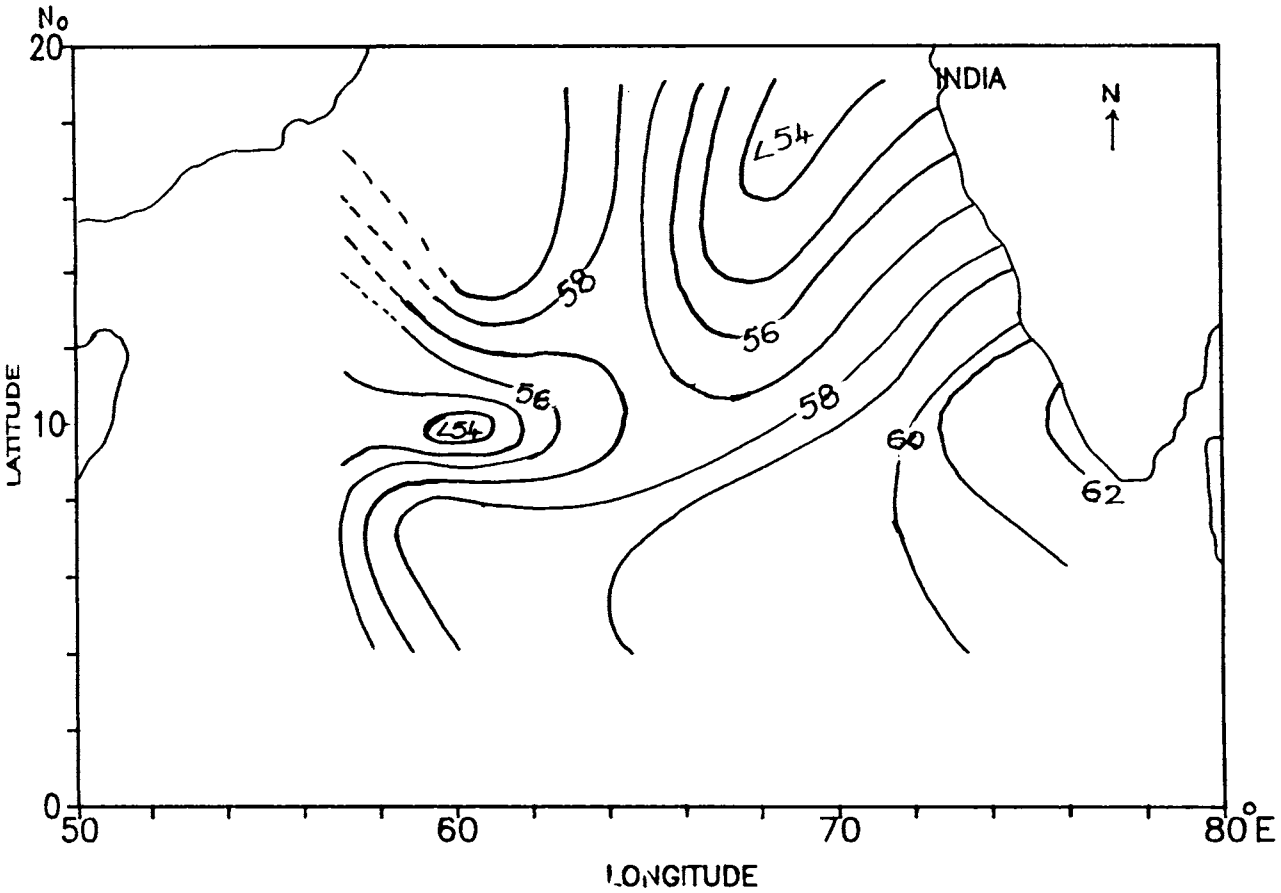

Fig.3.1 Distribution of heat content in 0-50m during pre-monsoon season ($10^8 J/M^2$)

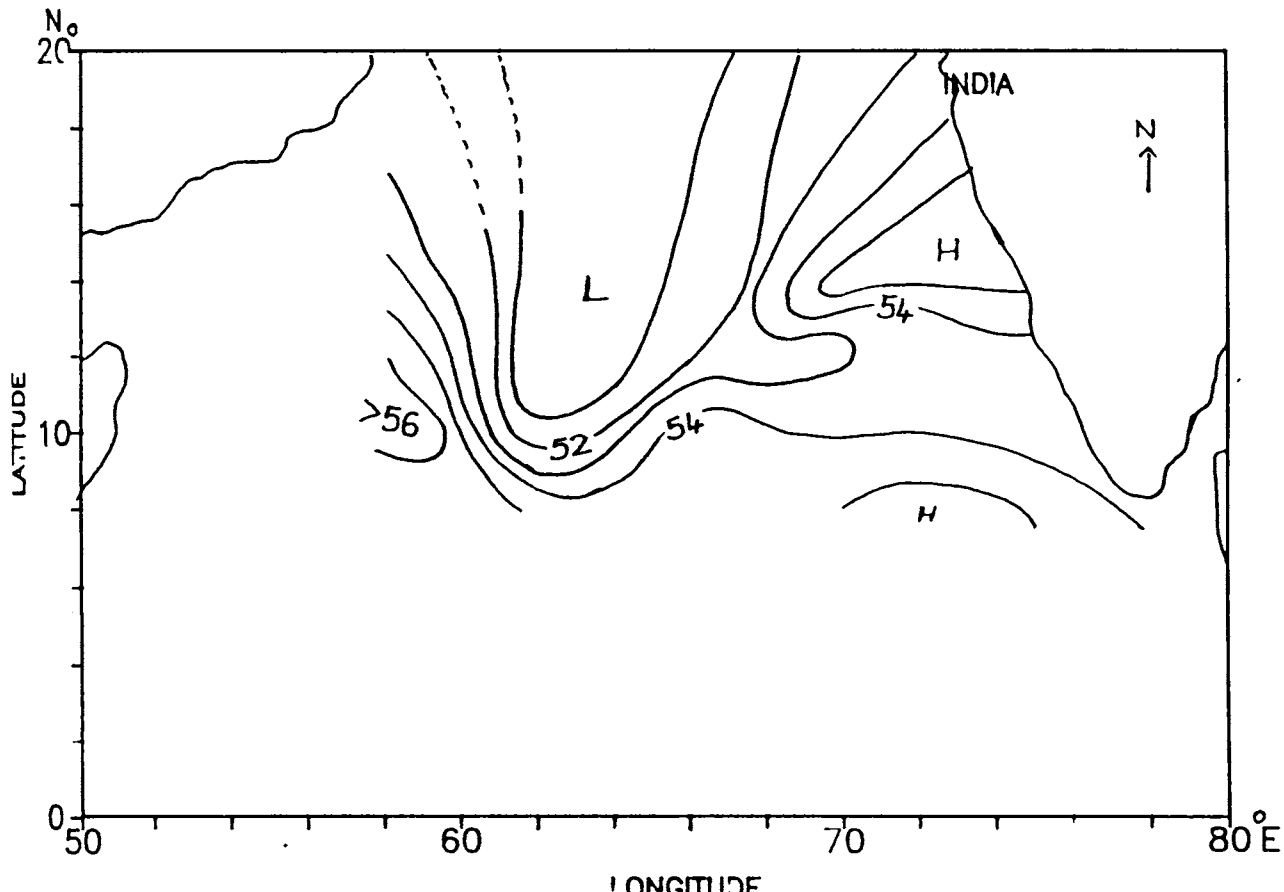

Fig.3.2 Distribution of heat content in 50-100m during pre-monsoon season (10^8 J/M^2)

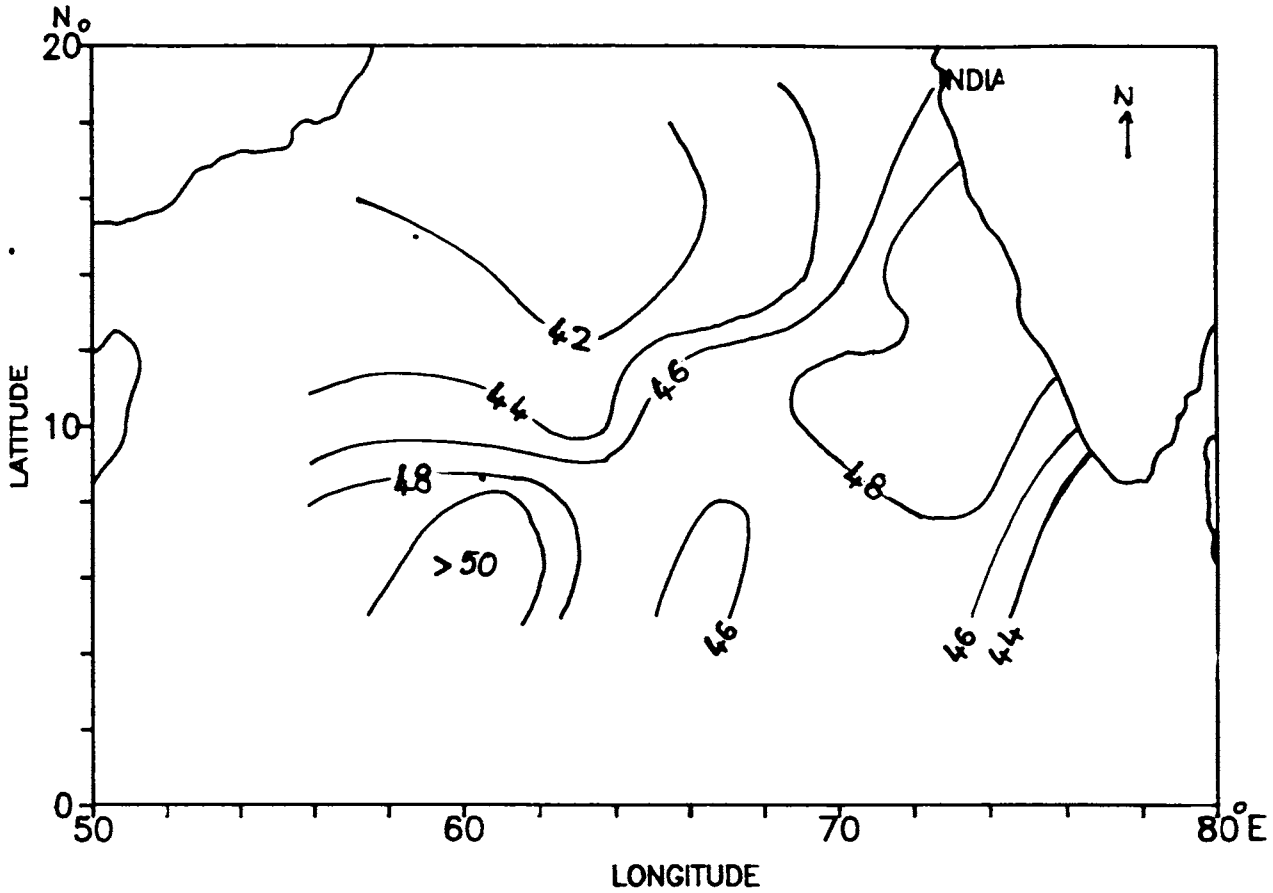

Fig.3.3 Distribution of heat content in 100-150m during pre-monsoon season (10^8 J/M^2)

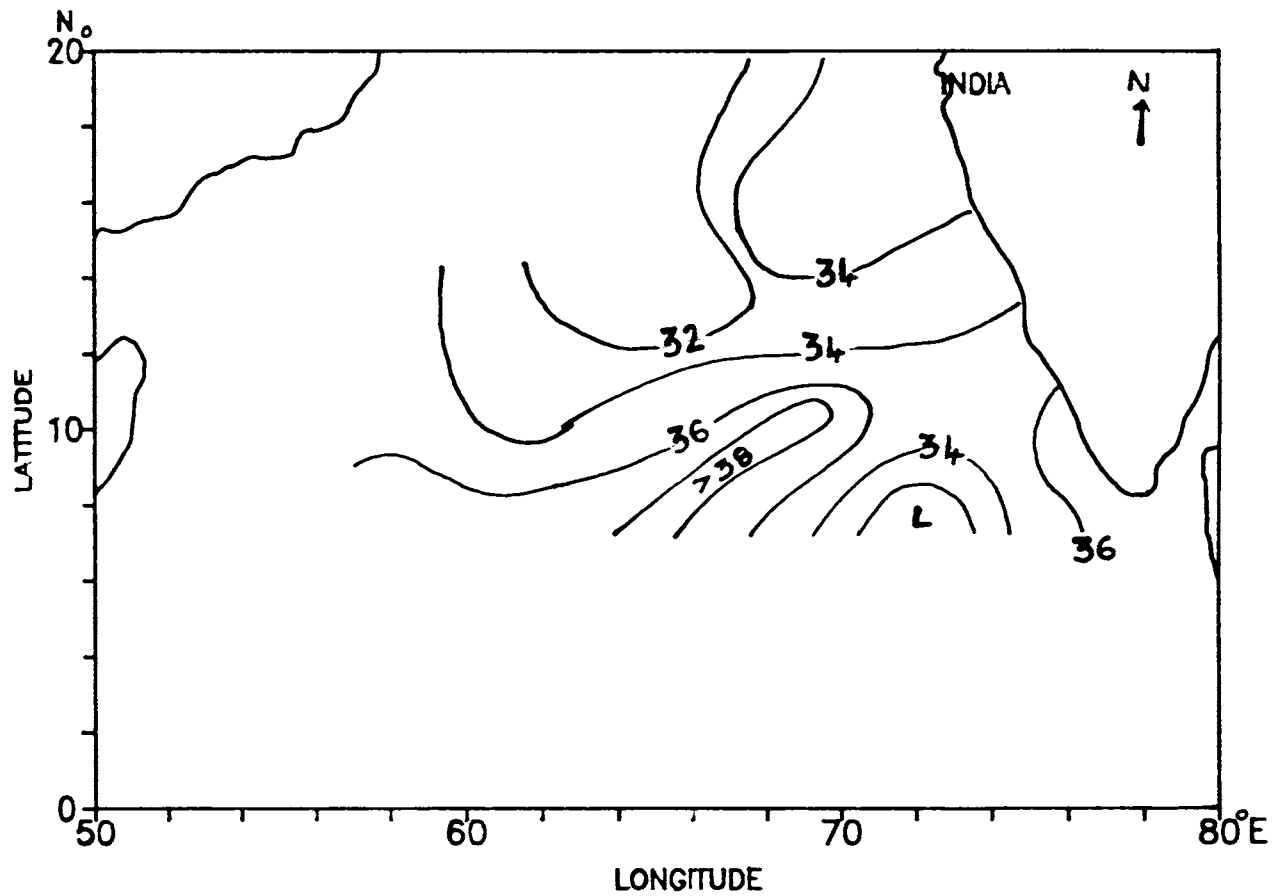

Fig.3.4 Distribution of heat content in 150-200m during pre-monsoon season (10^8 J/M^2)

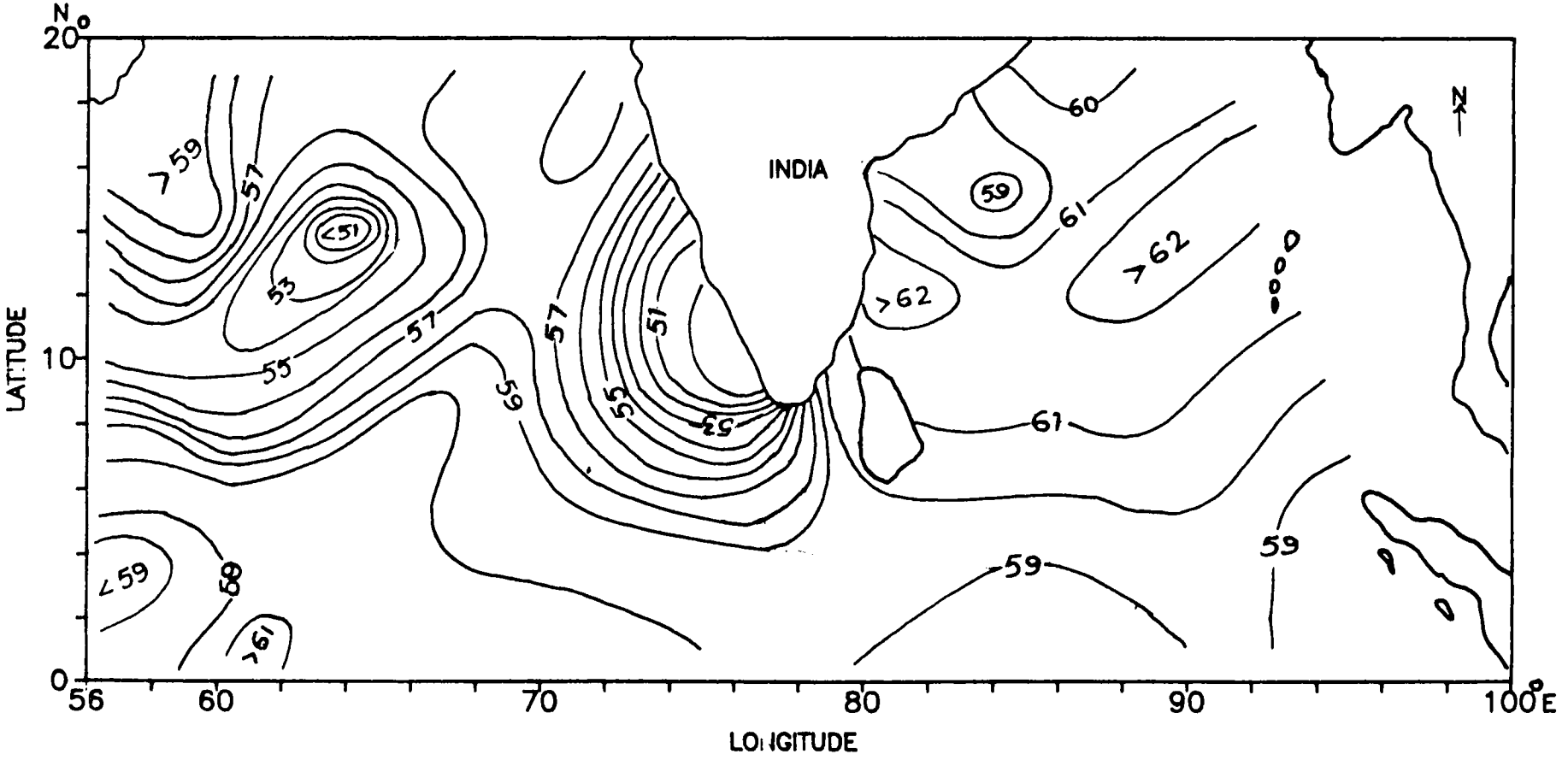

Fig.3.5 Distribution of heat content in 0-50 m during monsoon season (10^8 J/M^2)

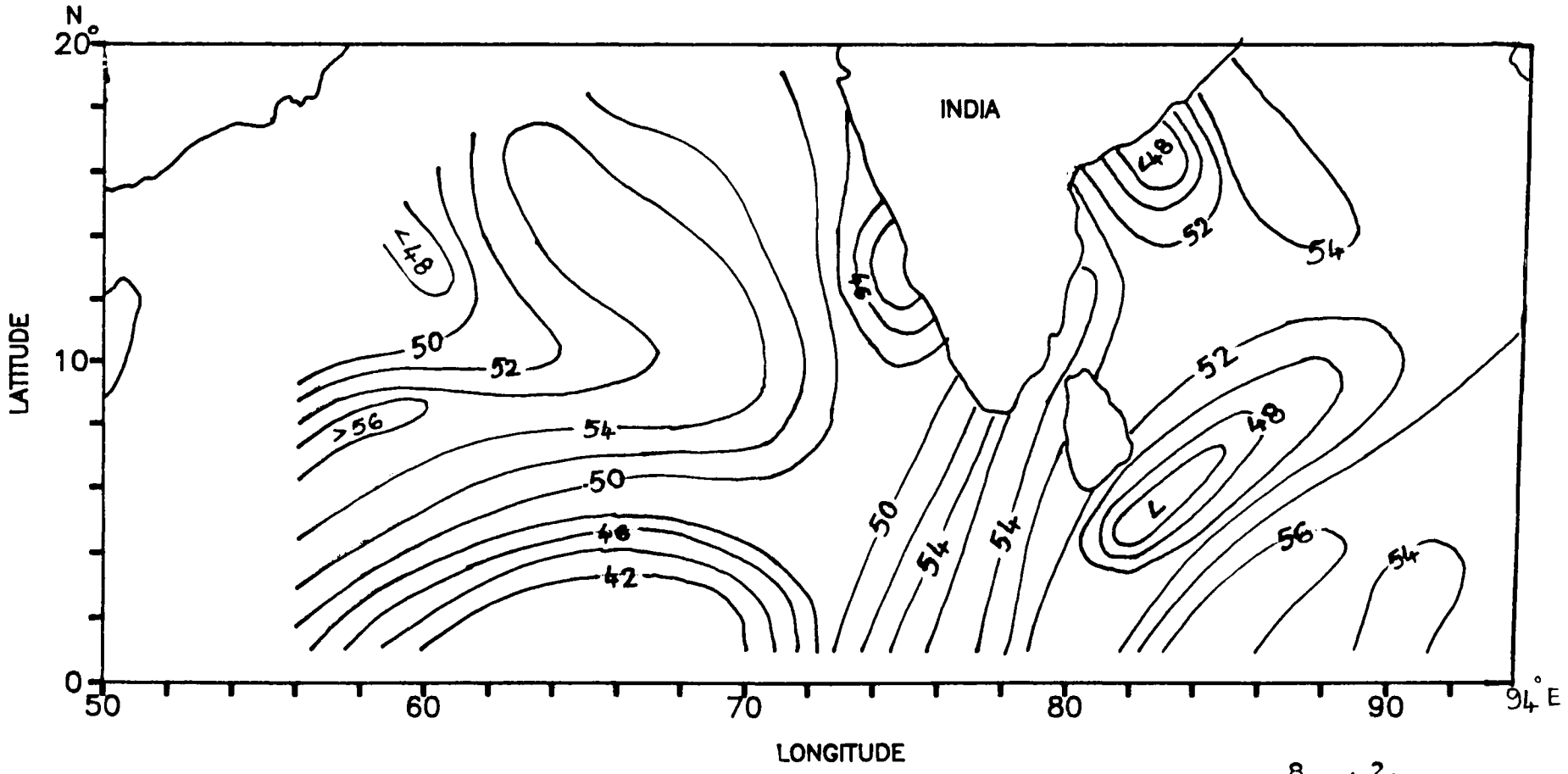

Fig.3.6 Distribution of heat content in 50-100m during monsoon season (10^8 J/M^2)

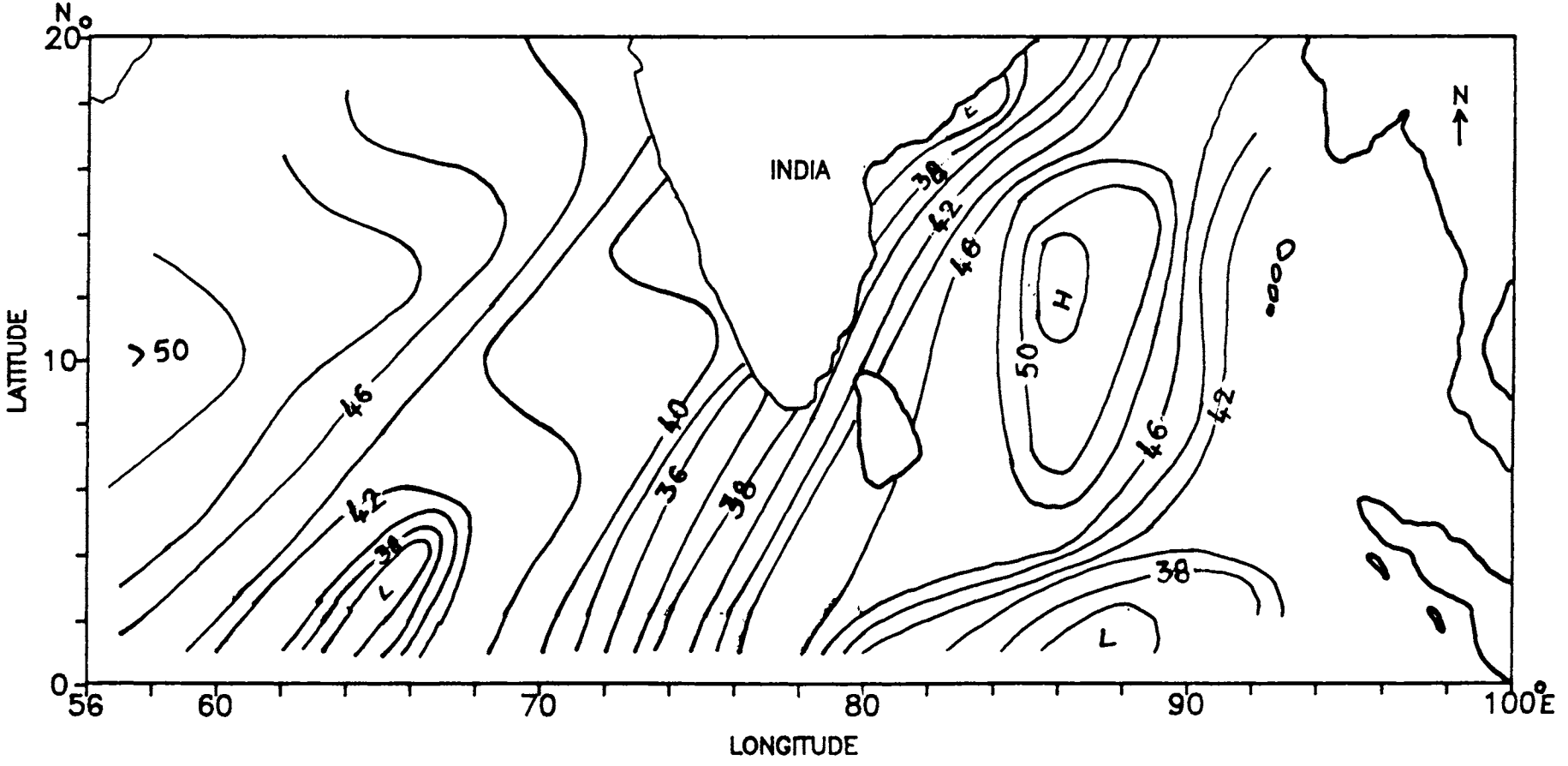

Fig.3.7 Distribution of heat content in 100-150m during monsoon season (10^8 J/M^2)

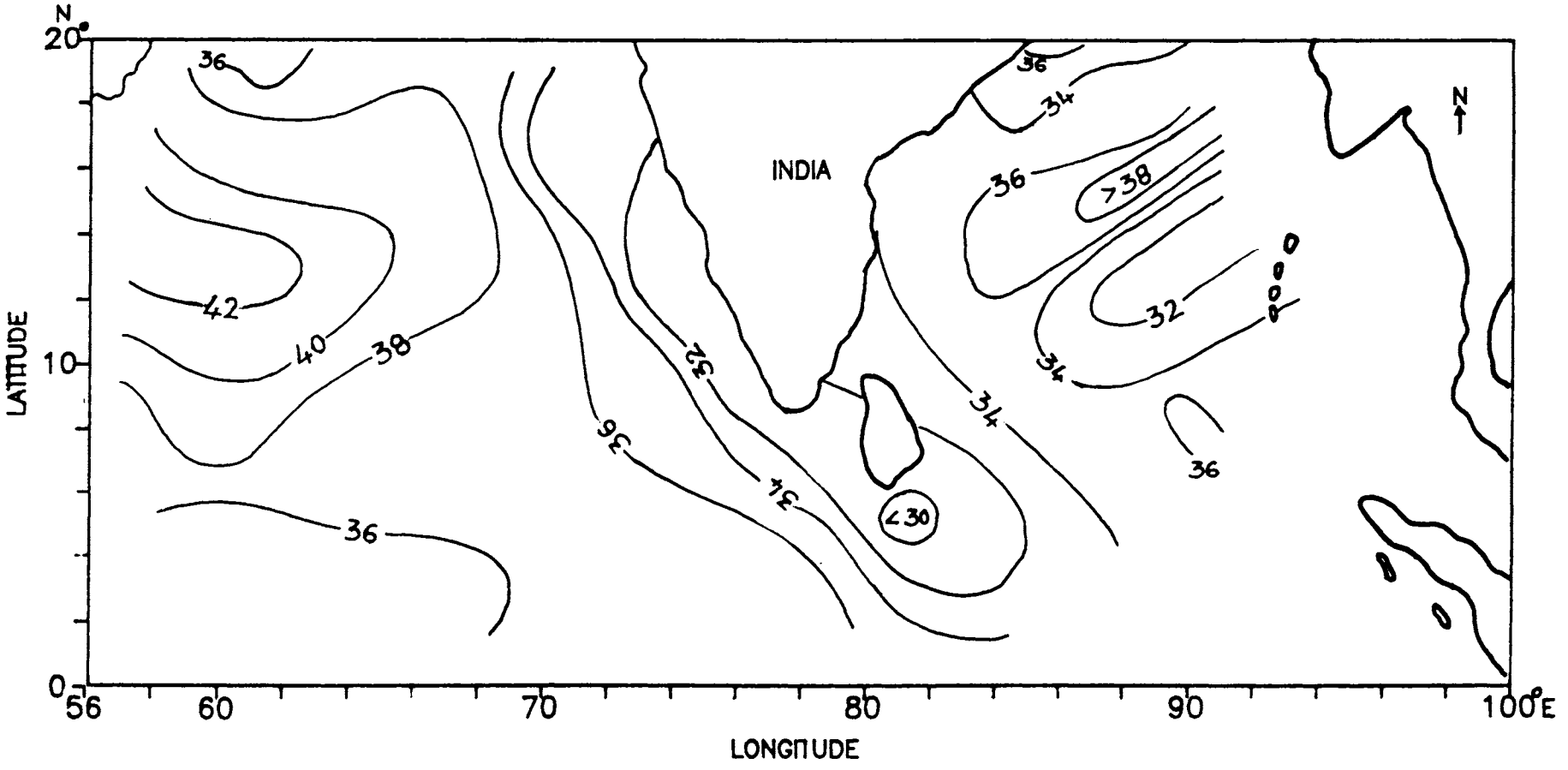

Fig.3.8 Distribution of heat content in 150-200m during monsoon season (10^8 J/M^2)

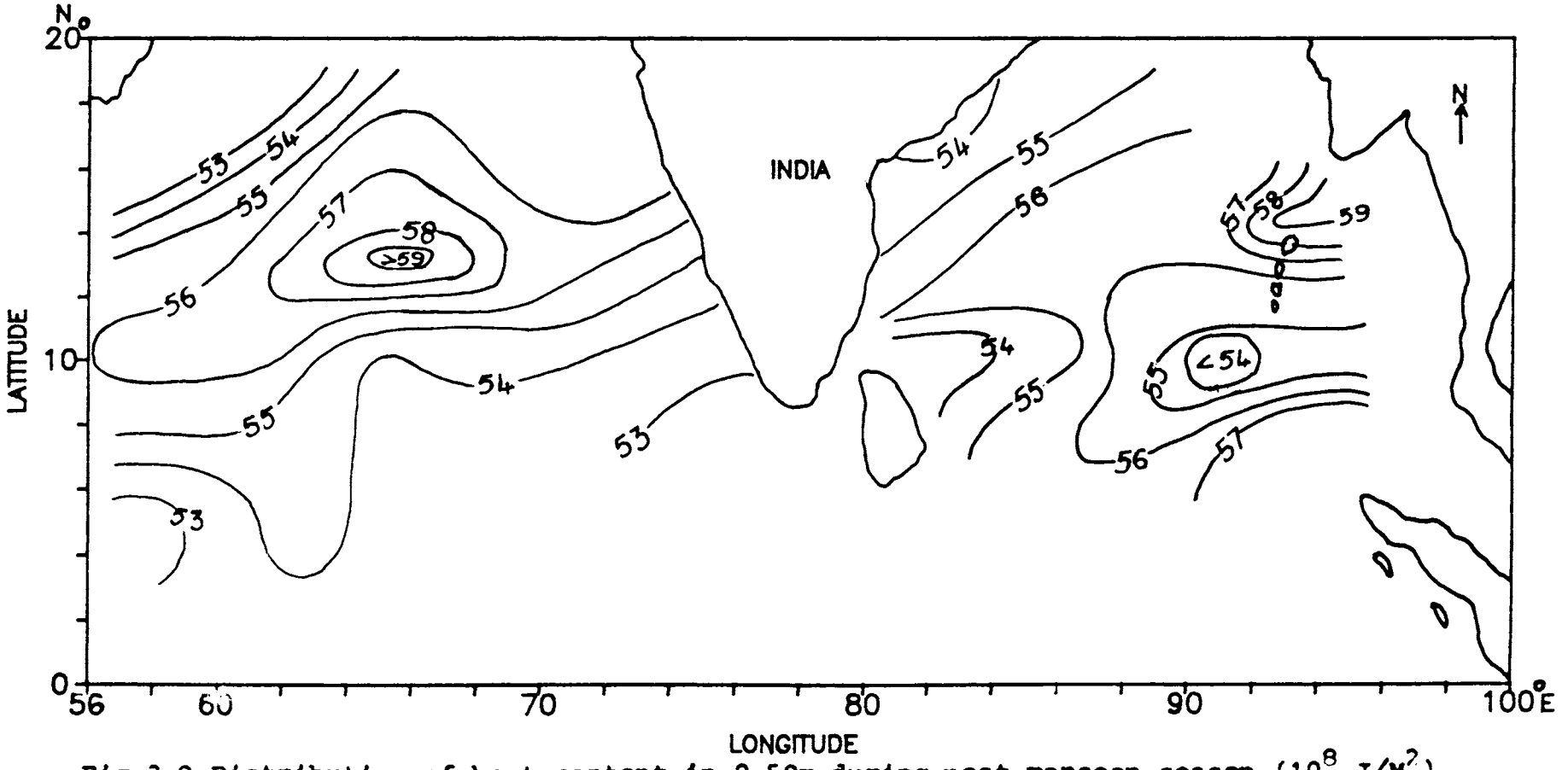

Fig.3.9 Distribution of heat content in 0-50m during post-monsoon season (10^8 J/M^2)

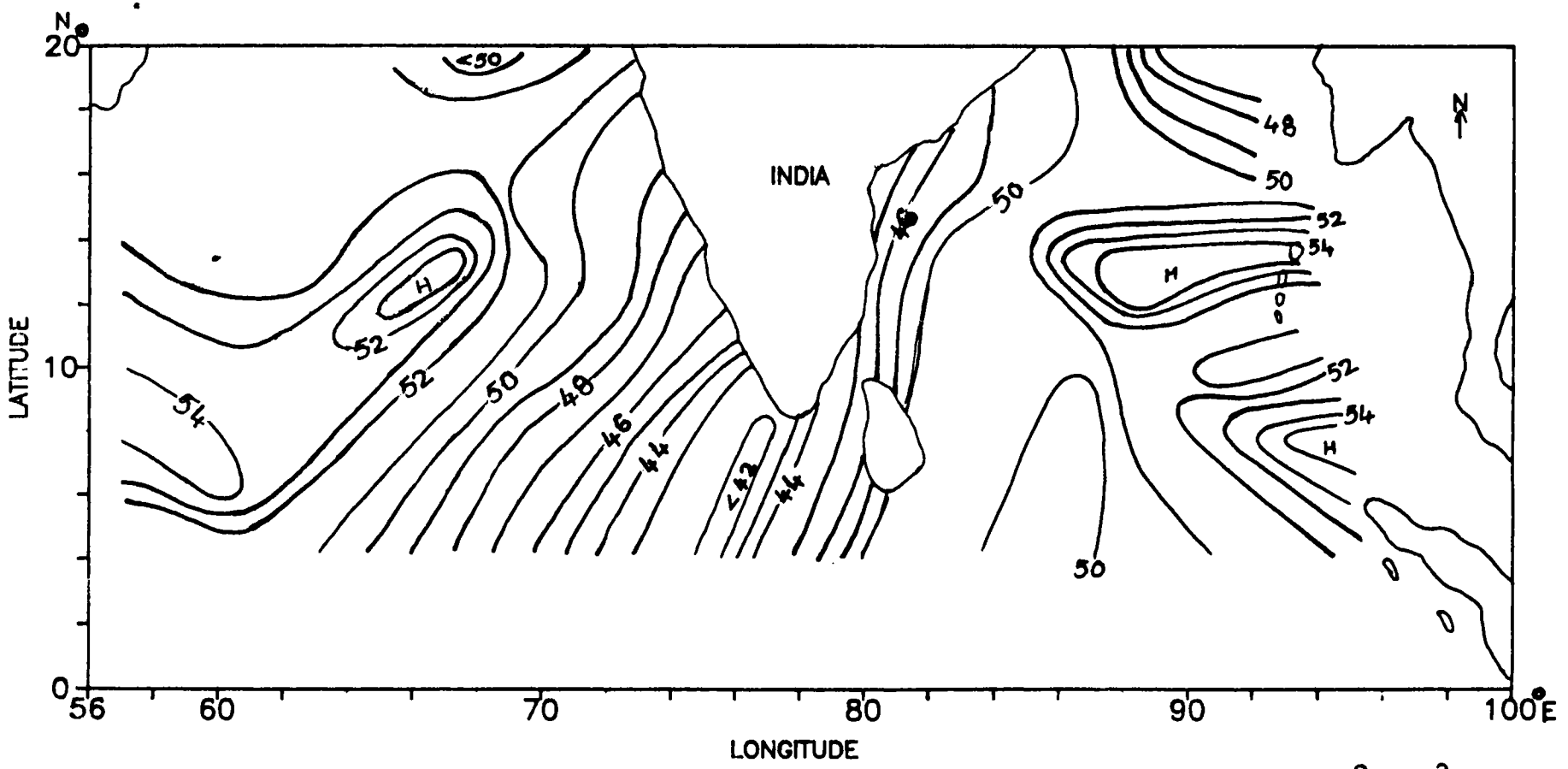

Fig.3.10 Distribution of heat content in 50-100m during post-monsoon season (10^8 J/M^2)

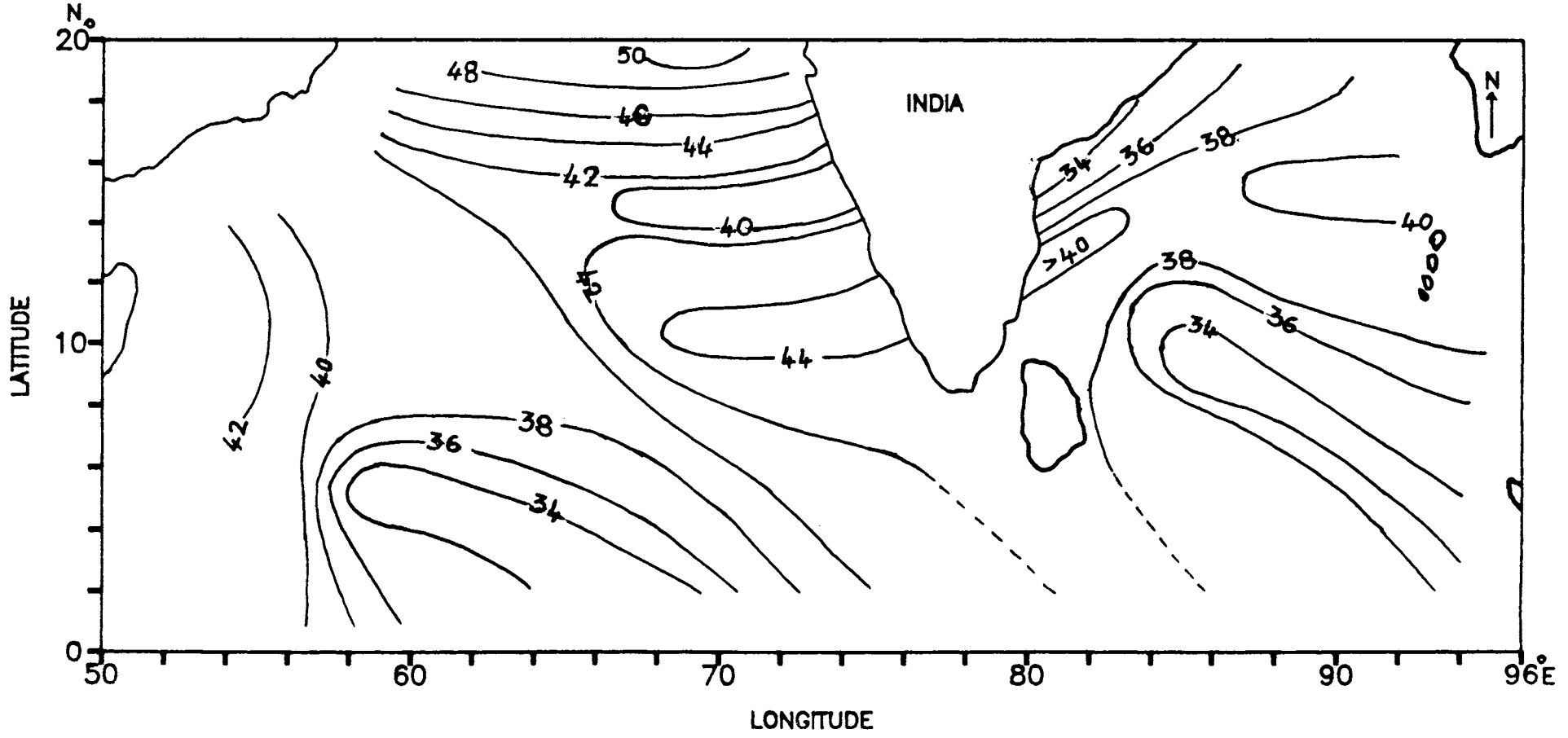

Fig.3.11 Distribution of heat content in 100-150m during post-monsoon season (10^8 J/M^2)

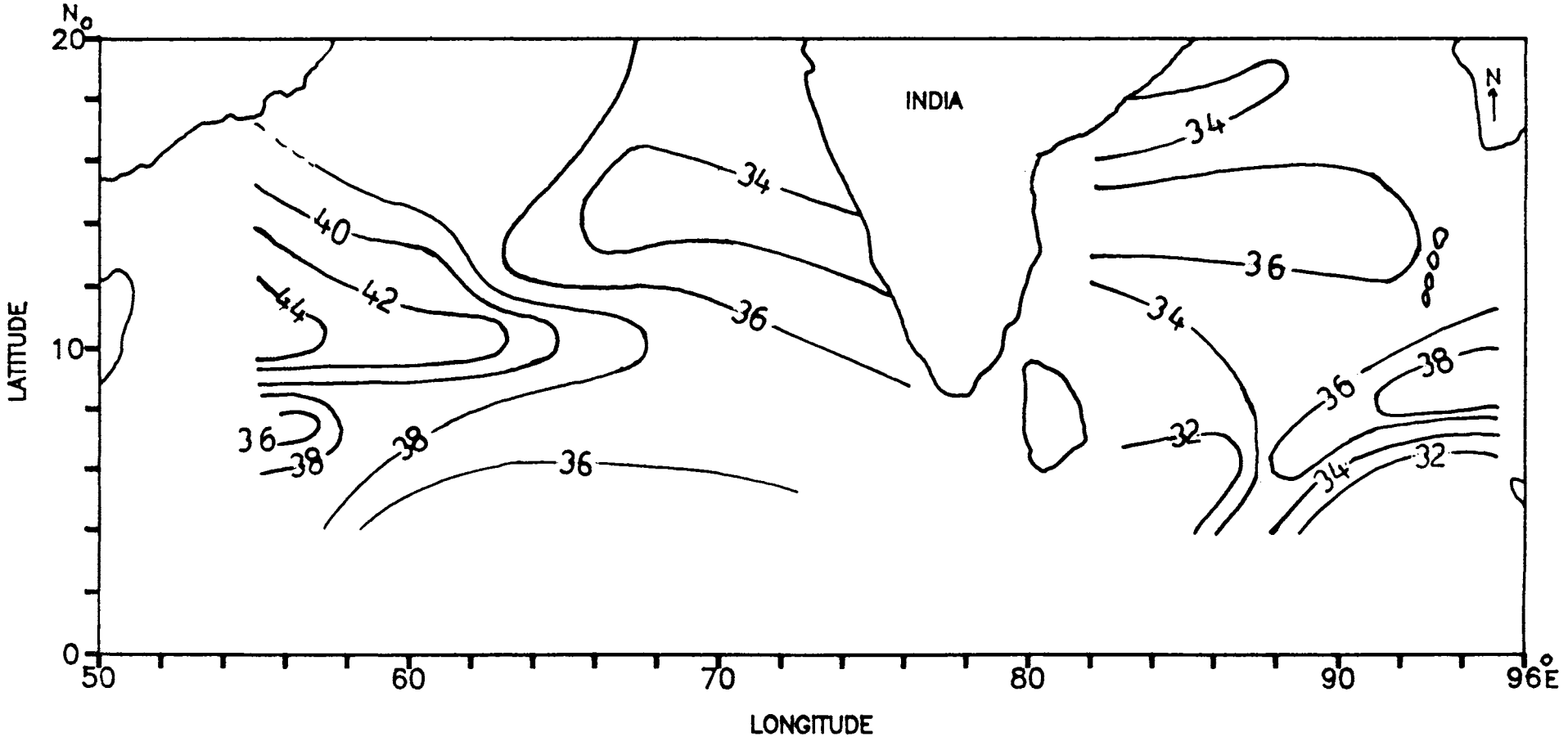

Fig.3.12 Distribution of heat content in 150-200m during post-monsoon season (10^8 J/M^2)

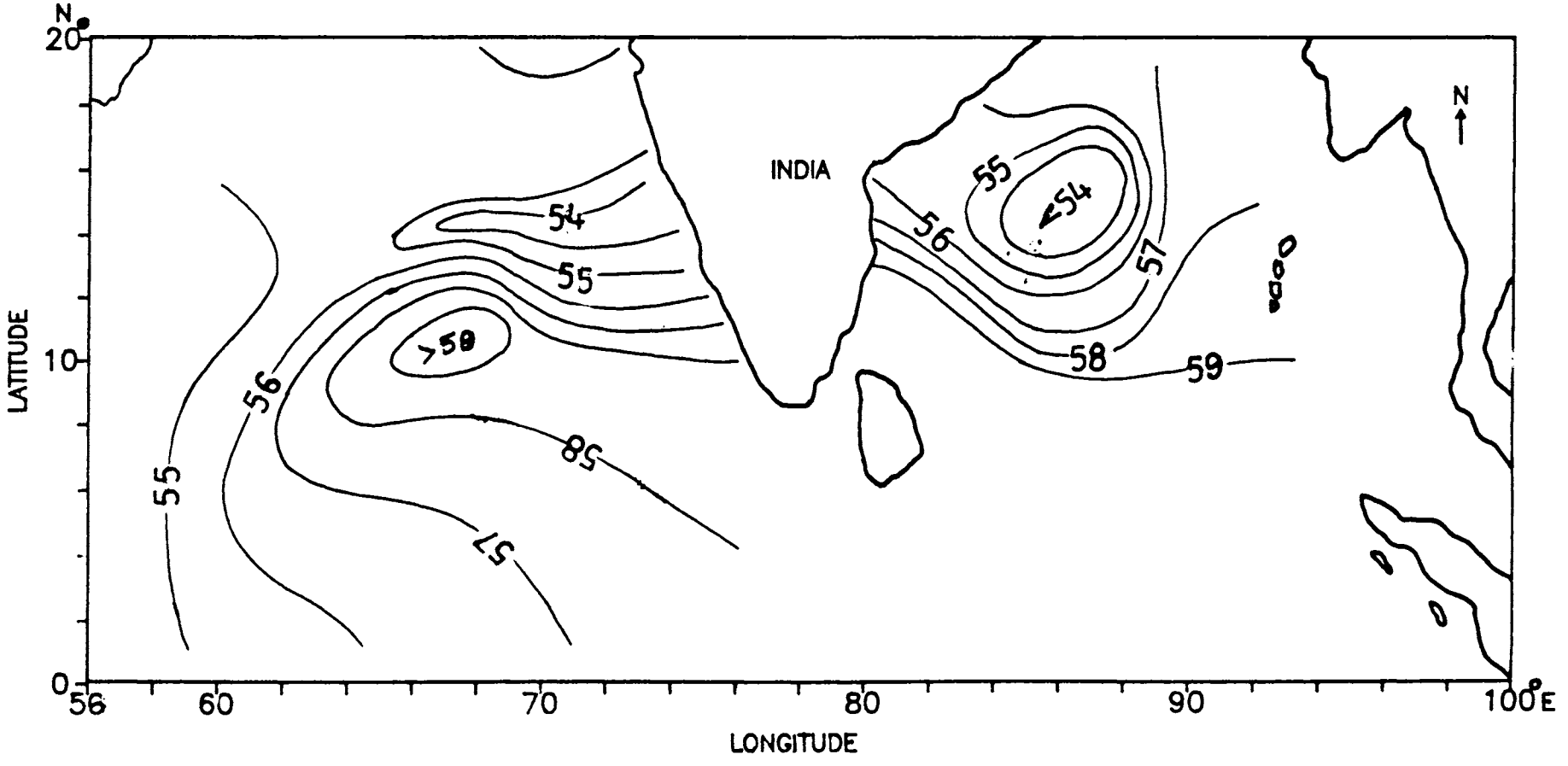

Fig.3.13 Distribution of heat content in 0-50m during winter season (10^8 J/M^2)

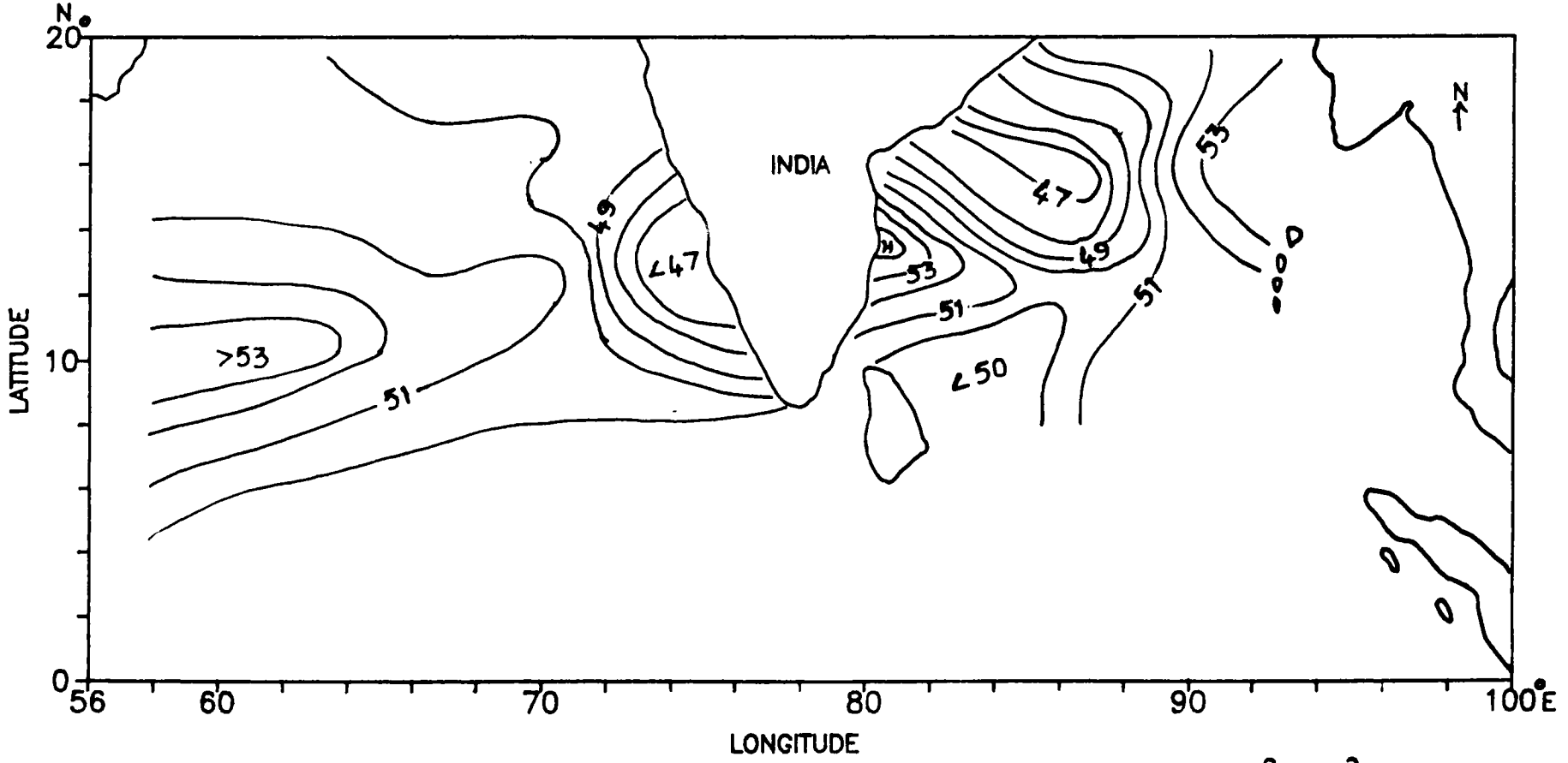

Fig.3.14 Distribution of heat content in 50-100m during winter season (10^8 J/M^2)

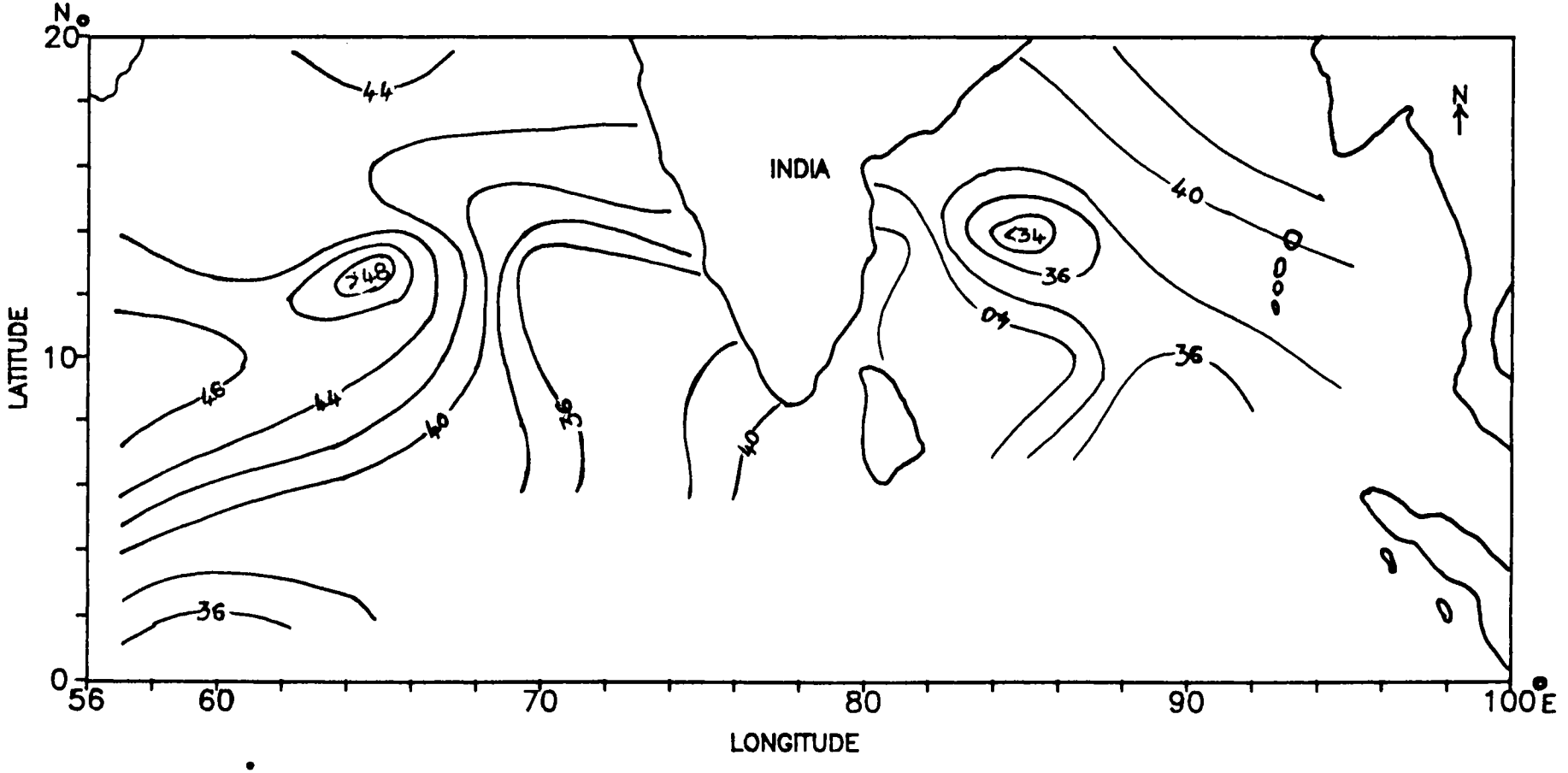

Fig.3.15 Distribution of heat content in 100-150m during winter season (10^8 J/M^2)

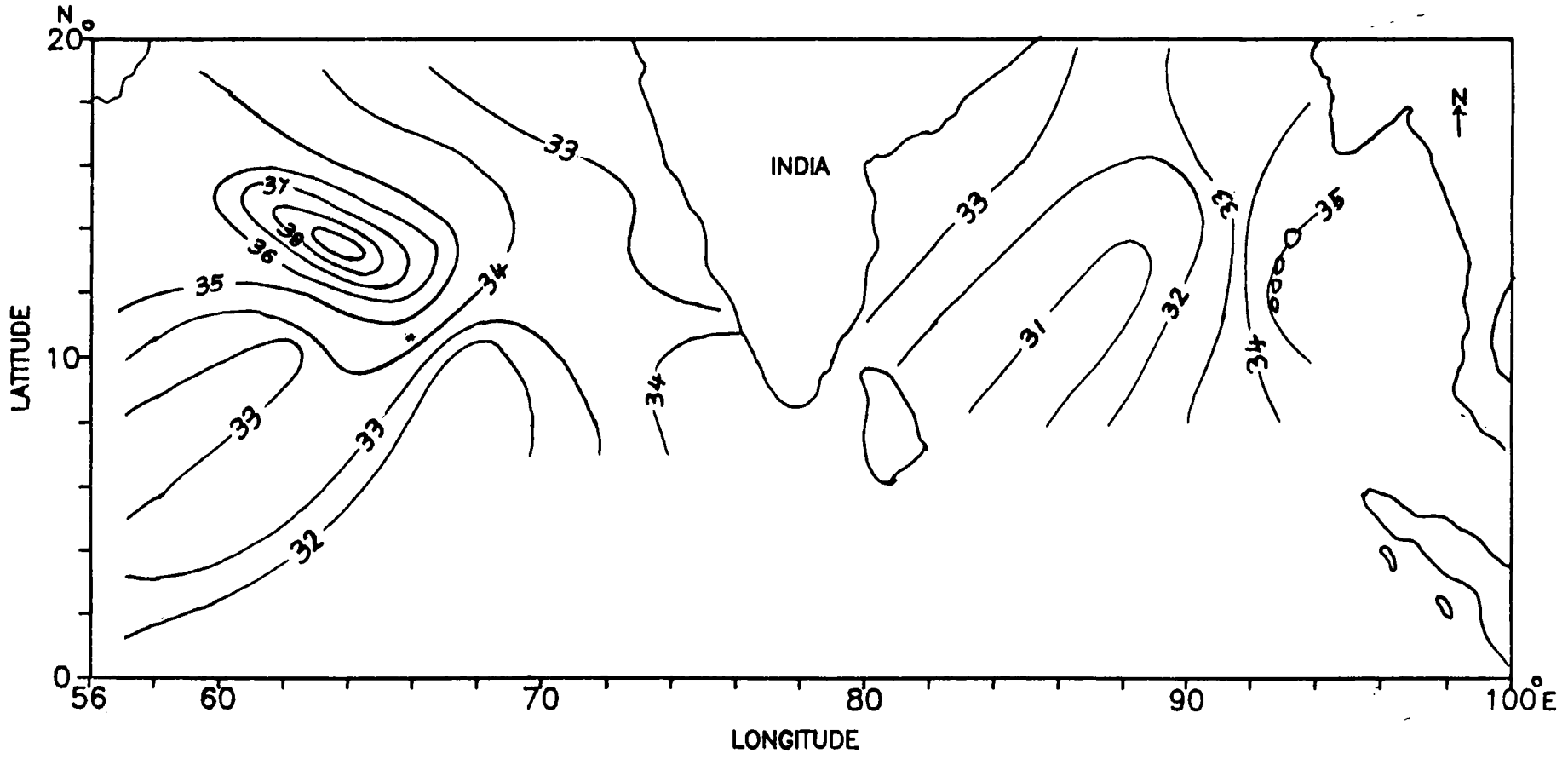

Fig.3.16 Distribution of heat content in 150-200m during winter season (10^8 J/M^2)

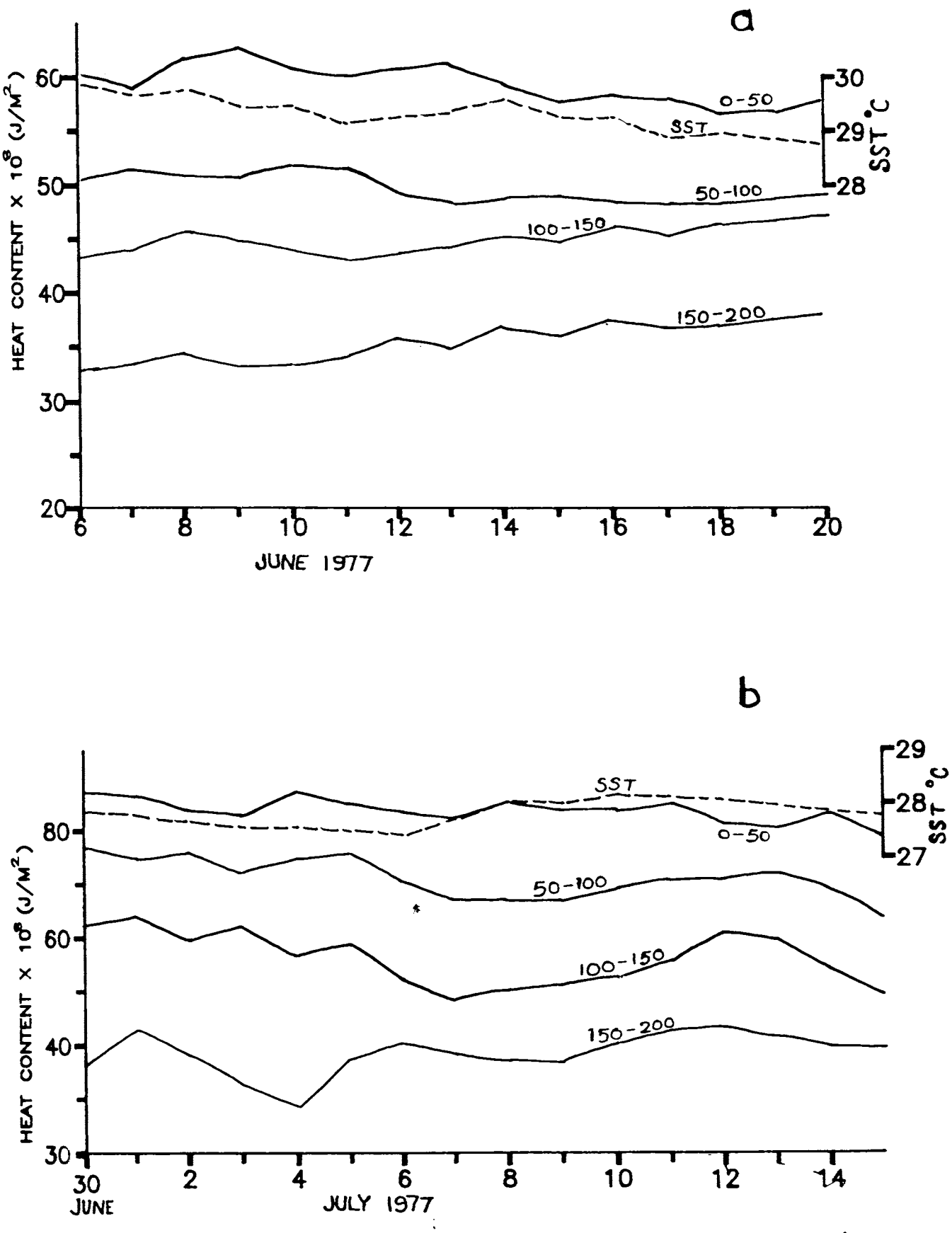

Fig.3.17 Daily variation of heat content in different layers in Area-I (a) Phase-I (b) Phase-II

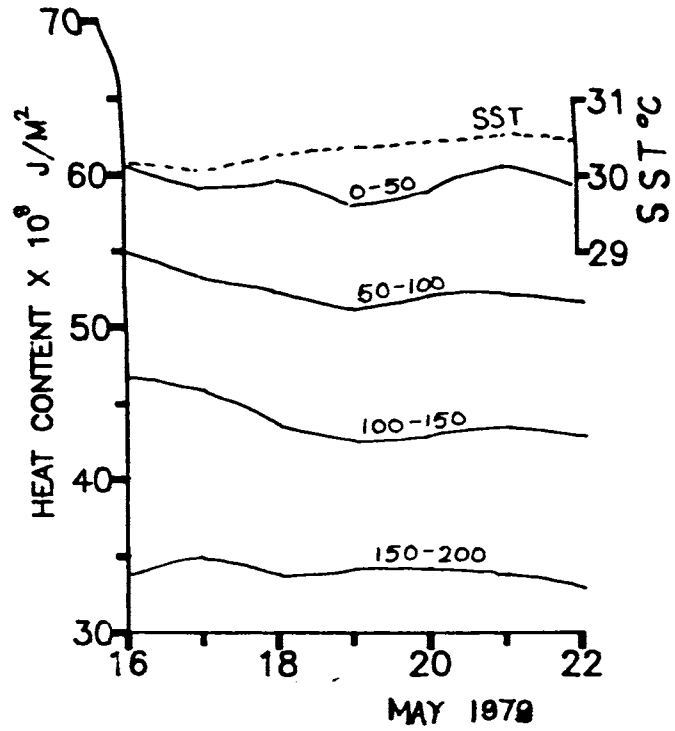

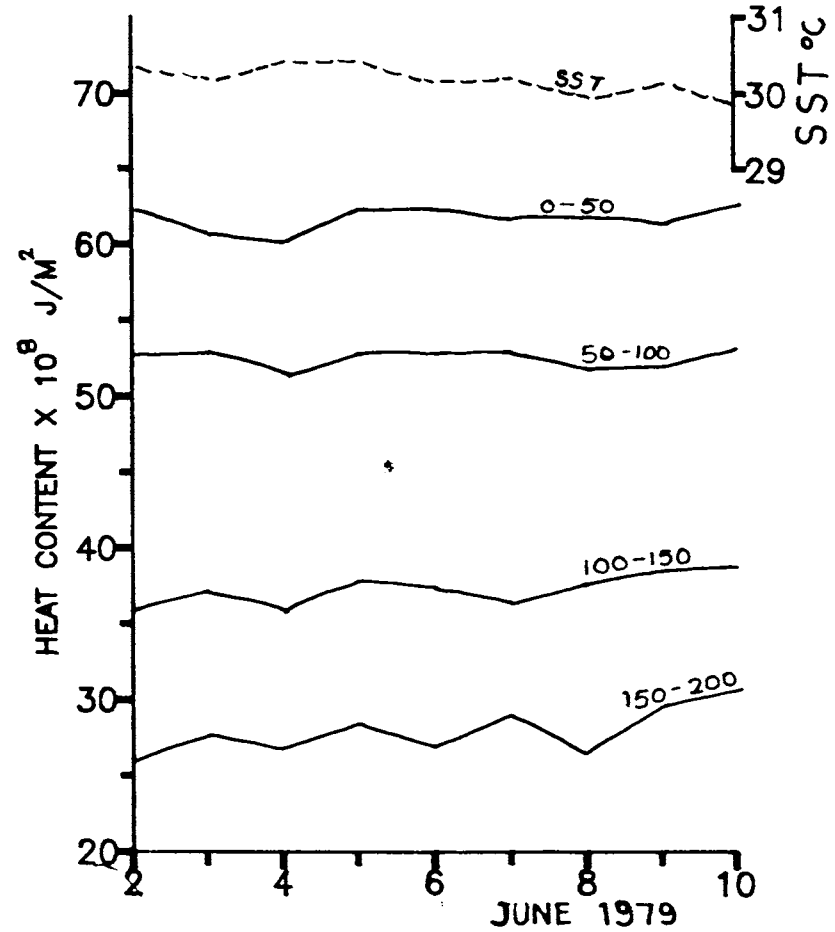

Fig.3.18 Daily variation of heat content in different layers in (a) Area-II (b) Area-III

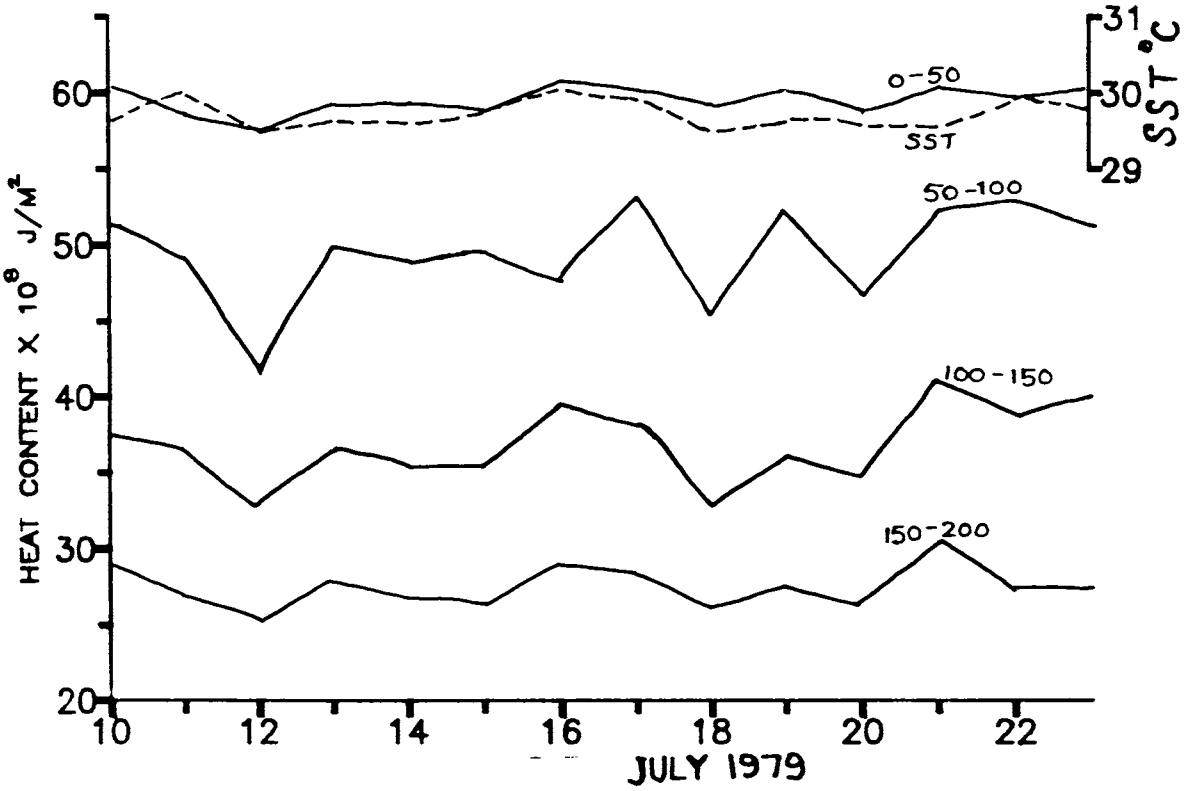

Fig.3.19 Daily variation of heat content in different layers in Area-IV.

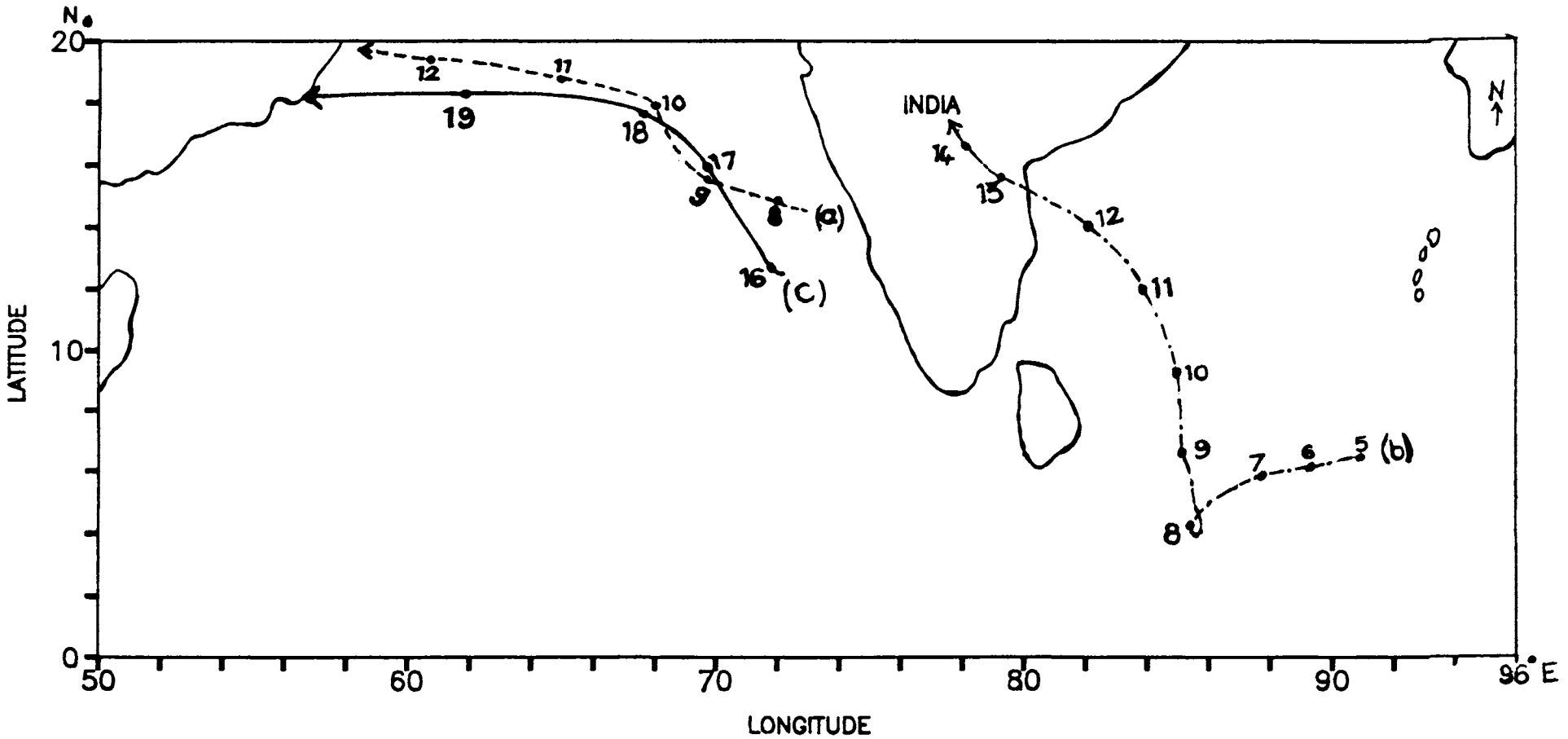

Fig.3.20 Track of cyclonic storms studied in Arabian Sea and Bay of Bengal
(a) during 8-12 June, 1975 (b) during 5-14 May, 1979 (c) during 16-19 June, 1979.

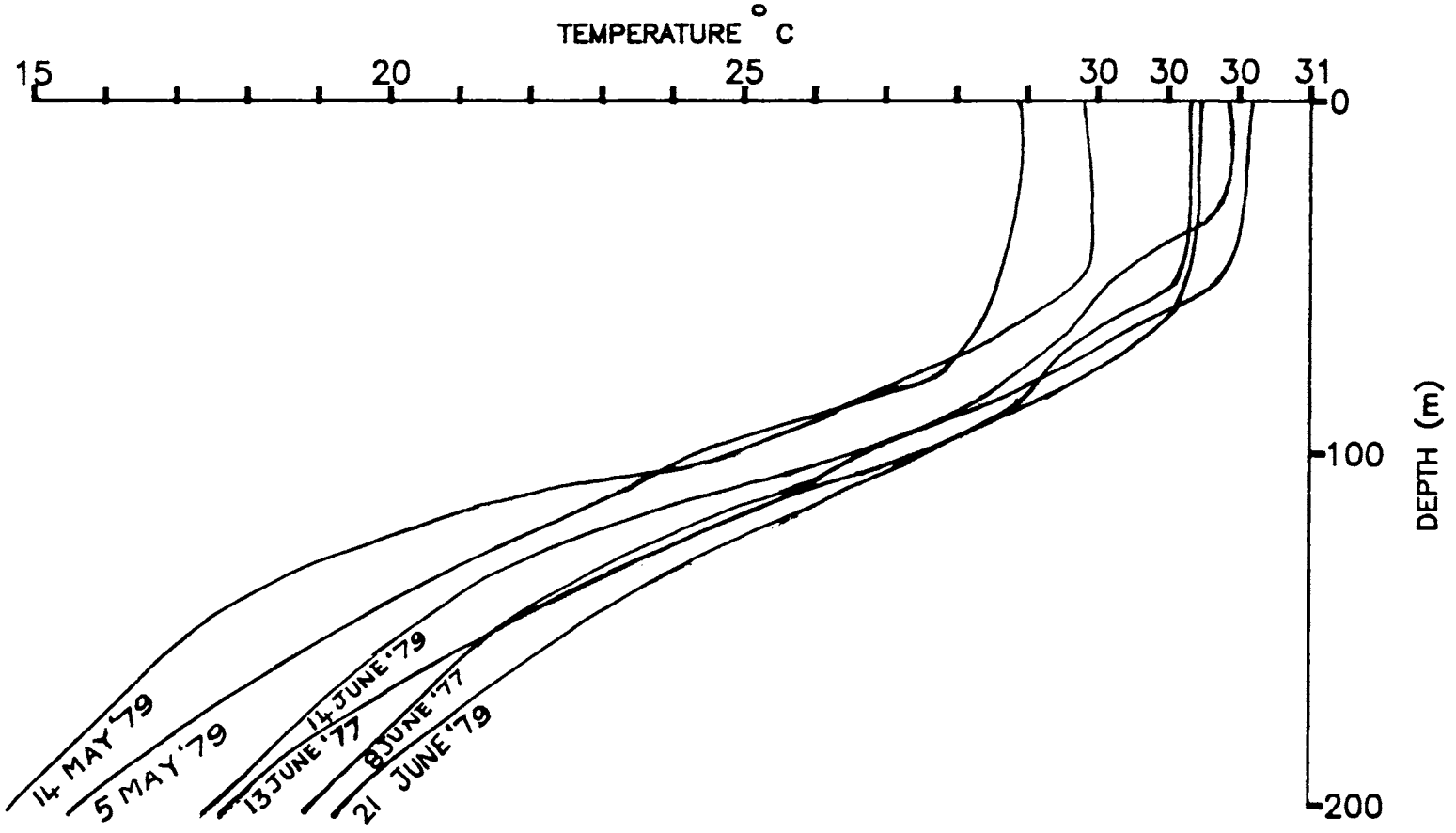

Fig.3.21 Temperature profiles before and after the three storms.

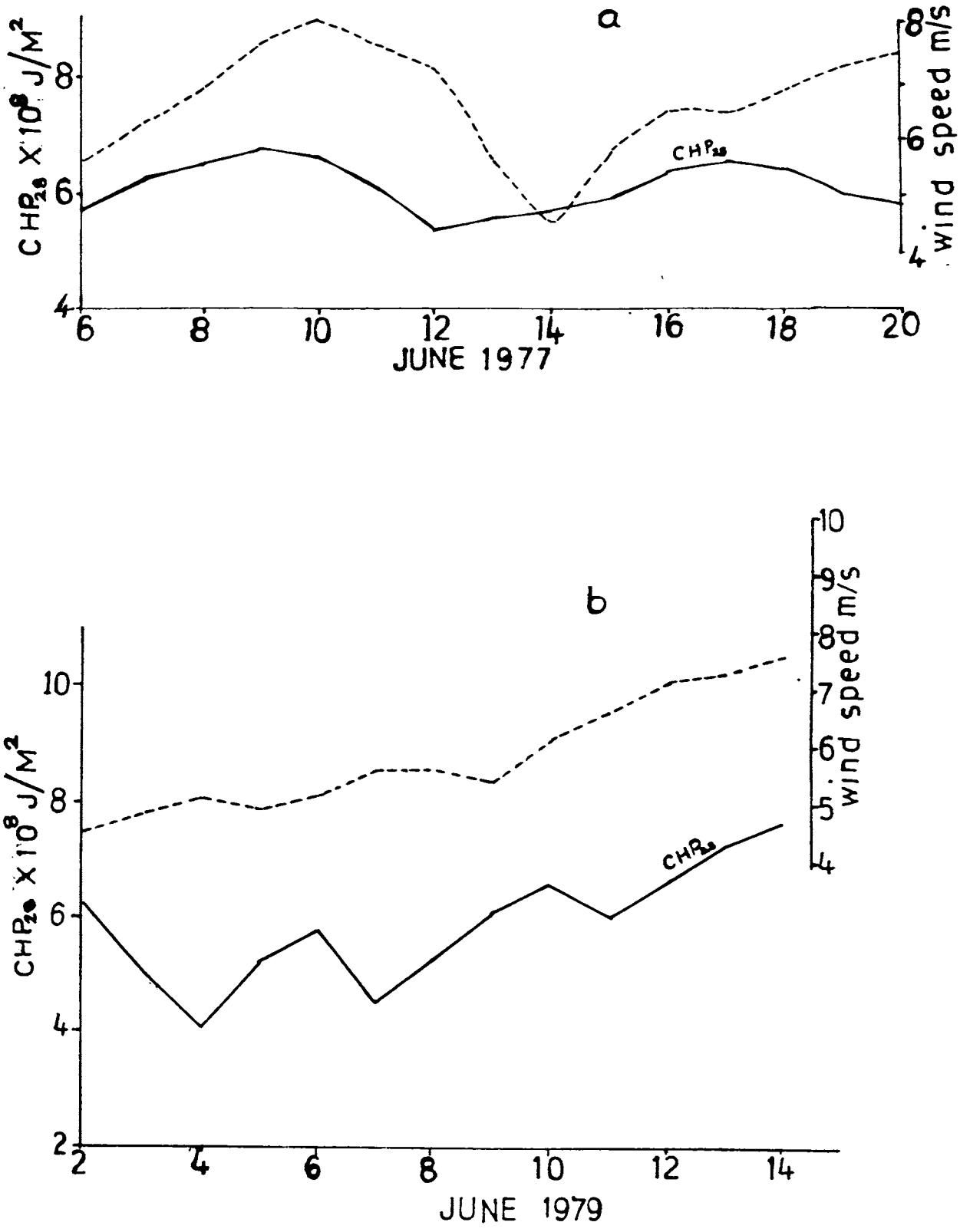

Fig.3.22 Daily variation of CHP_{28} and wind speed in (a) Area-I, storm -a (b)Area-III, storm-C

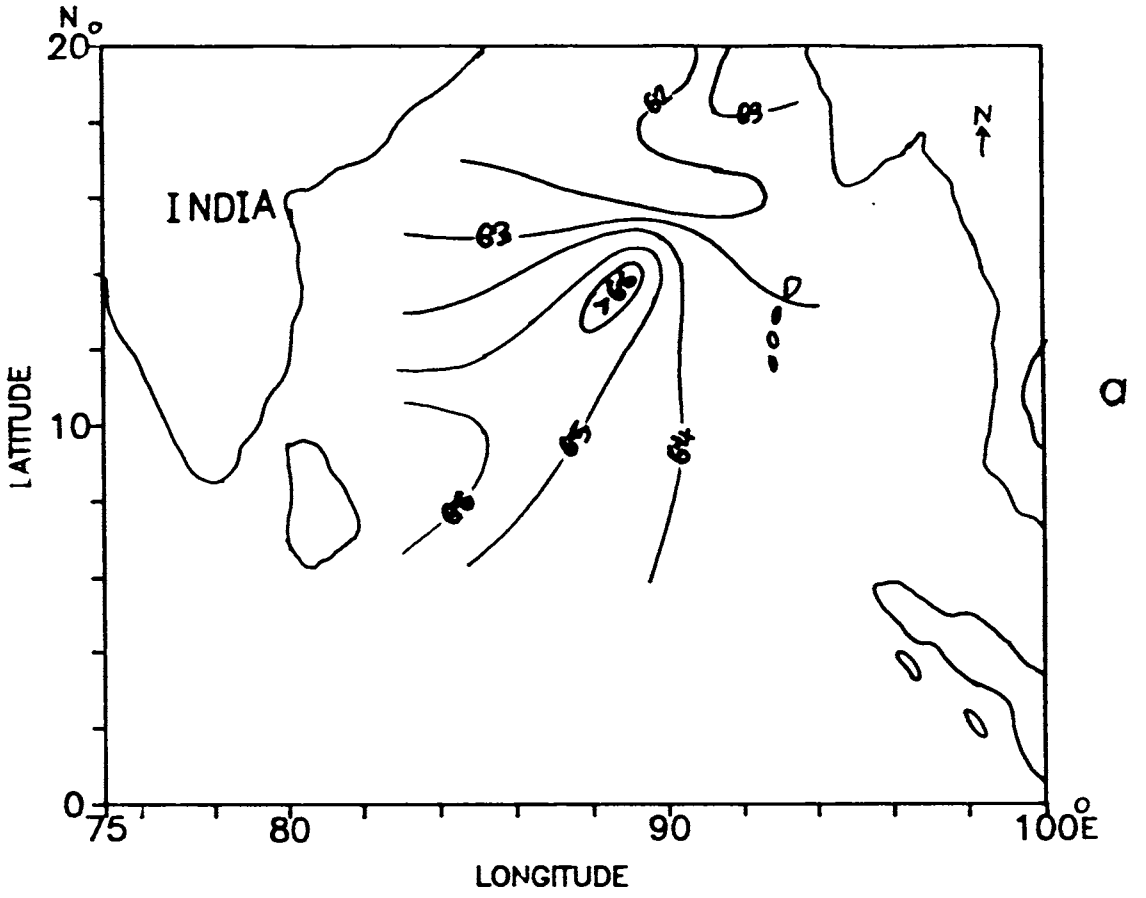

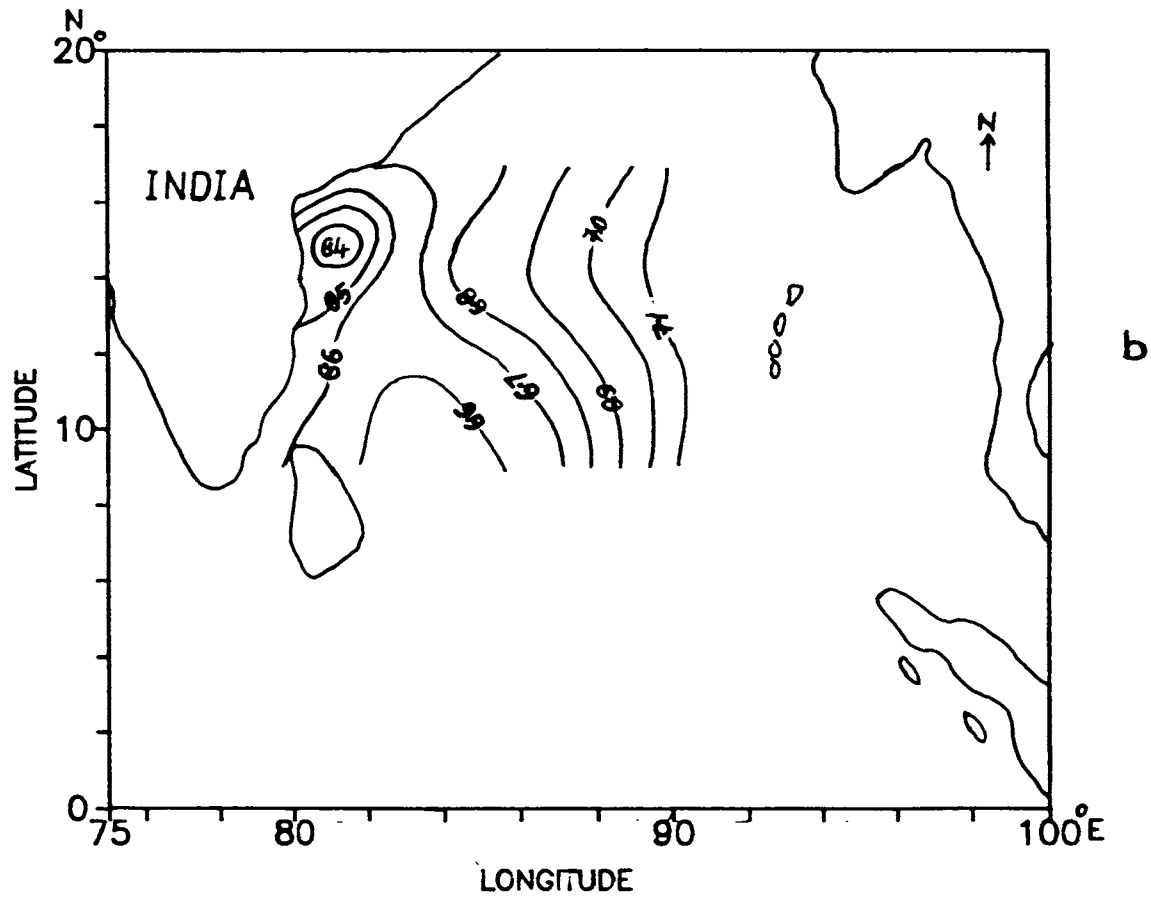

Fig.3.23 Distribution of CHP_{28} on (a) 1st May (b) 17th May 1979 (10^8 J/M^2)

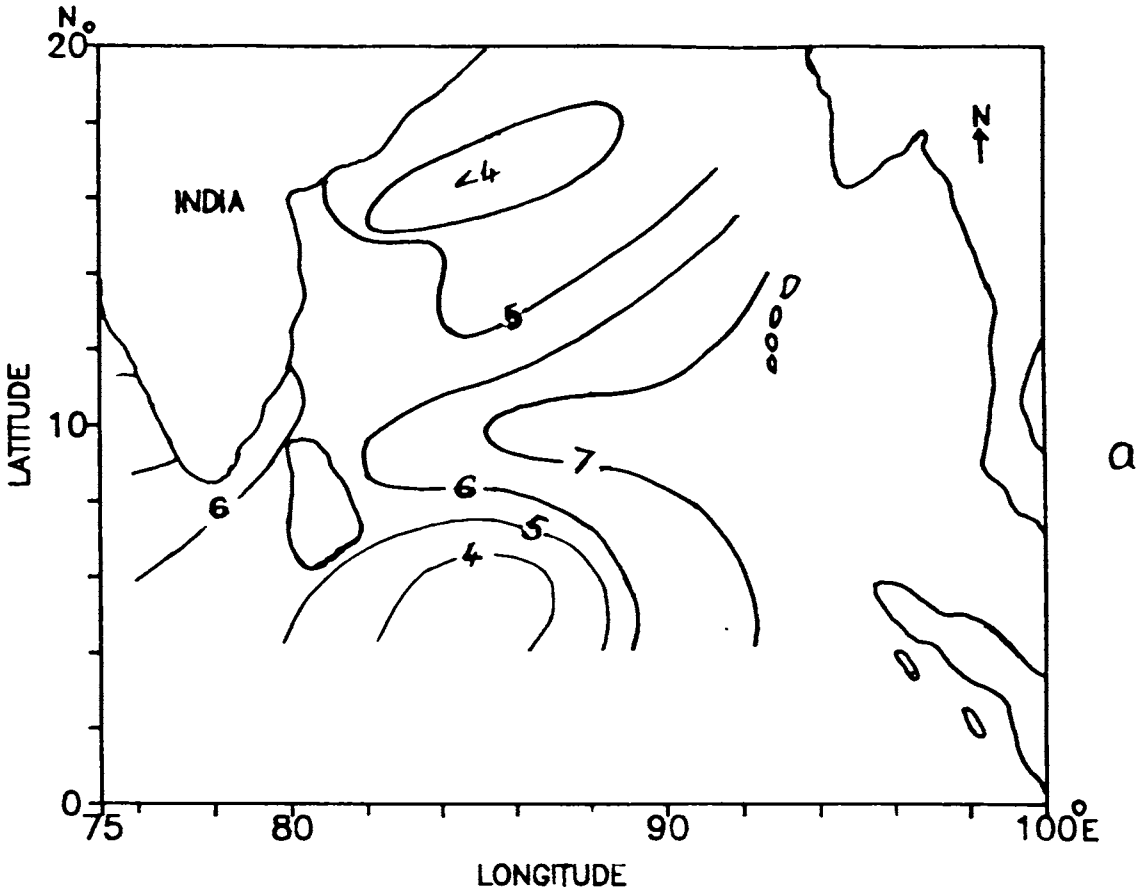

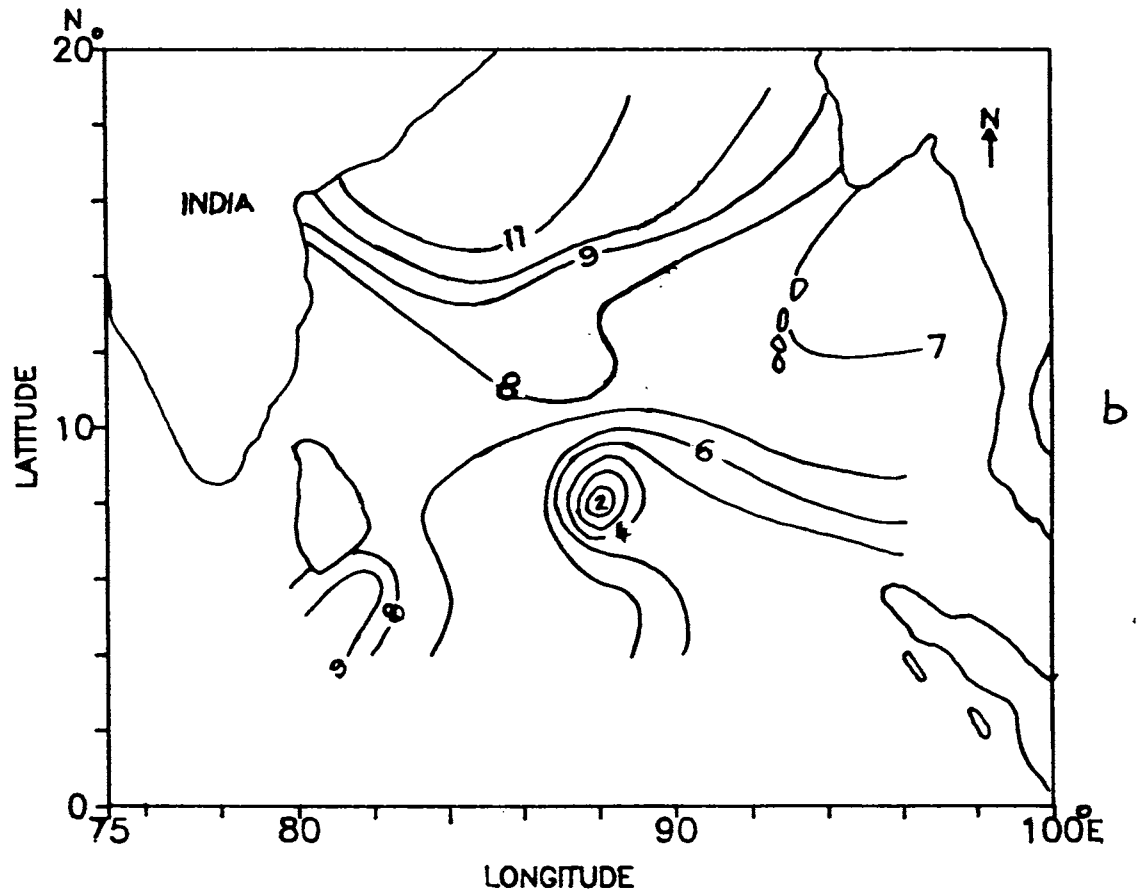

Fig.3.24 Distribution of surface wind speed on (a) 1st May (b) 17th May 1979 M/s

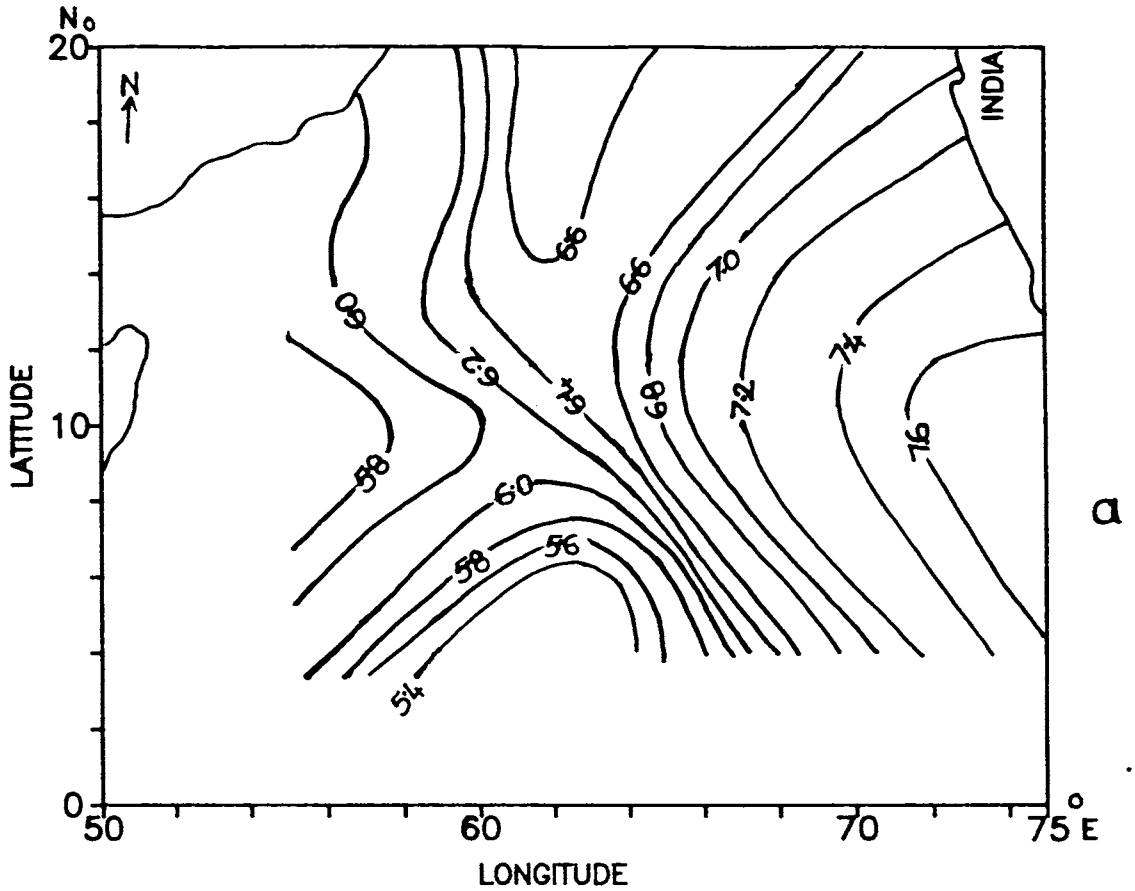

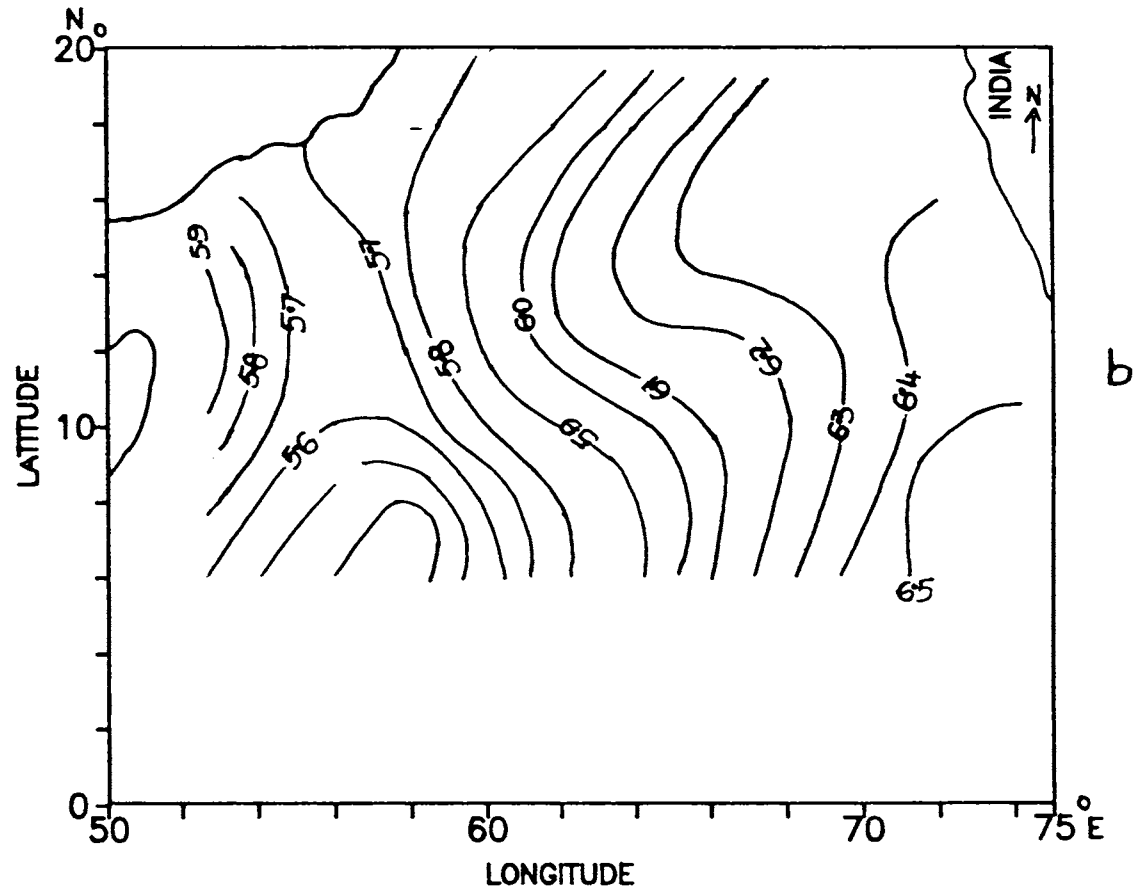

Fig.3.25 Distribution of CHP_{28} on (a) 10th June 1979 (b) 30th June-1979 (10^8 J/M^2)

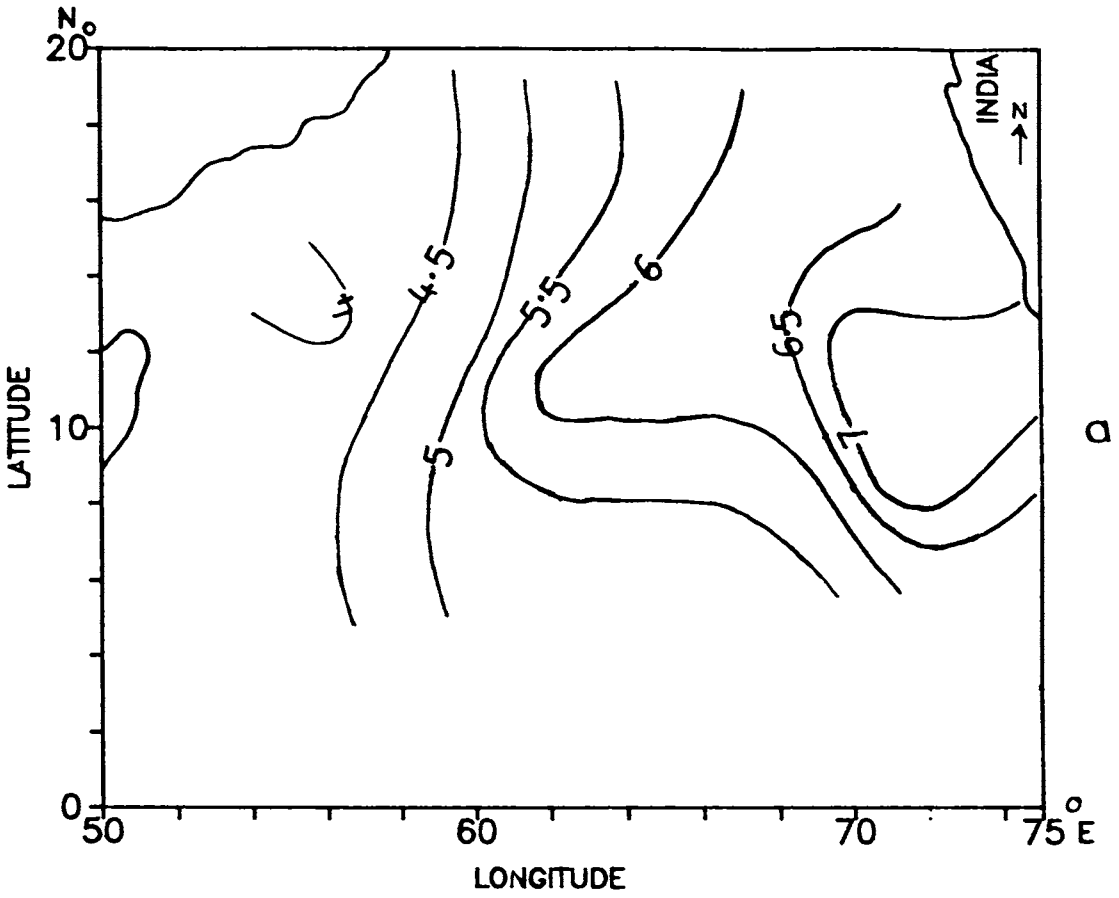

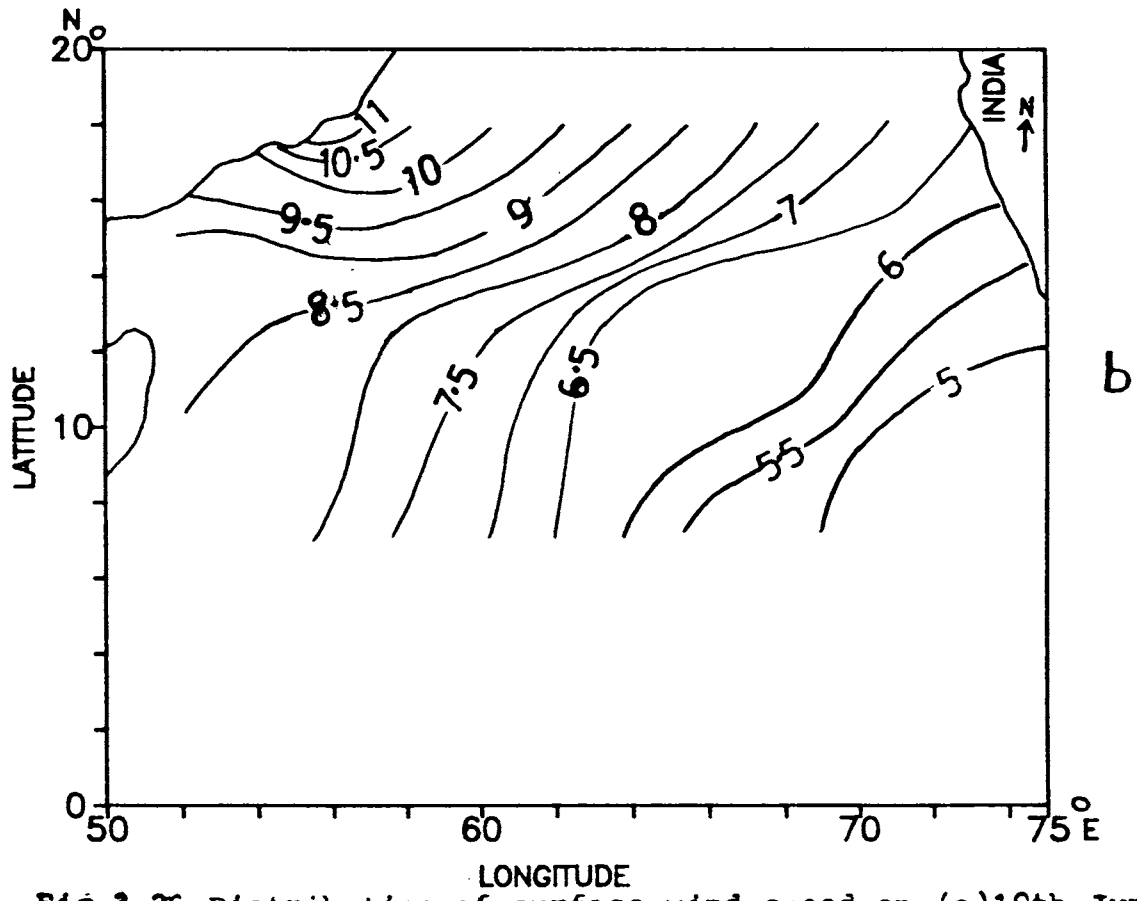

Fig.3.26 Distribution of surface wind speed on (a)10th June (b) 30th June 1979 M/s

CHAPTER-IV

HEAT BUDGET COMPONENTS

4.1 Introduction

The importance of different heat budget components in the air- sea interaction was highlighted in the first chapter. The methodology of estimating the various components was given in detail in the same chapter. This chapter discusses the variation of different energy exchange parameters namely, Net radiation, Latent heat flux, Sensible heat flux and the Net heat gain or loss during pre-onset, onset and break-period of monsoon 1979 in the northern Indian Ocean, utilizing satellite and ship data. The daily variations of these components are also discussed for different polygon areas. The total heat storage during four seasons and heat advection during monsoon season have also been studied in detail.

Much of the energy which drives the atmospheric circulation comes from the solar heat collected by the oceans and returned to atmosphere as latent and sensible heat. The oceans, to a large extent control the climate of the earth due to thier larger thermal capacity. The latent heat energy partially sustains the major features of the general circulation by supplying water vapour to the environment during condensation. The surface boundary layer of the ocean plays a very crucial role in the air-sea exchanges of momentum, heat and moisture. Hence, surface radiation budget and its spatial and temporal variations are important to all aspects of the study of weather and climate.

The major factors affecting heat exchange parameters are length of the day which changes the incoming radiation, atmospheric absorption, clouds, surface albedo and surface wind speed.

Earlier important works on heat budget include the world maps of global solar radiation by Black (1956), Budyko (1956), Ashbel (1961), and Landsberg et al,(1963) and the atlas of heat balance by Budyko (1963). Monthly and annual maps of global solar radiation and net radiation over the Indian Ocean have been presented by Mani et al, (1967).

Conventional method of estimating incoming solar radiation at the ocean surface using solar constant, cloud amount and albedo of the sea surface had been used by Reed (1977) and Rao et al, (1978). Kelkar and Pradhan (1977) found out a numerical relation and presented the diurnal and seasonal observations of earth's radiation budgets during 1962-1965. Vonder Haar and Socomi (1979), presented a comprehensive radiation climatology of the earth-atmosphere system and observed a net gain of energy at major energy exporting areas.

Until very recently, our only knowledge of solar radiation input in large oceanic regions comes from sparse cloud observations used in empirical formulae, and only composite over several years could give us an idea of the field (Hastenrath and Lamb, 1980). Rao et al, (1981) attempted to evaluate the

radiation fluxes over the northern Indian Ocean using climatological data for normal and break monsoon conditions.

There has not been much work done on the marine boundary layer due to paucity of observations over the oceans. However, in recent years, with the advent of global satellites, observations over the oceans have been taken at regular intervals of time to get global coverage needed for climatic studies. Measurements of surface radiation is difficult to be made by satellites due to the intervening atmosphere, whereas radiation balance at the top of the atmosphere can be measured directly. Net radiation and the incoming radiation at the ocean surface have been estimated from satellite radiation parameters with reasonable accuracy (Tarpley, 1979). In tropical regions. where ocean-atmosphere system receives the maximum heat, conventional methods are almost inexistent and hence satellite estimates have certain advantage in estimating the surface radiation budgets.

Tarpley (1979) and Gautier et al, (1980) have shown that it is possible to estimate the downward solar radiation and the net short-wave radiation at the surface over land using repeated measurements of geostationary satellites. Gautier (1982) designed a simple radiative model to estimate the insolation from geostationary satellite data, utilizing the satellite derived net radiation at the top of the atmosphere. Mohanty et al,(1982) studied the effect of large scale heat budget during the onset and active phases of south west Asian monsoon for the tropical belt, utilising FGGE data for May-July 1977. The evolution of net

short-wave radiation fields computed using geostationary satellite data, before during and after the monsoon onset in the Indian Ocean has been presented by Gautier (1986) who also documented the westward propagation of large scale convective activity in the equatorial regions. Ali (1990,a) estimated SST from absorbed solar radiation at the ocean surface using NOAA radiation parameters.

Rao et al,(1984) estimated the evaporation rates over the Arabian Sea for June 1982, utilizing the SAMIR brightness temperature of Bhaskara-II and GOSSTCOMP charts of NOAA series. They pointed out that the spatial distribution of evaporation estimated using satellite coincides with that obtained from ship observations as well as from climatological data. Simon and Desai (1986) computed evaporation over the equatorial India Ocean using TIROS-N moisture profile and extrapolated GOES low level cloud motion vector winds to the surface.

The present chapter deals with the analysis of surface energy parameters viz. net radiation, latent heat flux, sensible heat flux and the net oceanic heat gain or loss at the ocean surface on a weekly basis during pre-onset, onset, and break-monsoon periods. Daily variations of these components at a particular station in the Arabian Sea (15^{o} N, 65^{o} E), and for a polygon area in Bay of Bengal are also studied during May-July 1979. The total heat gain/loss, heat storage of the mixed layer and 0-200m layer and the heat advection during monsoon periods have been presented for different latitude belts.

Net radiation is computed from a regression analysis (Ref. qn.1.2, Chapter-I) utilising the satellite derived planetary osorbed radiation, available radiation at the top of the tmosphere, cloud amount and the total water vapour content of ne atmosphere. Latent and sensible heat fluxes have been stimated from bulk aerodynamic formula utilising satellite erived SST, air temperature and GOES cloud motion vector winds xtrapolated to the surface. Since the surface pressure and umidity is difficult to be retrieved from satellites, latent eat has been calculated using the ship observed dew-point emperature and surface pressure. Details regarding the data and omputation have already been discussed in chapter-I. Heat budget arameters have been analysed only for the year 1979 for which he satellite derived radiation parameters were obtained.

The net radiation values obtained from satellite radiation arameters were compared with ship observations. The accuracy is ound to be about 20% in a root mean square sense with a orrelation coefficient equal to 0.86 for the range of 1-60W/M^2. 'able.4.1 gives the comparison of estimated and observed net 'adiation values.

.2. Spatial and temporal variations of energy exchange components during monsoon 1979.

.2.1 Pre-onset period (16-25th May 1979)

The spatial distribution of net radiation averaged for the eriod during 16-25 May is presented in fig (4.1). In the Arabian ea,an east-west gradient in the net radiation is observed

ble.4.1. Comparison of net radiation values estimated and observed (W/M^2) for the monsoon season.

Satellite derived	ship observed	difference
139	101	38
103	104	1
165	109	54
173	112	61
195	136	59
169	138	31
191	163	28
221	161	60
136	163	27
160	172	12
171	173	2
148	179	31
151	196	45
168	210	42
175	180	5
182	186	4
183	190	7
189	205	16
193	202	9
200	206	6
205	195	10
207	197	10
208	196	12
215	194	21
232	198	34
238	206	32
239	208	31
234	203	31

varying from 160W/M^2 at the equator to 250W/M^2 near the Somali coast. Whereas maximum value o about 210W/M^2 is observed in the central Bay of Bengal which decreases to 180W/M^2 on either side. This gradient in the net radiation almost followed the distribution of cloud amount. In general, net radiation increases towards east both in the Arabian Sea and Bay of Bengal. Maximum radiation (about 250W/M^2) is recorded in the northwestern Arabian Sea and minimum (about 130W/M^2) near the equator around 2^o N,73.5^o E. There is a general increase in net radiation towards north in the Arabian Sea. The net radiation thus exhibits a large zonally oriented field with strong east west gradients during this period. It can be seen that, the cloud cover during this period is almost maximum near the minimum net radiation area and vice-versa (fig.4.2). Cloud cover increases from west to east with maximum near the southwest coast of India. In Bay of Bengal, it decreases towards east.

During this period, latent heat flux shows gradual increase towards north both in Arabian Sea and Bay of Bengal (fig.4.3). In the Arabian Sea, latent heat shows an increase towards east up to mid Arabian Sea afterwhich it decreases towards the Indian coast. In the Bay of Bengal, the zonal variations of latent heat shows an increasing trend from east to west. Maximum latent heat of about 150W/M^2 is observed in the central Arabian Sea and minimum of 75W/M^2 near the central and western parts of north equatorial Indian Ocean. This may be because of low cloud cover and comparatively light winds during the pre-onset period. Variations in sensible heat flux during this period are limited

for a minimum of $3W/M^2$ to a maximum of $9W/M^2$ in magnitude (fig 4.4). The maximum sensible heat is encountered in the Central Bay of Bengal and minimum in the south central Arabian Sea. Compared to Bay of Bengal, Arabian Sea shows lower sensible heat flux. The low sensible heat observed during pre-onset may be because of minimum sea-air temperature difference.

By adding all the above three heat fluxes, considering the latent and sensible heat fluxes as loss terms, net heat gain/loss is estimated. It is seen that, Ocean gains maximum heat of $120W/M^2$ in the western Arabian Sea and a minimum of 50 W/M^2 in the Central parts of north equatorial Indian Ocean and western Bay of Bengal (fig.4.5). The maximum gain in the western Arabian Sea is because of maximum net radiation and less latent heat release.

4.2.2 Onset period (9-16th June 1979)

During the onset period, net radiation shows a drastically different picture (fig.4.6). The maximum net radiation near 11^{o} N,64^{o} E during the earlier period is replaced by almost minimum values due to more cloudiness and strong winds associated with monsoon onset. Maximum net radiation is concentrated around 19^{o}N,$58\text{-}61^{o}$E and the minimum in the eastern Arabian Sea. In the southern side, (south of 10^{o} N) small areas of alternate high and low net radiations are noticed. In this region, the variations in net radiation show an increasing trend from west to east. Lower values are encountered in the southern parts compared to north of

10^{o} N. The zonal variations in net radiation during this period are more in the Arabian Sea compared to Bay of Bengal. This may be because of maximum cloud cover over the Arabian Sea than Bay of Bengal. Comparatively very low values are observed during this period than the pre-onset period.

The distribution of cloud cover during onset period indicates intensification and migration of the southwest monsoon along the west coast of India (fig.4.7). Area of maximum cloud cover corresponds to area of minimum net radiation seen in the southeastern Arabian Sea and northern Bay of Bengal.

In the Arabian Sea, latent heat flux increases generally from west to east (fig 4.8). Eastern Arabian Sea exp[illegible]nces maximum latent heat of 200W/M^2 coinciding with maximum cloud cover area. This could be due to maximum condensation caused by more latent heat release. Minimum latent heat of 130W/M^2 is found around 15^{o} N, 65^{o} E. Latent heat varies between 130-200W/M^2 in the Arabian Sea and between 150 and 190W/M^2 in Bay of Bengal. Higher latent heat release is found in this period compared to the pre-onset period in accordance with the more cloud cover.

The horizontal distribution of sensible heat flux during the onset period is shown in fig (4.9). Sensible heat exhibits more variations in the Bay of Bengal than in the Arabian Sea. northern equatorial Indian Ocean shows almost uniform distribution of sensible heat of around 8W/M^2. The values ranges from 10-2 W/M^2 in Bay of Bengal and between 8 and 16W/M^2 in Arabian Sea. The increase in sensible heat compared to the pre-

onset period is more in Bay of Bengal. The increase in sensible heat observed during this period may be because of high wind speed prevailing during monsoon onset.

From fig(4.10) it can be seen that, ocean loses heat in the eastern Arabian Sea and in most parts of Bay of Bengal during the period of monsoon onset. A maximum loss of $60W/M^2$ is noticed around 12^{o} N,74^{o} E. During this period ocean gains heat in the western Arabian Sea and in some parts of Bay of Bengal. Maximum heat gain of $65W/M^2$ is centered around 3^{o} N,63^{o} E. Compared to the previous period, net heat gain shows lower magnitudes both in Arabian Sea and Bay of Bengal due to low net radiation and high latent heat release.

4.2.3 Break-monsoon period (14-21st July 1979)

During this period, western part of north equatorial Indian Ocean experiences higher net radiation compared to the onset period except off the western coast of India where it does not show such increase due to high cloud cover in this region (fig.4.11). Net radiation increases in a southwesterly direction from a minimum of $160W/M^2$ off the northwestern coast of India to a maximum of $215W/M^2$ in the western parts of north equatorial Indian Ocean. Bay of Bengal also experiences higher net radiation with a maximum of $225W/M^2$ near the central Bay compared to the onset period. This increase in net radiation could be the result of low cloud cover and surface winds during the break period. The corresponding cloud cover distribution exhibits lower

cloud amount than the previous period (fig.4.12). The maximum net radiation area corresponds to minimum cloud cover of 3 parts in ten and the minimum net radiation in the western coast of India corresponds to higher cloud amounts.

The distribution of latent heat flux during break period shows a minimum core of 139W/M^2 around 10^o N,66^o E from where it increases in all directions in the Arabian Sea (fig.4.13). In the northern Bay of Bengal, latent heat shows higher values reaching a maximum of 160W/M^2 in the area of minimum net radiation recorded during this period. Minimum latent heat of 130W/M^2 is observed around 10^o N,88^o E. Compared to the onset period, higher latent heat is noticed in the western Arabian Sea and northern Bay of Bengal. However, a decrease of about 70W/M^2 is observed off the north western coast of India. This lowering of latent heat could be due to low evaporation rate because of low surface winds.

Sensible heat flux shows considerable variations in the eastern part of north equatorial Indian Ocean (fig.4.14). Compared to the pre-onset phase, the region of maximum latent heat flux migrated towards southwest both in the northwestern Arabian Sea and the eastern parts of north equatorial Indian Ocean. Low wind speed provides minimum sensible heat in the area of maximum net radiation.

During this period, a heat loss of 5W/M^2 is noticed in a limited area in the northeastern Arabian Sea (fig.4.15). Maximum gain of 80W/M^2 is found in the south western Bay of Bengal.

Contrary to the earlier period, Bay of Bengal gains more heat than Arabian Sea.

4.3. Daily variations of surface energy parameters

Daily values of heat budget components, have been computed for May and June 1979 for a fixed position at 15^{o} N,65^{o} E in the Arabian Sea. Daily average values of these components have been estimated for a polygon area in the northern Bay of Bengal in order to study the daily variations during the break-monsoon period.

4.3.1 May 19-30, 1979

Fig (4.16) depicts the daily variations of different heat budget components during May and June 1979. The net radiation increases from 149W/M^2 on 19th to 230W/M^2 on 22nd May (fig.4.16,a). Net radiation fluctuates by about 35W/M^2 during the period between 22-26th and then decrease to 165W/M^2 on 29th. The corresponding cloud cover shows inverse relation with the net radiation. Latent heat flux increases from 125W/M^2 on 19th to a maximum of 240W/M^2 on25th and afterwards it decreases to 180 W/M^2 on 30th May. Sensible heat varies between 5W/M^2 on 19th to 15W/M^2 on 30th May. Net gain of heat is indicated upto 24th May with a maximum of 60W/M^2 on 22nd and a maximum loss of about 30W/M^2 on 25th May. The maximum loss on 25th May could be because of intensive cloud cover on this day as observed by Krishnamurthy et al,(1979). A loss of 10W/M^2 is noticed on 29th May with slight gain on the preceding and following days. On 29th relatively high latent heat release and low net radiation is noticed.

4.3.2 June 1-11, 1979

Net radiation shows a gradual increases from 230W/M^2 on 1st June to 238W/M^2 on 2nd June (fig.4.16,b). Rapid decrease of 60W/M^2 in net radiation is seen on 3rd June thereafter it fluctuates by about 35W/M^2 upto 10th June and decreases sharply on 11th, the actual day of onset of monsoon in this year. The corresponding cloud cover increases throughout these days reaching a maximum of 8.4 parts out of ten on 11th June. The daily variations of net radiation shows a clear inverse relation with the day to day variations of cloud cover. Latent heat flux during this period continuously increases from a minimum of 110W/M^2 on 1st to 235W/M^2 on 11th June. Sensible heat flux is slightly higher than the pre-onset period. The significant increase in latent heat flux influences the net oceanic gain during this period. The net heat gain/loss more or less follows the variations in net radiation. Though the net radiation is maximum on 2nd June, net heat gain is more on 1st June due to minimum latent heat. After 1st June, oceanic heat gain decreases reaching zero on 4th June and subsequently ocean starts losing heat at a maximum rate of 50W/M^2 on 11th June, the day of onset of monsoon.

4.3.3 July 10-23, 1979

Net radiation varies between 130W/M^2 and 220W/M^2 during this period (fig.4.17). The variations show three maxima on 11th,17th and 23rd with intervening minima on 13th and 21st July. The cloud cover during this period varies between 3 and 6 parts

out of ten. The variations in cloud amount shows an inverse relation with the variations in net radiation. Latent heat shows an almost opposite variations as that of net radiation. This could be because of the increased water vapour content due to cloudiness which controls the evaporation rate. Latent heat varies between minimum of $105W/M^2$ on 14th to a maximum of $150W/M^2$ on 18th July. Sensible heat shows lower magnitudes compared to the onset period may be due to the less air-sea temperature difference during the break-period. It varies between $7W/M^2$ and $15W/M^2$ during 10-23rd July. The net heat gain/loss closely follows the variations in net radiation. Ocean loses heat on 13th and 21st July amounting to $5W/M^2$ is mainly due to large latent heat release and low net radiation. A maximum gain of $115W/M^2$ is observed on 14th July as a result of maximum net radiation. The oceanic heat gain during this period is more compared to the onset period.

Average values of heat budget components during the monsoon season of 1979 are presented in Table 4.5. All the components show a northward increase with the maximum centered around 15-20^{o} N latitude belt.

4.4 Seasonal heat storage and heat advection

While redistributing the heat received from the sun, the ocean currents transports heat from warmer regions to colder regions. Of the various processes contributing to world climate, the heat advection by the ocean is the least understood. This is

because of the difficulty in obtaining this component by direct method. In the direct method, simultaneous measurements of temperature and velocity are needed on an annual basis which is very difficult to be carried out in oceanic areas. The study of oceanic heat flux by direct method is, therefore practically impossible.

The heat transport in the ocean is therefore, obtained by indirect methods. One method is to compute the geostrophic current using the density field and then to use the mean temperature field to estimate the heat flux (Model,1950; Jung,1952; Bryan,1962; Barnett,1978; Wunch,1980; Bruce and Beatty,1985) The more common method to obtain advection is from the heat balance of the ocean. Knowing the net heat exchange at the sea surface and heat storage in the ocean, the residual can be estimated to give the heat advection. This approach was followed by Merle (1980) for the equatorial Atlantic, Lamb (1981) and Lamb and Bunker (1982) for the north Atlantic, Etter (1983) for the Gulf of Mexico, Hastenrath and merle (1986) for the tropical Atlantic, Bruce (1987) for the Somali basin, Levitus (1987) for the world Oceans and Varma (1989) for the northern Indian Ocean.

There are several difficulties in evaluating the heat storage. The main difficulty is regarding the estimation of the depth upto which the annual variation of heat content extends. In most of the areas, the main influence is seen up to 100m, but in some isolated areas, it may extend beyond 500m (Oort and Vonder Haar,1977). Further individual temperature profiles terminate at

different depths so that average profiles will become less representative with increase in depth. Different depth limits have been used by several authors for the estimation of heat storage in various oceanic regions (Bathen,1971; Merle,1980; Bruce,1987)

In the present study, the seasonal average of heat storage and heat advection of the mixed layer and the 0-200m layer have been computed for each 5^{o} latitude belts in the northern Indian Ocean. The computation is based on equation (1.13) discussed in chapter-I. The seasonal average heat content values from the previous chapter have been taken as the input for calculating the heat storage. While the heat storage has been estimated for different seasons, heat advection has been analysed for monsoon season only as the surface heat budget estimates have been calculated for this season.

Table 4.2 illustrates the heat storage of the mixed layer during different seasons. It is seen that maximum heat storage occurs during pre-monsoon season between 5-10^{o} N. During this season, oceanic heat storage is seen in all the latitude belts. During monsoon season, on the other hand, heat is depleted in all the latitude belts with a maximum depletion of about $51W/M^{2}$ between 10-15^{o} N. Decrease in heat storage is observed south of 10^{o} N, during three season other than pre-monsoon, while there is an increase of heat storage in the northern regions (north of 10^{o} N) except during monsoon season. Varma (1989) also observed a cooling during winter and monsoon seasons and maximum warming in

February in the northern Indian Ocean using the zonally averaged heat storage from Meehl (1984). Using continuous data for about 2 years, Mc Phaden (1982) noted heat depletion during April to September in the western Indian Ocean.

From Table4.3, it is seen that the total teat storage in the 0-200m layer is negative in the north equatorial region during February to October and it becomes positive during winter season. Heat depletion is observed during monsoon and post-monsoon seasons especially between 5-15^{o} N due to heat transport from this region by currents generated by the monsoon winds. This could be due to the reduction in insolation caused by the increased cloud cover in these season. During winter, heat storage shows an increase in all the latitude belts with a maximum of 123W/M^{2} between 5-10^{o} N. Generally, heat storage variations are prominent between 5-15^{o} N belt compared to the northern and southern regions.

Table.4.4 represents the degree of heat advection in the mixed layer and in the 0-200m layer during monsoon season. As the negative values indicate, heat is exported during monsoon season both in the mixed layer and in 0-200m layer. In the latitude belts of 0-5^{o} N and 15-20^{o} N mixed layer exports more heat than the 0-200m layer. This is due to large negative heat storage of the mixed layer. The maximum heat export of 114W/M^{2} observed between 10-15^{o} N in the 0-200m layer is also related to maximum negative heat storage of this layer. The heat export in the mixed layer is about three times more than the surface heat gain in the 0-5^{o} N latitude belt. 0-200m layer shows a heat export of

Table. 4.2. Average heat storage of the mixed layer during different seasons (W/M^2)

Latitude	Pre-monsoon	Monsoon	Post-monsoon	Winter
0-5° N	+21.5	-19.5	-40.5	-10.5
5-10° N	+58.5	-1.5	-21.3	-36.2
10-15° N	+9.1	-51.0	+27	+15.2
15-20° N	+9.3	-25.5	+9.0	+7.5

Table 4.3. Average heat storage of the 0-200m layer during different seasons (W/M^2)

Latitude	Pre-monsoon	Monsoon	Post-monsoon	Winter
0-5° N	-66.6	-5.3	-10.1	+83
5-10° N	+20.3	-66.6	-53.3	+123.1
10-15° N	+53.3	-73.1	-53.3	+80.3
15-20° N	+16.6	+3.3	-33.1	+36.6

Table.4.4. Heat advection in the mixed layer and 0-200m layer during monsoon season (W/M^2)

Latitude	Mixed layer	0-200m layer
0-5° N	-28.2	-14.5
5-10° N	-30.6	-95.1
10-15° N	-92.1	-114.1
15-20° N	-72.5	-43.7

Table 4.5. Average values of heat budget parameters during monsoon 1979 for 5° latitude belts (W/M^2)

Latitude	Net radiation	Latent heat flux	Sensible heat flux	Net heat gain/loss
0-5° N	160.2	142.1	8.8	9.1
5-10° N	194.6	135.5	13.5	28.6
10-15° N	195.8	142.3	12.1	40.4
15-20° N	204.6	144.6	13.0	47.0

$14.5W/M^2$ in this region. In the latitude belt 5-10° N, heat export from the mixed layer is almost equal to the net heat gained at the surface while, the export from 0-200m layer approximates thrice the surface heat gain. For the 10-15° N latitude belts the heat export from the mixed layer is about two times the surface heat gain and that from the 0-200m layer amounts to thrice the surface heat gain. Between 15-20° N latitude belt, the heat export from the mixed layer is almost equal to twice the surface heat gain while, the export from 0-200m layer almost equals with the surface heat gain.

4.5 Discussion

In the previous sections we have seen the distribution of different heat budget components during pre-onset, onset and break periods of monsoon on a daily and weekly basis. The heat storage and heat advection in the mixed layer and 0-200m layer have also been presented.

The net radiation in the northern Indian Ocean during the pre-onset period shows its maximum in the northwestern Arabian Sea and minimum in the central part of north equatorial Indian Ocean. The short-wave radiation also shows similar locations of maxima and minima in the northern Indian Ocean (Gautier, 1986). The reduced net radiation near the equatorial region is associated with maximum convective clouds observed during the period as evidenced by the satellite cloud pictures presented by Krishnamurthy et al. (1979). Earlier studies by Gautier (1986), Rao (1987,b) and Mohanty and Mohan Kumar (1990) have related the

considerable reduction in net short-wave radiation as due to intense convective clouds. Cloud cover during pre-onset period indicates the northward intensification of convergence zone near the Kerala coast. The magnitude of latent heat flux during this period varies between 75-150 W/M^2. More or less comparable values of latent heat are observed by Mohanty and Mohan Kumar (1990) using ship observed marine meteorological parameters. Sensible heat flux varies between 3-9 W/M^2 during this period with its maximum in the central Bay of Bengal. In the north equatorial Indian Ocean, the sensible heat is about $5W/M^2$ on an average. Simon and Desai (1986) observed a mean sensible heat value of 16.9 W/M^2 in the equatorial belt (6^o S-6^o N,50- 100^o E) during May 1979. Maximum net heat gain of $120W/M^2$ is observed during pre-onset period in the western part of Arabian Sea. This indicates the increased amount of net radiation and almost low latent heat release in this region. The minimum gain of $50W/M^2$ in the western Bay of Bengal corresponds to higher latent heat and low net radiation. In the Arabian Sea, the net heat gain varies between $50W/M^2$ and $120W/M^2$. Varma (1989) also observed almost a similar range of $75W/M^2$ and $200W/M^2$ for the Arabian Sea during pre-onset period. Near the Somali basin, surface heat gain ranges between $40W/M^2$ and $60W/M^2$ while Hastenrath and Lamb (1979,b) observed a minimum of $40W/M^2$ and a maximum of $50W/M^2$ during May.

During the monsoon period, a considerable reduction in net radiation is noticed in the southern Arabian Sea, which is mainly due to the development of convective clouds associated with the onset of monsoon. The latent heat flux is maximum in this region

due to enhanced evaporation during the monsoon onset period. The intensification and migration of cumulus convective clouds towards north is clearly noticed from the cloud distribution. Sikka and Gadgil (1980) found from satellite observations that, the cloud patches propagate northward in the Indian monsoon region. Yasunari (1980), using the satellite pictures of cloudiness in south Asia, reported the meridional movement of convective clouds and their association with the active and break monsoon cycles. Krishnan et al.(1992) analysed the northward propagation of convective activity in the Indian monsoon region in relation to the equatorial 30-50 day oscillations. The net radiation shows much variations in the area of maximum cloud cover. Northwest increase in net radiation is noticed with maximum on the western corner of the Arabian Sea.

During the onset period, latent and sensible heat fluxes show higher values compared to the previous period. Maximum Latent heat of $200W/M^2$ is noticed in eastern Arabian Sea and maximum sensible heat of $22W/M^2$ is the south western Bay of Bengal. A marked increase in sensible heat and latent heat fluxes was noticed in the equatorial India Ocean during mid-June by Simon and Desai (1986) and they concluded that this increase is due to high SST and not due to wind speed. In the present study, sensible and latent heat shows northward increase in the eastern Arabian Sea and western Bay of Bengal, mostly following the similar pattern of cloud cover. Strong winds associated with the passage of monsoon onset vortex observed during this period

(discussed in the earlier chapter) also enhances the latent heat release.

During the onset period, eastern Arabian Sea and most parts of Bay of Bengal show heat loss, which suggest that a net oceanic heat loss produces a positive feed back for the maintenance and development of deep cumulus convection. This is also evident in the large latent heat release observed during this period. A significant heat loss from the ocean and reduction in net radiation was reported earlier by Rao (1987,b), Ali and Desai (1989) and Varma (1989). The net heat gain/loss obtained in the present study varies between 65W/M^2 and -60W/M^2 in the Arabian Sea and between 40W/M and -30W/M^2 in Bay of Bengal. Southeastern Arabian Sea experiences a net heat loss of 40 W/M^2 and a loss of more than 10W/M^2 in the southern Bay of Bengal. Mohanty and Mohan Kumar (1990) observed a variation between 100W/M^2 and -170W/M^2 in the south eastern Arabian Sea. In a stationary position in southern Bay of Bengal, Rao(1987,b) found a net heat gain/loss of 50-100W/M^2 during June 1979. In the present study, the maximum heat loss observed in the southeastern Arabian Sea is associated with intense convective clouds and strong trade winds observed during the onset of monsoon.

The net radiation has been increased both in Arabian Sea and Bay of Bengal during the break period due to low cloud cover. A decrease of 70 W/M^2 in latent heat flux is also noticed in this season. Sensible heat shows comparatively low values than the onset period. A heat loss of 5W/M^2 observed in the

northeastern Arabian Sea is because of maximum latent heat release and low net radiation. In general, ocean gains heat throughout the area and the maximum is concentrated in Bay of Bengal. The increase in net radiation and net heat gain is consistent with the studies on the energy fluxes over the north Indian Ocean during different epochs of summer monsoon (Mohanty and Mohan Kumar,1990), and the heat budget of the equatorial Indian Ocean (Ali and Desai,1989). The daily variations of heat budget components also reveal an increased net radiation, reduced latent heat flux and large oceanic heat flux during the pre-onset and break monsoon periods, and decreased net radiation, high latent heat release and less heat gain at the ocean surface during onset of monsoon. It is thus clear that, oceanic heat gain/loss is very much controlled by the net radiation, cloud cover and latent heat flux.

The analysis of heat storage of the mixed layer and 0-200m layer indicates positive heat storage in the pre-monsoon season and heat depletion during monsoon season. Maximum depletion of heat is observed in the monsoon season between 10-15^{o} N for both mixed layer and 0-200m layer. Heat depletion in the surface layers has been observed by Bruce (1987), Rao et al,(1985) and Varma (1989) during monsoon season. The results of heat advection during monsoon season reveal that heat is exported from the mixed layer as well as from the 0-200m layer because of maximum heat depletion observed during this season. Heat export from the mixed layer in the 0-5^{o} N latitude belt is about three times the surface heat gain and the export from the 0-200m layer is about

twice the surface heat gain. Between 5-15^{o} N latitudes, the heat export from the 0-200m layer is more than that exported from the mixed layer. In the latitude belt 15-20^{o} N, the heat exported from the mixed layer is three times the surface heat gain and the export of heat from the 0-200m layer is nearly equal to the heat gained at the surface.

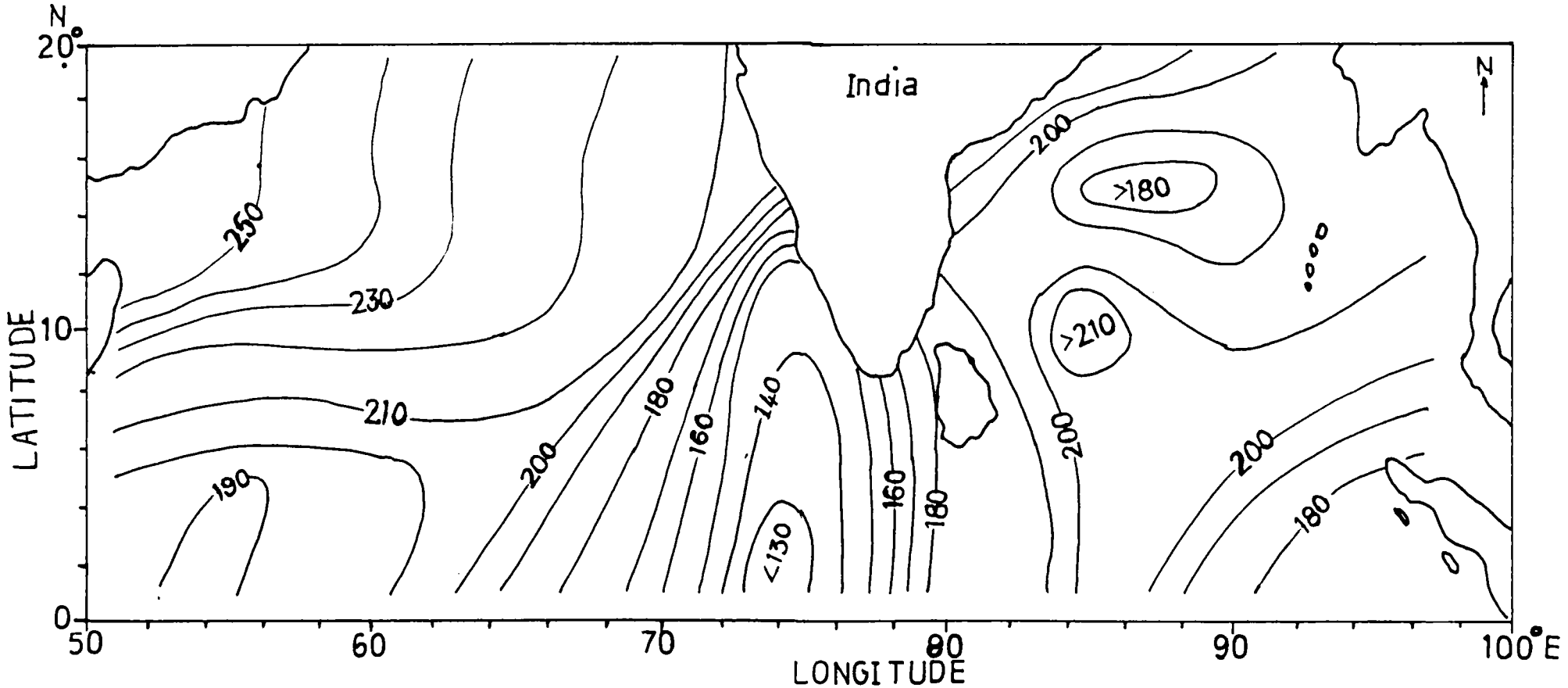

Fig.4.1 Distribution of net radiation during pre-onset period (16-25 May, 1979) W/M^2

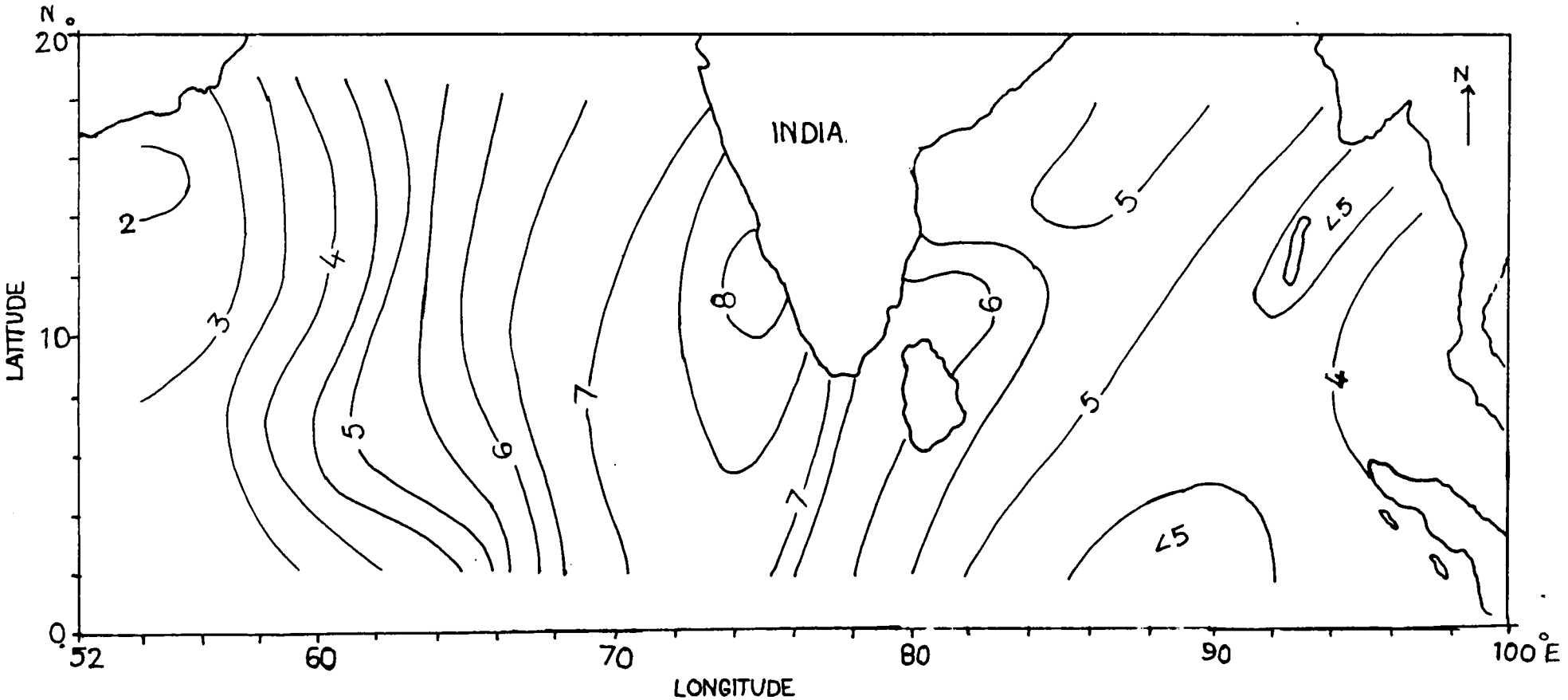

Fig.4.2 Distribution of cloud cover during pre-onset period (16-25 May, 1979) Tens

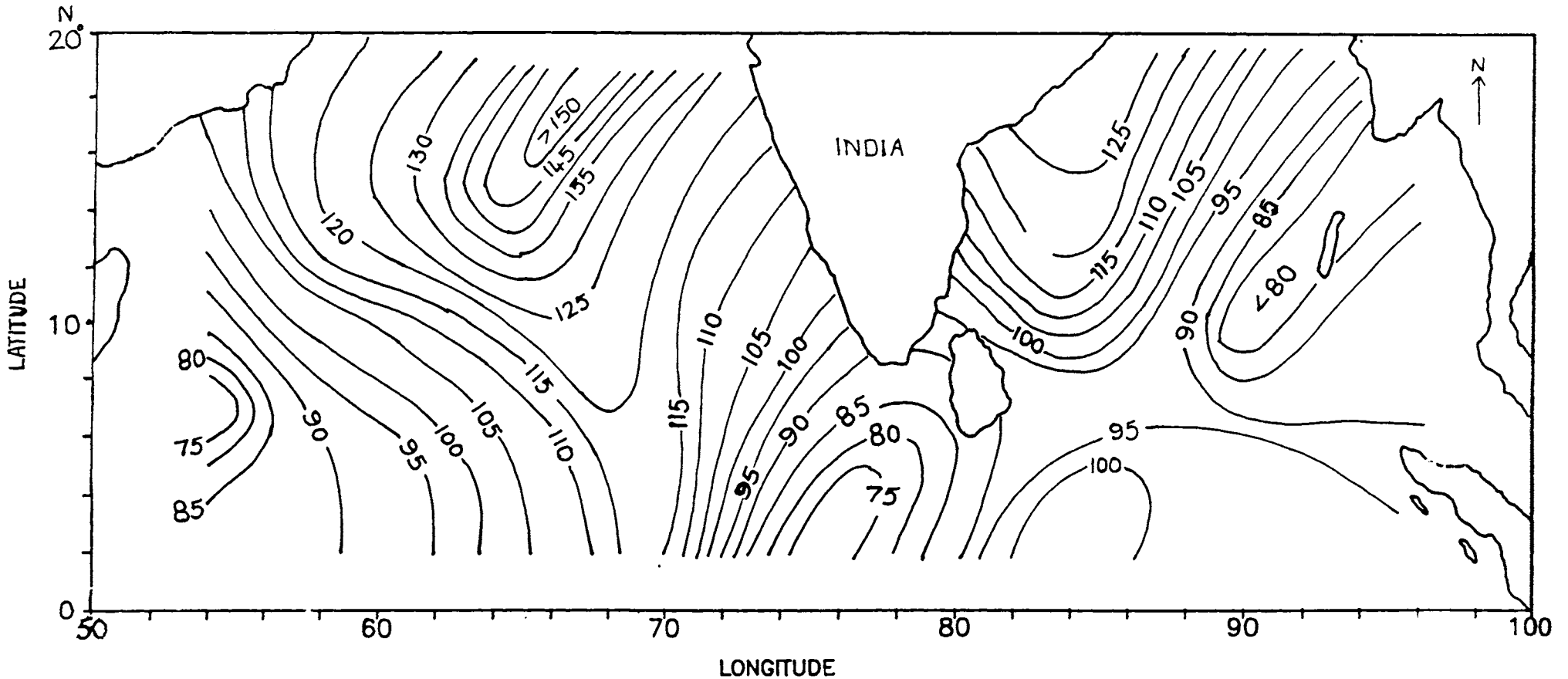

Fig.4.3 Distribution of latent heat flux during pre-onset period (16-25 May, 1979) W/M^2

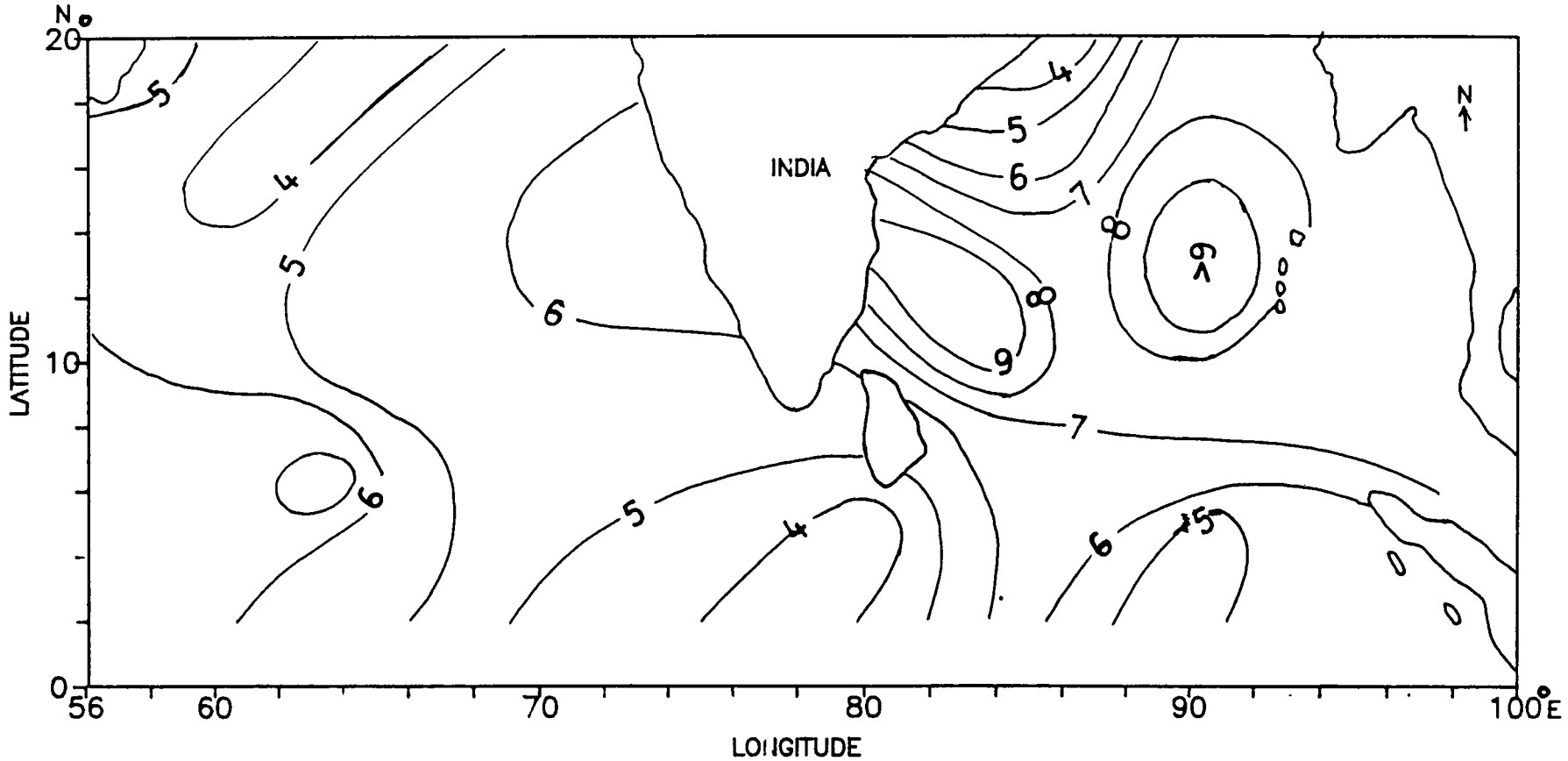

Fig.4.4 Distribution of sensible heat flux during pre-onset period (16-25 May, 1979) W/M^2

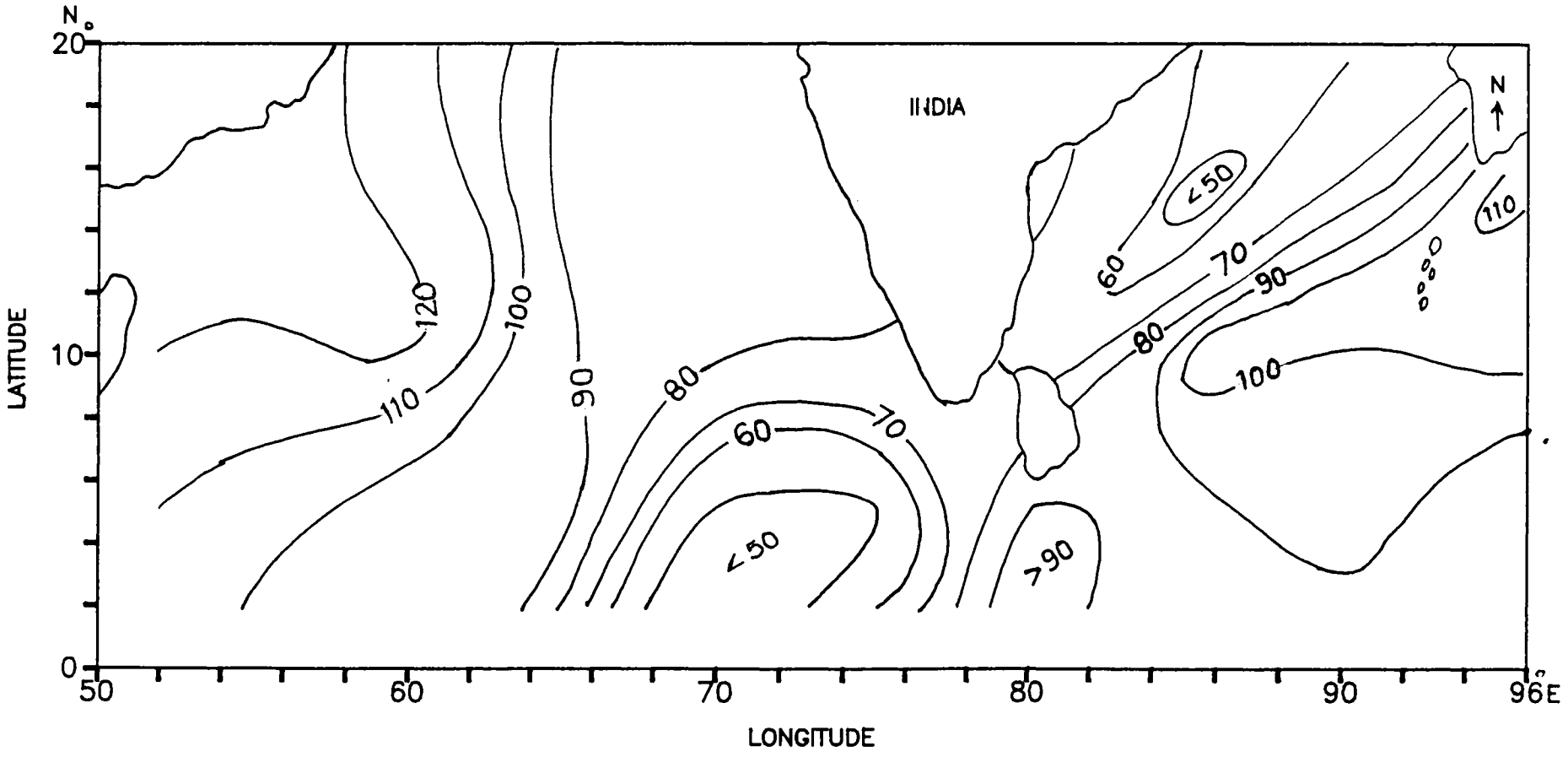

Fig.4.5 Distribution of net heat gain during pre-onset period (16-25 May,1979)

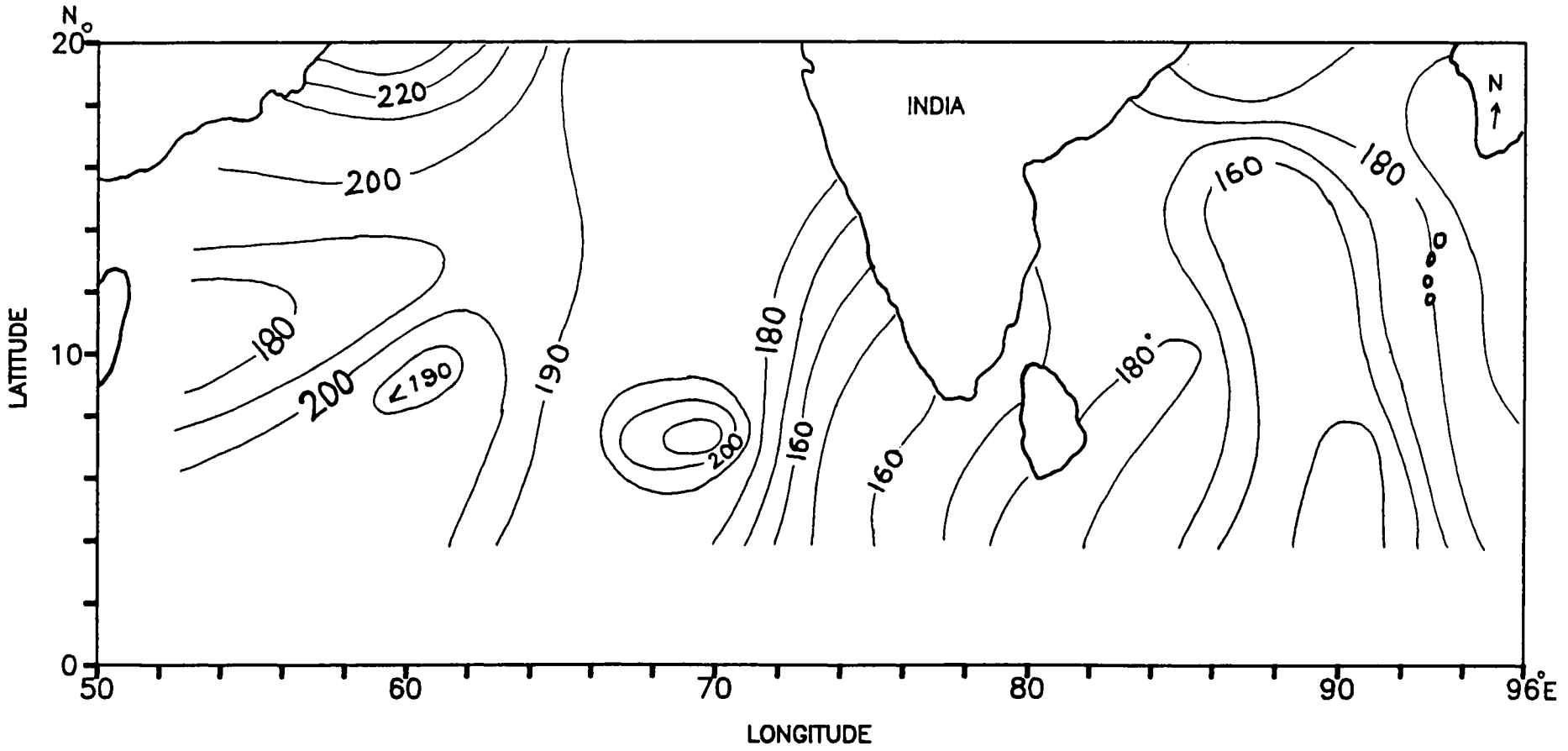

Fig.4.6 Distribution of net radiation during onset period (9-16 June, 1979) W/M^2

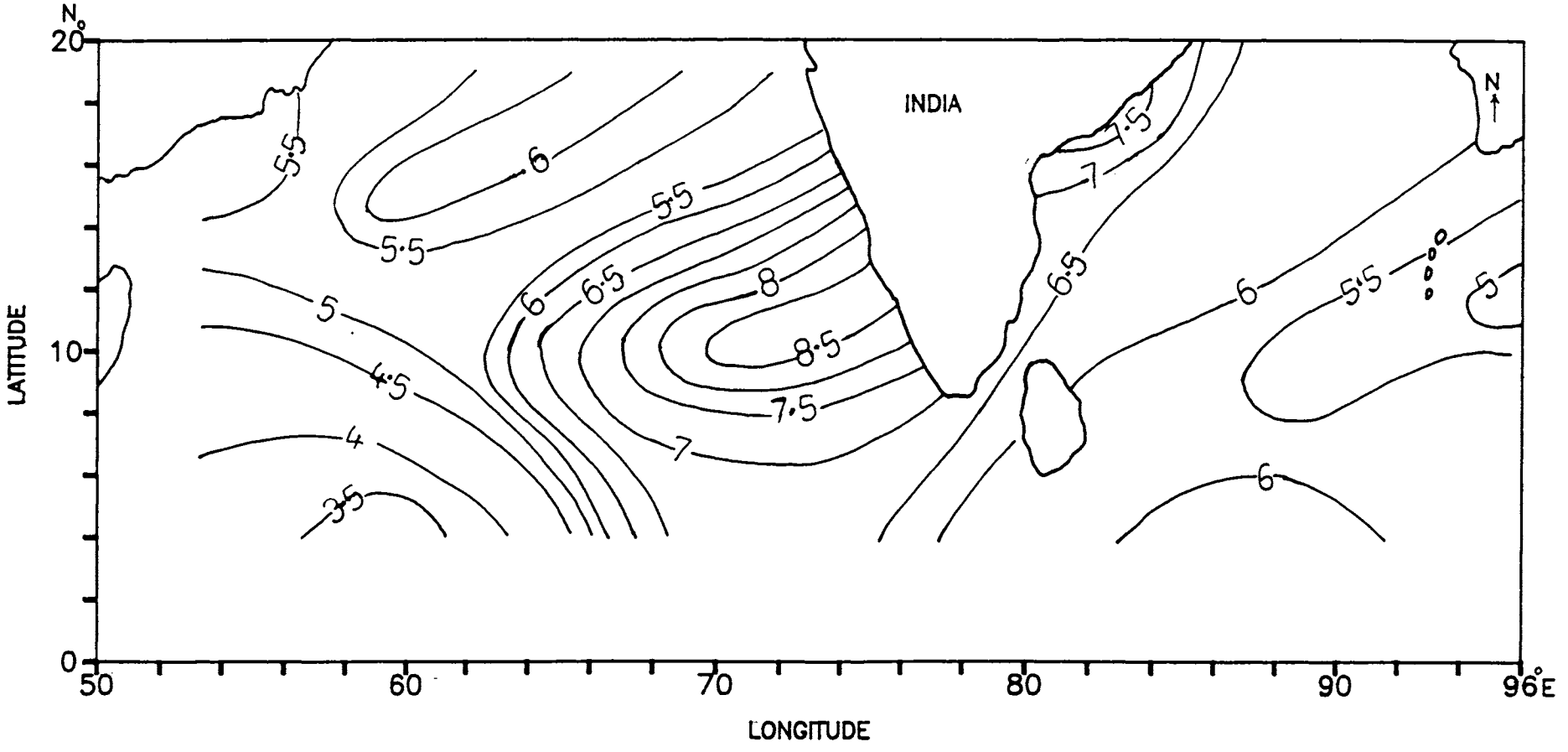

Fig.4.7 Distribution of cloud cover during onset period (9-16 June, 1979) Tens

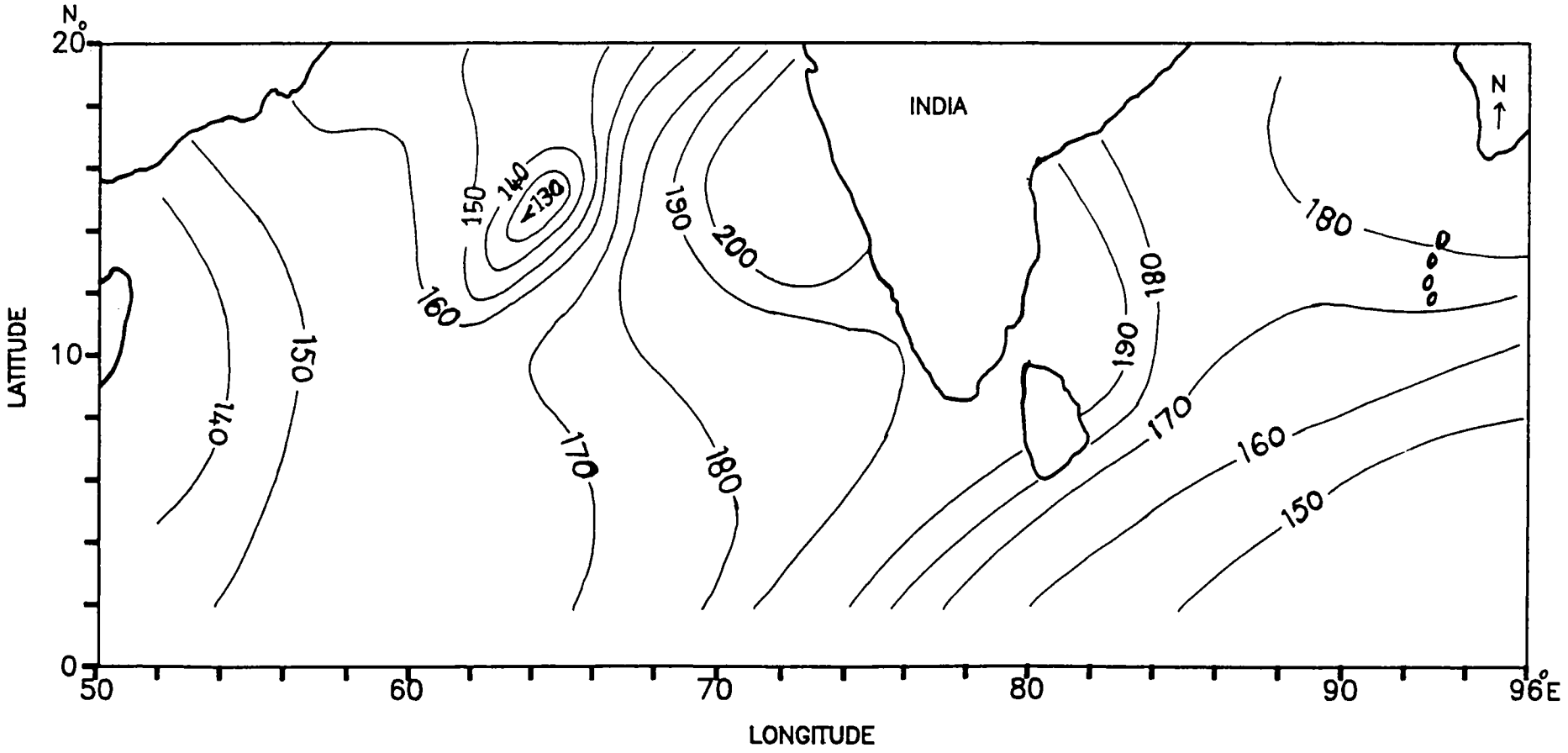

Fig.4.8 Distribution of latent heat flux during onset period (9-16 June, 1979) W/M^2

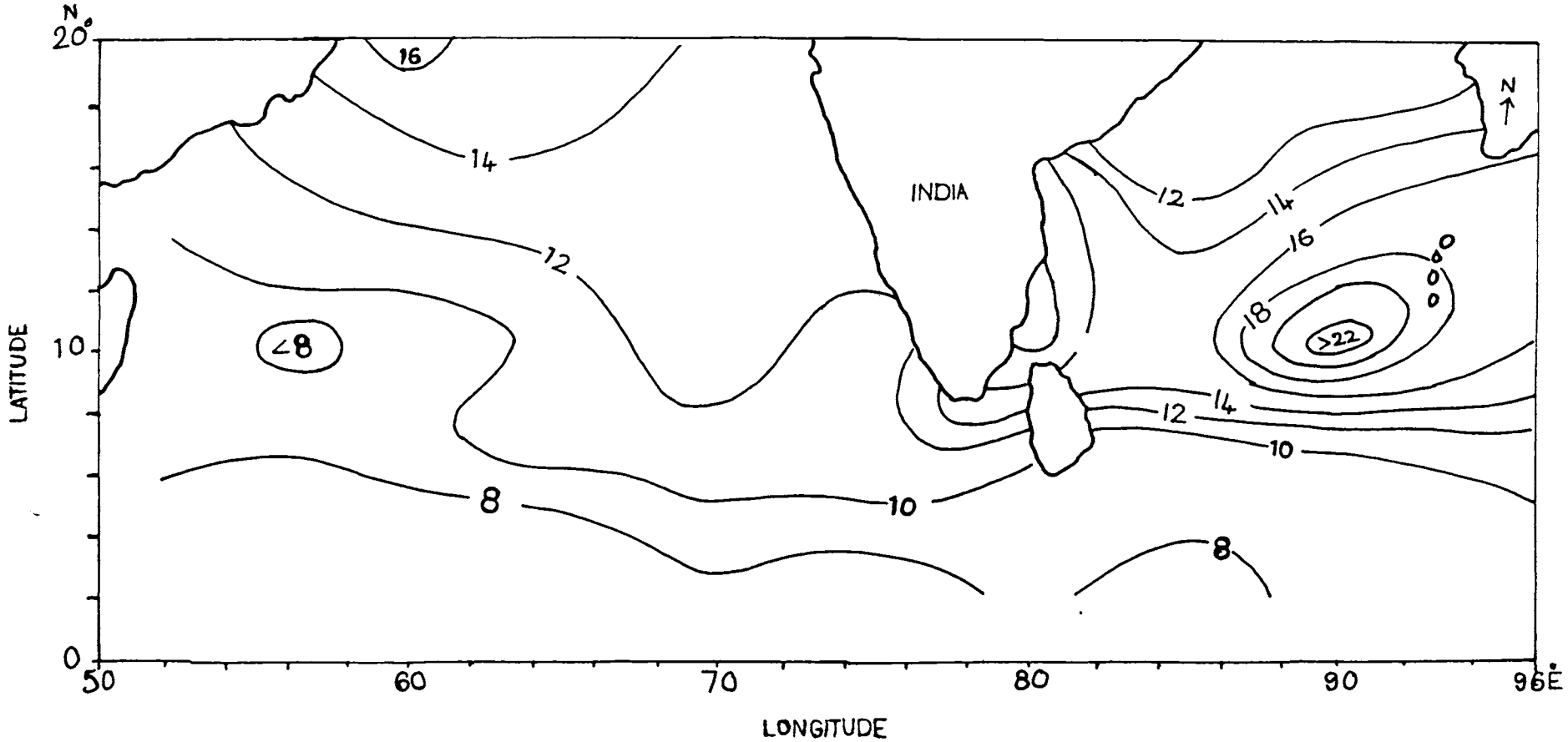

Fig.4.9 Distribution of sensible heat flux during onset period (9-16 June, 1979) W/M^2

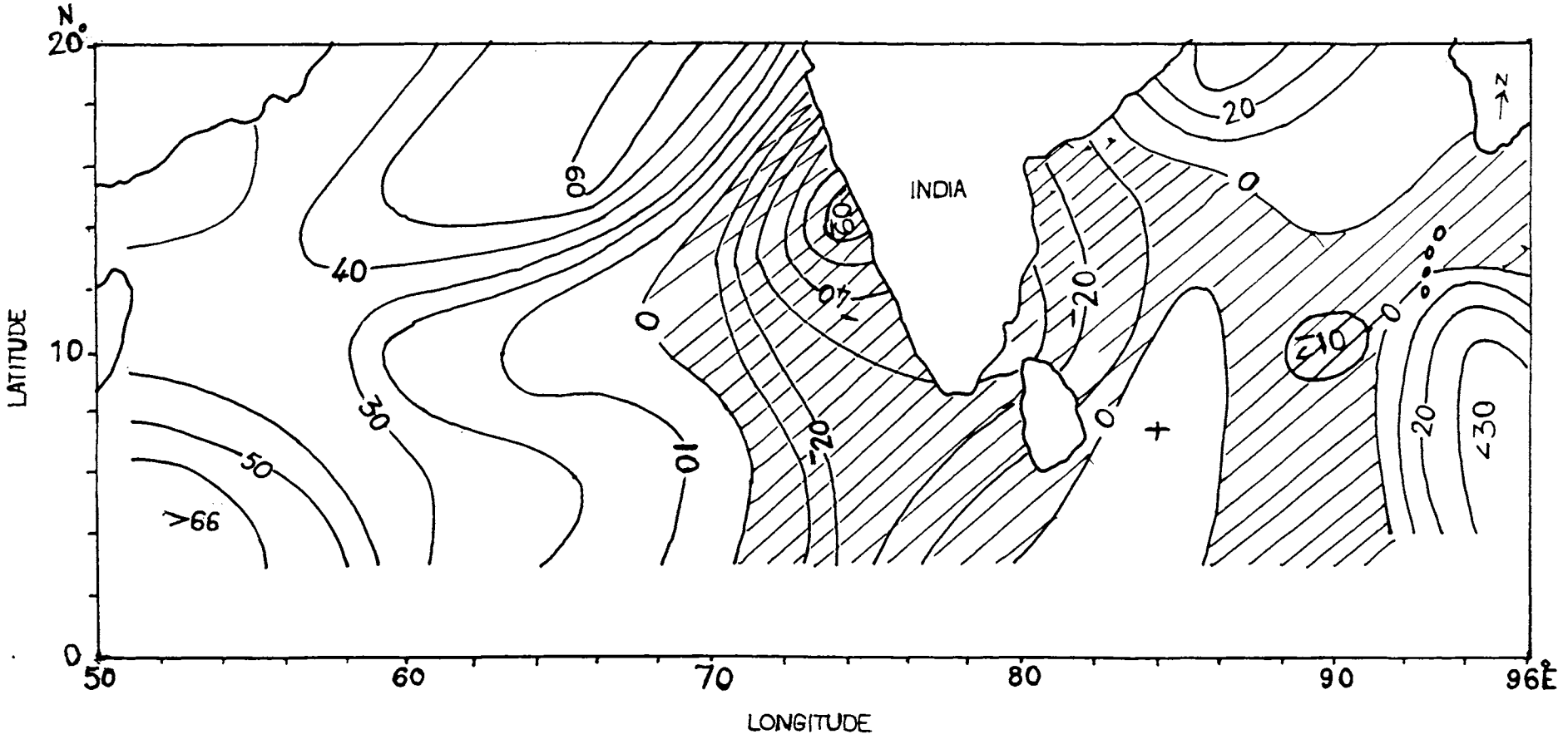

Fig.4.10 Distribution of net heat gain/loss(shaded) during onset period (9-16 June 1979) W/M^2

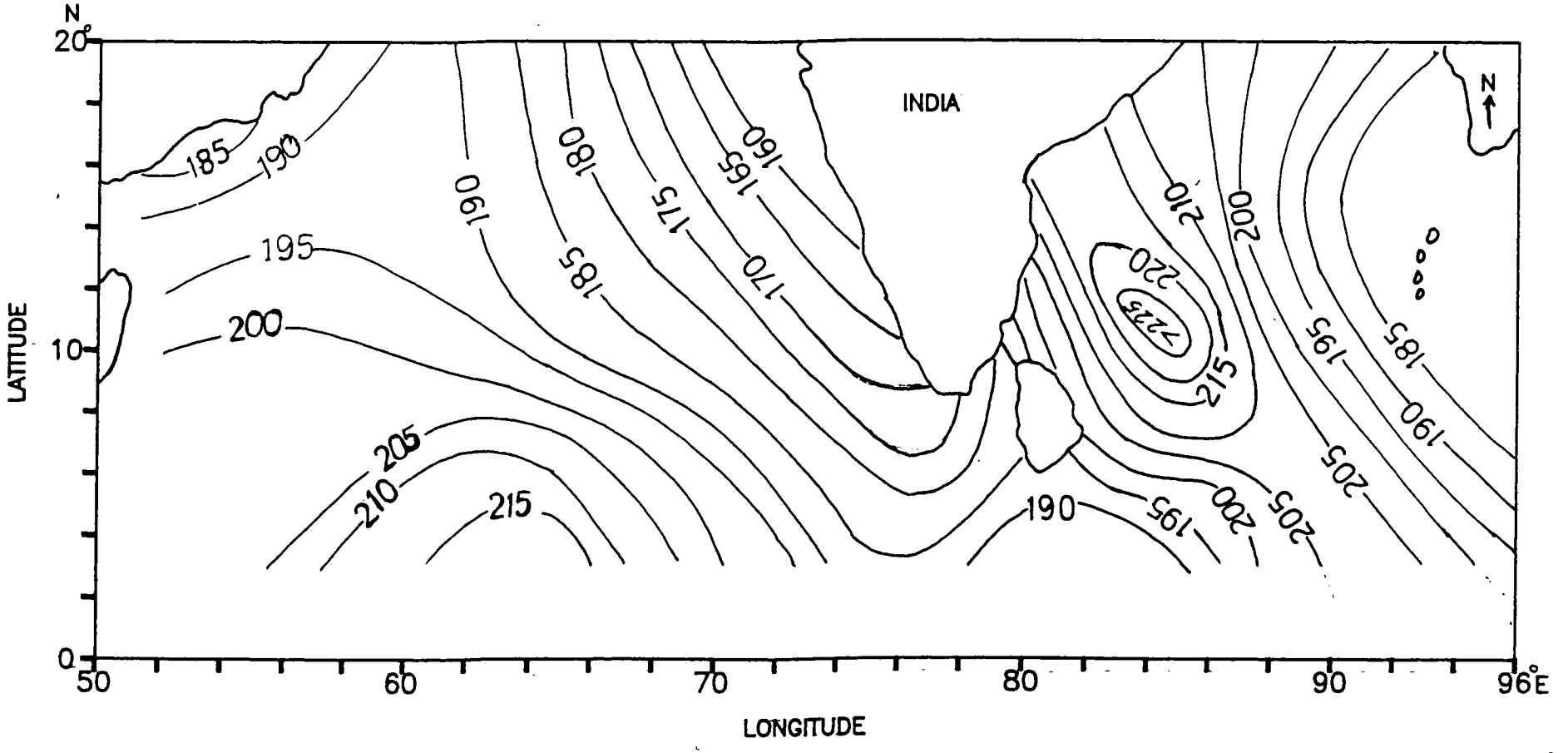

Fig.4.11 Distribution of net radiation during break-monsoon period (14-21 July, 1979) W/M^2

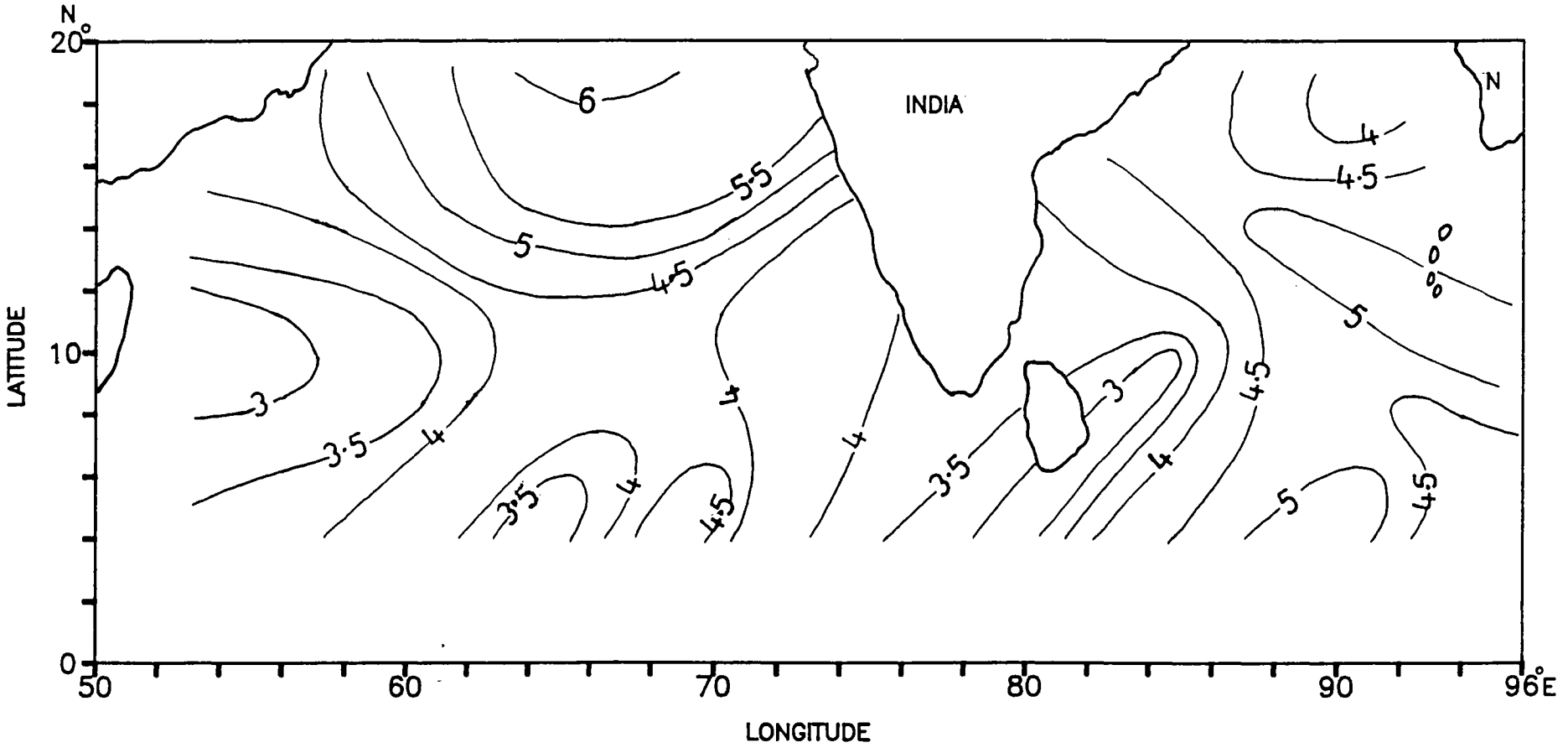

Fig.4.12 Distribution of cloud cover during break-monsoon period (14-21 July, 1979) Tens

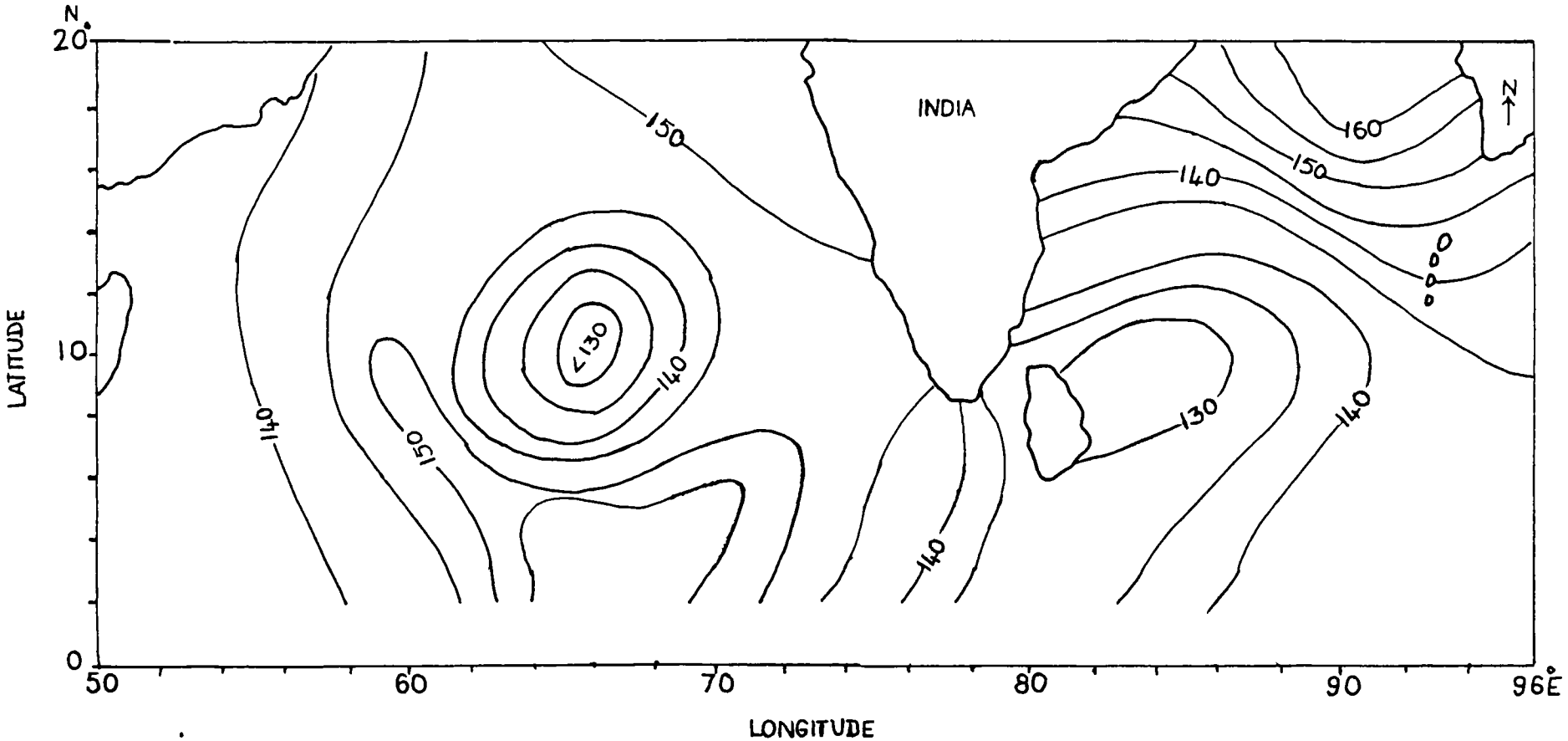

Fig.4.13 Distribution of latent heat flux during break-monsoon period (14-21 July, 1979) W/M^2

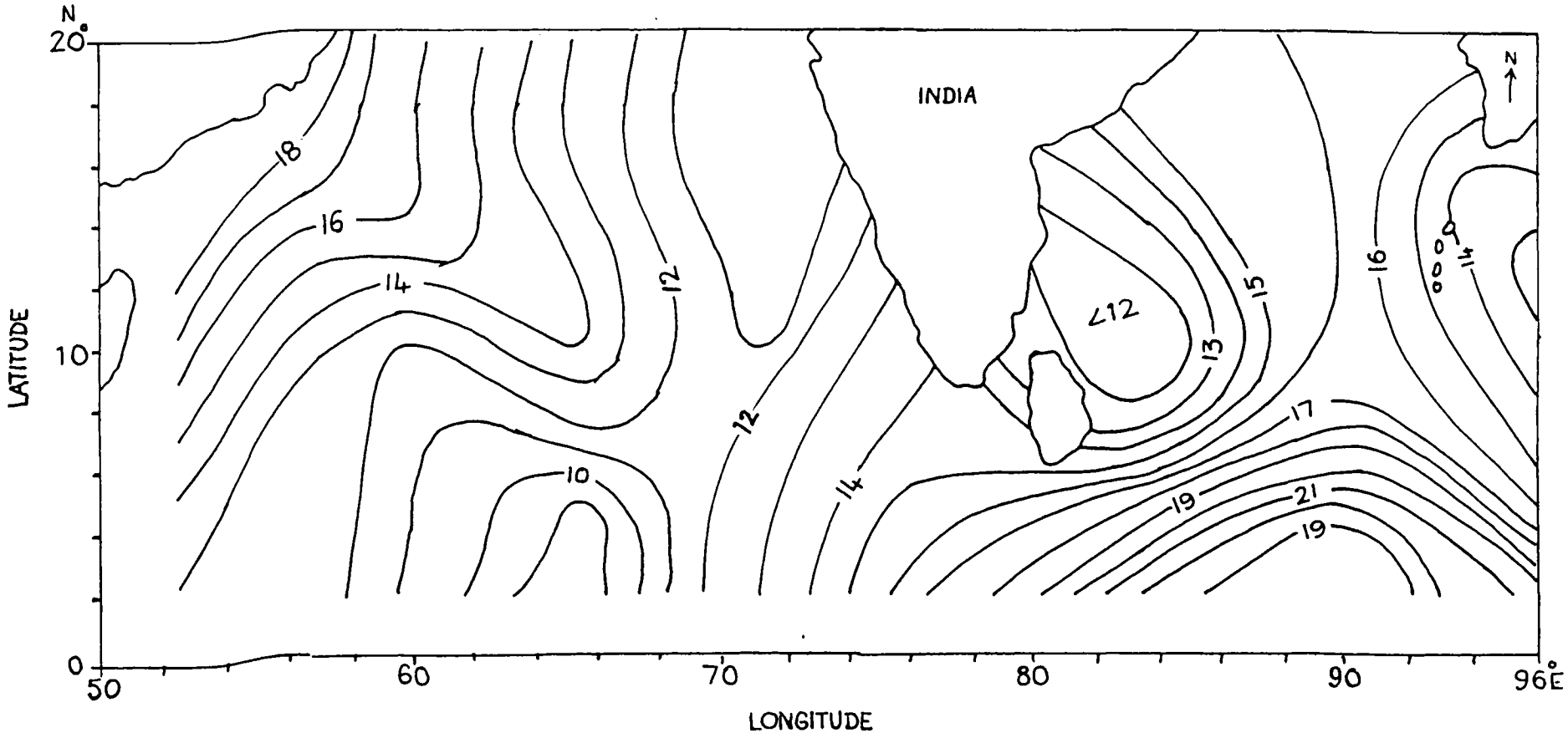

Fig.4.14 Distribution of sensible heat flux during break-monsoon period (14-21 July, 1979) W/M^2

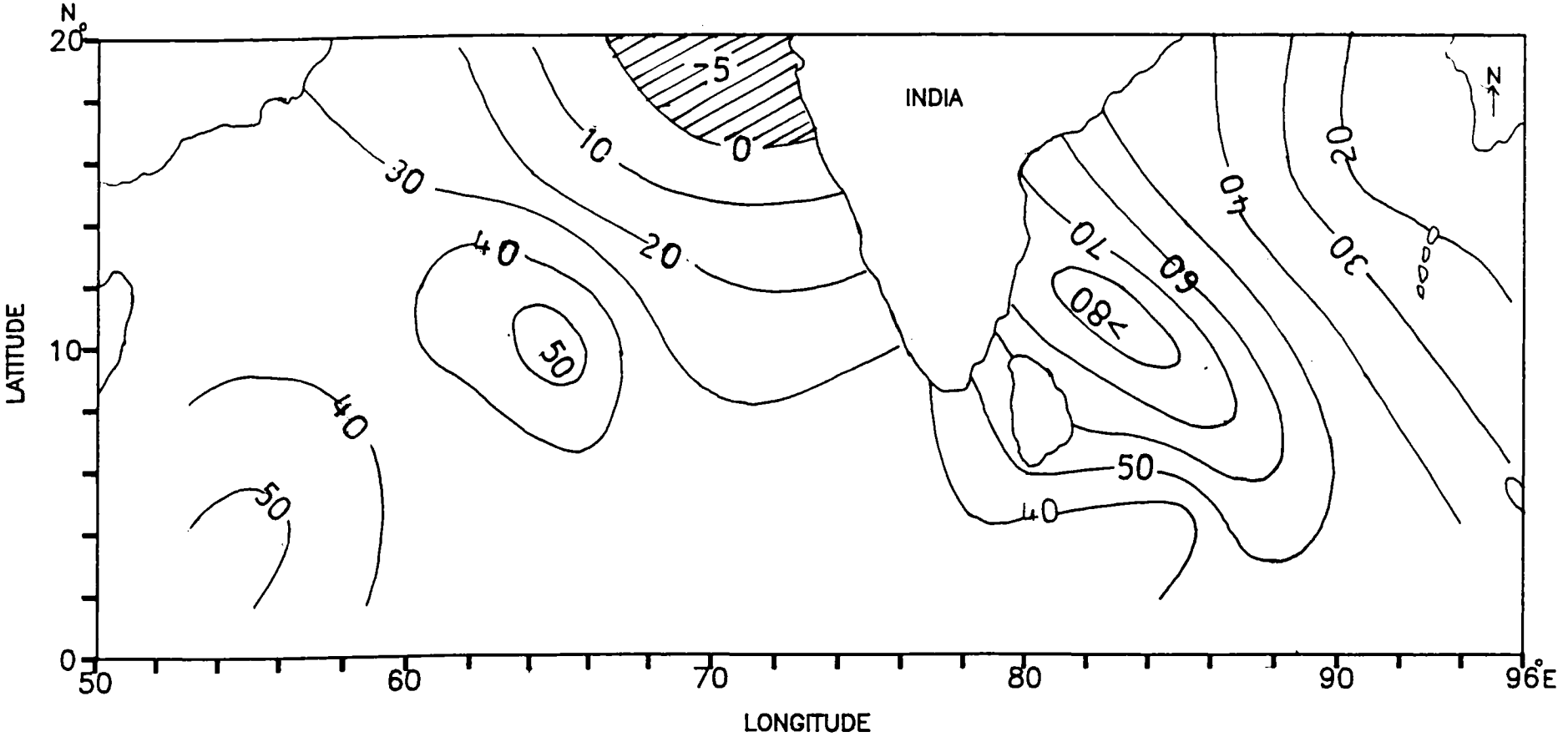

Fig.4.15 Distribution of net heat gain/loss (shaded) during break - monsoon period (14-21 July, 1979)
(W/M^2)

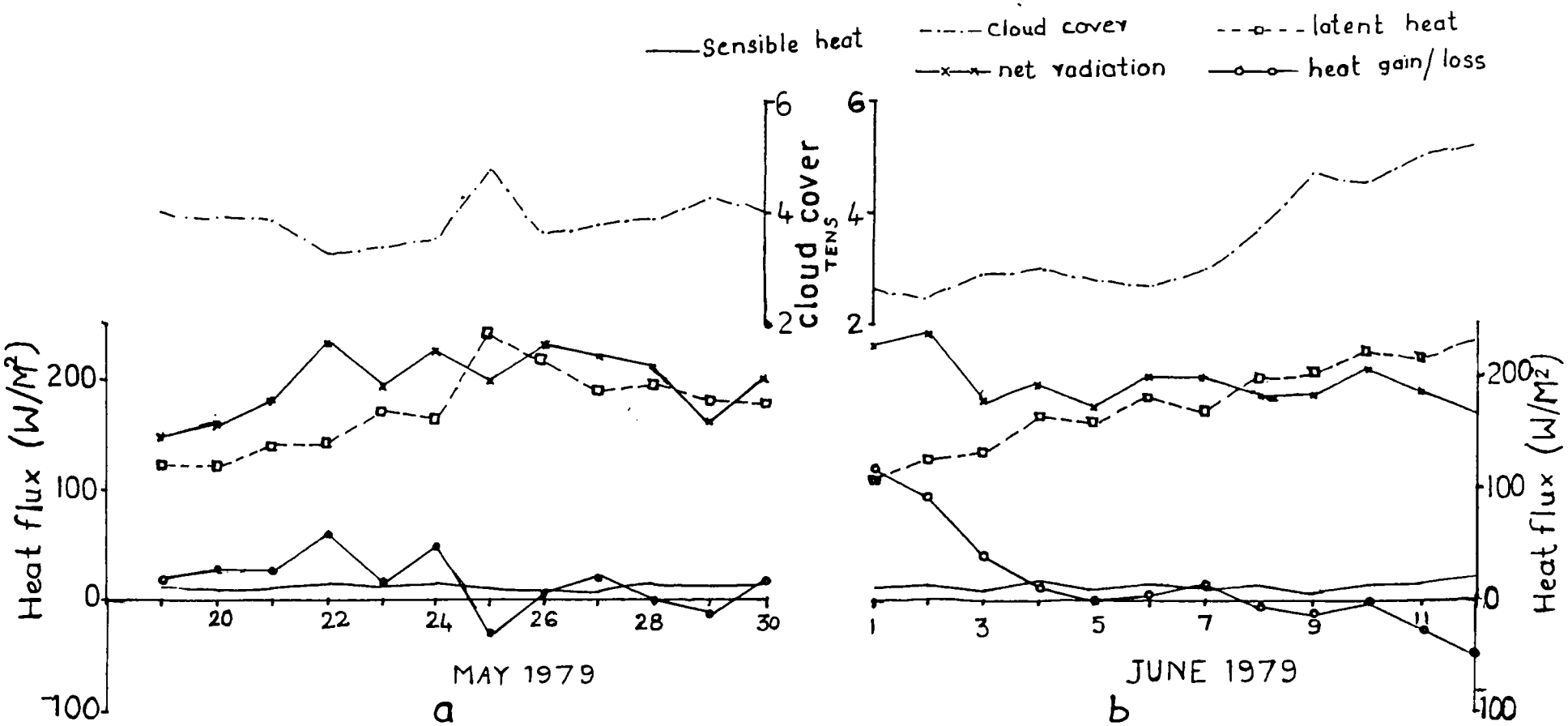

Fig.4.16 Daily variation of energy exchange parameters during (a) pre-onset period (b) onset period

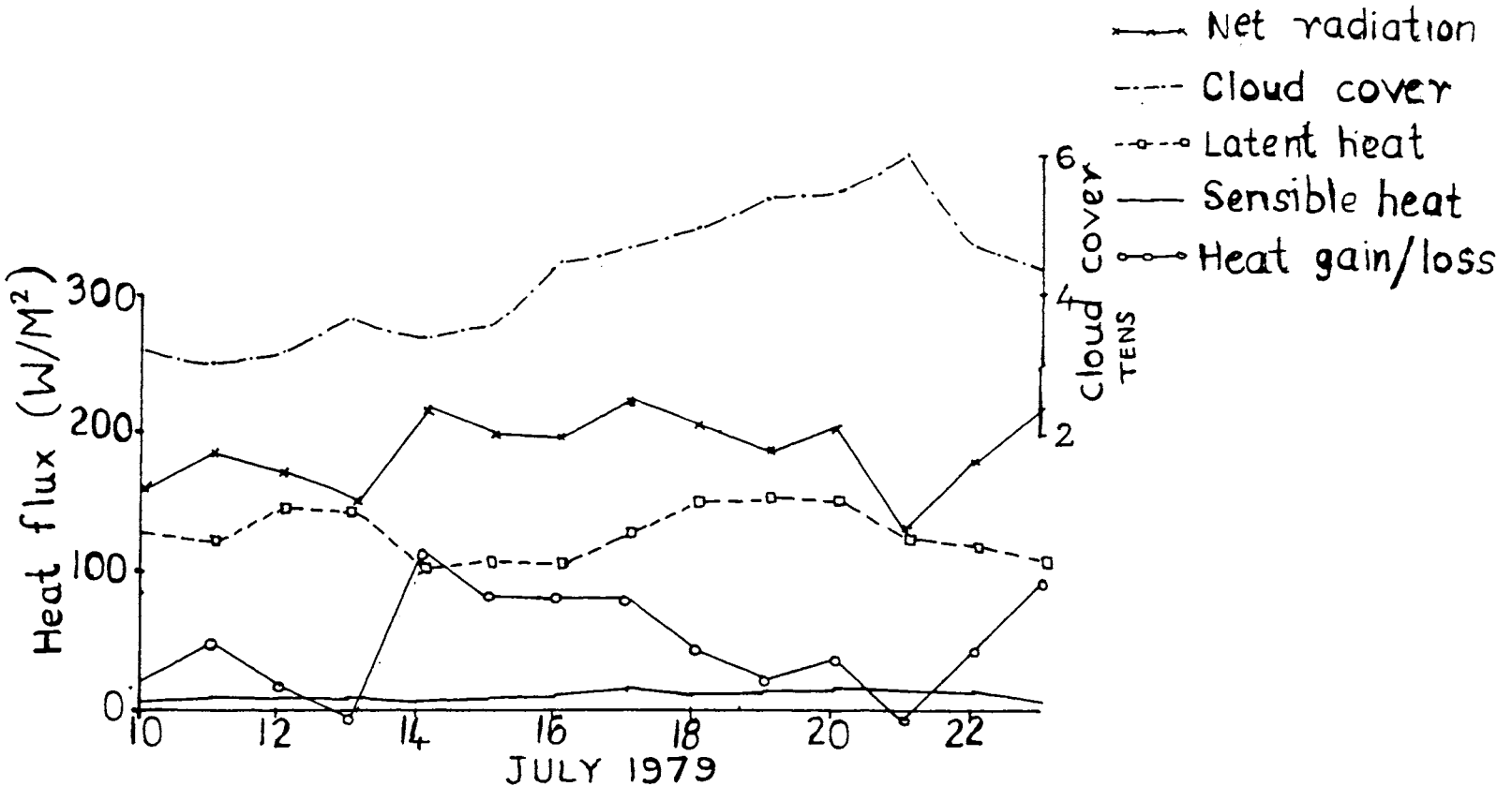

Fig.4.17 Daily variation of energy exchange parameters during break-monsoon period

CHAPTER - V

SUMMARY AND CONCLUSIONS

An assessment of the role of air-sea interaction on monsoon variability in the Indian Ocean has to begin with an examination of the various energy exchange parameters. Heat budget of the ocean is controlled by the exchange of net radiation, latent heat and sensible heat at the ocean-air interface. Thermal conditions in the upper layers of the Indian Ocean are very much influenced by these energy exchanges and hence influence the oceanic and atmospheric circulations.

Northern Indian Ocean is unique in nature in its seasonally reversing monsoonal winds and surface currents. In order to understand the complex nature of Indian monsoon, study of mixed layer dynamics and heat budget of the northern Indian Ocean is required. This thesis attempts to study the seasonal and daily variations in mixed layer depth (MLD), sea surface temperature (SST), heat content of different layers up to 200m, cyclone heat potential, heat budget and heat advection of the mixed layer and 0-200m layer and the various factors controlling them.

As the mixed layer controls most of the energy exchange processes, an accurate method to estimate MLD is of atmost importance. MLD has been estimated by different methods and compared with that obtained from actual temperature profiles. It has been found that the gradient method followed by Ali et al,

(1987) gives satisfactory results. Hence in this study, MLD is estimated using the gradient method. In order to analyse seasonal variations of MLD and SST, seasonal averages were determined using the temperature profiles during 1977-1986. To match with the Levitus (1982) climatology, MLD has been calculated for the following seasons viz. pre-monsoon (February-April), monsoon (May-July), post-monsoon (August- October) and winter (November-January). Using the temperature climatology of Levitus (1982), climatic variations of MLD and SST have also been studied for comparison with those obtained during 1977-1986. Day to day variations of MLD and SST were also analysed in four polygon areas during May-June 1977 and May-July 1979.

The distribution of heat content in different layers of 50m thickness from surface upto a depth of 200m has been carried out from the temperature profiles during 1977-1986. The variations in heat content have been analysed on a seasonal as well as daily basis during May-July 1977 and 1979. A regression equation to estimate cyclone heat potential (CHP_{28}) has been developed uising in-situ SST, wind speed and heat content of 28^{o} C isotherm. Using this regression equation, CHP_{28} has been computed utilizing the satellite derived wind speed and SST during 1979. Besides, daily CHP_{28} has also been computed using MONSOON-77 in-situ data. Variations of CHP_{28} during three storm events in the Arabian Sea and Bay of Bengal have been thus analysed in relation to wind speed.

The radiation data and marine meteorological data obtained from NOAA satellite, GOES satellite derived cloud motion winds and ship measured SST, air temperature, dew point temperature and surface pressure were used for the computation of energy exchange parameters (net radiation, latent heat flux and sensible heat flux) during May-July 1979. Net radiation has been estimated from a regression analysis utilizing the planetary absorbed radiation, available radiation at the top of the atmosphere, total water vapour content and cloud cover. Fluxes of latent and sensible heat were evaluated by bulk aerodynamic method using a constant drag coefficient. Heat storage of the mixed layer and 0-200m layer for different seasons and heat advection during monsoon season have been estimated following Hastenrath and Merle (1986).

Variations of MLD have been studied in relation to the change in SST. Shallow mixed layer is observed in the western side of Arabian Sea during pre-monsoon corresponding to the high SST using Levitus (1982) temperature climatology. MLD increases from west to east in the north equatorial Indian Ocean during monsoon season. SST variations during this period show a increasing trend from west to east. During post-monsoon season, high MLD values are seen in the Arabian Sea compared to Bay of Bengal while the reverse is true during winter season. SST exhibits a gradual increasing trend towards east in both Arabian Sea and Bay of Bengal during the post-monsoon season and the trend is similar for Arabian Sea during the winter season also.

In Bay of Bengal, SST inc es towards southwest during the winter season.

The distribution of MLD and SST using the seasonal averages for the period 1977-1986 shows a gradual increase in MLD towards northeast reaching a maximum of 65m around 16^{o} N,72^{o} E during the pre-monsoon period. In this region more or less low SST prevails. During monsoon season, the minimum MLD observed in the Arabian Sea during the previous season has been replaced by deeper MLD. Bay of Bengal exhibits shallow MLD. Reversal of the zonal slope in MLD is noticed in this season in the north equatorial region in association with the wind reversal. A surface cooling of about $3-4^{o}$ C is noticed in the western Arabian Sea and it is about 2^{o} C in the Bay of Bengal. Comparatively deep MLD is found during post-monsoon season in the western region which shows a shoaling towards east both in Arabian Sea and Bay of Bengal. The .pa variations in SST are reflected in the corresponding MLD variations. During the winter season, deep MLD is noticed in the northwestern Arabian Sea and in the central Bay of Bengal in association with low SST.

Studies on the daily variations of SST and MLD in various polygon areas show an increase in MLD during 6-20 June and 30 June to 15 July 1977 in the central Arabian Sea. The corresponding variations in SST show a decreasing trend. During 10-22 May 1979, a gradual fall in MLD (about 10m) is noticed to an increase in SST of 0.3^{o} C in the western Arabian Sea.

It is found that mixed layer depth varies with the variations in SST in many cases. During monsoon season, the MLD deepens in the Arabian Sea as a result of increased mixing provided by the rough sea conditions.

Analysis of vertical temperature sections in the equatorial Indian Ocean shows a decreasing trend (about 20m over a 14^{o} longitude) in MLD from west to east before the onset of monsoon and a deepening of 18m over 8^{o} longitude from west to east after the onset of monsoon 1977. The magnitude of decrease from west to east is about 15m over 16^{o} longitude before onset and the increase is about 22m over 17^{o} longitude from west to east after the onset of monsoon during 1979. In the equatorial Indian Ocean, MLD dynamics is not controlled by SST alone but, surface wind stress also plays a major role.

In general, it can be seen that when the SST increase is due to the heating caused by increased insolation, the upper mixed layer gets heated up resulting in a shallow MLD. For example, during pre-monsoon season, shallow MLD is obesrved in the western Arabian Sea due to high SST. Similarly, when the decrease in SST is due to the heat loss caused by reduced insolation, or increased net loss from the ocean surfcae, mixed layer deepens. This is true during monsoon season especially in the Arabian Sea. On the other hand, when the increase/decrease in SST is due to an oceanic phenomena, MLD increases/decreases. For example, during upwelling, SST decreases when the cooler water reaches the surface, as can be seen in the vertical section of

the equatorial region between 75^{o} to 77^{o} E during 19-23 July. Similarly, when the MLD increases at the eastern end of the equatorial Indian Ocean as a result of the piling up of warmer surface water, there exists a direct correlation between SST and MLD. Thus depending upon the phenomena SST and MLD are correlated either directly or indirectly.

The variations of heat content in the surface (0-50m) layer show a maximum heat content of $62*10^{8}J/M^{2}$ during pre-monsoon season in the Arabian Sea and a minimum of $50*10^{8}J/M^{2}$ during monsoon season. This layer shows a heat content of $58*10^{8}J/M^{2}$ during post-monsoon and about $53*10^{8}$ J/M^{2} during winter season in the central Arabian Sea. In Bay of Bengal, higher heat content is noticed during monsoon season compared to Arabian Sea, and more or less same magnitude during pre-monsoon season and lower heat content during post-monsoon and winter seasons. The zonal variations of heat content in all the lower three layers beyond 50m show similar trend as the surface layer during monsoon and winter seasons, but, the trend is reversed during the other two seasons.

The decrease in heat content between the first and second layers is about $9*10^{8}J/M^{2}$ in the eastern Arabian Sea which shows a regular fall towards west during pre-monsoon season. During monsoon season, it is about $16*10^{8}J/M^{2}$ on the eastern side and about $2*10^{8}J/M^{2}$ on western side of the Arabian Sea, whereas in Bay of Bengal, this type of conspicuous zonal variations are not

present. This heat content variations are mostly controlled by the variations in SST, mixed layer cooling and vertical advective processes in the upper thermocline. During post-monsoon season, the lowering is less on the western side than the eastern section both in Arabian Sea and Bay of Bengal. This is because of the cooling and deepening of mixed layer on the western and shallow MLD on the eastern side.

Beyond 100m, the successive layers show larger heat loss on the eastern Arabian Sea during monsoon and winter seasons, but, this trend is reversed during pre and post-monsoon seasons in Arabian Sea and Bay of Bengal. This difference in heat content is mostly associated with the temperature gradient in the thermocline.

Day to day variations of heat content of the surface layer mostly follow the variations in SST. The lower three layers show more or less opposite trend in heat content variations as compared to the surface layer. The heat loss between successive 50m layers increases downwards during 30th june to 15th July 1979, because of the decrease in downward advective transfer of heat from the surface to lower layers. During 6-20th June 1977, the heat loss between the second and third layer is less compared to the layers above and below. The heat loss in each 50m layer exhibits almost similar magnitudes during 16-23rd May 1979. In June 1979, the reduction in heat between second and third layers appears to be higher than the layers above and below. This is due

to sharp temperature gradient in the thermocline up to 150m. In Bay of Bengal, during July, the surface layer shows minor fluctuations in heat content, but, the lower three layers exhibit large variations. This may be due to the vertical oscillations of thermocline.

Analysis of CHP_{28} during three storm events reveals that increase in heat potential is accompanied by high SST and low MLD before the formation of storm and decreased heat content, low SST and deep MLD after the storm events. This implies that heat has been taken away by the storm in the form of latent heat along its track.

Spatial distributions of heat budget components in the northern Indian Ocean show dramatic changes during different phases of southwest monsoon. Maximum variations in net radiation are noticed in the southwestern Arabian Sea associated with the intensification of convective clouds just before the onset. Latent and sensible heat show comparatively lower values than those during the onset period. Ocean gain a maximum heat of $120W/M^2$ in the western Arabian Sea due to increased net radiation and low latent heat release. A minimum gain of $50W/M^2$ is noticed in the Bay of Bengal.

Considerable reduction in net radiation is noticed during the onset period due to the intensification and migration of convective clouds. Eastern Arabian Sea registered maximum latent heat of $200W/M^2$ where the cloud cover shows maximum variations.

This is due to maximum condensation as a result of more latent heat release. Sensible heat flux increases by $10W/M^2$ both in Arabian Sea and Bay of Bengal. During onset period, ocean loses a maximum heat of $60W/M^2$ near the southwest coast of India. In most parts of Bay of Bengal also recorded heat loss of about $30W/M^2$ in association with low net radiation and high latent heat.

Net radiation recovers its maximum during break period. Latent heat, sensible heat and cloud cover show low values compared to the onset period. Ocean gains heat during this period throughout the study area except in a limited area in the northern Arabian Sea where a loss of $5W/M^2$ is noticed. In the daily variations also, heat exchange components exhibit similar variations. The oceanic heat gain is, in general, mainly controlled by variations in net radiation and latent heat flux. Heat loss during monsoon season produces a positive feed back for the development and intensification of convective clouds.

Variations in heat storage of mixed layer and 0-200m layer indicate an overall positive heat storage during pre-monsoon and heat depletion during monsoon season. Heat storage minus surface heat gain gives the degree of heat advection indicating heat export during monsoon season in the north Indian Ocean. On an average, heat export from both the mixed layer and 0-200m layer is found to be more than twice the surface heat gain during this season.

The present investigations have brought out the role played by the various air-sea interaction parameters during the different phases of Indian monsoon. The advective transfer of heat in different latitude belts in the north Indian Ocean has been established and quantified. The studies also enable us to highlight the influence of oceanic heat content in the genesis of cyclonic storms in the Indian Ocean.

REFERENCES

Ali,M.M.,Simon,B.,Desai,P.S.,1987: Inference of vertical motions in the equatorial Indian Ocean using satellite data., Oceanologica acta, NSP, 71-75.

Ali,M.M and Desai,P.S.,1989: Heat budget study of the equatorial Indian Ocean using satellite data., Contributions in Marine Sciences, Dr.S.Z. Qasim's sixtieth birthday felicitation volume, 227-236.

Ali,M.M.,1990(a): Role of absorbed solar radiation on Indian Ocean surface temperature- A case study for calm winds using satellite data., Remote Sens. Environ.,30,107-111.

Ali,M.M.,1990(b): Inference of the zonal slope of marine boundary layer from GEOSAT altimeter data., Paper presented at the TOGA scientific conference held at Hawai during 1990. Full paper communicated to Indian J. Rem. Sens.

*Anderson,E.R.,1952: Energy budget studies.,U.S Geological survey circulation,229,71-119.

Anjaneyulu,T.S.S.,1980: A study of air and sea surface temperature over the Indian Ocean, Mausam, 31,551-560.

Ashbel,P.,1961: New world maps of global solar radiation during IGY 1957-58,Hebrew University, Dept. of climatology and meteorology, Jerusalem, Israel.

Basil Mathew.,1982: Studies on upwelling and sinking in the seas around India., Ph.D Thesis, University of Cochin, 159pp.

Bathen,K.H.,1971: Heat storage and heat advection in the north Pacific Ocean.,J.Geophys. Res. 76,676-687.

Barnett,A.F., 1978: Poleward heat flux in southern Hemispheric ocean.,J. Phys. Oceanogr.,8,785-798.

Bjerkness,J.,1966: A possible response of the atmospheric Hadley circulation to the equatorial anomalies of ocean temperature.,Tellus,18,820-829.

*Black,J.H.,1956: The distribution of solar radiation over the earth's surface.,Arch. Meteorol. Geophys., B(7),166-189.

Bruce,J.C and Beatty,W.,1985: Some observations of currents off Somali coast during the southwest monsoon.,J.Geophys.Res., 74(8),1958-1967.

Bruce,J.G.,1987: Seasonal heat content variations in the north western Indian Ocean., Oceanologica acta, Symposium on vertical motion,F 137a.149.

Bryan,K.,1962: Measurement of meridional heat transport by ocean currents., J. Geophys. Res.,67,3403-3414.

Budyko,M.I.,1956: Heat balance of the earth's surface (translated from Russian)., U.S weather Beaur. Washington,D.C,259pp.

*Budyko,M.I.,1963: Atlas of the heat balance of the earth., Kartfabrika gosgeoltehizdala (in Russian), Lenigard,pp75.

Bunker,A.F.,1978: Computations of surface energy flux and annual air-sea interaction cycles of the North Atlantic Ocean.,Mon.Wea. Rev.,104,1122-1140.

*Burdicky,F.,1958: Remarks on the distribution of solar radiation on the surface of the earth., Arch. Meteorol. Geophys. B(8),326-335.

Camp,N.T and Elsberry,R.L., 1978: Ocean thermal response to strong atmospheric forcing Part-II The role of one

dimensional processes.,J.Phys.Oceanogr. 8,215-224.

Colon,J.A.,1964: On the interaction between the southwest monsoon current and the sea surface over the Arabian Sea., Indian J. Meteorol. Geophys. 15,183-200.

Colborn,J.G.,1975: The thermal structure of the Indian Ocean.,The University press of Hawai, Honolulu,161pp.

Christenson,E.M. and Mascarenhas,A.,1979: Heat storage in the oceanic upper mixed layer inferred from LANDSAT data.,Science,203,653-654.

Creegan,A and Johnson,J.A.,1978: An advective mixed layer model with imposed surface heating and wind stress.,Deep Sea Res.,26-A 357-368.

Das,V.K, Gouveria,A.D and Varma,K.K., 1980: Circulation and water characteristics on isanosteric surfaces in the North Arabian Sea during Feb-April.,Indian J. Mar.Sci.,9,156-165.

David,H.,1974: Observations of the deepening of the wind mixed layer in the Northeast Pacific Ocean.,J. Phys. Oceanogr.,4,1-15.

Dhoulath,K.A, Ali,M.M, Desai,P.S and Kurup,P.G.,1990: Estimation of cyclone heat potential over Bay of Bengal using satellite and ship data., Current Sci. 59,No.16,790-793.

Dhoulath,K.A, Ali,M.M, Kurup,P.G and Desai.P.S., Analysis of net shortwave radiation over the Arabian Sea from satellite data., Proc. Natl. Symp. on Advances in satellite meteorology held at Space Applications Centre, Ahmedabad during February 1992 (in press).

Deshamps,P.V and Frouin,R.,1983: Large diurnal heating of the sea

surface observed by the HCMR experiment., J.Phys. Oceanogr. 14, 177-184.

Duing,W.,1970: The monsoon regime of the current in the Indian Ocean., IIOE Oceanogr. Monograph, 1, East-west centre press (Honolulu), 68pp.

Duing, W and Leetma,A.,1980: Arabian Sea cooling - A Preliminary heat budget.,J.Phys. Oceanogr.,10,307-312.

Elsberry,R.L and Camp,N.T., 1978: Oceanic thermal response to strong atmospheric forcing Part-II Characteristics of forcing events., J. Phys. Oceanogr.,8,206-214.

Elsberry,R.L and Raney,S.D 1978: Sea surface temperature response to variations in atmospheric wind forcing., J.Phys. Oceanogr.,8, 881-887.

Etter,P.C.,1983: Heat and freshwater budget of Gulf of Mexico.,J.Phys. Oceanogr., 13, 2058-2069.

Gautier,C, Diak,G. and Masse,S.,1980: A simple physical model to estimate incident solar radiation at the surface from GOES satellite data., J. Appl.Meteorol.,19,1005-1012.

Gautier,C.,1981: Daily short-wave energy budget over the ocean from geostationary satellite measurements., Oceanography from space, Plenum press,201-206.

Gautier,C.,1982: Mesoscale insolation variability derived from satellite data. J.Appl.Meteorol., 21,51-58.

Gautier,C.,1986: Evolution of the net surface short-wave radiation over the India Ocean during summer MONEX-79-A satellite description., Mon.Wea.Rev.,114,525-537.

Gautier,C and Frouin,R.,1988: An attempt to remotely sense from space the surface heat budget over the Indian Ocean during

the 1979 monsoon.,Geophys. Res. Letters,15,No.10,1121-1124.

*Gibblett,M.A.,1921: Some problems connected with evaporation from large expenses of water.,Proc.Roy.Soc.London,Series-A,99,472-490.

Hastenrath,S and Lamp,P.,1979(a): climatic Atlas of the Indian Ocean Part-I-Surface circulation and climate.,Uty. of Wisconsin press,104pp.

Hastenrath,S and Lamb,P.,1979(b): Climatic atlas of the Indian Ocean Part-II-The oceanic heat budget. Uty. of Wisconsin press,93pp.

Hastenrath,S.,1980: Heat budget of the tropical ocean and atmosphere.,J.Phys.Oceanogr.,10,159-170.

Hastenrath,S and Lamb,P.,1980: On the heat budget of the hydrosphere and atmosphere in the Indian Ocean.,J.Phys. Oceanogr.10,694-708.

Hastenrath,S and Merle,J.,1986: Annual march of heat storage and export in the tropical Atlantic Ocean. J.Phys.Oceanogr.,16, 694-708.

Hsiung,J,Reginald,E.N and Houghtby,T.,1989: The annual cycle of oceanic heat storage and oceanic meridional heat transport.,Quart.J.Roy.Meteor.Soc.,115,1-28.

Jacob,S., 1951: The energy exchange between the sea and atmosphere and some of its consequences., Bull.Scripts.Inst. Oceanogr.,Uty. of Calofornia,6,27-122.

*Jeffry,S.,1918: Some problems of evaporation, Phil. Magazine and J. Science, London,series-6,35,270-280.

Joseph,P.V and Pillai,P.V.,1986: Air-sea interaction on monsoonal

scale over northern Indian Ocean-Part-II-Monthly mean atmospheric and ceanic parameters during 1972 and 1973.,Mausam,37,159-168.

Joseph,M.G.,1987: Studies on mixed layer depth in the Arabian Sea.,Ph.D Thesis, Cochin Unty. of Sci. and Tech., 162pp.

Joshi,P.C and Desai,P.S.,1986: Thermal response of monsoon circulation observed with NOAA data.,Presented at the workshop on 'Satellite Meteorology',IISc Bangalore, Dec-22-27.

Jung,G.H.,1952: Note on meridional transport of energy by oceans., J. Mar. Res.,11,39-146.

Kaiser,A.C.J.,1976: Heat balance of the upper ocean under light winds.,J.Phys.Oceanogr.,8,1-12.

Kelkar,R.R. and Pradhan,T.D.,1977: Measurement of radiation balance components over a water surface.,Indian J.Meteorol. Hydrol.Geophys.,28,349-354.

Koteswaram,P., 1958: The Asian summer monsoon and the general circulation over the tropics- Monsoons of the world, 105-110.

Krishnamurthy,T.N, Rananatham.Y, Ardanuy,P and Pasch,R.,1979: Quick look Summer MONEX Atlas, Part-II-The onset phase. Dept. of Meteorology, Florida state Uty., Tallahassee, Florida, FSU Report No.75.

Krishnan,R, Kasture,S.V and Keshvamurthy,R.V.,1992: Northward movement of the 30-50 day mode in an axisymmetric global spectra model.,Current Science,62(11),732-735.

La Fond, E.C., 1966: Temperature structure in the sea in

Encyclopedia of ocean.,Edited by K.W. Fairbridge, New York, Reinhold.

Lamb,P.J.,1981: Estimates of annual variation of Atlantic Ocean heat transport., Nature, 290,766-768.

Lamb,P.J and Bunker, A.F.,1982: Tha annual march of the heat budget of the north Atlantic Ocean.,J. Phys. Oceanogr.,12,1388-1410.

*Landsberg,H.E, Idppmann,K,Pattan,H and Troll,L.,1963: Weltkorten Sur Kil makunde., Springer-Verlog,Berlin.

*Leipper,D.F., 1967: Observed ocean conditions and hurricane Hilda-1964., J. Atm. Sci.,24,182-196.

Levitus,S.,1982: Climatological Atlas of the World Ocean., NOAA Proc. Paper No-13, U.S. Govt. Printing office, Washington,D.C,173 pp.

Levitus,S., 1987: Rate of change of heat storage of the world oceans., J.Phys. Oceanogr., 17,518-528.

Mani,A,Chacko,O,Krishnamurthy,V and Desikan,V.,1967: Distribution of global and net radiation over the Indian Ocean and its Environment. Arch. Meteor. Geophys., 15(12), 82-98.

Mc Alister, E.D and Mc Leish, W.,1969: Heat transfer in the top millimeter of the ocean., J.Geophys. Res. 74(13),3408-3414.

Mc Phaden, M.J.,1982: Variability in the central equatorial Indian Ocean. Part-II Oceanic heat and turbulent energy balance. J. Mar. Res.,40,403-419.

Merle,J., 1980: Seasonal heat budget in the equatorial Atlantic Ocean.,J.Phys. Oceanogr.,10,464-471.

Meehl,G.A.,1984: A calculation of ocean heat storage and effective ocean surface layer depths for the northern

hemisphere., J. Phys. Oceangr.,14,1747-1761.

Mishra,D.K.,1981: Satellite derived SST distribution over the North Indian Ocean during southwest monsoon season.,Mausam,32,59-66.

Miller,P.R, Sivaramakrishnan,M.V and Suryanarayana,R.,1963: Preliminary results and future plans of IIOE meteorology programme- Computer plans. Porc. seminar jointly sponsored by NSF (USA), IMD and USIS,30-41.

Miller,J.R.,1978: Monitoring changes in upper ocean heat storage from satellites.,TM No.79601.Goddard space flight centre,1-28.

Miller,J.R.,1985: Variations in upper heat storage determined from satellite data. Remote Sen. Environ.,11,473-482.

*Model.F.,1950: Warm waserheizang Europs.Ber. Deut. Welterdienstes.,12,51-60.

Mohanty,U.C, Dube,S.K and Sinha,P.C.,1982: On the role of large scale energetics in the onset and maintenance of summer monsoon.,Mausam,33,139-152.

Mohanty,U.C and Mohan Kumar,N.,1990: A study on energy fluxes in the surface boundary layer of the Indian seas during different epochs of the Asian monsoon., Atm. Envt.,24A,No.4,823-828.

Molinari,R.C, Swallow,J.C and Fests,J.F.,1986: Evolution of the near surface thermal structure in the western Indian Ocean during FGGE 1979., J. Mar. Res.,44,739-762:

Murthy,V.S.N, Rao,D.P and Sastry,J.S.,1983: The lowering of sea surface temperature.,Mahasagar,16,67-71.

Niiler,P.P and Kraus,E.B.,1977: One dimensional models of the upper ocean-in modelling and prediction of upper layers of the ocean., (Ed. Kraus,E.B) Pergamon press,143-172.

Oort,A.H and Vonder Haar,T.H.,1977: On the observed annual cycle in the Ocean-Atmosphere heat balance over the northern hemisphere., J.Phys.Oceanogr.,6,781-799.

Ohring,G and Gruber,A.,1984: Satellite determination of the relationship between total long-wave radiative flux and infra-red window radiance.,J. Appl. Meteorol.,23,416-425.

Ostapoff,F and Worthem, S.,1974: The intra-diurnal temperature variations in the upper ocean layer. J. Phys. Oceanogr., 4,601-612.

Pant,M.C.,1977: Wind stress and fluxes of sensible and latent heat over the Arabian Sea during ISMEX-73.,Indian J. Meteorol. Hydrol. Geophys.,28,189-196.

Patil,M.R and Ramamirtham,C.P.,1962: Hydrography of the Laccadives offshore waters- A study of the winter conditions., J.Mar.Biol.Ass.India, 4,159-169.

Patil,M.R, Ramamirtham,C.P, Udayavarma,P, Nair,C.P.A and Maryland,P., 1964: Hydrography of the west coast of India during the pre-monsoon period of the year 1962.,J.Mar. Biol.Ass. India, 6,151-164.

Pathak,P.N.,1982: Comparison of SST from TIROS-N and ships in the Indian Ocean during MONEX (May-July)., Remote Sen. Environ.,12,363-369.

Pickard,G.L.,1965: Descriptive physical oceanography- An Introduction., Pergamon press,200pp.

Pickard,G.L and Emery,W.J., 1983: Descriptive physical oceanography., Pergamon press,249pp.

Pisharoty, P.R.,1965: Evaporation from Arabian Sea and the Indian southwest monsoon.,Proce. Symp. on the International Indian Ocean Expedition of meteorological results, Bombay,43-54.

Polousky,A.B and Shapiro,N.B.,1983: Variability of hydrographical fields in the western equatorial zone of the Indian Ocean., Oceanography,23,2,172-175.

Pond.S and Pickard, G.L., 1983: Introductory dynamical oceanography.,Pergamon press,316pp.

Raghavan,K, Puranik,P.V, Mujundar,V.R, Ismail;P.M.M and Paul,D.K., 1978: Interaction between the west Arabian Sea and the Indian Monsoon.,Mon.Wea.Rev.,106,719-724.

Ramage,C.S, Miller,F.R and Jeffry,C., 1972: Meteorological Atlas of IIOE, Uty. of Hawai, Honolulu.

Ramam,K.V.S,Murthy,P.G.K and Kurup,C.K.B.,1979: Thermal structure variation in the Arabian Sea May-July1978.,Mausam,30,105-112.

Ramam,K.V Prasada Rao,C.V.K and Durga Prasad N., 1982: On the time varying current and hydrographic conditions in the central Arabian Sea during summer MONSSON-77. Mausam, 33-4, 451-458.

Ramamaswamy,C.,1962: Break in the monsoon as a phenomenan of interaction of easterlly and sub-tropical weterly jet-stream., Tellus,14,337-343.

Ramesh Babu,V, Rao,L.V.G, Varkey,M.J and Udayavarma,P.,1978: Tempearture distribution of the upper layers of northern

and eastern Arabian Sea during ISMEX-73.,Indian J. Meteorol.Hydrol.Geophys.,27,291-293.

Ramesh Babu,V, Varkey,M.J, Keasavadas and Gouria,A.D., 1980: Water masses and general hydrography along west coast of India during early March.,Indian J. Mar. Sci.,9,82-89.

Ramesh Babu,V and Sastry,J.S.,1984: Summer cooling in the east central Arabian Sea- A processe of dynamic response to the southwest monsoon.,mausam,35,17-26.

Ramesh Babu,V,Sastry,J.S,Gopalakrishna,V.V and Rama Raju,D.V., 1991: Premonsoonal water charecteristics and circulation in the east central Arabian Sea., Proc. Indian Acc. Sci. Earth and planetary science,100, No.1,55-68.

Rao, D.P, Sarma,V.N, Sastry,J.S and Premchand,K.,1978: On the lowering of SST in the Arabian Sea with the advance of southwest monsoon season. Proce. Symp. on 'Tropical Monsoon'., Pune,106-115.

Rao,R,R, Murthy, P.G.K, Joseph,M.G and Raman,K.V.S.,1981: On the space-time variability of ocean surface mixed layer charecteristics of central and eatern Arabian Sea during monsoon-77.,International conference on early results of FGGE and large scale aspects of its monsoon experiments, Geneva,9,20-27.

Rao,R.R,Rao,D.S,Murthy,P.G.K and Joseph,M.X.,1983: A premilinary investigation on the summer monsoonal forcing on the thermal structure of upper Bay of Bengal during MONEX-79, Mausam, 34, 239-250.

Rao,M.V, Ramesh Babu,V, Rao,L.V.G and Sastry,J.S.,1984:

Estimation of evaporation rates over the Arabian Sea from satellite data, Proc. Indian Acc. Sci.

Rao,R.R, Raman,K.V.S, Rao,D.S and Joseph,M.X.,1985 : Surface heat budget estimates at selected areas of north Indian ocean during monsoon-77, Mausam, 36, 21-32.

Rao,D.S and Rao,R.R., 1986: A case study of the genisis of a monsoon low and the thermal structure of the upper northern Bay of Bengal during MONEX-79. Mahasagar,19(1),1-9

Rao,R.R.,1987(a): Further analysis of the thermal response of the upper Bay of Bengal to the forcing of pre-monsoon cyclonic storm and summer monsoonal onset during MONEX-79., Mausam, 38, 2, 147-156.

Rao,R.R.,1987(b): On the thermal response of upper eastern Arabian sea to the summer monsoonal forcing during monsoon-77, Mausam, 37, 77-84.

Rao,R.R.,1988: Seasonal heat budget estimates of the upper layers in the central Arabian Sea., Mausam,39,241-248.

Reed,R.K.,1977: On estimating insolation over sea surface., J.Phys.Oceanogr.,7,482-485.

Riverdine,G.,1983: Heat budget of the tropical Atlantic Ocean-Seasonal upwelling.,Deep Sea Res. 32-A 216-222.

Roll,H.U.,1965: Physics of the Marine Atmosphere.,Acadamic press,426pp.

Saha,K.R.,1970: Zonal anomaly of sea surface temperature in equatorial Indian Ocean and its possible effert on mnsoon , Tellus,22,403-409.

Sastry,J.S, and D'souza,R.S.,1970: Oceanagraphy of Arabian Sea during southwest monsoon-Part-I Thermal structure., Indian

J. Meteorol. Geophys.,21,367-382.

Sastry,J.S and Ramesh Babu,V.,1985: Summer cooling of the Arabian Sea-A review., Proc. Indian Acc.sci. 94,117-128.

Seetharamayya,P and Mullan,A,H.,1987: Storm induced vertical thermal variations (warming and cooling) in eastern Arabian Sea during MONEX-79. Proc. Sym. short-term varaibility of physical oceanographic features in Indain waters, 19-20 Feb.1987,Cochin (suupliment).

Shetye,S.R.,1986: A model study of the seasonal cycle of the mixed layer.,Proc. Indain Acc. Sci., 94,129-137.

Sikka,D.R and Gadgil,S.,1980: On the maximum cloud zone and the ITCZ over Indian Ocean longitudes during the southwest monsoon., Mon. Wea. Rev.,108,1840-1853.

Simon,B and Desai,P.S.,1986: Equatorial Indian Ocean evaporation estimates from operational meteorological satellites and some inferences in the context of monsoon onset and activity., Boundary layer Meteorology,37,37-52.

Simpson,J.J and Paulson,C.A., 1980: Small scale SST structure.,J.Phys. Oceanogr.,10,399-410.

Suryanarayana,R and Sikka,D.R.,1965: Evaporation over the Indian Ocean during 1963.,Proc. Synp. on 'Meteorolgical results of IIOE',Bombay,68-69.

Tarpley,J.D.,1979: Estimating incident solar radiation at the surface from geostationary satellite data.,J. Appl. Meteorol.,18,1172-1181.

Timothy Liu, W.,1983: The effect of variation in SST and

atmospheric stability in the estimation of average wind speed by SEASAT-SASS., J. Phy. Oceanogr. 14,392-401.

Varma,K.K, Kesavadas,V and Gouvia,A.,1980: Thermocline structure and water masses in the northern Arabian Sea during February-April.,Indian J. Mar. Sci.,9,148-155.

Varma,K.K., 1989: Studies on energy exchange and upper ocean thermal structure in Arabian Sea and heat transport in Northern Indian Ocean., Ph.D Thesis, Cochin university of Science and Technology, 140pp.

Vonder Haar,T.H and Ellis,J.S.,1974: Atlas of radiation budget measurements from satellites., Atmos. Sci. Pap.No.231,Colorado State Unty.,180pp.

Vonder Haar T.H and Socomi,V.E.,1979: Satellite observations of the earth's radiation budget-1962-1965,WMO Tech. Rep.,104pp

Washburn.L and Gibson C.H.,1984: Horizontal variability of temperature microstructure at the base of mixed layer during MILE., J. Geophys. Res.,89,3507-3522.

Weisberg,R.H,Miller,L,Horigan,A and Knauss,J.,1980: Velocity observations in the equatorial thermocline during GATE, Deep Sea Res.,26, suppl.

Wunch,C and Gill,A.E.,1976: Observations of equatorially trapped waves in Pacific sea level variations.,Deep Sea Res.,23,371-390.

*Wunch,C.,1978: Observations of equatorially trapped waves in the ocean-A review., Prepared for equatorial workshop-July 1977,FINE workshop Proc. NOVA/NYIT,Uty. Press,Fort, Lauderdale,37pp.

Wunch, C.,1980: Meridional at flux of North Atlantic Ocean.,Proc. Natl. Acc. Sci.,77,5043-5047.

Wylie,D.P and Hinton,B.B.,1982: The wind stress pattern of the Indian Ocean during the summer monsoon of 1979. J.Phys.Oceangr.,12,1,186-199.

Wyrtki,K.,1971: Oceanographic Atlas of IIOE., Natl. Sci. Foundation, Washington,D.C,531pp.

Wyrtki,K.,1973: An equatorial jet in the Indian Ocean., Science, 181,262-264.

Yamamotto,G and Wark,D.Q.,1962: Methods of estimating infra-red flux and SST from meteorological satellites., J. Atm. Sci.,19, 369-384.

Yasunari,T., 1980: A quasi- stationary appearance of 30-40 day period in the cloudiness fluctuations during summer monsoon over India., J. Meteorol. Soc. Japan, 58,225-229.

Zandlo,J.A, Smith,W.L,Menzel,W.P amd Hayden,C.M.,1981: Surface temperature determination from an amalgamation of GOES and TIROS-N radiance measurements., J. Appl. Meteorol.,21,44-50.

---

* Not reffered in original.